A THEORETICAL STUDY OF THE CATION – π INTERACTION IN ALKALI METAL POLYENES AND POLYENE COMPLEXES

THESIS

Submitted to the
University of Calicut
in partial fulfillment of the requirements
for the award of the degree of
Doctor of Philosophy
in Chemistry,
under the Faculty of Science

By

FR. JOSE T. M.

Forwarded

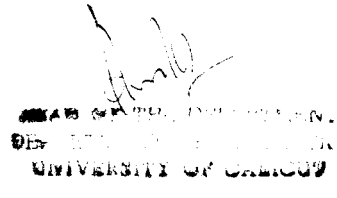

Department of Chemistry,
University of Calicut,
Calicut University P.O.,
673 635

April 2007

A THEORETICAL STUDY OF THE CATION – π INTERACTION IN ALKALI METAL POLYENES AND POLYENE COMPLEXES

THESIS

Submitted to the
University of Calicut
in partial fulfillment of the requirements
for the award of the degree of
Doctor of Philosophy
in Chemistry,
under the Faculty of Science

By

FR. JOSE T. M.

Forwarded

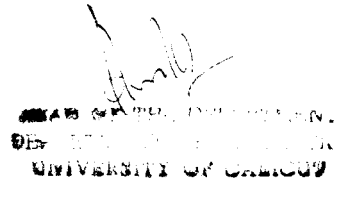

Department of Chemistry,
University of Calicut,
Calicut University P.O.,
673 635

April 2007

DEPARTMENT OF CHEMISTRY
UNIVERSITY OF CALICUT

Dr. M. P. Kannan
Professor and Former Head

Phone: Office: 0494-2401144
Extn: 413, 414
Res. : 0494-2400045
Fax : 0494-2400269
E-mail: mpkannan@gmail.com
Calicut University P. O.
673635 Kerala India

CERTIFICATE

This is to certify that the work embodied in this thesis entitled "A THEORETICAL STUDY OF THE CATION-π INTERACTION IN ALKALI METAL POLYENES AND POLYENE COMPLEXES" has been carried out by Fr. Jose T. M., under my guidance, and the same has not been submitted elsewhere for a degree or diploma.

Calicut University
20th April 2007

Dr. M. P. Kannan

Dr. M. P. KANNAN
Professor
Department of Chemistry
University of Calicut
Kerala - 673635

A THEORETICAL STUDY OF THE CATION – π INTERACTION IN ALKALI METAL POLYENES AND POLYENE COMPLEXES

THESIS

Submitted to the
University of Calicut
in partial fulfillment of the requirements
for the award of the degree of
Doctor of Philosophy
in Chemistry,
under the Faculty of Science

By

FR. JOSE T. M.

Forwarded

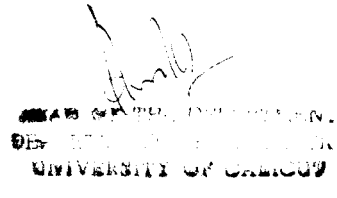

Department of Chemistry,
University of Calicut,
Calicut University P.O.,
673 635

April 2007

DECLARATION

This is to certify that the thesis entitled "**A THEORETICAL STUDY OF THE CATION-π INTERACTION IN ALKALI METAL POLYENES AND POLYENE COMPLEXES**" is an authentic record of the research work carried out by me, under the guidance of Dr. M. P. Kannan, Department of Chemistry, University of Calicut and the same has not been submitted elsewhere for any degree or diploma. In keeping with the general practice of reporting scientific observation, due acknowledgement has been made wherever the work described is based on the findings of other investigators.

It is also certified that I have fulfilled the course requirements and passed the qualifying examination for the Ph.D. degree of this university.

Calicut University
20th April 2007

Fr. JOSE T. M.
Candidate

A THEORETICAL STUDY OF THE CATION – π INTERACTION IN ALKALI METAL POLYENES AND POLYENE COMPLEXES

THESIS

Submitted to the
University of Calicut
in partial fulfillment of the requirements
for the award of the degree of
Doctor of Philosophy
in Chemistry,
under the Faculty of Science

By

FR. JOSE T. M.

Forwarded

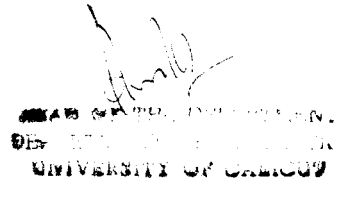

Department of Chemistry,
University of Calicut,
Calicut University P.O.,
673 635

April 2007

ACKNOWLEDGEMENT

With immense pleasure, I record my deep sense of gratitude to my research guide, ***Dr. M. P. Kannan****, Professor and Former Head of the Department, for suggesting the research topic and for leading me in my research work with his scholarly guidance and constant encouragement. It is his timely interventions and intuitive suggestions that helped me to complete this work on a satisfactory note.*

I express my sincere thanks to ***Dr. K. Krishnankutty****, Prof. & Head of the Department, Dr. K. K. Aravindakshan, former Head of the Department and all the teachers of Department of Chemistry, University of Calicut, for their support and encouragement during the research programme.*

I thankfully acknowledge the help and support of Mr. Aneesh M. H., my research colleague, Mr. Ramachandran Chelattu, Mr. V. P. Abdul Raheem, and all the research scholars of Department of Chemistry, University of Calicut. I also thank Mr. Satheesan K., the technical assistant, library staff and other members of the non-teaching staff.

I am grateful to the Principal and the Management of Christ College Irinjalakuda for deputing me for the research work under FIP of UGC. I am indebted to the UGC, New Delhi for granting me the Teacher Fellowship under FIP.

The constant support and encouragement from the colleagues of my department in Christ College, Irinjalakuda, inmates of Christ Monastery, Irinjalakuda, inmates of Deepthy Bhavan, Thenhipalam and the members of my Congregation and family are also gratefully acknowledged.

Finally, I thank the Almighty God for his divine providence, which was the leading light throughout this scientific endeavor.

Fr. Jose T. M.

A THEORETICAL STUDY OF THE CATION – π INTERACTION IN ALKALI METAL POLYENES AND POLYENE COMPLEXES

THESIS

Submitted to the
University of Calicut
in partial fulfillment of the requirements
for the award of the degree of
Doctor of Philosophy
in Chemistry,
under the Faculty of Science

By

FR. JOSE T. M.

Forwarded

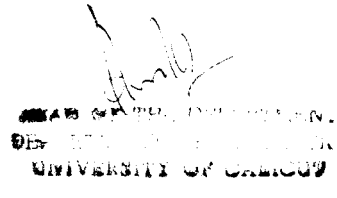

Department of Chemistry,
University of Calicut,
Calicut University P.O.,
673 635

April 2007

Dedicated to

My dear teachers who led me to the horizons of knowledge ...

A THEORETICAL STUDY OF THE CATION – π INTERACTION IN ALKALI METAL POLYENES AND POLYENE COMPLEXES

THESIS

Submitted to the
University of Calicut
in partial fulfillment of the requirements
for the award of the degree of
Doctor of Philosophy
in Chemistry,
under the Faculty of Science

By

FR. JOSE T. M.

Forwarded

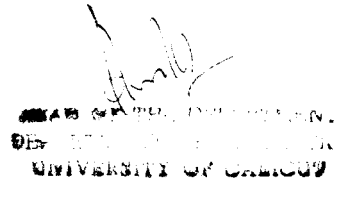

Department of Chemistry,
University of Calicut,
Calicut University P.O.,
673 635

April 2007

ABBREVIATIONS USED IN THE THESIS

AM1	Austin model 1
AO	Atomic orbital
Arg	Arginine
B.E	Binding energy
B3LYP	Becke3 Lee Yang & Parr
CC	Coupled cluster
CGTO	Contracted Gaussian type orbital
CI	Configuration interaction
DFT	Density functional theory
DZ	Double zeta
E_{bend}	Bending energy
E_{el}	Electrostatic energy
E_{HF}	Hartree-Fock energy
E_{st}	Stabilisation energy
E_{str}	Stretching energy
E_{tors}	Torsional energy
E_{vdw}	van der Waal's energy
E_{XC}	Exchange correlation energy
FF	Force field
GTO	Gaussian type orbital
HF	Hartree Fock
HOMO	Highest occupied molecular orbital
IR	Infrared
KS	Kohn - Sham
LCAO	Linear combination of atomic orbitals
LDA	Local density approximation
LSDA	Local spin density approximation

LUMO	Lowest unoccupied molecular orbital
Lys	Lysine
MBPT	Many body perturbation theory
MD	Molecular dynamics
MM	Molecular mechanics
MNDO	Modified neglect of diatomic overlap
MO	Molecular orbital
MP	Moller Plesset perturbation
NMR	Nuclear magnetic resonance
PA	Poly acetylene
PES	Potential energy surface
PGTO	Primitive Gaussian type orbital
Phe	Phenyl alanine
PM	Parameterization method
QM	Quantum mechanics
SCF	Self consistent field
SE	Semi empirical
SOMO	Singly occupied molecular orbital
STO	Slater type orbital
SV	Split valence
Trp	Tryptophan
Tyr	Tyrosine
TZ	Triple zeta
UMO	Unoccupied molecular orbital
V_{NN}	Potential energy due to inter nuclear interaction
V_{XC}	Exchange correlation potential

A THEORETICAL STUDY OF THE CATION – π INTERACTION IN ALKALI METAL POLYENES AND POLYENE COMPLEXES

THESIS

Submitted to the
University of Calicut
in partial fulfillment of the requirements
for the award of the degree of
Doctor of Philosophy
in Chemistry,
under the Faculty of Science

By

FR. JOSE T. M.

Forwarded

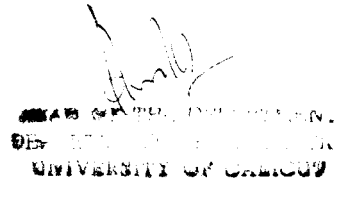

Department of Chemistry,
University of Calicut,
Calicut University P.O.,
673 635

April 2007

TABLE OF CONTENTS

A THEORETICAL STUDY OF THE CATION – π INTERACTION IN ALKALI METAL POLYENES AND POLYENE COMPLEXES

THESIS

Submitted to the
University of Calicut
in partial fulfillment of the requirements
for the award of the degree of
Doctor of Philosophy
in Chemistry,
under the Faculty of Science

By

FR. JOSE T. M.

Forwarded

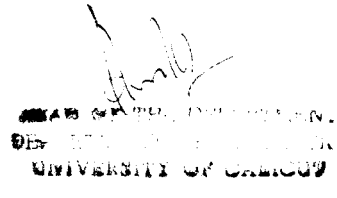

Department of Chemistry,
University of Calicut,
Calicut University P.O.,
673 635

April 2007

CHAPTER 1

A GENERAL SURVEY OF FORCES OF INTERACTION

1.1 Introduction

Chemistry is the branch of science dealing with construction, transformation and properties of molecules [1]. The molecules are obtained by the 'play' of atoms. Usually this 'play' of atoms is governed by the charged particles in them, positive nuclei and negative electrons, as well as their size. Molecules differ because they contain different nuclei and different number of electrons or the nuclear centres may be in different geometrical positions. Depending upon the elements involved in the bond making and breaking, chemistry was divided into organic and inorganic chemistry. Later on chemistry was categorized into different branches such as physical chemistry, theoretical chemistry, industrial chemistry, biochemistry, photochemistry, pharmaceutical chemistry, forensic chemistry etc., depending upon the emphasis of the discussion, though none of them are mutually adiabatic. Comparatively new entrants in this area, which gained prominence these days, are computational chemistry, bioinorganic chemistry, combinatorial chemistry, femtochemistry and nano chemistry. All these branches have contributed a lot to the integral growth of chemistry as a branch of science, always pursuiting for the greater welfare of humanity. A scenario has dawned on us where a world without chemistry is simply virtual and a chemical branch without the mission of human uplift is non-existing. As chemists, we should somehow partake creatively in the construction of a new world through the advances of chemistry, which will be the only solace for us in the ultimate run.

This thesis is primarily concerned with a theoretical study on the designing of molecules that can show some interesting kind of motion under the influence of the interactive forces operating in the molecular environment, which may modify their electronic and optical properties. Thus, this introductory chapter deals with a general survey of the forces of interaction.

1.2 Interactive forces in the realm of Chemistry

Since the molecules differ from one another, there is a chance for interaction between them and these interactions are generally called chemical interactions. Depending on the nature of players (particles) involved, these interactions are termed as ionic, covalent or coordinate; the ionic interactions entail in ionic compounds, the covalent interactions in covalent compounds and the coordinate interactions in complexes.

All these interactions that, in one way or other, influence the formation, stability and sustenance of the molecules, are the concern of chemistry. As we discussed earlier, there are interactions of construction, interactions of stabilization and interactions of transformation. Comprehensive information of these interactions will be immensely helpful for our subsequent discussion about the various chemical phenomena and hence a survey of such interactions is presented here.

1.2.1 Coulombic interaction

The strong interactive force existing between two ions is called Coulombic interaction. When the ions are of opposite charges, the interaction is attractive and it may entail in the formation of a chemical bond known as ionic bond. On the other hand, when the ions are of same charge, there occurs repulsion between them and hence they move apart so as to minimize the repulsive interaction. In either case, a charge on the interacting species is

necessary to evoke Coulombic interaction. This means only point charges involve in Coulombic interactions.

A point charge is an idealized model of a particle that has an electric charge. The charge is assumed to be confined to an infinitely small region of space from which a completely uniform electric field surrounds the point. The fundamental equation of electrostatics is Coulomb's law, which describes the force between two point charges. Coulomb's law is an inverse square law indicating the magnitude and direction of electrostatic force that one stationary, electrically charged object of small dimensions (ideally, a point source) exerts on another. Coulomb's law states that the magnitude of the electrostatic force (F) between two point charges (Q_i, Q_j) is directly proportional to the magnitudes of the charges and inversely proportional to the square of the distance (r_{ij}) between the charges in vacuum:

$$F = Q_i Q_j / r_{ij}^2$$

Ionic bonding, the result of Coulombic attraction, occurs only if the overall energy change for the reaction is favourable, i.e., when the bonded atoms have a lower energy than the free ones. Larger the energy change due to interaction between the atoms, stronger will be the bond. Such a bond is stronger than a hydrogen bond (see section 1.1.4.1), but similar in strength to a covalent bond (see section 1.1.2). Typical examples for ionic compounds are the chlorides of alkali metals like Na, K, Rb and Cs. Strength of an ionic bond is ca. 60 to 80 kcal/mol.

However, pure ionic bonding is not known to exist. All ionic bonds have some degree of covalent bonding.

1.2.2 Covalent Interaction

The interaction between two species arising out of the sharing of their electrons for the formation of a covalent bond is known as covalent interaction. Quantum mechanically, the sharing of electrons between two atoms resulting in a covalent bond, considerably decreases the energy of the system and hence it can be said that the covalent interaction stabilizes the system. Generally a covalent bond is formed between two atoms of comparable electronegativities. Methane is a classical example for such a covalent compound.

However, a pure covalent bond exists only in homogeneous diatomic molecules or in such mega molecules like diamond. When there is difference in the electronegativities of the bonding atoms, there occurs a polarisation in the bond, namely the shift of shared pair of electrons towards the atom of higher electronegativity. Covalent compounds of this type are thus polar compounds in which there exists slight Coulombic interaction between atoms. Water, ammonia, hydrogen chloride, etc., are examples for polar compounds.

The polarity of the atoms involved in the covalent bond formation gives rise to certain non-covalent interactions like hydrogen bonding, dipole-dipole interaction, etc. The larger the difference in electronegativity between two atoms, the larger will be the Coulombic interaction and the bond will be ionic. Since the different atoms forming bonds will have slight differences in their electro negativities, it is possible that they will possess some charge leading to some Coulombic interaction between them, though it may not end up with the formation of an ionic bond.

The strength of a covalent bond differs from bond to bond and system to system. For example, the C-C bond strength in methane is different from the C-C bond strength in ethylene, which in turn differs from the C-C bond

strength in benzene. Usually a covalent bond will have strength between 25 to 100 kcal/mol.

1.2.3 Coordinate Interaction

In coordinate interaction, an electron rich species, called donor or ligand (an anion or a Lewis base), interacts with an electron deficient species, called acceptor (a metal atom or a cation or any Lewis acid), by donating an electron pair, so as to establish a strong bond, called coordinate bond or dative bond. An arrow pointing from the donor of the electron pair to the acceptor of the electron pair represents a coordinate bond. Once the bond has been formed, its strength is not different from that of a covalent bond. The process of forming a dative bond is called coordination. The resultant compound is called an adduct (a compound formed by the addition reaction between two molecules).

Coordinate bonds can be found in many different substances. For example, in carbon monoxide, CO, there exists a coordinate bond and two normal covalent bonds between the carbon and the oxygen atom. Similarly, the ammonium ion, $(NH_4)^+$, has a coordinate bond, formed between a proton (H^+ ion) and the nitrogen atom.

Coordinate interaction can also be found in coordination complexes involving metal atoms or ions, especially if they are transition metal atoms or ions. In such complexes, the ligands interact strongly with the central metal atoms by donating their pair of electrons to the vacant d-orbitals or hybrid orbitals. Since this interaction involves the same nature of covalent interaction, the strength of such bonds will be almost equal to that of covalent bonds and the bond strength varies from 10 to 100 kcal/mol.

1.2.4 Non-covalent Interactions

Besides the above three interactions of construction, there exists certain other interactions, generally called non-covalent interactions, that stabilize the constructed molecules. There are inter molecular and intra molecular non-covalent interactions. Comparatively they are weak interactions, but are capable of stabilizing certain systems, which are otherwise very unstable. Many of the biological molecules are having this type of interactions. According to Dougherty [2], non-covalent intermolecular forces play a major role in determining the structures of biological macromolecules and in mediating processes such as receptor- ligand interactions, enzyme- substrate binding and antigen- antibody recognition. Wang and co-workers [3] claim that the non-covalent interactions appear ubiquitously in biology, with particular reference to the protein chemistry. In some other cases they are the guiding forces behind the structures of certain systems. Lisy et al. [4] state that the non-covalent inter molecular interactions play an important role in the molecular level design of functional materials, because they are responsible for the structure and properties exhibited by these materials. Some important non-covalent interactions are detailed below.

1.2.4.1 Hydrogen bonding

One of the important non-covalent interactions in chemistry is hydrogen bonding. It is a type of attractive force that exists between two atoms of opposite polarity. Although stronger than most other non-covalent interactions, the typical hydrogen bond is much weaker than both the ionic bond and the covalent bond. However, the presence of hydrogen bond very much affects the physical properties like boiling point and melting point and even the material state of the compounds. A classical example is water which, as per the group characteristics, must be a gas, but instead is a liquid, which is exclusively due to the inter molecular hydrogen bonding. Within

macromolecules such as proteins and nucleic acids, hydrogen bonding can exist between two parts of the same molecule, and figures as an important constraint on such molecules' overall shape. The strength of a hydrogen bond varies from 2 to 15 kcal/mol.

1.2.4.2 Ion- dipole interaction

Attractive electrostatic force existing between neutral and charged (ionic) molecules is termed ion-dipole interaction. It involves an interaction between a charged ion and a polar molecule (i.e., a molecule with a dipole). Cations are attracted to the negative end of a dipole and anions are attracted to the positive end of a dipole. The magnitude of the interaction energy (E) depends upon the charge of the ion (Q), the dipole moment of the molecule (μ) and the distance (r) from the centre of the ion to the midpoint of the dipole.

$$\text{i.e., } E \alpha Q\mu/r^2$$

Ion-dipole forces are important in solutions of ionic substances in polar solvents (e.g., a salt in aqueous solvent). The strength of ion- dipole interaction varies from 10 to 50 kcal/mol.

1.2.4.3 Dipole- dipole interaction

Dipole- dipole interaction is defined as the interaction between molecules or groups having a permanent electric dipole moment. It can be intra molecular or inter molecular. Usually this type of dipole-dipole force exists between polar molecules. The interaction energy depends on the strength and relative orientation of the dipoles as well as on the distance between the centres of the dipoles. The energy of interaction is directly proportional to the product of dipole moments and inversely proportional to

the sixth power of the distance between the molecules and to the temperature. It is given by the equation,

$$E = (-2/3kT)\ (\mu_1\mu_2/4\pi\varepsilon_0)\ (1/r^6),$$

where μ_1 and μ_2 are the dipole moments of the interacting dipoles, 'r' is the distance between the interacting molecules, T is the temperature, k is the Boltzmann constant and ε_0 is the permittivity due to free space.

In HCl gas, the molecules of HCl are polar and dipole- dipole interactions contribute about 15% towards the total intermolecular forces. In weakly polar molecules like CO and NO, the contribution is very small. The term dipole- dipole interaction also applies to the intra molecular interactions between bonds having permanent dipole moments. The energy of dipole-dipole interactions can approach the energy of a weak chemical bond. Usually its strength is between 1 to 12 kcal/mol.

1.2.4.4 Dipole- induced dipole interactions

The dipole moment induced in a non-polar molecule due to the presence of an electric field or a charged species or a polar molecule is known as induced dipole. The non-polar molecule should be polarisable in order to possess a dipole moment in such conditions. The induced dipole moment in the presence of an electric field is given by,

$$\mu_{ind.} = \alpha E$$

where, α = polarizability of the molecule and E = the electric field strength.

The energy due to dipole- induced dipole interaction, E, is given by,

$$E = (-\mu^2\ \alpha/\ 4\pi\varepsilon_0)\ r^{-6}$$

Where, μ = dipole moment of the first molecule, α is the polarizability of the second molecule and r is the distance between them. Such interactions are

evoked when a non-polar molecule dissolves in a polar or dipolar solvent. Example is the interaction between HCl and C_6H_6 when the latter is dissolved in the former.

1.2.4.5 Induced dipole- induced dipole interaction

This is a weak type of interaction existing between neighbouring non-polar molecules. It is also called London- Dispersion forces. Even if the molecule is totally non-polar, the movements of electrons of it may induce an instantaneous dipole moment in it. This induced dipole influences the electron distribution in a nearby non-polar molecule causing a slight polarity in it. Thus a weak dipole- dipole interaction is induced known as induced dipole-induced dipole interaction.

Larger the molecule, larger will be the momentary distortions in the electron cloud of the molecule. Hence, dispersion forces between molecules increase with their relative molecular masses. Another factor, which determines the strength of dispersion forces, is the polarizabilities of the molecules. If α_1 and α_2 are the polarizabilities of the first and second molecules, the energy, E, due to induced dipole- induced dipole interaction is given by,

$$E = (-3\ \alpha_1\ \alpha_2/2)\ (I_1\ I_2 / I_1+I_2)\ r^{-6}$$

where, I_1 and I_2 are the first ionization energies of the first and second molecules and 'r' is the distance between them. The types of interactions existing in noble gases or in a sample of oxygen are examples for induced dipole- induced dipole interaction. Higher boiling point of HI as compared to HCl could be explained by the induced dipole- induced dipole interactions between HI molecules.

1.2.4.6 Cation- π interaction

Another important non-covalent interaction is cation- π interaction. It is a strong non-covalent force by which cations strongly bind to the π- face of benzene and other aromatic structures [2]. Usually, cation-π interaction occurs between two species, one rich with a π-electron cloud and the other a Lewis acid (e.g., cation). Since aromatic systems are rich with π- electrons, when we speak of cation- π interaction, the emphasis will be on the binding of cations to aromatic systems. However, it should be remembered that it is not exclusively a "cation- aromatic" interaction. Ethylene, acetylene and other simple π-systems are fully anticipated to and are documented to be involved in cation- π interactions [5]. And not only simple cations, but all cations, from Li^+ to very complex organic structures like acetylcholine (Ach) are involved in this type of interactions. Very often it is stronger than a hydrogen bond and the strength varies from 2 to 20 kcal/mol.

The first indications about this interaction came from two directions: one, from analysis of protein crystal structures [6]; and the other, from studies involving artificial cyclophane receptors in aqueous media [7-9]. Cyclophane structures with aromatic residues bind quaternary ammonium compounds with high affinities and the major factor in this binding was the interaction between the positive charge of the ammonium compounds and the electron rich aromatic face of the cyclophane structure. Both theoretical and empirical evidences indicate that this kind of interaction is relatively strong. Many studies have looked at the interaction of benzene and cations in the gas phase, meaning that there are no solvent molecules to interfere. These studies have established the magnitude and generality of this interaction. For example, in gas phase, potassium ion (K^+) and benzene molecule are attracted to each other, with a stabilisation energy of 18.3 kcal/mol [10]. Here, the binding is

evidently due to the interaction between the cation and the cloud of the π-electrons and is found to be quite significant. In fact, in the gas phase, K^+ is more strongly attracted to benzene than to the highly polarised water molecule, K^+.....water interaction energy being 17.9 kcal/mol [10]. This clearly demonstrates the existence as well as the importance of cation- π interaction in molecular systems. Average hydrogen bonds, the all-important intermolecular interactions, are very often weaker than this. The studies using synthetic receptors, mostly cyclophane structures in aqueous media, have proved clearly that a hydrophobic binding site comprised of aromatic rings can compete with full aqueous solvation in the binding of highly solvated cations [5].

Qualitative model for cation-π interaction

On the basis of their studies with gas phase complexes, Ma and Dougherty [5] state that electrostatic interactions play a prominent role in prototypical cation-π interactions. They developed a qualitative model for cation- π interaction by emphasizing very simple electrostatic effects. Experimental measurements have shown that the alkali metal cations Li^+, Na^+ and K^+ interact with benzene, a prototype of aromatic systems, with binding energies of 38.3, 28.0 and 19.2 kcal/mol respectively [11]. Computational studies have given the stabilisation energy of Rb-benzene complex to be 15.8 kcal/mol [12]. The stabilisation energy trend, i.e., $Li^+ > Na^+ > K^+ > Rb^+$, shows a classical electrostatic sequence-a sequence which we will observe when benzene is replaced by Cl^- ion. If polarizability, dispersion forces and charge transfer effects were the dominant factors in determining the strength of cation-π interaction, Rb^+ would have been the strongest binder [5]. Since we get a reverse order in the ab initio calculations as well as in the experiments, the polarizability of the cation seems to be less important. The electrostatic reasoning can also explain the variations due to changes in the

aromatic ring. Furan and thiophene exhibit poor cation- binding ability, both in gas phase and in cyclophane hosts [13] even though they are two electron rich heterocyclic compounds. This is explained in terms of less negative electrostatic potential over the centre of their aromatic, presumably due to the presence of electro negative oxygen and sulphur in the rings. This observation also supports electrostatic model of cation-π interaction. It is reported that across a series of 11 aromatics, 100% of the variation in cation-π binding energy for Na^+ was due to variation in the electrostatic component of the binding [14]. Above all these, this model rationalizes most of the trends observed both in experiments as well as in computational results.

However, it is not true that 100% of the cation-π binding energy is electrostatic. At times, the "non electrostatic" component of cation-π interaction, which is a combination of effects mostly related to the polarizability of the aromatic, becomes a major factor. Hence, cation-π interaction cannot be qualitatively modelled unless additional terms, such as induced dipoles, polarizabilities, dispersion forces and charge transfer are not included. The relevance of polarization effects in this interaction has been emphasized by Kollman and Caldwell [15] using classical force-field calculations. Cubero et al. [16] explain how polarization contribution to the strength of cation-π interaction becomes significant in cases where the different aromatic cores are used with the same cation. But, the fact is that the polarizability of the aromatic is not the defining feature of the cation-π interaction. Across a series of aromatics, it makes a constant contribution to the total stabilisation energy [14]. Thus, to the first order, cation-π interaction can be considered as an interaction primarily governed by the electrostatics of the cation (guest) and the π-face of aromatic residue (host) [2].

It has been established by Reisse [17] that a point charge experienced a comparable stabilization while interacting at long range with a point dipole,

significantly larger than that of water or with a point quadrupole comparable to that of benzene. (A quadrupole can be thought of as two dipoles aligned in such a way that there is no net dipole. Topologically, quadrupoles are equivalent to d-orbitals). Since benzene possesses a permanent quadrupole moment, the question may arise whether cation-π interaction is something new or it is merely an "ion-quadrupole" interaction. An ion- quadrupole interaction is expected to show $1/r^3$ distance dependence for the stabilization energy [18], whereas the distance dependence of a prototype cation-π interaction is $1/r^n$ with $n < 2$ [2], where 'r' is the distance between the centre of the cation and that of the quadrupole. A real cation-π interaction involves a cation that is typically at van der Waals contact with the aromatic. In Na^+...benzene complex, the distance is ca. $2.4A^0$ and such a range is observed in all other cases. Hence, the cation-π interaction cannot be quantitatively modelled as just an ion- quadrupole interaction. The usefulness of the quadrupole moment is that it provides an easy way to visualize the charge distribution of aromatics and leads naturally to the expectation of significant electrostatic interactions [5]. Also it is helpful in giving explanation for the variation in ion-π interaction strength in some of the π-complexes.

The other major factor proposed to model cation-π interaction is the induced dipole that arises in the aromatic, in response to the nearby charge. If this were the dominating factor, polarizability should be of major importance. However, the fact that a less polarizable benzene is a stronger binder than a more polarizable cyclohexane makes us rule out the induced dipole factor. It should be noted that the quadrupole moment of cyclohexane is much smaller than that of benzene, which again is a supporting evidence for holding quadrupole moment partially controlling the strength of cation-π interaction [2].

1.3 Relevance of the study of cation - π interaction

A major focus of modern organic chemistry has been to develop an understanding of the weak, non-covalent binding forces. This is because of their ubiquitous nature throughout the chemical and biological sciences. Some of them are very crucial to a large number of biological processes. One important non-covalent binding force of this type is cation- π interaction. Studies of organic model systems, coupled with a wide range of results from structural biology, have established the relevance of cation-π interactions to biological recognition through interactions with aromatic side chains from the amino acids, phenyl alanine (Phe), tyrosine (Tyr) and tryptophan (Trp) [2]. Also, this interaction is found to be common among structures in the Protein Data Bank, and it is clearly demonstrated that, when a cationic side chain, lysine (Lys) or arginine (Arg) is near to an aromatic side chain Phe, Tyr, or Trp, the geometry is biased towards one that would experience a favourable cation-π interaction [19]. The dependence of enzyme activity on the presence or absence of the alkali metal cations like Na^+ and K^+ is ascribed to their interaction with the active sites of the proteins [20]. There is now sufficient evidence that the ammonium cation-π interaction can be considered as an important non-covalent interaction in protein stabilization [19, 21] and molecular recognition [5, 22]. Since a great deal of direct and circumstantial evidences indicate that cation- π interactions are important in a variety of proteins and other biomolecules that bind cationic ligands or substrates [2], a detailed study of this interaction will be a stepping stone to the chemistry of biomolecules.

Another area of chemistry inviting considerable attention today is the field of conducting polymers. In fact, the discovery of Poly acetylene (PA) film has dawned an era of conducting polymers [23]. The study of conducting polymers is particularly exciting because it opens the way to progress in

understanding the fundamental chemistry and physics of macromolecules [24]. Also, it offers the promise of achieving a new generation of polymers exhibiting the electrical and optical properties of metals or semi conductors, while retaining their mechanical properties. Here too, we may find the relevance of the study of cation-π interaction.

PA (Figure 1.1) was the first organic polymer to be converted to a conducting substance by alkali metal doping.

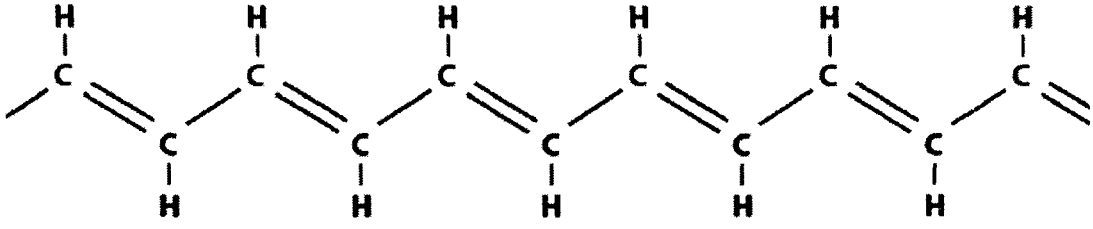

Figure 1.1: Poly Acetylene

It has been suggested [25] that in alkali metal doped conducting polymers, the doped metal loses its outer-most electron to the polyenic part, creating a charge- charge interaction in the complex. Actually, the new electron enters into the antibonding π-band of the polyene, reducing the gap between the π-band and the π* band of the system, and effectively increases the conductivity of the polyene. Basing on this, MacDiarmid states that the Coulombic interaction between the charge on the chain and dopant ion is a very strong interaction that can totally alter the energetics of the system [25]. It should be recollected that the organic conductors, which depend badly on the presence of π- electrons for their electron transport properties [26] are systems with conjugated double bonds extending from one end to the other. There is every possibility for an interaction between the cationic species

resulting from the injected metal to the polyene and the enhanced π-cloud of the system. Such an interaction will exhibit the characteristics of the so-called "cation- π interaction". The theoretical study done by Mpourmpakis et al. [27] on the behaviour of alkali metal cations in carbon nanotubes lends a supporting hand to the above assumption. According to them the cation-carbon nanotube interaction has a cation-π character and follows the same stabilisation energy (E_{st}) trend as in the case of benzene in gas phase [12]. Basing on their experiments with two armed lariat ethers having double bonds and Na and K cations, Hu et al. [28] states that when double bonds are positioned appropriately, cation -π interactions are possible between the neutral double bonds and the macro-ring bound cations. Recall that Dougherty et al. [5], who have done extensive research on cation– π interaction in different type of systems, have observed that ethylene, acetylene and other simple π-systems are fully involved in cation- π interactions. If so, cation - π interaction is very much a force to be reckoned with, in the domain of metal-doped conjugated polymers, an extension of such π- systems. The study of such an interaction, which is the major objective of this research, may help us to understand better the underlying mechanism of transition from non metal to metal as the result of alkali metal doping in PA type molecules.

Further, polyenes with extended conjugation are not totally foreign to biological systems. In fact, the carotenoids with a polyenyl part of extended conjugation (Figure 1.2) resemble very much to substituted PA. Another example is Vitamin A (Figure 1.3), derivative of beta-carotene. Therefore, the study of interactions in metal polyenes may be a good start for an exploration in the field of biomolecules with aliphatic fragments of extended conjugation.

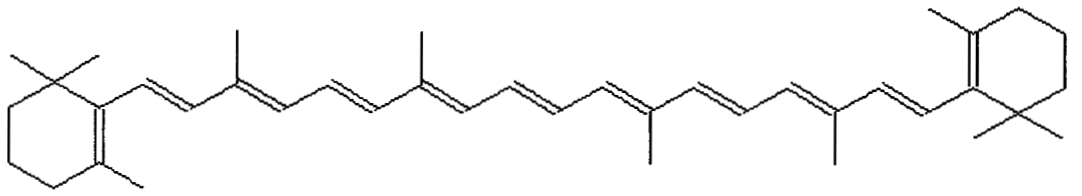

Figure 1.2: Beta-carotene

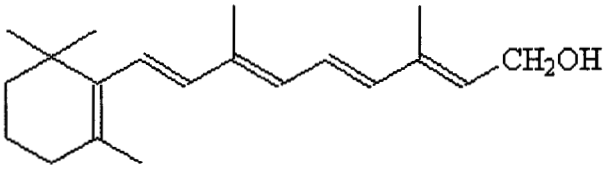

Figure 1.3: Vitamin A

1.4 Objectives of the work

The physical model appropriate for describing the highly conducting, heavily doped phase of PA is still being debated in the field of conjugated polymers, despite a considerable activity since its discovery. A number of physical models were proposed, the soliton model [29-31], Peierls insulator model [32, 33], polaronic metal model [34] etc., but all of them were insufficient to explain the characteristics of metal-doped PA. There is no consensus about the proper picture to apply to the metallic nature of metal-doped PA [35]. Perhaps, the failure to propose a clear model to the above stemmed from the under-exploration of the interactive forces existing between the alkali metal dopants and the conjugated polyenic substrates in such systems. Besides, cation-π interaction involving aliphatic π-systems is less-well addressed, though such interaction can play a significant role in biological systems with aliphatic fragments of extended conjugation, as mentioned above.

Computational Nanotechnology: A major objective of computational nanotechnology is the designing, modeling and fabrication of novel molecular structures. In this investigation, we are interested in designing molecular systems that model the interactions of the metal species with long aliphatic π-systems as in PA and biomolecules. Hence we have embarked on a systematic study of the interactions in metal-polyene complexes by computational technique. The interaction between a long chain polyene and a metal atom can lead to a large number of isomers of the metal-polyene complex. Computational experiments allow us to examine all of them quickly and easily and reject the energetically unstable ones. Such a study can easily unveil the most favourable position(s) of the metal in the polyene matrix and the consequent characteristics of the metal polyene complex.

Instead of taking mega molecules like PA or the biomolecules, it is better to start with small molecules, which somehow mimic the actual molecular environment. This saves time, and very often serves the purpose. Hence, we have chosen all-trans conjugated polyenes, ranging from C_5 to C_{13} as our representative samples. As dopants, we have employed alkali metal atoms Li, Na, K and Rb and their ions, as they are the best species to represent quaternary nitrogen of biosystems [5].

A detailed study of such systems, in their free and doped state, may throw some insight into their structure and the probable interactive forces in them, which may ultimately lead to a better understanding of systems such as conducting polymers, biomolecules, etc.

1.5 Scope of the work

The vast possibilities with the metal-doped polyenes are yet to be explored. The study may be extended to several other fields. For example, an important question often addressed in the study of carbon gasification and

adsorption of gases in carbonaceous materials is the catalytic role of alkali metals [36-41]. The layers of carbonaceous substances can be considered as an extended array of ethylene molecules (or small fragments of PA). The distribution of different metals into such layers will have some impact on them. The computational studies on metal-doped PA may offer some clues to the above question.

Further, interactions between organic cations and protein aromatic residues are widespread and of considerable biological importance. Several neurotransmitters have a positively charged nitrogen portion in their chemical structure that is made use of for its interaction with the protein residue. For example, serotonin, a neurotransmitter involved in processes such as migraine, depression, and anxiety contains a methyl ammonium portion. Many of the bioorganic cations are monovalent species with quaternary nitrogen, which is very much similar to the monovalent alkali metal ions. Hence, the interactions involving alkali metal cations are somewhat analogous to those involving such organic cations. The study of the interactions of alkali metal ions with π- electron cloud will, therefore, help us to make some searches into the interactions existing in biomolecules. It could entail in designing such molecules in such a way that they contribute to the more efficient functioning of the organism.

Non-covalent interactions are ubiquitous throughout chemical and biological sciences. Many of the biological systems, especially the 3-D structured proteins, are stabilized by the non-covalent interactions like hydrogen bonds, salt bridges, cation-π interactions, hydrophobic effects, etc. [19]. Nowadays these molecules are studied computationally rather than experimentally. Though our study may confine to the cation-π interactions in conjugated polynes, its extension to protein chemistry may offer immense possibilities to those involved in experimental work.

1.5 References:

1. F. Jensen, " Introduction to Computational Chemistry", John Wiley & Sons Ltd., (1999) W. Sussex, 1-2.
2. D. A. Dougherty, Science, 271 (1996) 163-168
3. W. Wang, O. Donini, C. M Reyes, P. A. Kollman, Annu. Rev. Biophys. Biomol. Struct., 30 (2001) 211-243.
4. D. Kim, S. Hu, P. Tharakeswar, K. S Kim, J. M. Lisy, J. Phys. Chem. A, 107 (2003) 1228-1238.
5. J. C. Ma & D. A. Dougherty, Chem.Rev., 97 (1997) 1303-1324.
6. S. K. Burly & G. A. Petsko, FEBS Lett., 203 (1986) 139-143.
7. T. J. Shepodd, M. A. Petti, D. A. Dougherty, J. Am. Che. Soc., 108 (1986) 6085- 6087.
8. T. J. Shepodd, M. A. Petti, D. A. Dougherty, J. Am. Chem. Soc., 110 (1988) 1983-1985.
9. M. A. Petti, T. J. Shepodd, J. R. E. Barrans, D. A. Dougherty, J. Am. Che. Soc, 110 (1988) 6825-6840.
10. J. Sunner, K. Nishizawa, P. Kebarle, J. Phys. Chem., 85 (1981) 1814-1820.
11. C. A. Deakyne & M. J. Meot-Ner, J. Am. Chem. Soc., 107 (1985) 474-479.
12. R. A. Kumpf & D.A. Dougherty, Science, 261 (1993) 1708-1710.
13. P. C. Kearney, L. S. Mizoue, R. A. Kumpf, J. E. Forman, A. McCurdy, D. A. Dougherty, J. Am. Chem. Soc., 115 (1993) 9907-9919.
14. S. Mecozzi, A. P. West Jr., D. A. Dougherty, J. Am. Chem. Soc., 118 (1996) 2307-2308.

15. J. W. Caldwell & P. A. Kollman, J. Am. Chem. Soc., 117 (1995) 4177-4178.

16. E. Cubero, F. J. Luque, M. Orozco, Proc. Natl. Acad. Sci. USA, 95 (1998) 5976-5980.

17. M. Luhmer, K. Bartik, A. Dejaegere, P. Bovy, J. Reisse, Bull. Soc. Chim. Fr., 131 (1994) 603-606.

18. S. K. Burly & G. A. Petsko, Adv. Protein Chem., 39 (1988) 125-189.

19. J. P. Gallivan & D. A. Dougherty, Proc. Natl. Acad. Sci. USA, 96 (1999) 9459-9464.

20. C. H. Suelter, Science, 168 (1970) 789-795.

21. D. A. Dougherty & D. A. Stauffer, Science, 250 (1990) 1558- 1560.

22. N. S. Scrutton & A. R. C. Raine, Biochem. J., 319 (1996) 1- 8.

23. H. Shirakawa, Synthetic Metals, 125 (2002) 3-10.

24. A. J. Heeger, Synthetic Metals, 125 (2002) 23- 42.

25. A. G. MacDiarmid, Synthetic Metals, 125 (2002) 11-22.

26. R. C. Haddon, Pure & Appl. Chem., 65 (1993) 11-15.

27. G. Mpourmpakis, E. Tylianakis, D. Papanikolaou, G. Froudakis, Rev. Adv. Mater. Sci., 11 (2006) 92-97.

28. J. Hu, L. J. Barbour, G. W. Gokel, Collection of Czechoslovak Chemical Communications, 69 (2004) 1050- 1062.

29. M. J. Rice, Phys. Lett. A., 71 (1979) 152-154.

30. W. P. Su, J. R. Schrieffer, A. J. Heeger, Phys. Rev. Lett., 42 (1979) 1698-1701.

31. S. Larsson & L. R. Monge, Int. J. Quant. Chem., 63 (1997) 655-665.

32. M. J. Rice, W. Schnieder, S. Strassler, Phys. Rev. B., 8 (1973) 474-482

33. X. Q. Yang, D. B. Tanner, M. J. Rice, H. W. Gibson, A. Feldblum, A. J. Epstein, Solid State Commin., 61 (1987) 335-340.

34. S. Kivelson & A. J. Heeger, Phys. Rev. Lett., 55 (1985) 308-311.

35. D. B. Tanner, G. L. Doll, A. M. Rao, P. C. Eklund, G. A. Arbuckle, A. G. MacDiarmid, Synthetic Metals, 141 (2004) 75-79.

36. Z. H. Zhu & G. Q. Lu, Langmuir, 20 (2004) 10751-10755.

37. P. L. Walker Jr., F. Rusinco Jr., L. G. Austin, "Advances in Catalysis", Volume II, Academic Press, (1959) New York, 133-220.

38. W. Y. Wen, Catal. Rev.- Sci. Eng., 22 (1980) 1-28.

39. C. Wong & R. T. Yang, Ind. Eng. Chem. Fundam., 23 (1984) 298-303.

40. S.G. Chen & R. T. Yang, J. Catal. 138 (1992) 12-23.

41. M. J. Illan-Gomez, A. Linnares-Solano, L. R. Radovic, C. Salinas-Martinez de Lecea, Energy Fuels, 10 (1996) 158-168.

A THEORETICAL STUDY OF THE CATION – π INTERACTION IN ALKALI METAL POLYENES AND POLYENE COMPLEXES

THESIS

Submitted to the
University of Calicut
in partial fulfillment of the requirements
for the award of the degree of
Doctor of Philosophy
in Chemistry,
under the Faculty of Science

By

FR. JOSE T. M.

Forwarded

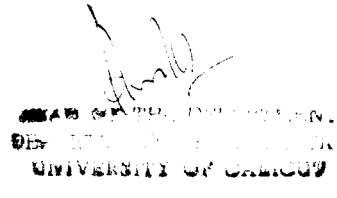

Department of Chemistry,
University of Calicut,
Calicut University P.O.,
673 635

April 2007

CHAPTER 2

COMPUTATIONAL DETAILS AND PROCEDURE

2.1 Introduction

The present age is an era of computer technology, which has transformed all branches of knowledge positively and revolutionarily. The communication of knowledge has been made easier and the whole world has transformed into a global village of interacting masses by the use of computer technology. All the branches of science have immensely benefited from its application. It has made the scientific tasks easier, the verification of scientific principles simpler and extension of the results of science to humanity much faster. The advent of computer technology has helped the chemists to make deep inroads in many a field of chemistry. In fact a new branch has developed in chemistry, known as computational chemistry, which now acts as the precursor of experimental chemistry.

2.2 An Overview of Computational Chemistry

Computational chemistry is a branch of theoretical chemistry whose major goals are to create efficient mathematical approximation and computer programmes that calculate the properties of molecules such as total energy, dipole and quadrupole moments, vibrational frequencies, reactivity and other diverse spectroscopic quantities and cross sections for collisions of molecules with diverse atomic or subatomic projectiles. It generates data that complement experimental details on the structures, properties and reactions of substances. The term is also sometimes used to cover the areas of overlap between computer science and chemistry [1]. It is simply the application of chemical, mathematical and computing skills to the solution of interesting

chemical problems. Therefore, it has become extremely important in the last few decades, as it is widely being used in academic and industrial research. It can be a useful way to investigate materials that are too difficult to find or too expensive to purchase. Computers are used to generate information such as the properties of molecules, simulated experimental results, feasibility of certain reactions, etc. Today, theory and experimentation combine together in the search for understanding the inner structure of matter.

One particularly important way in computational chemistry is to model a system prior to synthesizing it in the laboratory [2]. Many professional computational chemists are using computational modeling to gain additional understanding of the compounds being examined in the laboratory. They apply existing computer programs and methodologies to specific chemical questions and try to find out acceptable answers to them. Computational chemistry also helps chemists to make predictions before running the actual experiments so that they can be better prepared for making observations. In some cases, the interactive forces active in a particular molecule are studied by obtaining the molecular parameters of that species with the application of the computer programmes. In other cases, computational studies are carried out in order to find a starting point for a laboratory synthesis. Computational studies are also used to explore reaction mechanisms and explain observations of laboratory reactions. Very often, those molecular properties, which are difficult to get experimentally, are determined or predicted by the computational studies. Thus, Computational chemistry is particularly useful for the determination of properties that are inaccessible experimentally and for the interpretation of experimental data. As a technique, computational chemistry has the advantage of producing answers cheaply and quickly (compared to, for example, thermodynamic measurements), especially for hypothetical structures like transition states.

Computational chemistry is today widely used within all branches of chemistry, physics, biology and pharmaceutical science. It produces quantitative information on molecules and their interactions; very often it affords deeper understanding of molecular processes that cannot be obtained from experiments alone. It can be used, for example, to predict how a molecule interacts with other molecules and charges in its environment. Such information may be used elsewhere, for example, to study how proteins (which are built up of amino acids) interact with different substrates, with special reference to the field of pharmaceuticals. Apart from the molecular level studies, computational chemistry can be applied to the macro world also. Such an example may be taken from the astronomical world, in which, apart from stars and planets, there are large quantities of interstellar matter, often collected in vast clouds. What does this matter consist of? It can be studied from the earth through the radiations that the molecules emit. The radiation occurs because of the molecular rotation. Hence, it is possible to determine the composition and appearance of the molecules using the frequency spectrum of the radiation. This, however, is an immensely difficult task, particularly because these molecules cannot always be produced in the laboratory so as to obtain material for comparative studies. Quantum chemistry, however, does not suffer from such limitations. Calculations based on assumed structures can give information on radio emission frequencies that can be directly compared with data collected by the radio telescope. In this way, theory and measurement together can give information on the molecular composition of interstellar matter.

Some of the functions which can be actualized using readily available computer programmes are electronic structure determinations, geometry optimizations, frequency calculations, locating transition structures, protein calculations, drawing potential energy surfaces (PES), rate constant

calculations (kinetics) and thermodynamic calculations (like, heat of reaction, energy of activation, etc.) for chemical reactions [3].

However, there is a point of concern in this whole exercise of computational chemistry: it is easy to make errors that remain undetected; it is often difficult to judge the significance of a result. Just by operating the computer programmes, which are readily available, one can produce volumes of huge output files containing a lot of information. Unless he has mastered in analysing the results and manipulating them properly, they may turn out to be useless junk; or sometimes they may be totally irrelevant on closer inspection. Therefore, literature research and comparison to known systems and data wherever possible are desirable to benefit from computational techniques.

2.3 Computational Methods

Researchers have long sought methods for understanding how bonds between the atoms in molecules function. With such methods, it would be possible to calculate the properties of molecules and the interplay between them. The growth of quantum mechanics in physics at the beginning of 19^{th} century opened new possibilities, but its applications within chemistry were too long and too complicated to be accomplished easily via human calculations. It was not practically possible to handle the complicated mathematical relations of quantum mechanics for such complex systems as molecules. Hence, the scientists were badly in need of certain techniques that would ease out the hardship of calculations.

With the advent of computers, a new era has dawned upon us where the calculations of quantum mechanics are no longer a laborious exercise. With the application of computers to solve the equations and problems of quantum mechanics, enormous theoretical and computational development has taken place- actually a revolution in the field of chemistry and its natural

allies. Walter Kohn and John Pople are the two prominent figures of this field and they were deservingly honoured with the Nobel Prize of 1998. W. Kohn's theoretical work has formed the basis for simplifying the mathematics in the descriptions of bonding of atoms, a prerequisite for many of today's calculations. J. Pople developed the entire quantum-chemical methodology now used in various branches of chemistry [4].

Computer-based calculations are now used generally to supplement experimental techniques. For several decades they have been developed and refined so that it is now possible to analyse the structure and properties of matter in detail. Conventional calculation of the properties of molecules is based on a description of the motion of individual electrons. For this reason, such methods are mathematically very complicated. W. Kohn showed that it is not necessary to consider the motion of each individual electron: it suffices to know the average number of electrons located at any one point in space. This has led to a computationally simpler method, the density functional theory (DFT). The simplicity of the method makes it possible to study very large molecules. Today, for example, calculations can be used to explain how enzymatic reactions occur. It has taken more than thirty years for a large number of researchers to render these calculations practicable, and the method is now one of the most widely used in quantum chemistry.

Depending on their nature of approach to the problem, computational methods are of two types- molecular mechanical methods and quantum mechanical methods. The former is based on classical (Newtonian) mechanics whereas the latter is based on quantum mechanics (QM).

2.3.1 Molecular Mechanical methods

Molecular mechanics (MM) is a method in which observable data are used to parameterize constants based on Hook's Law, allowing systems to be

represented by classical physics and simple potential energy functions. The equations used to calculate the components of potential energy, together with the data required to describe the behaviour of different kinds of atoms and bonds are called a force field and hence this method is also called Force Field (FF) method. It represents molecules as spheres connected by springs and uses the classical physics to explain and interpret the behaviour of atoms and molecules. In this type of methods, the calculations are limited to the consideration of nuclear movements and the electrons are not considered explicitly. Since it is based on Newtonian mechanics it is widely applied in molecular structure refinement, molecular dynamic simulations, Monte Carlo simulations and ligand docking simulations.

FF methods are based on the following principles:

a) Nuclei and electrons are considered as single atom-like particles

b) Atoms are spherical and are assigned a net charge.

c) Interactions are based on springs and classical potentials

d) Interactions determine the spatial distribution of atom-like particles and their energies

In the broadest sense, molecular mechanics is concerned with molecular motion. During the calculation it gives the molecular geometry, heat of formation, energy, dipole moment, ionization potential and charge density. Also it is the cornerstone of computer simulations. Computer modeling with molecular simulations has been developed and widely applied in studying molecules of biological interest. Two interesting areas of this branch are (a) studying enzyme catalytic mechanisms using a combination of QM and MM. (b) studying macro molecular dynamics using molecular dynamics (MD) and Free energy calculation methods [5].

Another objective of MM is to predict the energy associated with a given conformation of a molecule. However the energy values have no meaning as absolute quantities. Only differences in energy between two or more conformations have meaning. A simple MM energy equation is given by:

Energy = Stretching energy + Bending energy + Torsional energy + Non bonded interaction energy + Coupling energy

i.e., $E_{FF} = E_{str} + E_{bend} + E_{tors} + E_{vdw} + E_{el} + E_{cross}$

Stretching energy, E_{str}, is the energy for stretching a bond between two atoms, A and B. E_{bend} represents the energy required for bending an angle formed by three atoms A-B-C, where there is a bond between A and B and between B and C. Torsional energy, E_{tors}, is the energy for rotation around a B-C bond in a four atom sequence A-B-C-D, where A-B, B-C and C-D are bonded. Looking down the B-C bond the torsional angle is defined as the angle formed by the A-B and C-D bonds. Van der Waal's energy, E_{vdw}, and electrostatic energy, E_{el}, together describe the non-bonded interaction energy. E_{vdw} is the energy describing the repulsion or attraction between atoms that are not directly bonded. The electrostatic term E_{el} is commonly taken as the sum of electrostatic interactions involving all pairs of atoms except 1, 2 and 1,3. Most force fields include E_{vdw}/ E_{el} for atom pairs, which are separated by three bonds or more. Finally, E_{cross} describes coupling between the first three terms. Given such an energy function of the nuclear coordinates, geometries and relative energies can be calculated [6].

Due to its simplicity and computational efficiency, MM is widely used for classical approximations. The main advantage of this method is that the calculations can be completed at tremendous speed and hence large systems can be studied in a short period of computational time. Also it is very efficient

in predicting the properties for classes of molecules where a lot of information already exists. The most reliable results are energy differences between conformers.

Although empirical force fields provide a good representation of potential energy surfaces in the regions of minima, one cannot use them to calculate the complete potential energy surface for a chemical reaction, since these fields are incapable of describing bond breaking. It is difficult to know which results we can trust. Besides, these methods are zero dimensional such that the probable error of a given result within the method cannot be assessed.

2.3.1.1 Important Force Field Methods

Some of the important Force Field methods are AMBER, CHARMM, MMFI, MM1, MM2, MM3, MM4, CFF, UFF and YETI. Some important methods are briefly mentioned below:

(a) AMBER

Assisted model building with energy refinement (AMBER) is the name of both a force field and molecular mechanics program. It was parameterized specifically for proteins and nucleic acids. AMBER uses only five bonding and nonbonding terms along with sophisticated electrostatic treatment. No cross terms are included. Results are very good for proteins and nucleic acids, but can be somewhat erratic for other systems.

(b) MM1, MM2, MM3, MM4

MM1, MM2, MM3 and MM4 are general-purpose organic force fields. There have been many variants of the original methods, particularly MM2. The MM2 and MM3 force fields perform best for a wide range of organic molecules.

2.3.2 *Quantum Mechanical Methods*

Quantum mechanical methods are based on Quantum mechanics. Quantum mechanics is primarily concerned with particles, which explicitly exhibit the dual nature-namely the wave nature as well as the particle nature. Evidently, they do not obey the classical mechanics. The examples for such particles are electrons and other fundamental particles of matter.

When quantum mechanics was introduced, its postulates suggest that the states of such systems are defined by certain mathematical functions called wave functions (ψ) and they should obey the Schrödinger equation having the general formula, $\boldsymbol{H}\psi = E\psi$, where E is the energy of the system and $\boldsymbol{H}$ is the total energy operator (Hamiltonian operator). Schrödinger equation addresses the following question: Where are the electrons and nuclei of a molecule in space? [4] This is a search into the electronic configuration of the system, its conformation, the size and shape of the electron cloud and hence that of the total system. Secondly, the Schrödinger equation tries to determine the energies of these systems under a given set of conditions. Here, along with the energy calculation, the heat of formation, conformational stability, chemical reactivity, spectral properties, etc. also may be taken into consideration.

Schrödinger equation is the basis for most of the computational chemistry programmes that scientists use. This is because the Schrödinger equation models the atoms and molecules with mathematics. Since Schrödinger equation is the basis of the programmes, their accuracy is very much dependent on the accuracy of the construction of the equation. This requires that we should mimic the actual system as near as possible. However, we should remember that only the Schrödinger equation for hydrogen atom is completely solvable and from here onwards the solution for other systems are often done with some or other approximations. Coming to molecular systems,

the Hamiltonian contains a number of terms accounting for various types of interactions, which makes the Schrödinger equation practically unsolvable that necessitates various types of approximations. The approximation methods can be categorized as either ab initio or semi empirical depending upon their approach to the problems concerned. Throughout the semi empirical and ab initio calculations, only gas phase systems are considered because this avoids the substantial contributions of inter molecular interactions in liquids and solids [7].

2.3.2.1 Semi Empirical Methods

Semi Empirical (SE) methods were developed to treat large molecules because of the difficulties met with in applying the ab initio methods to such molecules. They use parameters that compensate for neglecting some of the time consuming mathematical terms in the Schrödinger equation, whereas ab initio methods include almost all such terms. The parameters used by semi empirical methods can be derived from experimental measurements or by performing ab initio calculations on model systems.

Most of the SE methods use only the s and p functions and the basis functions taken are the Slater type orbitals (STOs). The central assumption of SE methods is the zero differential overlap approximation, which neglects all products of basis functions depending on the same electron coordinates when located on different atoms [8]. This means that the product of the functions on different atoms is set equal to zero. Here, in effect, the overlap matrix is reduced to unit matrix, one-electron integrals involving three centres are set to zero and all three and four centre 2-electron integrals are neglected. These approximations considerably decrease the complexities in the computation process. However, to compensate for these approximations, the remaining integrals are made into parameters and their values are assigned on the basis of calculations or experimental data.

Since the SE calculations are much faster than the ab initio methods, they are extensively applied in organic chemistry, where there are only a few elements involved in bond making and the molecules in that section are of moderate size. Usually, SE methods are used in organic, inorganic, organo-metallic and oligomeric systems where hundreds of atoms are present. These can also be used to study ground, transition and excited states of molecules. Some SE methods have been devised specifically for the description of molecules of inorganic chemistry [9].

The advantage of SE calculation is that they are much faster than ab initio calculations even if they are applied to systems where large number of molecules is interacting. The disadvantage of using this method is that the results can be erratic and fewer properties can be predicted reliably [10]. Nevertheless, it is a fact that this method can give reliable information regarding the structure and bonding, which has to be modified using ab initio methods. For beginners in this field SE methods are good starters to study molecules, as this will involve less computational time.

2.3.2.1.1 Important SE methods

Important SE methods are HUCKEL, PPP, CNDO, MNDO, INDO, AM1, SAM1 and PM3. Though several methods are available, nowadays only AM1 and PM3 are widely used.

(a) MNDO

The modified neglect of diatomic overlap (MNDO) method gives reasonable qualitative results for many organic systems. However its application is limited as it gives qualitatively and quantitatively incorrect results in most of the cases.

(b) AM1

Austin Model 1 (AM1) method is applied for modeling organic compounds. It generally predicts the heats of formation more accurately than MNDO; however the predicted heat of formation tends to be inaccurate for molecules with a large amount of charge localization. Though not reliable for accurate results, this method can throw important insights into the nature of the system under consideration, without much time lag.

(c) PM3

Parameterization method 3 (PM3) uses nearly the same equations as the AM1 method along with an improved set of parameters. It has the algorithms for including solvation effects and hence the calculations can be extended to that level also. Still, there are many instances when PM3 also gives erratic results. On average, PM3 predicts energies and bond lengths more accurately than MNDO or AM1 methods.

2.3.2.2 Ab initio methods

The term *ab initio* in Latin means "from the beginning". This name is given to computations that are derived directly from theoretical principles or from the first principles without the inclusion of experimental data. It does not mean that we are solving the Schrödinger equation exactly. Ab initio methods also contain some kind of approximations; but such methods can lead us to a reasonable solution of the Schrödinger equation giving somewhat acceptable values to the problem in question.

There are several ab initio methods. A method and basis set that is quite adequate for one application may be totally inadequate for another application. So, selection of appropriate method for the particular problem in question is of utmost importance. An insufficient method and an inappropriate

basis set may totally mislead us to highly erroneous conclusions. We also have to take into account the cost of doing calculations and the total amount of computer time required. For a simple problem that requires a simple ab initio method only, we need not go for highly advanced calculations. Similarly, if the results are not adequate for the purpose, there is no point in doing the calculation, however cheap it may be.

Though a wide range of ab initio methods have been employed in computational chemistry, we will restrict ourselves to only three methods which have been frequently and consistently used in our calculations. They are Hartree-Fock (HF) method, Moller Plesset perturbation (MP2) method and Density Functional (B3LYP) method.

(a) Hartree – Fock (HF) method

Of the several ab initio methods, the most common one is the Hartree-Fock method. It is also known as the self-consistent field (SCF) method. Here the primary approximation is the central field approximation, i.e., Coulombic electron – electron repulsion is taken into account by integrating the repulsion term. This gives the average effect of repulsion, but not the explicit repulsion interaction. In this method, a many electron Schrödinger equation is split into many simpler one- electron equations, the solutions of which gives as many single electron wave functions and their energies. The actual wave function of the system is the linear combination of these wave functions.

The HF calculation starts with an initial guess of orbital coefficients for all the electrons in the system. One electron is selected, and the potential in which it moves is calculated by freezing the distribution of all the other electrons and treating their averaged distribution as the centro symmetric source of potential. The Schrödinger equation is solved for this potential, which gives a new orbital for it. The procedure is repeated for all the other

electrons in the system, using the electrons in the frozen orbitals as the source of the potential. At the end of one cycle, there are new orbitals from the original set. This process is repeated until there is little or no change in the orbitals as well as the energy value. Since this is a variational calculation, the calculated energy value will be always higher than the actual value. The more correct the wave function is, the closer will be the energy to the actual value.

The energies calculated by the Hartree- Fock method are typically in error by about 0.5% for light atoms. This error is mainly due to the fact that HF SCF wave function takes into account the interactions between electrons only in an average, but not the instantaneous electron correlation. Actually, the electrons repel each other that they tend to stay apart as far as possible. Hence, in order to minimize the error in HF energy, the calculation should take into account the electron correlation completely. For this, the wave function is modified by introducing inter electronic distances into it. Accordingly, Fock operator is also modified including the Coulomb operator $\boldsymbol{J}_j$ and exchange operator $\boldsymbol{K}_j$. Solution of the HF equation using this new operator gives the orbital energy ε_i. Summation of ε_i over n/2 occupied orbitals (where n= number of electrons) gives the total orbital energy. Total HF energy is then calculated using the equation,

$$E_{HF} = 2\Sigma\, \varepsilon_i - \Sigma_i \Sigma_j (2J_{ij}-K_{ij}) + V_{NN},$$

where i= 1.... n/2 and j= 1...n/2 and V_{NN} is the potential energy due to internuclear interaction.

Roothan modified the calculation process by introducing basis sets to represent spatial orbitals and thus modifying the Schrödinger equation. Iterative solution of the new equation, known as HF-Roothan equation, helps to reach a SCF wave function, very close to the actual wave function and a better energy value.

(b) Moller Plesset perturbation (MP) method

Moller- Plesset method may be considered as the extension of the HF method as it involves the perturbation treatment of atoms and molecules, taking HF function as the unperturbed wave function. Though it was proposed by Moller and Plesset in 1934 as one form of many body perturbation theory (MBPT), the actual molecular application of MP perturbation theory began only in 1975 with the work of Pople and co-workers and Bartlett and co-workers [11]. The treatment of this section will be restricted to closed shell, ground state molecules. Depending upon the correlations added as the perturbation terms, the method becomes MP2 (second order), MP3 (third order), MP4 (fourth order) and so on.

In MP2 calculation, $\boldsymbol{H}^0$ is taken as the unperturbed Hamiltonian and its eigen functions are the zeroth-order wave functions. One of the wave functions is the HF ground state function Φ_0 and others are all possible Slater determinants formed using any 'n' of the infinite number of possible spin orbitals. The perturbation $\boldsymbol{H}^1$ is the difference between the true molecular electronic Hamiltonian $\boldsymbol{H}$ and the HF inter- electronic potential, $\boldsymbol{H}^0$.

i.e., $\boldsymbol{H}^1 = \boldsymbol{H} - \boldsymbol{H}^0$

Thus, the MP first order correction to the ground state energy, E_0 (1), is given by,

E_0 (1) = $< \psi_0(0) \,|\boldsymbol{H}^1|\psi_0(0)> = <\Phi_0|\boldsymbol{H}^1|\Phi_0>$, as $\psi_0(0) = \Phi_0$. The subscript '0' denotes the ground state.

Therefore, $E_0 + E_0(1) = <\psi_0(0) \,|\mathbf{H}^0|\psi_0(0)> + <\Phi_0|\boldsymbol{H}^1|\Phi_0>$

$$E_0 + E_0(1) = < \psi_0(0) \,|\boldsymbol{H}^1|\psi_0(0)> + < \Phi_0 \,|\boldsymbol{H}^1|\Phi_0 >$$

$$= <\Phi_0| \boldsymbol{H}^0 + \boldsymbol{H}^1|\Phi_0 >$$

$$= < \Phi_0 \mid \mathbf{H} \mid \Phi_0 >$$

Since $< \Phi_0|\boldsymbol{H}|\Phi_0 >$ is the variational integral for the Hartree- Fock wave function Φ_0, it equals the Hartree- Fock energy E_{HF}. i.e., $E_0(0) + E_0(1) = E_{HF}$ The eigen value of Φ_0 of $\boldsymbol{H}^0$ is equal to $\Sigma_{m=1\ldots n}\ \varepsilon_m$ and hence $E_0(0)=\Sigma_{m=1\ldots n}\ \varepsilon_m$

The 2nd order energy correction as per perturbation method is,

$$E_0(2) = \Sigma_{s\neq 0}\ \{| <\psi_s(0)|\ \boldsymbol{H}^1|\Phi_0>|^2\}\ /\ E_0(0) - E_s(0),$$

where $\psi_s(0)$ = unperturbed functions and Φ_0 = ground state HF function. Evaluation of $E_0(2)$ gives a calculated value as MP2 or MBPT (2) where '2' indicates the inclusion of energy corrections through 2nd order.

To do a MP electron correlation calculation, one first chooses a basis set and carries out a SCF calculation to obtain Φ_0, E_{HF} and virtual orbitals. E (2) is found out by evaluating the integrals over spin orbitals in terms of integrals over basis functions.

Moller-Plesset calculations are not variational. It is not uncommon to find MP2 calculations that give total energies below the exact total energy. Depending on the nature of the chemical system, there seems to be two patterns in using successively higher orders of perturbation theory. For some systems, the energies become successively lower and closer to the total energy in going from MP2 to MP3, to MP4 and so on. For other systems, MP2 will have energy lower than the exact energy, MP3 will be higher, MP4 will be lower... with each having an error that is lower in magnitude but opposite in sign [12].

One advantage of Moller- Plesset method is that it is size extensive. It is much faster than Configuration Interaction calculation, another ab initio method. The energy gradient in MP2 calculations is readily evaluated analytically and this allows MP2 geometry optimization and vibrational calculations to be done easily. It is to be noted that MP2 method is one of the

two most commonly used methods for including correlation effects on molecular ground-state equilibrium properties (the other being Density Functional method) because of its high computational efficiency and good results for molecular properties.

However, for those species involving open shell ground states (e.g., O_2, NO_2, OH^-, etc.), 'spin contamination' can occur to produce serious errors. Also the MP2 calculations do not work well at geometries far from equilibrium, though they work well near the equilibrium geometry [13]. Another limitation of MP calculations is that they are not generally applicable to excited electronic states.

(c) Density Functional Theory (DFT) Methods

Density functional theory is an extremely successful approach for the description of ground state properties of metals, semiconductors, and insulators. The success of density functional theory (DFT) not only encompasses standard bulk materials but also complex materials such as proteins and carbon nanotubes.

The wave function of a many electron system contains '3n' spatial and 'n' spin coordinates. This much information is more than what is needed; at the same time it lacks the physical significance. Also it makes the energy calculation a tedious process. Hence the search was on for functions involving fewer variables and it ended up in the formulation of Density Functional method. The goal of DFT methods is to design functionals connecting the electron density with the energy.

Pierre Hohenberg and Walter Kohn proved that for molecules with non-degenerate ground state, the molecular electronic properties are uniquely determined by the ground state electron probability density, ρ_0 (x, y, z), a function of three variables only, independently of the number of electrons.

Electron density is the square of the wave function, integrated over N-1 coordinates. Hence the ground state electronic energy E_0 can be considered to be dependent on ρ_0. This implies E_0 is a functional of ρ_0. i.e., $E_0 = E_0[\rho_0]$.

The external potential ν (r) is given by $-\Sigma_\alpha \{Z_\alpha / r_{i\alpha}\}$ where Z_α is the charge of the nucleus and $r_{i\alpha}$ is the distance of the i^{th} electron from nucleus. It is nothing other than the potential energy of interaction between electrons and the nuclei and it is acting on the electrons. The external potential is rather easily determined by the ground state electron probability density $\rho_0(r)$. Also $\rho_0(r)$ is employed to find out the number of electrons in the system. i.e., $\int\rho_0(r)\, dr = n$, where n = the number of electrons. Once the number of electrons and the external potential is specified, the electronic wave functions and allowed energies are determined as the solutions of the electronic Schrödinger equation. Therefore, the ground state electronic energy E_0 is a functional-function of the function of electron density. i.e., $E_0 = E_\nu [\rho_0]$ where 'ν' emphasizes the dependence of E_0 on the external potential ν (r), which differs for different molecules.

Since it was practically impossible to calculate $E_\nu [\rho_0]$, Kohn in association with L. J. Sham modified DFT and introduced Kohn-Sham (KS) orbitals from which exact ground state 'ρ' can be found out. The exchange-correlation energy, which is the sum of exchange energy and correlation energy, E_{xc}, is a functional of 'ρ'. If $E_{xc}[\rho]$ is exactly known, the ground state energy of the molecule can be found out. But, no one knows what the correct functional $E_{xc}[\rho]$ is for molecules. Hence approximations are needed for finding out exchange correlation energy.

Considering the molecular system consisting of noninteracting electrons and the electron density 'ρ' varying extremely slowly with position,

$E_{xc}[\rho]$ may be considered as the sum of exchange and correlation energy of all the electrons in the homogeneous electron gas.

i.e., $E_{xc} = \int \rho\,(x)\, \varepsilon_{xc}(\rho)\, dr$,

where $\varepsilon_{xc}(\rho)$ is the exchange and correlation energy per electron.

This method, known as local density approximation (LDA), is further modified by local spin density approximation (LSDA), where different orbitals and different densities are taken for electrons with different spins. The DF calculations in LDA start with an initial guess for 'ρ'. Basing on 'ρ', E_{xc} is determined followed by V_{xc}, where V_{xc} is the exchange-correlation potential. This helps the solution of the orbital equation to get the first set of KS orbitals. Further iterations improve ρ, E_{xc} and KS orbitals and finally the most appropriate wave function and ground state energy E_0 is reached from these DFT calculations.

Despite the fact that 'ρ' in a molecule is not a slowly varying function of position, the LSDA works surprisingly well for calculating molecular equilibrium geometries, vibrational frequencies and dipole moments, even for transition metal compounds, where HF calculations often give poor results. However, calculated LSDA molecular atomization energies are very inaccurate. This requires functionals that go beyond LDA and LSDA.

In order to overcome the difficulties met with LSDA method in DFT, gradient corrected and hybrid functionals were incorporated into the energy equation. Approximate gradient corrected exchange and correlation energy functionals were developed using theoretical considerations such as the known behaviour of the true functionals E_x and E_c in various limiting situations as a guide, with some empiricism thrown in. The DFT methods with such modified functionals are BLYP, B3LYP, B3PW91 and B1B95. These methods using gradient corrected functionals and hybrid functionals

give good equilibrium geometries, vibrational frequencies and dipole moments. Besides these, they also give generally accurate molecular atomization energies.

Although the results obtained with the modern density functional methods are usually sufficiently accurate for most applications, there is no systematic way of improving them [in contrast to some of the traditional wave function-based methods like configuration interaction (CI) or coupled cluster (CC) theory]. Hence, in the current DFT approach, it is not possible to estimate the error of the calculations without comparing them to other methods or experiments.

In Table 2.1 the specifics of each of these three methods are presented along with their thrust area

Method	Type of calculation	Advantages	Disadvantages	Applicable to
Molecular Mechanics	Uses classical physics; Relies on force field with embedded empirical properties	Fast and useful with limited computer resources; Can be used for large molecules	Less accurate; does not calculate electronic properties	Large systems with thousands of atoms
Semi-Empirical	Uses quantum physics; uses experimentally derived empirical parameters and approximations	Less computation time; calculates transition states and excited states	Less accurate; requires data from ab initio methods or from experiments	Medium sized systems with hundreds of atoms involving electronic transitions
Ab Initio	Uses quantum physics; highly rigorous steps; less approximations	Does not depend on experimental data; more accurate; calculates transition states and excited states	Computationally expensive	Small systems; for systems without experi-mental data; for systems where high accuracy needed

2.4 Ab initio procedures

There are several procedures that can be carried out with any ab initio program. The important steps are single point calculation, geometry optimization and frequency calculation. Usually, with these steps we will have an idea about the molecule, its structure and other relevant details.

2.4.1 Single point calculation

This procedure simply calculates the energy, wave function and other requested properties at a single fixed geometry. It is usually done first at the beginning of a study on a new molecule to check out the nature of the wave function. It is also frequently carried out after a geometry optimization, but with a larger basis set or a more superior method than is possible with the basis set and method used to optimize the geometry. Thus for a very large system the geometry may be optimized at HF level with the 3-21G basis set, but energy differences between isomers are then explored with a higher method like B3LYP or MP2 using a higher basis set like 6-31G**, 6-311G**, depending upon the nature of the molecule and purpose of the calculation.

2.4.2 Geometry Optimization

The process of finding the energy minimum point on the Potential Energy Surface (PES)[a] is called geometry optimization. This is also called energy minimization process. During this process, the molecule/species in study attains its stable structure close to the starting point by rearranging the structural parameters like the bond lengths, bond angles and dihedral angles.

Experience has shown that it is essential to find the geometry of a molecule accurately by geometry optimization. The procedure calculates the

[a] *The PES is the plot obtained when electronic energy, E, is plotted against some variables. If E is dependent on one variable only, we get the PES in a two dimensional space. If there are two variables, we get the PES in a 3-D space and so on.*

wave function and energy at a starting geometry and then proceeds to move to a new geometry that will give a lower energy. This is then repeated until we have the lowest energy geometry close to the starting point. Ideally this procedure calculates the forces on the atoms by evaluating the gradient (first derivative) of the energy with respect to atomic coordinates analytically. In some cases the gradients have to be estimated numerically. Sophisticated algorithms are used to select a new geometry at each step that give rapid convergence to the geometry with the lowest energy.

Calculation of E at one particular arrangement of the nuclei is called single point calculation. During geometry optimization, different possible structures for the molecule are explored and their energies are calculated and finally a molecular structure, for which the energy is minimum, is reached. In this energy minimization process, the gradient points on the PES with respect to the electronic energy are found out first. Gradient is the vector constituted by a set of (3N-6) first partial derivatives of E with respect to each of the variables on which E is dependent. Any point on the PES where the gradient is zero is called a stationary (critical) point and many such points are obtained on the PES during the optimization process. Such points may denote a minimum, maximum or a saddle point.

A saddle point corresponds to the energy maximum with respect to one variable, but energy minimum for the remaining variables; i.e., a point on the PES that is a maximum in one direction and a minimum in the other. Saddle points represent a transition structure connecting two equilibrium structures. The energy minimum on the PES than all the points in the immediate vicinity is called the local minimum. A conformation of a molecule, which corresponds to the local minimum on the PES, is called a conformer. A global minimum is the lowest energy point on the PES and it corresponds to the most stable isomer/conformer of the species in study.

For large molecules, there may be too many conformations and to get the true global minimum, several examinations are to be done. To be sure that one has found a minimum and not a saddle point, it is essential to test the nature of the located stationary point. Usually, this is done by performing a frequency calculation at the optimized geometry using the same basis set. For a true minimum, all the calculated frequencies will be real. For a first order saddle point, one of the calculated frequencies will be imaginary [14]. However, there is no short cut to find out the most stable conformer or isomer. Once all the possible stable structures are located, the species with the least energy will be the most stable one. A typical diagram of a PES is given in Figure 2.1.

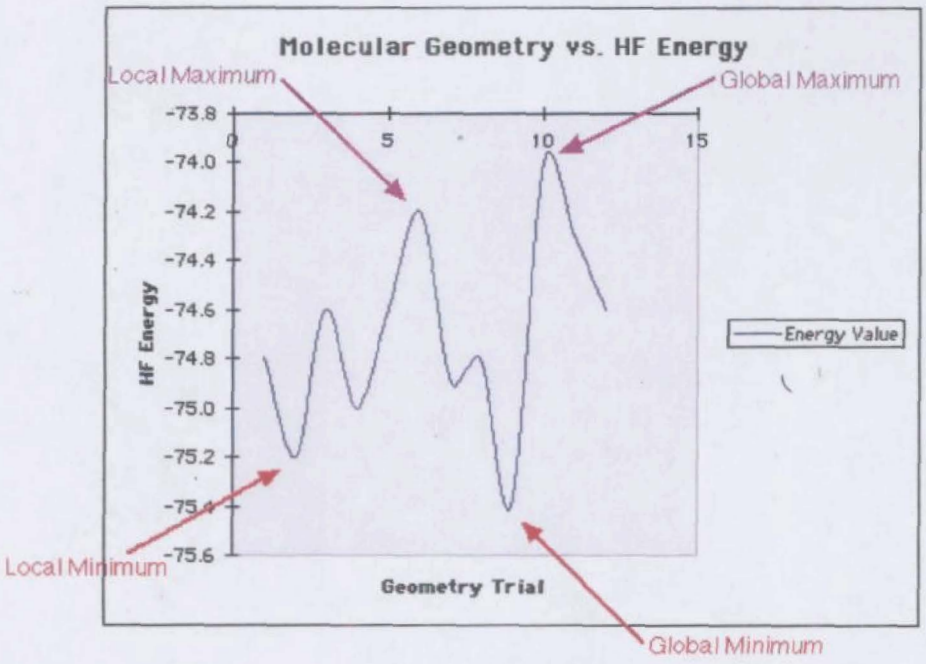

Figure 2.1: PES diagram of a large molecule

2.4.3 Frequency calculation

We carry out frequency runs for two reasons. First, we may want to actually predict the frequencies and the infrared (IR) and Raman intensities. Here we note that the frequencies are harmonic frequencies - they are those obtained by assuming that the potential energy surface is harmonic.

However, we carry out frequency calculations much more often than this. If the geometry obtained from an optimization run is a local, or indeed the global, minimum, all the frequencies will be real and positive. Getting such a result confirms we have obtained a local or global minimum. If we have a transition structure or any stationary point other than a minimum, some of the frequencies will be complex. These are printed out as negative numbers and are often called "imaginary frequencies". A well-behaved transition structure for a reaction will have one imaginary frequency. If we have restrained the symmetry in the optimization, we may get more than one imaginary frequencies.

Note that frequency calculations should only be carried out at the geometry obtained from an optimization run and with the same basis set and method. Any other calculation will give meaningless results.

2.5 Outline of a calculation

The QM calculation of a system involves several steps. At first, we have to construct an input file that includes the description of the geometry of the system, known as the Z-matrix, its electronic structure and charge, followed by the QM method and the basis set to be employed. The geometry of the system is described in terms of the structural parameters such as bond length, bond angle and dihedral angle. Electronic structure is expressed by giving the multiplicity of the system; charge and multiplicity together state whether the system has an open shell configuration or a closed shell

configuration. Depending on this information, the method of calculation and the basis set are specified. When we optimize geometry, it is always good to start with a poor basis set such as STO-3G or 3-21G for organic compounds, and then use the optimized geometry with this basis set as a starting geometry for a better basis set. During the optimization process, nuclear repulsion energy and electronic energy are calculated in separate steps and then total energy is determined. By rearranging the molecular parameters, the most stable configuration (with the lowest energy) within a particular region is arrived at. Some of the steps we come across during the optimization are: generating initial guess, self–consistent field iterations, electron density analysis, etc. All these culminate in the calculation of total energy of the system. One might next carry out a post-correlation energy calculation, or calculation of the first derivatives of the energy with respect to atomic coordinates. Calculation of the second derivatives of the energy with respect to atomic coordinates will give the vibrational frequencies for the optimized structure.

2.5.1 Z- matrix

Z- matrix is a list of bond lengths, bond angles and dihedral angles (conformation angles) used to describe the geometry of a molecule in a QM calculation [15]. A well-constructed Z-matrix can often help a programme run more efficiently. Such an efficient run reduces the computational time considerably. On the other hand, if a poorly constructed Z-matrix is used to define a molecule in QM calculations, we will end up with a less efficient geometry optimization, i.e., with unfavourable results- such as reaching an incorrect structure or an unstable isomer or spending unusually long time for optimization.

The use of Z-matrix is slowly declining because a number of graphic user input programmes are available, which can be used for the construction

of the molecule from which the programme itself will deduce the geometry. However, Z-matrix geometry specification is a skill still necessary for using some software and it remains the best way of incorporating symmetry constraints.

2.5.1.1 How to construct a Z-matrix

In order to construct an efficient Z-matrix, the following steps are to be followed:

a) Draw the possible structure of the molecule.

b) Assign one atom, preferably the central atom, the number "1".

c) All other atoms are given sequential numbers. The numbering is done in an order such that a specific symmetry is developed in it.

d) Starting from atom 1, all are written in the order at the extreme left column of the Z-matrix.

e) The first atom is the originating point that needs no specification.

f) The second atom is connected to the first through a bond length.

g) The third is linked to the second/first atom through a bond length and then angled with the first / second through any value except 180.

h) The fourth atom is connected to any one of the former three through a bond length and then angled with another of the remaining two. Its connection with the remaining atom is then defined through a dihedral angle.

It is to be noted that no three atoms should be collinear in the same card of the Z-matrix, even if they are so in the molecule and if such a system is to be constructed, it is done using dummy atoms such that linearity in the same card is avoided. As an example, the Z-matrix of ethylene molecule (D_{2h}) is given below:

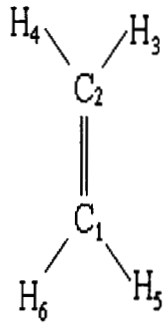

C

C 1 b1

H 2 b2 1 a1

H 2 b2 1 a1 3 d1

H 1 b2 2 a1 3 d2

H 1 b2 2 a1 3 -d1

b1 = 1.33

b2 = 1.09

a1 = 120.0

d1 = 180.0

d2 = 0.0

2.5.2 Basis Sets

According to molecular orbital (MO) theory, the molecular orbitals are obtained by the linear combination of atomic orbitals. Nowadays the term 'atomic orbital (AO)' is replaced by the term 'basis function'. In QM calculations, the set of one-electron wave functions (atomic orbitals) used to

construct LCAO-molecular orbitals is called the basis set [16]. Hence, basis set may be defined as a collection of basis functions (AOs) used to construct molecular orbitals. It can also be defined as the mathematical representation of the atomic orbitals in a molecule. Thus, it can be generally represented as:

$$\psi_i = \sum_i C_{\mu i}\, \phi_\mu, \text{ where i varies from 1 to n.}$$

Here, Ψ_i is the i^{th} MO, $C_{\mu i}$ are the coefficients of linear combination, ϕ_μ is the μ^{th} AO and n is the number of AOs.

The basis set may be interpreted as restricting each electron to a particular region of space. Larger basis sets impose fewer constraints on electrons and more accurately approximate exact molecular orbitals in the given system.

The hydrogen-like wave functions, modified for electron correlation, are generally represented as,

$\Psi_{nlm} = R_{nl}(r)\, Y_l^m\, (\theta,\phi)$, where $R_{nl}(r) = r^l\, e^{-Zr/na} \sum b_j r^j$, j varies from 0 to (n-l-1). They are not used per se because they lead to mathematical complications and time-consuming calculations. Instead, wave functions are used in which the radial terms R(r) are simplified. J. C. Slater suggested the use of functions that consisted only the spherical harmonics and the exponential term and such functions are known as Slater Type Orbitals (STOs), represented as,

$$S_{nlm}(r,\theta,\phi) = \{(2\zeta)^{n+0.5}/[(2n)!]^{0.5}\}\, r^{n-1} e^{-\zeta r}\, Y_l^m\, (\theta,\phi)$$

The difference between the STO and the hydrogen like orbital is that the STO has no nodes and the orbital exponent, ζ, is not necessarily equal to Z/n. The node, for example, in the 2s orbital would simply "come out in the wash" by a mixture of the 1s and 2s Slater-type functions when the molecular orbital calculation is done. The orbital exponent should be chosen to minimize the

energy, but this selection is still a formidable task even with modern computers.

Slater-type orbitals (STOs) represent the real situation for the electron density in the valence region and beyond, but are not so good nearer to the nucleus. Many calculations over the years have been carried out with STOs, particularly for diatomic molecules. The first basis set used in large-scale computational studies of polyatomic molecules consisted of STOs.

There were different terminologies used to describe STO basis sets. A minimal basis set consists of one STO for each inner shell and valence shell AO of each atom. Thus, the numbers of basis functions in a minimal set of an atom or molecule is equal to the number of AOs in it. A double-zeta (DZ) basis set is obtained by replacing each STO of a minimal basis set by two STOs that differ in their orbital exponents ζ (zeta). Similarly, a split-valence (SV) basis set uses two STOs for each valence AO but only one STO for each inner shell AO. Hence, this basis set is minimal for the inner shell AOs, but DZ for the valence AOs.

Although Slater orbitals were used for many years, they are not used directly anymore because the integrals in the resulting secular determinant are difficult to evaluate (especially the integrals involving more than one nuclear centre). Instead, nowadays we use Gaussian type functions (GTOs), suggested by Frank Boys, represented by,

$$G_{nlm}(r, \theta,\phi) = N_n r^{n-l} \exp.(-\alpha r^2) Y_l^m (\theta,\phi)$$

The GTOs contain the exponential $\exp(-r^2)$, rather than the $\exp(-r)$ of the STOs, and are very easy to evaluate. Of course they do not represent the electron density of the real situation as well as the STOs, but we can overcome this to a large extent by using more GTOs. The individual GTOs are called primitive Gaussian type orbitals (PGTOs), while the combined

functions are called contracted Gaussian type orbitals (CGTOs). Some early calculations used a large number of individual GTOs. It was then suggested that the GTOs be contracted into separate functions. The current practice is to take each basis function as a linear combination of a small number of Gaussians. Thus, in modern basis sets, the STOs are replaced by CGTOs, which in turn are the linear combinations of several PGTOs or Gaussian primitives.

Basing on the number and type of GTOs used for the construction of molecular orbitals, they are classified into different groups, such as Minimal basis sets, Scaling basis sets, Extended basis sets,etc.

(a) Minimal basis sets

The essential idea of a minimal basis set is that we select one basis function for every AO that is required to describe the free atom. Thus for hydrogen, the minimal basis set is just one 1s orbital. For carbon, the minimal basis set consists of a 1s orbital, a 2s orbital and the full set of three 2p orbitals. For methane the minimal basis set consists of nine basis functions; four 1s orbitals from each hydrogen atom, and the set of 1s, 2s and 2p orbitals from carbon atom.

Several minimal basis sets are in common use, but by far the most common are the STO-nG basis sets devised by John Pople and his group. The most common of these is STO-3G where a linear combination of three GTOs is fitted to a STO. Or we can say each STO is replaced by a CGTO, which is the linear combination of three PGTOs. The STO-3G basis set for methane thus consists of a total of nine CGTOs built from 27 PGTOs.

Other commonly used STO-nG basis sets are STO-4G and STO-6G where each STO is fitted to 4 and 6 GTOs respectively. The STO-nG basis sets are available for almost all elements in the periodic table.

(b) Scaling basis sets

The STO-nG basis sets use fixed orbital exponents, which suggests that the orbitals of a given type are of identical size. However in actual molecules this will not be the case, especially in those molecules having both σ bonds and π bonds. The π MOs will be different from the σ MOs. This necessitates different orbital exponents for different types of MOs. Also, the MOs of different molecules will have different orbital exponents. Another defect with STO-nG basis set is its inability to describe the anisotropic distribution of the electron density along the bond direction.

In order to overcome the above difficulties and to present the orbitals differently in different molecular environments, each AO is expressed as the sum of two STOs that differ only in the value of their exponent, ζ. Thus the combination of a large orbital and a small orbital is essentially equivalent to an orbital of intermediate size and minimized energy. Figure 2. 2 will highlight the concept.

(a)

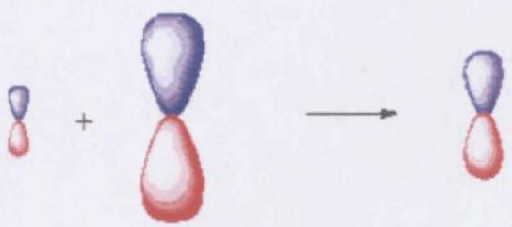

(b)

Figure 2.2: (a) mixing of two 's' functions of different 'ζ' values (b) mixing of two 'p' functions of different 'ζ' values

The resulting orbital is of a size that best fits the molecular environment since it is obtained from energy minimizing process. The nice thing about this procedure is that the mixing coefficients in the molecular orbitals now appear in a linear fashion. This simple dodge is equivalent to scaling the single minimal basis set orbital.

(i) Double zeta basis sets

A set of orbitals, generated from a sum of two STOs of different orbital exponents (replaced by equal number of CGTOs which are linear combinations of PGTOs), constitutes a double zeta (DZ) basis set. In other words, DZ basis set is the representation of AOs, each AO being expressed as the sum of two STOs of varying orbital exponent values.

In a genuine double zeta basis set, every member of a minimal basis set is replaced by two functions. In this way both core and valence orbitals are scaled in size. The normal abbreviation for a double zeta basis set is DZ, but the D95 (pronounced "dee nine five") basis set built into the program, Gaussian, is a double zeta basis set. Care should be taken in using the abbreviation because it does not describe a basis set as accurately as, say, 6-31G does. It is necessary to be clear which author constructed the basis set.

Split valence double zeta basis sets

This is a different category of DZ basis set. Instead of expressing all the atomic orbitals as the sum of two STOs, the inner orbitals are described by a single STO and the valence orbitals, by a sum of several STOs of differing orbital exponents. Such a representation is commonly referred to as split valence basis set. The general notation for split valence basis set is n-MPG, where n= number of GTOs used to describe the inner shell orbitals, the hyphen indicates that we have a split valence basis set and the numbers M and P designate the number of Gaussian functions that are used to fit the STOs. M

corresponds to the number of GTOs used to express smaller STO and P, the number of GTOs for larger STOs. G simply tells us that we are using Gaussian functions. Examples for split valence double zeta basis sets are 3-21G and 6-31G.

(ii) Triple zeta basis sets

Triple zeta (TZ) basis set is the representation of atomic orbitals, generated from a sum of three STOs of different orbital exponents and they are referred to as TZ. It is an extension of double zeta basis set.

Split valence triple zeta basis sets

It is another split valence basis set where the core orbitals are a contraction of N primitive Gaussians and the valence orbitals are split into three functions of differing 'ζ ' values. It is represented by N-MPQG. Example for triple valence basis set is 6-311G.

(c) Extended basis sets

There are certain systems where electrons are relatively far from the nucleus. Examples for them are molecules with lone pairs, anions, other systems with significant negative charge, systems in their excited states, systems with low ionization potential, systems where absolute acidities are described, etc. In these, larger orbitals are needed to accommodate the electron cloud more efficiently [17]. To allow orbitals to occupy a larger region of space, diffuse functions are introduced. Similarly, when systems with distorted electron cloud are considered, basis functions with usual shape will not suffice. Consideration of these factors accounts for the introduction of extended basis sets.

(i) Polarization basis sets

In the formation of a molecule, due to the influence of other nuclei, the orbitals in its proximity will get distorted or polarized, which necessitates orbitals, which are more flexible in shapes than the s, p, d etc. shapes in the atoms. To accomplish this, basis functions of higher angular quantum number are mixed with the original basis functions. Thus 's' is mixed with 'p', 'p' is mixed with 'd' and so on as shown in the figure 2.3.

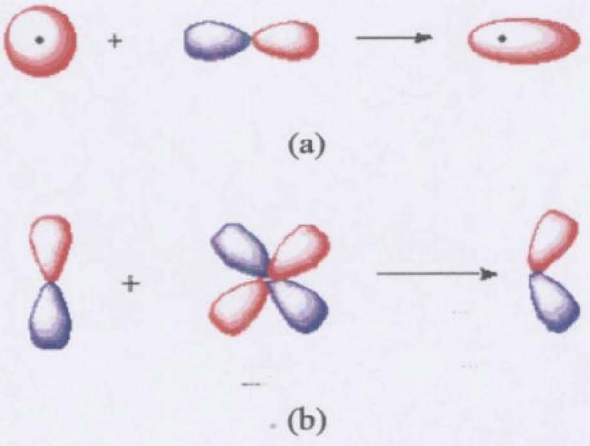

Figure 2.3: (a) mixing of 's' and 'p' (b) mixing of 'p' and 'd'

The polarization functions are generally represented with an asterisk mark (*) or (**) super fixed to G of the split valence basis set. '*' denotes the mixing of 'd' functions with the 'p' functions of atoms, Li to Cl. '**' denotes the mixing of 'd' functions with the 'p' functions of atoms from Li to Cl and 'p' functions to the 's' functions of hydrogen atoms. i.e., N-MPG*. Examples for polarized basis sets are 6-31G* and 6-31G**. Here in 6-31G*, the core orbitals are the CGTOs of six primitive Gaussians. The valence orbitals are split into two CGTOs of differing orbital exponents, the lower CGTO being constructed from three Gaussian primitives and the higher CGTO being constructed from a single Gaussian primitive.

(ii) Diffuse basis sets

Diffuse functions are large size versions of 's'- and 'p'- type functions as opposed to the standard valence size functions of neutral atoms. To denote the diffuse basis sets, '+' is added before G of the basis set. If one '+' is added, it denotes one set of diffuse 's' and 'p' functions on heavy atoms and the second '+' indicates that a diffuse 's' function is also added to hydrogen. A diffuse basis set is generally represented, as N-MP+G. Example for diffuse basis set is 6-31+G – a split valence basis set with one set of diffuse 'sp'- functions on heavy atoms.

For a comparative study, the different basis sets for water molecule is given below in Table 2.2.

Table 2.2: Basis sets and orbitals of atoms used for their construction in water molecule

Basis set	Orbitals of Hydrogen	Orbitals of Oxygen
STO-3G	1s	1s, 2s, $2p_x$, $2p_y$, $2p_z$
3-21G	1s, 2s	1s, 2s, 3s, $2p_x$, $2p_y$, $2p_z$, $3p_x$, $3p_y$, $3p_z$
6-31G	1s, 2s	1s, 2s, 3s, $2p_x$, $2p_y$, $2p_z$, $3p_x$, $3p_y$, $3p_z$
6-31G*	1s, 2s	1s, 2s, 3s, $2p_x$, $2p_y$, $2p_z$, $3p_x$, $3p_y$, $3p_z$, 4xx, 4yy, 4zz, 4xy, 4xz, 4yz
6-31G**	1s, 2s, $3p_x$, $3p_y$, $3p_z$	1s, 2s, 3s, $2p_x$, $2p_y$, $2p_z$, $3p_x$, $3p_y$, $3p_z$, 4xx, 4yy, 4zz, 4xy, 4xz, 4yz
6-31+G*	1s, 2s	1s, 2s, 3s, 4s, $2p_x$, $2p_y$, $2p_z$, $3p_x$, $3p_y$, $3p_z$, $4p_x$, $4p_y$, $4p_z$, 5xx, 5yy, 5zz, 5xy, 5xz, 5yz
6-311G	1s, 2s, 3s	1s, 2s, 3s, 4s, $2p_x$, $2p_y$, $2p_z$, $3p_x$, $3p_y$, $3p_z$, $4p_x$, $4p_y$, $4p_z$
6-311+G*	1s, 2s, 3s	1s, 2s, 3s, 4s, 5s, $2p_x$, $2p_y$, $2p_z$, $3p_x$, $3p_y$, $3p_z$, $4p_x$, $4p_y$, $4p_z$, $5p_x$, $5p_y$, $5p_z$, $6D_0$, $6D_{+1}$, $6D_{-1}$, $6D_{+2}$, $6D_{-2}$
6-311++G*	1s, 2s, 3s, 4s	1s, 2s, 3s, 4s, 5s, $2p_x$, $2p_y$, $2p_z$, $3p_x$, $3p_y$, $3p_z$, $4p_x$, $4p_y$, $4p_z$, $5p_x$, $5p_y$, $5p_z$, $6D_0$, $6D_{+1}$,$6D_{-1}$, $6D_{+2}$, $6D_{-2}$
6-311++G**	1s, 2s, 3s, 4s, $5p_x$, $5p_y$, $5p_z$	1s, 2s, 3s, 4s, 5s, $2p_x$, $2p_y$, $2p_z$, $3p_x$, $3p_y$, $3p_z$, $4p_x$, $4p_y$, $4p_z$, $5p_x$, $5p_y$, $5p_z$, $6D_0$, $6D_{+1}$, $6D_{-1}$, $6D_{+2}$, $6D_{-2}$

2.6 Introduction to GAUSSIAN Programme [18]

Though a number of computer programmes are available to calculate the molecular properties, the most widely used programmes are SPARTAN, GAMESS and GAUSSIAN [19]. Of these three, GAUSSIAN is more user friendly and it can serve as a powerful tool for exploring areas of chemical interest like substituent effects, reaction mechanisms, potential energy surfaces and excitation energies [20].

GAUSSIAN is a computer programme existing in various versions, labelled by release year and the latest version is GAUSSIAN-2003. It includes all common ab initio methods like HF, CI, DFT, MP, CC, many SE methods and also the MM methods [21]. It can predict many properties of molecules and reactions such as energies and structures of molecules and their transition states, bond and reaction energies, molecular orbitals, multipole moments, atomic charges and electrostatic potentials, vibrational frequencies, IR and Raman spectra, NMR properties, polarizabilities and hyper polarizabilities, thermo chemical properties and reaction pathways.

Wide application and high reliability of the results make GAUSSIAN a powerful tool in examining different pathways of reactions. It is specifically because of this reason that we opted for GAUSSIAN for our computational work to find out the structural and electronic characteristics of alkali metal substituted (or doped) conjugated polyenes so as to determine the interactive forces in such complexes.

2.7 Computational Procedure

The goal of our work is the study of the cation – π interaction in metal-polyenes and metal polyenyl complexes. This involves the study of the interactions existing in the systems of our study. Theoretical explorations were made into the alkali metal polyenes and alkali metal doped polyene

complexes to find out their correct structures, total energies, binding energies and other parameters. The structure, stabilisation energy and other characteristics will give reliable insights about the interactive forces that stabilize them. For the theoretical calculations, we employed the software GAUSSIAN-03.

At first, the geometry of the system in study is optimized employing the HF method with 6-31G* basis set. The optimized parameters are then substituted in the parent system and again optimized at the MP2 and B3LYP levels with the same basis set. Normal mode analysis was performed on the optimized structures at B3LYP level to determine whether they correspond to energy minima or transition states. The structural parameters were then analysed using the soft ware MOLDA [22] and Gauss View [23]. From the total energy values of the individual species and the product species, the energy of formation of the complex is calculated. Since that much energy is released during the product formation as the result of various interactive forces, it is taken as the stabilisation energy of the product.

In fact, the computational calculations were started with the SE method AM1. It was a good method to start with, as it gave certain valuable hints about the effect of metal doping and substitution. The trends observed in these calculations were followed with higher-level ab initio calculations employing HF, B3LYP and MP2 methods. In all these calculations, the split valence polarized basis set, 6-31G* were mainly employed. In those systems where Rb is one of the several atoms, the calculations were performed with the basis set, 3-21G. In order to verify the accuracy and reliability of these methods, higher level calculations were also done at MP2 level in selected systems, using the extended basis set, 6-311+G*.

2.7.1 Molecular Modeling

The effects of three types of metallic manipulations in conjugated polyenes were studied using the computational techniques. They are:

(a) Metal substitution in conjugated polyenes

(b) Metal doping in conjugated polyenes

(c) Metal ion doping in conjugated polyenes

In each stage, conjugated polyenes of odd and even number are studied separately, using the metals lithium (Li), sodium (Na) and potassium (K). In some cases, rubidium (Rb) is also used to ascertain whether the trends are the same.

For the geometry optimization, the molecule or the system in study is introduced in the form of a Z-matrix. The route of the calculation, the file name, charge of the system and the multiplicity are specified in the input file. If the calculations are to be retrieved for further higher-level calculation, the checkpoint file is preserved in appropriate folders. The Z- matrix should be as close as possible to the system that is represented by it, in order to obtain the best results at a very low computational cost.

In metal substitution, the metal was introduced into the sp^3 carbon of the polyene in place of hydrogen. In order to pinpoint all the possible stable isomers of the same system, metal ion was introduced on to different carbons of the polyenyl anion at right angles. In metal/cation doping, the metal/cation was placed perpendicularly on different carbons of the polyene at a small bondable distance (e.g.,2.1 A^0 for Li, 2.2 A^0 for Na and 2.5 A^0 for K). In order to get the vibrational frequencies, the term 'freq' is added in the route section. As an example of the input file, the doping of K^+ onto the third carbon of the polyenyl anion is modelled via the Z-matrix and presented below:

Checkpoint File: %chk=F:\TMJHF\C5H7K (3)

Route Section: # T HF/6-31G* OPT

File Name: C5H7K (3)

Charge & Multiplicity = 0,1

Symbolic Z-matrix:

C						
C	1	1.3574				
H	1	1.0798	2	122.0191		
H	1	1.0781	2	121.2568	3	-180.0,0
H	2	1.0874	1	114.8331	3	180.0,0
C	2	1.4116	1	131.2925	3	0.0,0
H	6	1.0815	2	118.7437	5	-180.0,0
C	6	1.4118	2	122.5033	1	-180.0,0
H	8	1.0873	6	113.8716	7	180.0,0
C	8	1.3572	6	131.2762	2	-180.0,0
H	10	1.0797	8	122.0040	9	-180.0,0
H	10	1.0782	8	121.2731	9	0.0,0
K	6	2.5	8	90.0	9	90.0,0

2.7.2 Dynamics of the calculation and excerpts from GAUSSIAN output file.

In the computational calculation, the Z-matrix, which we present in terms of bond lengths, bond angles and dihedral angles, is further developed into a file of initial parameters, presenting almost a complete list of possible bond lengths, bond angles and dihedral angles between different atoms of the molecular system we have considered. This gives us a chance to compare the initial and final optimized parameters. The file of initial parameters, basing on the above Z- matrix, is given below:

! Name	Definition	Value	Derivative Info.	!
! R1	R(1,2)	1.3574	estimate D2E/DX2	!
! R2	R(1,3)	1.0798	estimate D2E/DX2	!
! R3	R(1,4)	1.0781	estimate D2E/DX2	!
! R4	R(2,5)	1.0874	estimate D2E/DX2	!
! R5	R(2,6)	1.4116	estimate D2E/DX2	!
! R6	R(2,13)	3.1182	estimate D2E/DX2	!
! R7	R(6,7)	1.0815	estimate D2E/DX2	!
! R8	R(6,8)	1.4118	estimate D2E/DX2	!
! R9	R(6,13)	2.7804	estimate D2E/DX2	!
! R10	R(7,13)	2.9833	estimate D2E/DX2	!
! R11	R(8,9)	1.0873	estimate D2E/DX2	!
! R12	R(8,10)	1.3572	estimate D2E/DX2	!
! R13	R(8,13)	3.1183	estimate D2E/DX2	!
! R14	R(10,11)	1.0797	estimate D2E/DX2	!
! R15	R(10,12)	1.0782	estimate D2E/DX2	!
! A1	A(2,1,3)	122.0191	estimate D2E/DX2	!
! A2	A(2,1,4)	121.2568	estimate D2E/DX2	!
! A3	A(3,1,4)	116.7241	estimate D2E/DX2	!
! A4	A(1,2,5)	114.8331	estimate D2E/DX2	!
! A5	A(1,2,6)	131.2925	estimate D2E/DX2	!
! A6	A(1,2,13)	107.3817	estimate D2E/DX2	!
! A7	A(5,2,6)	113.8744	estimate D2E/DX2	!
! A8	A(5,2,13)	100.5574	estimate D2E/DX2	!

! A9	A(2,6,7)	118.7437	estimate D2E/DX2	!
! A10	A(2,6,8)	122.5033	estimate D2E/DX2	!
! A11	A(7,6,8)	118.753	estimate D2E/DX2	!
! A12	A(6,8,9)	113.8716	estimate D2E/DX2	!
! A13	A(6,8,10)	131.2762	estimate D2E/DX2	!
! A14	A(9,8,10)	114.8522	estimate D2E/DX2	!
! A15	A(9,8,13)	100.5574	estimate D2E/DX2	!
! A16	A(10,8,13)	107.3779	estimate D2E/DX2	!
! A17	A(8,10,11)	122.004	estimate D2E/DX2	!
! A18	A(8,10,12)	121.2731	estimate D2E/DX2	!
! A19	A(11,10,12)	116.7229	estimate D2E/DX2	!
! A20	A(2,13,7)	41.2279	estimate D2E/DX2	!
! A21	A(2,13,8)	46.7714	estimate D2E/DX2	!
! A22	A(7,13,8)	41.2328	estimate D2E/DX2	!
! D1	D(3,1,2,5)	180.0	estimate D2E/DX2	!
! D2	D(3,1,2,6)	0.0	estimate D2E/DX2	!
! D3	D(3,1,2,13)	69.1202	estimate D2E/DX2	!
! D4	D(4,1,2,5)	0.0	estimate D2E/DX2	!
! D5	D(4,1,2,6)	180.0	estimate D2E/DX2	!
! D6	D(4,1,2,13)	-110.87	estimate D2E/DX2	!
! D7	D(1,2,6,7)	0.0	estimate D2E/DX2	!
! D8	D(1,2,6,8)	180.0	estimate D2E/DX2	!
! D9	D(5,2,6,7)	180.0	estimate D2E/DX2	!
! D10	D(5,2,6,8)	0.0	estimate D2E/DX2	!
! D11	D(1,2,13,7)	-99.2319	estimate D2E/DX2	!

! D12	D(1,2,13,8)	-159.6695	estimate D2E/DX2	!
! D13	D(5,2,13,7)	140.3709	estimate D2E/DX2	!
! D14	D(5,2,13,8)	79.9334	estimate D2E/DX2	!
! D15	D(2,6,8,9)	0.0	estimate D2E/DX2	!
! D16	D(2,6,8,10)	180.0	estimate D2E/DX2	!
! D17	D(7,6,8,9)	180.0	estimate D2E/DX2	!
! D18	D(7,6,8,10)	0.0	estimate D2E/DX2	!
! D19	D(6,8,10,11)	0.0	estimate D2E/DX2	!
! D20	D(6,8,10,12)	180.0	estimate D2E/DX2	!
! D21	D(9,8,10,11)	180.0	estimate D2E/DX2	!
! D22	D(9,8,10,12)	0.0	estimate D2E/DX2	!
! D23	D(13,8,10,11)	-69.1128	estimate D2E/DX2	!
! D24	D(13,8,10,12)	110.8872	estimate D2E/DX2	!
! D25	D(9,8,13,2)	-79.9342	estimate D2E/DX2	!
! D26	D(9,8,13,7)	-140.3619	estimate D2E/DX2	!
! D27	D(10,8,13,2)	159.6487	estimate D2E/DX2	!
! D28	D(10,8,13,7)	99.2211	estimate D2E/DX2	!

The above step is followed by the input orientation whereby the positions of different atoms are presented in terms of Cartesian coordinates. Note that unless otherwise restricted, the first atom (1) is taken as the origin and the second atom is placed along the *Z*-axis. The other atoms are positioned accordingly. It is followed by the distance matrix in which the distances between the atoms of the molecule in discussion are presented. It is followed by the stoichiometry, degrees of freedom and the point group of the molecule.

Distance matrix (angstroms):

		1	2	3	4	5
1	C	0.000000				
2	C	1.357400	0.000000			
3	H	1.079800	2.136061	0.000000		
4	H	1.078100	2.126850	1.837192	0.000000	
5	H	2.065133	1.087400	3.052032	2.374378	0.000000
6	C	2.522705	1.411600	2.865107	3.470175	2.101800
7	H	2.828345	2.151874	2.749589	3.890779	3.065790
8	C	3.779778	2.475389	4.257239	4.596536	2.617705
9	H	3.972356	2.617702	4.675817	4.582845	2.290565
10	C	5.026808	3.779473	5.357474	5.905959	3.972183
11	H	5.356970	4.256426	5.477425	6.333491	4.675219
12	H	5.906325	4.596655	6.334283	6.708055	4.583146
13	K	3.754286	3.118211	3.992426	4.446655	3.485425

		6	7	8	9	10
6	C	0.000000				
7	H	1.081500	0.000000			
8	C	1.411800	2.152154	0.000000		
9	H	2.101865	3.065897	1.087300	0.000000	
10	C	2.522544	2.828282	1.357200	2.065093	0.000000
11	H	2.864461	2.749003	2.135643	3.051760	1.079700
12	H	3.470325	3.890892	2.126921	2.374774	1.078200
13	K	2.780400	2.983331	3.118301	3.485464	3.754178

		11	12	13
11	H	0.000000		
12	H	1.837181	0.000000	
13	K	3.991962	4.446771	0.000000

Stoichiometry C5H7K

Framework group C1[X(C5H7K)]

Deg. of freedom 33

Point group C1

This is followed by the standard orientation of the molecule. In the next step nuclear repulsion energy is calculated, symmetries of the occupied and unoccupied orbitals are guessed and the corresponding HF energy is determined based on the first guess orbitals.

Standard orientation:

Center Number	Atomic Number	Atomic Type	Coordinates (Angstroms) X	Y	Z
1	6	0	2.513486	-0.930241	0.157985
2	6	0	1.237629	-0.997378	-0.300510
3	1	0	2.739065	-0.777285	1.202823
4	1	0	3.353897	-1.028041	-0.510180
5	1	0	1.145269	-1.154315	-1.372554
6	6	0	0.000003	-0.899061	0.371228
7	1	0	0.000061	-0.742410	1.441322
8	6	0	-1.237760	-0.997437	-0.300667
9	1	0	-1.145296	-1.154355	-1.372604

10	6	0	-2.513323	-0.930303	0.158055
11	1	0	-2.738360	-0.777351	1.202907
12	1	0	-3.354158	-1.028073	-0.509741
13	19	0	-0.000036	1.852018	-0.031501

SCF Done: E (RHF) = -792.458031568 A.U. after 16 cycles

Convg = 0.4747D-08 -V/T = 2.0003

S**2 = 0.0000

The next step of calculation is the determination of population analysis using the self-consistent field density. All the orbitals, occupied and unoccupied, are categorized with their respective symmetries and energies. The presentation of this part of the file is given below:

****

Population analysis using the SCF density

****

Orbital symmetries:

Occupied (A) (A) (A) (A) (A) (A) (A) (A) (A) (A) (A) (A)
(A) (A) (A) (A) (A) (A) (A) (A) (A) (A) (A) (A)
(A) (A) (A) (A)

Virtual (A) (A) (A) (A) (A) (A) (A) (A) (A) (A) (A) (A)
(A) (A) (A) (A) (A) (A) (A) (A) (A) (A) (A) (A)
(A) (A) (A) (A) (A) (A) (A) (A) (A) (A) (A) (A)
(A) (A) (A) (A) (A) (A) (A) (A) (A) (A) (A) (A)
(A) (A) (A) (A) (A) (A) (A) (A) (A) (A) (A) (A)
(A) (A) (A) (A) (A) (A) (A) (A) (A) (A) (A) (A)
(A) (A) (A) (A) (A) (A) (A) (A) (A) (A) (A) (A)

The electronic state is 1-A.

Alpha occ. eigenvalues --	-129.79920	-13.23514	-10.57707	-10.57661	-10.57641
Alpha occ. eigenvalues --	-10.14891	-10.14154	-10.11457	-10.11270	-10.11129
Alpha occ. eigenvalues --	-1.40222	-0.77342	-0.77033	-0.76689	-0.74835
Alpha occ. eigenvalues --	-0.70274	-0.61606	-0.51807	-0.50605	-0.42352
Alpha occ. eigenvalues --	-0.39755	-0.36633	-0.33713	-0.30903	-0.29951
Alpha occ. eigenvalues --	-0.28160	-0.21801	-0.11053		
Alpha virt. eigenvalues --	-0.06093	-0.01183	-0.00361	0.01307	0.03001
Alpha virt. eigenvalues --	0.04920	0.05506	0.06358	0.08376	0.13292
Alpha virt. eigenvalues --	0.15959	0.17497	0.19742	0.20748	0.21211
Alpha virt. eigenvalues --	0.24763	0.25555	0.26757	0.27267	0.29018
Alpha virt. eigenvalues --	0.30366	0.32367	0.35358	0.38229	0.41550
Alpha virt. eigenvalues --	0.41727	0.45111	0.51242	0.57851	0.61474
Alpha virt. eigenvalues --	0.64225	0.67164	0.68844	0.70407	0.72936
Alpha virt. eigenvalues --	0.74338	0.76147	0.79230	0.86064	0.89345
Alpha virt. eigenvalues --	0.91097	0.91375	0.93807	0.95287	1.00355
Alpha virt. eigenvalues --	1.01170	1.03474	1.07026	1.11205	1.12290
Alpha virt. eigenvalues --	1.18792	1.28735	1.32266	1.40651	1.44288
Alpha virt. eigenvalues --	1.49180	1.55337	1.65573	1.78621	1.85306
Alpha virt. eigenvalues --	1.87733	1.93572	1.97693	2.04311	2.07781
Alpha virt. eigenvalues --	2.10936	2.13472	2.22050	2.31352	2.36786
Alpha virt. eigenvalues --	2.38703	2.40839	2.54763	2.57200	2.68266
Alpha virt. eigenvalues --	2.74856	2.90487	3.06403	3.07229	4.17161
Alpha virt. eigenvalues --	4.21178	4.25999	4.38062	4.55493	

In the next part of the output file, the Mulliken charge of each atom is presented. It is followed by a table in which the charges of hydrogens are summed up on the heavier atoms.

Mulliken atomic charges:

		1
1	C	-0.541980
2	C	-0.089517
3	H	0.131575
4	H	0.138342
5	H	0.146931
6	C	-0.477494
7	H	0.132245
8	C	-0.089511
9	H	0.146989
10	C	-0.541887
11	H	0.131615
12	H	0.138373
13	K	0.774318

Sum of Mulliken charges= 0.00000

Atomic charges with hydrogens summed into heavy atoms:

		1
1	C	-0.272063
2	C	0.057414

3 H 0.000000

4 H 0.000000

5 H 0.000000

6 C -0.345249

7 H 0.000000

8 C 0.057478

9 H 0.000000

10 C -0.271899

11 H 0.000000

12 H 0.000000

13 K 0.774318

Sum of Mulliken charges= 0. 00000

In the final part of the file, electronic spatial extent, net charge on the system and its dipole moment are presented.

Electronic spatial extent (au): <R**2>= 975.7187

Charge= 0.0000 electrons

Dipole moment (field-independent basis, Debye):

X= -0.0037 Y= 10.4391 Z= -1.0825 Tot=10.4951

The calculation steps are continued till a local minimum (stationary point) is reached. In such a condition, the maximum force, RMS force, maximum displacement and RMS displacement will be converged, which is a necessary condition to conclude the iterations. The conclusion of optimization steps is presented in the format given below.

Item	Value	Threshold	Converged?
Maximum Force	0.000017	0.000450	YES
RMS Force	0.000005	0.000300	YES
Maximum Displacement	0.001199	0.001800	YES
RMS Displacement	0.000181	0.001200	YES

Optimization completed.

-- Stationary point found.

The output file continues with optimized parameters, distance matrix, standard orientation, population analysis using the SCF density, optimized eigen values, Mulliken atomic charges, electronic spatial extent, net charge on the system and dipole moment and they are presented exactly in the same mode which we found above. The final part of the output file is the description of the molecule with its various parameters. So it can be called as the result chart and it will be of the following form:

1|1| UNPC-UNK | Fopt | RHF |6-31G(d)|C5H7K1|PCUSER|12-Aug-2005|0||# T HF/6-31G* OPT/ FREQ|| C5H7K (3) || 0, 1| C, -0.8106635075, -0.5669968546, -2.2802837335 | C, -0.9011635552, -0.9623241063, -0.9804448277 | H, 0.1386334524, -0.5637340656, -2.7958530915 | H, -1.6886244388, -0.4802326891, -2.8952401916 | H, -1.9049067542, -1.0218915104, -0.5738423486 | C, 0.1413048442, -1.1793824334,-0.0513299291 | H, 1.1603335148, -1.650221584, -0.4214795662 | C, -0.0618321917, -0 .9623379099, 1.3302407582 | H, -1.0925306633, -1.0219183811, 1.6626341077 | C, 0.8418052738, -0.5670183001, 2.2689722556 | H, 1.9006871768, -0.5637447973, 2.0550887329 | H, 0.5632002223, -0.4802677165, 3.3040412529 | K, 0.2982369, 1.6171141549, -0.1083303177 || Version = x 86 – Win 32-G03 Rev B.04 | State = 1-A | HF = -792. 465942 | RMSD = 9.151e-009 | RMSF = 1.475e-005 | Dipole = 0.2890304, 3.2382539, -0.1049728 | PG=C01 [X (C5H7K1)]||@

In order to proceed the work with frequency calculation, the following command is given: #T HF/6-31G* OPT/FREQ/geom=allcheckpoint. All the vibrational frequency modes are obtained during this calculation. Imaginary frequency value indicates the optimized system is only a transition state. If all the frequency values are positive, it is a clear assertion about the stability of the isomer. The energy and other characteristics of such isomers are computed for further examinations and detailed analysis.

2.7.3 Procedure of the work

Geometry optimisation processes are done with the polyenes, metal substituted polyenes, metal-doped polyenes and cation- doped polyenes to locate their stable isomers. Their energies and other molecular parameters are computed from the output file. The process is repeated with substituted polyenes too. The nature of the π-electron cloud along the polyene before and after the metal/ metal ion addition (substitution or doping) may be assessed from the carbon- carbon bond lengths. From the energies of the different species, energy of reaction, which is equal in magnitude to the total stabilisation energy of the species, is calculated. The different type of interactions contributing to the total stabilisation energy is then explored. The position of the metal along the carbon skeleton, its charge, etc., will be the pointers to the type of interactions existing in them. The magnitude of the stabilisation energy for different systems is also a good indicator to the nature of interaction. The factors favouring strong metal-polyene bonding are determined taking note of the changes effected by the electron withdrawing and donating groups in the metal polyenes and polyene complexes. A correct assessment of these factors will provide a good opening to the chemistry involving metal polyenes and metal-polyene complexes.

2.7.4 Selection of ab initio method and basis set

The selection of appropriate ab initio method and basis set is the important step of any computational work. Throughout our calculations, we have relied more or less on the DFT method B3LYP, employing the split valence polarized basis set, 6-31G*. The criteria for selecting this method and the said basis set are two: attaining a lower energy and comparatively lower computational cost. Of the three methods employed, namely HF, MP2 and B3LYP, the last one gave the lowest energy value at the lowest computational time. In our calculations, we are concerned more about the trend and geometry rather than the absolute values. Since we study the interacting forces in metal polyenes and polyenyl complexes, the energy difference between the products and the substrates is important rather than the absolute energy values. Our calculations with HF, MP2 and B3LYP levels using lower and higher basis sets have given almost agreeable values. The system for which the calculation was performed, the method, the basis set, relevant results and the approximate time taken for each calculation in a Pentium IV PC are given in Table 2.3.

Table 2.3: Comparison of the different characteristics of the same system obtained in different calculations using different basis sets

Method	Basis set	[a]System	[b] E (Hartree)	[c] E_{st} (kcal/mol)	[d] $\Delta E=E_L-E_H$ (Hartree)	[e]Ri (A^0)	[f] Q_M (a.u)	Time for calculation
HF	6-31G*	$C_9H_{11}K$ (3)	-946.2480	98.96	0.16830	2.8115	0.761576	0h 46m 49s
MP2	6-31G*	$C_9H_{11}K$ (3)	-947.4715	105.23	0.17421	2.7751	0.746230	3h 23m 42s
MP2	6-311+G*	$C_9H_{11}K$ (3)	-948.0228	**101.82**	0.18052	2.7419	0.969968	18h 14m 31s
B3LYP	6-31G*	$C_9H_{11}K$ (3)	-949.4184	**100.47**	0.05942	2.7816	0.659998	0h 46m 58s
B3LYP	6-311+G*	$C_9H_{11}K$ (3)	-949.5448	95.05	0.07622	2.7411	0.929877	3h 26m 24s
HF	6-31G*	C_7H_9K (3)	-869.3574	105.23	0.17274	2.8062	0.751992	0h 11m 16s
MP2	6-31G*	C_7H_9K (3)	-870.3181	112.18	0.18075	2.7686	0.735440	2h 55m 23s
MP2	6-311+G*	C_7H_9K (3)	-870.8142	**107.71**	0.18640	2.7338	0.961547	7h 52m 1s
B3LYP	6-31G*	C_7H_9K (3)	-871.8743	**107.71**	0.06293	2.7773	0.643907	1h 9m 4s
B3LYP	6-311+G*	C_7H_9K (3)	-872.1182	101.25	0.08938	2.7325	0.920545	1h 29m 53s

HF	6-31G*	C_5H_7K (3)	-792.4659	114.63	0.18195	2.8015	0.714560	0h 11m 19s
MP2	6-31G*	C_5H_7K (3)	-793.1640	122.41	0.19015	2.7625	0.698270	0h 20m 3s
MP2	6-311+G*	C_5H_7K (3)	-793.6048	**115.78**	0.19489	2.7234	0.938663	1h 59m 18s
B3LYP	6-31G*	C_5H_7K (3)	-794.5986	**118.50**	0.06954	2.7807	0.589575	0h 13m 7s
B3LYP	6-311+G*	C_5H_7K (3	-794.6914	109.92	0.09507	2.7255	0.890589	1h 4m 54s
HF	6-31G*	$C_9H_{11}Na$ (2)	-508.9655	117.72	0.18285	2.4645	0.584548	0h 43 m 1s
MP2	6-31G*	$C_9H_{11}Na$ (2)	-510.1699	121.47	0.17963	2.4370	0.582925	2h 55m 24s
MP2	6-311+G*	$C_9H_{11}Na$ (2)	-510.5651	111.70	0.17868	2.4441	0.819542	14h 29m 27s
B3LYP	6-31G*	$C_9H_{11}Na$ (2)	-511.8026	117.83	0.05626	2.4290	0.483759	0h 41m 52s
HF	6-31G*	C_7H_9Na (2)	-432.0757	124.50	0.18805	2.4629	0.577145	0h 23m 42s
MP2	6-31G*	C_7H_9Na (2)	-433.0177	129.17	0.18705	2.4350	0.573420	1h 8m 35s
MP2	6-311+G*	C_7H_9Na (2)	-433.3574	118.16	0.18542	2.4412	0.811068	4h 59m 6s
B3LYP	6-31G*	C_7H_9Na (2)	-434.3936	125.68	0.06014	2.4276	0.471582	0h 24m 24s
HF	6-31G*	C_7H_9Li (2)	-354.5831	143.70	0.20115	2.0921	0.383565	0h 20m 2s
MP2	6-31G*	C_7H_9Li (2)	-278.6349	155.55	0.20110	2.0692	0.373835	0h 29m 33s
MP2	6-311+G*	C_7H_9Li (2)	-278.8532	**152.11**	0.22097	2.0535	0.539596	3h 16m 36s
B3LYP	6-31G*	C_7H_9Li (2)	-279.6371	**149.83**	0.10100	2.0563	0.295067	0h 22m 45s
HF	6-31G*	C_5H_7Li (2)	-200.8044	161.46	0.24643	2.0871	0.367560	0h 9m 58s
MP2	6-31G*	C_5H_7Li (2)	-201.4833	167.33	0.24682	2.0649	0.360135	0h 10m 55s
MP2	6-311+G*	C_5H_7Li (2)	-201.6462	**161.71**	0.23304	2.0489	0.530967	1h 4m 17s
B3LYP	6-31G*	C_5H_7Li (2)	-202.2290	**161.88**	0.10946	2.0503	0.268910	0h 12m 20s
HF	6-31G*	$C_9H_{12}K^+$ (7)	-946.7351	16.84	0.27192	3.1213	0.877931	1h 1m 54s
MP2	6-31G*	$C_9H_{12}K^+$ (7)	-947.9377	19.44	0.26943	2.9870	0.869054	5h 50m 54s
MP2	6-311+G*	$C_9H_{12}K^+$ (7)	-948.4709	**19.33**	0.27639	2.9644	1.011971	12h 35m 47s
B3LYP	6-31G*	$C_9H_{12}K^+$ (7)	-949.8819	**19.00**	0.12756	3.0431	0.829745	3h 46m 18s

[a] The numeral in parentheses corresponds to the carbon to which the metal has least distance.

[b] E = Total energy; [c] E_{st}= Stabilisation energy; [d] E_H= energy of HOMO, E_L= energy of LUMO; [e] Ri = Metal-carbon distance; [f] Q_M= Mulliken charge on the metal.

It can be found from the table that the lower level B3LYP calculation, employing 6-31G* basis set, gives almost identical values as the higher level MP2 with 6-311+G* basis set. At the same time, the computational cost for the higher-level calculation is very large. Hence, unless otherwise required, we employed the B3LYP level of calculation using 6-31G* basis set.

Another comparison we make here is between the charges on the atoms in different notations. The Mulliken charges given in the GAUSSIAN output are used to explain certain phenomena observed in the complexes. Here too, we rely only on the trends of the charge on different carbons. When we analysed charges in terms of MK, ChelpG and NPA types, though the absolute values differ, the same trends were found to exist in the systems we studied. Hence, for our discussion based on the charges on the atoms, we have opted for the Mulliken charges only. The different types of theoretically defined charges for some systems are compared in Table 2.4.

Table 2.4: Charges (a.u) on the heavy atoms of Li/Na/K substituted C_5H_8 (B3LYP/ 6-31G*)

Charge-type	System	C1	C2	C3	C4	C5	Metal
Mulliken	C_5H_7Li (2)	-0.445	-0.081	-0.228	-0.038	-0.389	+0.2685
CHelpG	C_5H_7Li (2)	-1.151	+0.545	-0.627	+0.030	-0.414	+0.5934
MK	C_5H_7Li (2)	-1.378	+0.703	-0.723	-0.041	-0.418	+0.6201
NPA	C_5H_7Li (2)	-0.849	-0.280	-0.564	-0.234	-0.494	+0.8980
Mulliken	C_5H_7Na (2)	-0.484	-0.109	-0.215	-0.050	-0.400	+0.4480
CHelpG	C_5H_7Na (2)	-1.228	+0.551	-0.530	-0.011	-0.438	+0.6445
MK	C_5H_7Na (2)	-1.587	+0.706	-0.480	-0.113	-0.486	+0.6905
NPA	C_5H_7Na (2)	-0.829	-0.264	-0.490	-0.240	-0.513	+0.8652
Mulliken	C_5H_7K (3)	-0.464	-0.093	-0.251	-0.093	-0.464	+0.5895
NPA	C_5H_7K (3)	-0.654	-0.255	-0.462	-0.255	-0.654	+0.8325

2.7.5 Classification of the results

The results of the present investigation and the theoretical explanations given to them are presented in the subsequent three chapters, namely chapter 3, 4 and 5. The effects of alkali metal substitution to conjugated polyenes and the interactive forces leading to such effects are discussed in chapter 3. In the next chapter, alkali metal doping in conjugated polyenes and the subsequent changes in their electronic and structural aspects are analysed. To get a comprehensive picture about the effects of alkali metal addition to conjugated polyenes, doping of alkali metal ions was also done and the results are presented in the fifth chapter. Along with these, the substituent effects on the metal substituted polyenes and metal/metal ion doped polyenes are also studied. For this, polyenes carrying electron releasing and electron withdrawing groups are subjected to the computational study and the results are arranged in the concerned chapters. In the last chapter, we present a summary of the whole work done with its important conclusions and possible extensions. An attempt is also made to discuss the results of our study in the light of some ongoing research works and emerging trends of modern chemistry.

2.8 References:

1. Wikipedia, the free encyclopedia
2. D. Young, "Computational Chemistry", Wiley Inter Science, 2001, 3
3. "Chem Viz Over view" The Shodor Education Foundation, Inc., 1999-2000.
4. Nobel Prize in Chemistry-1998, Press Release by Nobel Foundation
5. W. Wang, O. Donini, C. M. Reyes, P. A. Kollman, Annu. Rev. Biophys. Biomol. Struct., 30 (2001) 211-243.

6. F. Jensen, " Introduction to Computational Chemistry", John Wiley & Sons Ltd, 1999, W.Sussex, 24

7. I. N. Levine, "Quantum Chemistry", 5th edn, 2003, Pearson Education, Singapore, 696.

8. F. Jensen, " Introduction to Computational Chemistry", John Wiley & Sons Ltd, 1999, W.Sussex, 81.

9 D. Young, "Computational Chemistry", Wiley Inter Science, 2001, 33.

10. D. Young, "Computational Chemistry", Wiley Inter Science, 2001, 32

11. I. N. Levine, "Quantum Chemistry", 5th edn, 2003, Pearson Education, Singapore, 511.

12. D. Young, "Computational Chemistry", Wiley Inter Science, 2001, 23.

13. I. N. Levine, "Quantum Chemistry", 5th edn, 2003, Pearson Education, Singapore, 567.

14. I. N. Levine, "Quantum Chemistry", 5th edn, 2003, Pearson Education, Singapore, 533.

15. D. Young, "Computational Chemistry", Wiley Inter Science, 2001, 67.

16. D. A. Mc Quarrie & J. D. Simon, "Physical Chemistry- A Molecular Approach", VLSE, 2003, New Delhi, 411.

17. J. B. Foresman & A. Frisch, "Exploring Chemistry with Electronic Structure Methods", 2nd edn, Gaussian, Inc, Pittsburgh, 2000, 99.

18. M. J. Frisch, G. W. Trucks, H. B. Schlegel, G. E. Scuseria, M. A. Robb, J. R. Cheeseman, J. A. Montgomery, Jr., T. Vreven, K. N.

Kudin, J. C. Burant, J. M. Millam, S. S. Iyengar, J. Tomasi, V. Barone, B. Mennucci, M. Cossi, G.Scalmani, N. Rega, G. A. Petersson, H. Nakatsuji, M. Hada, M. Ehara, K. Toyota, R.Fukuda, J. Hasegawa, M. Ishida, T. Nakajima, Y. Honda, O. Kitao, H. Nakai, M. Klene, X. Li, J. E. Knox, H. P. Hratchian, J. B. Cross, C. Adamo, J. Jaramillo, R.Gomperts, R. E. Stratmann, O. Yazyev, A. J. Austin, R. Cammi, C.Pomelli, J. W. Ochterski, P. Y. Ayala, K. Morokuma, G. A. Voth, P. Salvador, J. J. Dannenberg, V. G. Zakrzewski, S. Dapprich, A. D. Daniels, M. C. Strain, O. Farkas, D. K. Malick, A. D. Rabuck, K. Raghavachari, J. B. Foresman, J. V. Ortiz, Q. Cui, A. G. Baboul, S. Clifford, J. Cioslowski, B. B. Stefanov, G. Liu, A. Liashenko, P. Piskorz, I. Komaromi, R. L. Martin, D. J. Fox, T. Keith, M. A. Al-Laham, C. Y. Peng, A. Nanayakkara, M. Challacombe, P. M. W. Gill, B. Johnson, W. Chen, M. W. Wong, C. Gonzalez, and J. A. Pople, Gaussian, Inc., Pittsburgh, PA, 2003.

19. D. A. Mc Quarrie & J. D. Simon, "Physical Chemistry- A Molecular Approach", VLSE, 2003, New Delhi, 427.

20. J. B. Foresman & A. Frisch, "Exploring Chemistry with Electronic Structure Methods", 2nd edn, Gaussian, Inc, Pittsburgh, 2000, xxv.

21. I. N. Levine, "Quantum Chemistry", 5th edn, 2003, Pearson Education, Singapore, 550.

22. Hiroshi Yoshida, "MOLDA for Windows- A Molecular Data Processor", Dept of Chemistry, Faculty of Science, Hiroshima University, Higashi- Hiroshima 739, Japan.

23. Gauss View, Inc., Pittsburgh PA, 2003.

A THEORETICAL STUDY OF THE CATION – π INTERACTION IN ALKALI METAL POLYENES AND POLYENE COMPLEXES

THESIS

Submitted to the
University of Calicut
in partial fulfillment of the requirements
for the award of the degree of
Doctor of Philosophy
in Chemistry,
under the Faculty of Science

By

FR. JOSE T. M.

Forwarded

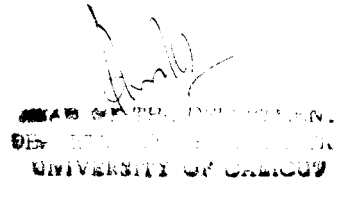

Department of Chemistry,
University of Calicut,
Calicut University P.O.,
673 635

April 2007

CHAPTER 3

ALKALI METAL SUBSTITUTED CONJUGATED POLYENES

3.1 Introduction

Since our objective is the study of poly acetylene (PA) type molecules, the best thing to start with such a study is to model PA type molecules by computer simulations and then to conduct the computational calculations on them. PA contains a delocalised electron cloud, which provides a highway for charge mobility [1]. Hence we started our computational analysis with conjugated polyenes with a delocalised electron cloud. Among the conjugated polyenes, there are odd numbered and even numbered polyenes. Also, there are all-cis and all-trans isomers. Fully conjugated odd polyenes will have one sp^3 carbon at the terminal position (C1) having three hydrogens, of which two are lying outside the plane of the carbons and the third, in the plane of the carbon itself. On the other hand, fully conjugated even polyenes will have only sp^2 carbons and hence all the hydrogens in it will be coplanar with the carbons. Example for an odd polyene is C_9H_{12} [Figure 3.1(a)] and example for an even polyene is $C_{10}H_{12}$ [Figure 3.1(b)]. Due to the alternate single and double bonds, there exists a delocalised electron cloud in the system, which is evident from the bond length values [see Table 3.1(b)].

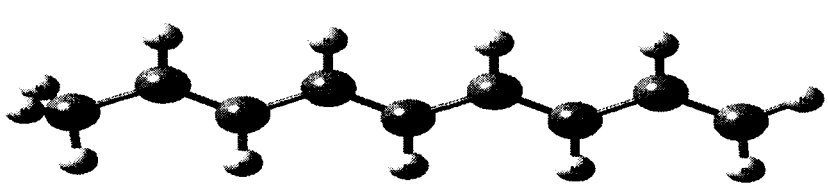

(a) C_9H_{12}

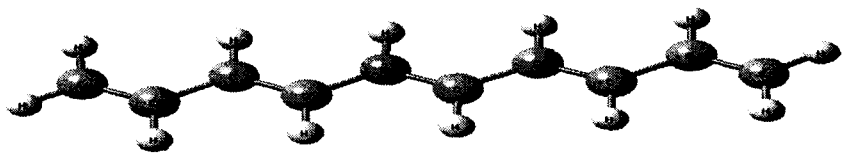

(b) $C_{10}H_{12}$

Figure 3.1: Optimized structures of C_9H_{12} & $C_{10}H_{12}$ (B3LYP/6-31G*)

3.2 Alkali metal substitution to all-trans conjugated polyenes

The substitution of the alkali metal to the polyene can be made in two modes- one, in place of the hydrogens on sp^3 carbon which are lying outside the plane of the carbon skeleton (non coplanar) and the other, in place of the hydrogens in the plane of the molecule (coplanar), either on the sp^3 carbon or on any other sp^2 carbon. Substitution of the metal to even polyenes is exactly similar to the latter, i.e., a coplanar substitution and hence the discussion related to the planar substitution in odd conjugated polyenes is applicable to the even polyenes also.

3.2.1 Coplanar Metal Substitution

When an alkali metal was substituted on the sp^3 carbon of a polyene in coplanar fashion, we got a species that was almost identical to the polyene itself. The frequency calculations showed that such metal-polyenes are unstable and they have considerably higher energy than non-coplanar isomers. However, when the metal was substituted on sp^2 carbons, either in odd or in even, the isomers obtained were stable. It was observed that the energies of such coplanar isomers from odd polyenes were much higher than their non-coplanar substituted counterparts.

The total energy of the system (E) expressed in Hartree (1 Hartree = 627.509 kcal/mol), the shortest metal- carbon distance (Ri), charge on the metal (Q_M), energy difference between the HOMO and the LUMO (ΔE) etc., are presented in Table 3.1(a).

Table 3.1(a): C_9H_{12} and its metal substituted (planar) isomers with their important characteristics (B3LYP/6-31G*).

System [a]	E (Hartree)	Ri (A^0)	Q_M (a.u)	$\Delta E = E_L - E_H$ (Hartree)	Number of imaginary frequencies
C_9H_{12}	-350.12588	---------	----------	0.13765	0
$C_9H_{11}Li$ (1p)	-357.01055	2.0032	0.380527	0.12186	1
$C_9H_{11}Li$ (8p)	-357.01780	1.9759	0.357302	0.11210	0
$C_9H_{11}Na$ (1p)	-511.77710	2.3223	0.381980	0.10750	1
$C_9H_{11}Na$ (8p)	-511.78330	2.3035	0.383828	0.09822	0
$C_9H_{11}K$ (1p)	-949.37826	2.7571	0.497937	0.08589	1
$C_9H_{11}K$ (5p)	-949.38870	2.7141	0.548393	0.09359	0
$C_9H_{11}K$ (8p)	-949.38641	2.7059	0.548287	0.09547	0
$C_9H_{11}K$ (9p)	-949.38647	2.6828	0.559800	0.08717	0
$C_{10}H_{12}$	-388.21308	--------	----------	0.12198	0
$C_{10}H_{11}Li$ (5p)	-395.10780	1.9888	0.364345	0.11928	0
$C_{10}H_{11}Na$ (5p)	-549.87368	2.3112	0.390319	0.09436	0
$C_{10}H_{11}K$ (5p)	-987.47801	2.7174	0.565879	0.09225	0

[a] The numeral in parentheses corresponds to the carbon to which the metal is substituted and 'p' to coplanar substitution

Except for the minor changes in bond lengths, there was no change in the planarity of the carbon skeleton. For comparison, the carbon-carbon bond lengths in free polyene (C_9H_{12}) and different metal substituted systems are given in Table 3.1(b).

Table 3.1(b): Carbon- carbon bond lengths (A^0) of free polyene and metal substituted polyenes (B3LYP/6-31G*)

System [a]	C1-C2	C2-C3	C3-C4	C4-C5	C5-C6	C6-C7	C7-C8	C8-C9	C9-C10
C_9H_{12}	1.4983	1.3469	1.4461	1.3563	1.4406	1.3560	1.4476	1.3442	-
$C_9H_{11}Li$ (1p)	1.4984	1.3530	1.4444	1.3579	1.4396	1.3568	1.4472	1.3448	-
$C_9H_{11}Li$ (8p)	1.4994	1.3471	1.4466	1.3570	1.4410	1.3577	1.4598	1.3578	-
$C_9H_{11}Na$ (1p)	1.4911	1.3521	1.4448	1.3577	1.4397	1.3568	1.4472	1.3447	-
$C_9H_{11}Na$ (8p)	1.4994	1.3471	1.4465	1.3571	1.4407	1.3581	1.4561	1.3528	-
$C_9H_{11}K$ (1p)	1.4905	1.3541	1.4437	1.3586	1.4391	1.3572	1.4469	1.3450	-
$C_9H_{11}K$ (5p)	1.5002	1.3482	1.4502	1.3648	1.4502	1.3600	1.4468	1.3459	-
$C_9H_{11}K$ (8p)	1.4997	1.3473	1.4462	1.3578	1.4400	1.3598	1.4574	1.3548	-
$C_9H_{11}K$ (9p)	1.4997	1.3445	1.4460	1.3581	1.4389	1.3597	1.4515	1.3615	-
$C_{10}H_{12}$	1.3446	1.4468	1.3573	1.4380	1.3598	1.4380	1.3573	1.4468	1.3446
$C_{10}H_{11}Li$(5p)	1.3453	1.4469	1.3593	1.4512	1.3719	1.4396	1.3591	1.4458	1.3456
$C_{10}H_{11}Na$ (5p)	1.3455	1.4467	1.3595	1.4472	1.3674	1.4395	1.3590	1.4458	1.3456
$C_{10}H_{11}K$ (5p)	1.3460	1.4465	1.3607	1.4493	1.3700	1.4394	1.3600	1.4453	1.3461

[a] The numeral in parentheses corresponds to the carbon to which the metal is substituted and 'p' to coplanar substitution.

Figure 3.2 highlights the minimal change to the planarity of the carbon skeleton, caused by the coplanar substitution of alkali metals to conjugated polyenes.

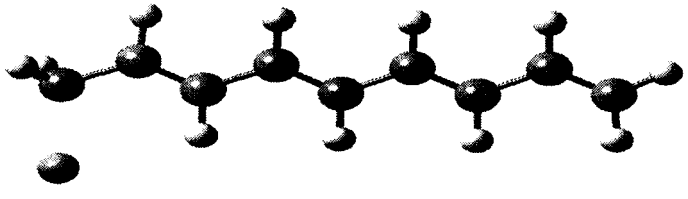

(a) $C_9H_{11}Li$ (1p)

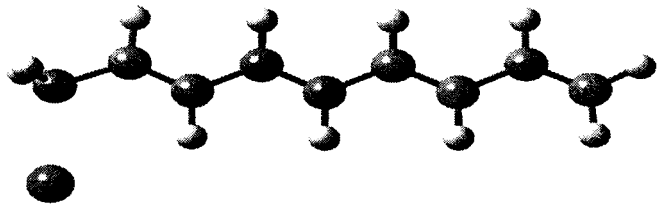

(b) $C_9H_{11}Na$ (1p)

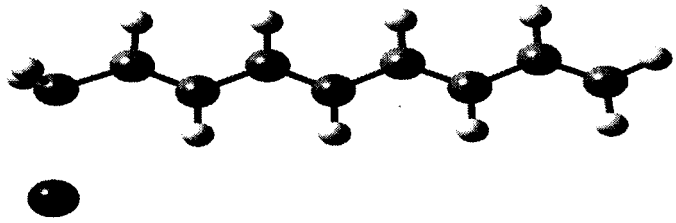

(c) $C_9H_{11}K$ (1p)

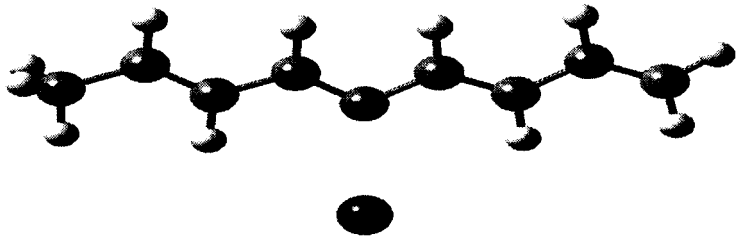

(d) $C_9H_{11}K$ (5p)

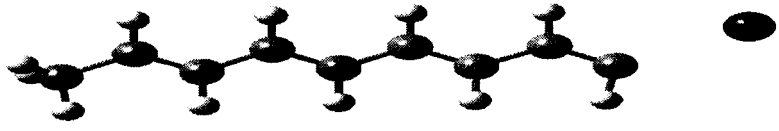

(e) $C_9H_{11}K$ (9p)

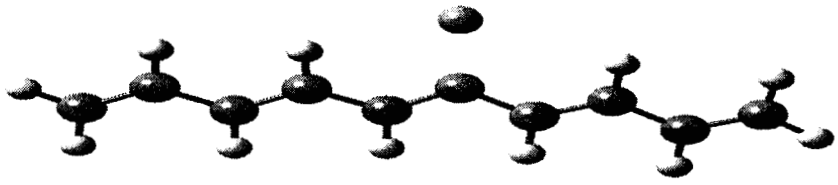

(f) $C_{10}H_{11}Li$ (5p)

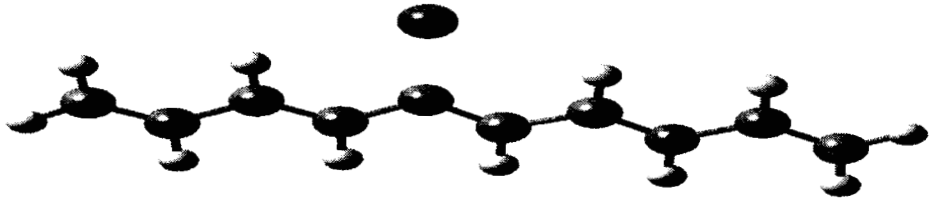

(g) $C_{10}H_{11}Na$ (5p)

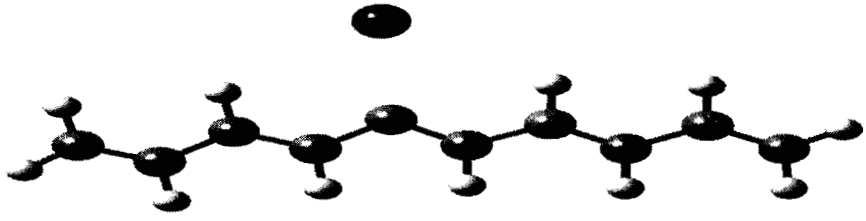

(h) $C_{10}H_{11}K$ (5p)

Figure 3.2: Optimized structures of (a) $C_9H_{11}Li$ (1p) (b) $C_9H_{11}Na$ (1p) (c) $C_9H_{11}K$ (1p) (d) $C_9H_{11}K$ (5p) (e) $C_9H_{11}K$ (9p) (f) $C_{10}H_{11}Li$ (5p) (g) $C_{10}H_{11}Na$ (5p) (h) $C_{10}H_{11}K$ (5p) [B3LYP/6-31G*]

3.2.2 Non coplanar metal substitution

The results of metal substitution primarily showed that the non-coplanar substitution of metallic species on odd polyenes induces a distortion in the planarity of the carbon skeleton, with considerable changes in the carbon-carbon bond lengths, bond angles and dihedral angles, in partial agreement with some earlier reports [2, 3, 4]. The distortion varies from minimum to intense, from system to system, depending upon the metal and substrate.

When the metal replaces a non-coplanar hydrogen on the sp^3 carbon (C1) in the polyene, at first the metal gets reduced to its cation and the polyene gets converted to an anion with a change of hybridization of C1 from sp^3 to sp^2. Therefore, metal substitution to odd numbered polyenes may be considered as identical to the doping of cations to the polyenyl anions. Non-coplanar substitution of the alkali metal on the sp^3 carbon of the conjugated polyene gave one isomer of the metal- polyene, with the metal being shifted to the adjacent carbon, either C2 or C3, depending on the nature of the metal. Besides, there occurred a rearrangement of the molecular parameters, giving a distorted or warped carbon skeleton. To probe into the possibility of existence of other stable isomers, if any, the metal ion was doped on different carbons of the polyenic anion and geometry optimizations were done. This procedure did reveal the existence of several isomers of polyenic metals with the metal positioned at a distance of 'Ri' above carbons other than C2 and C3. All these isomers were having lesser energy than their coplanar counterparts. The isomers thus obtained for various systems during the ab initio calculations have considerably high energy of reaction. The negative of the energy of reaction of the complex is taken as the stabilisation energy, E_{st}, of the species. It was determined by subtracting the energy of the optimized metal-polyene complex from the sum of the energies of metal ion (M^+) and

the polyenic anion $(C_nH_{n+2})^-$. The stable isomers obtained by the non-coplanar substitution of the metals with some of their notable characteristics are listed in Table 3.2.

Table 3.2: Stable isomers of different metal-polyene systems and their selected characteristics (6-31G* basis set)

Metal-polyene system	Method	Stable isomer [a]	E (Hartree)	Ri (A°)	E_{st} (kcal/mol)	Q_M (a.u)
C_3H_5Li	MP2	C_3H_5Li (2)	-124.31866	C2-Li=2.0681	187.21	0.321613
	B3LYP	C_3H_5Li (2)	-124.82471	C2-Li=2.0427	187.21	0.226123
C_3H_5Na	MP2	C_3H_5Na (2)	-278.69519	C2-Na=2.4290	156.90	0.513930
	B3LYP	C_3H_5Na (2)	-279.57534	C2-Na=2.3969	158.30	0.413044
C_3H_5K	MP2	C_3H_5K (2)	-715.99024	C2-K=2.8053	136.52	0.695855
	B3LYP	C_3H_5K (2)	-717.18307	C2-K=2.8074	135.69	0.603036
C_5H_7Li	MP2	C_5H_7Li (2) C_5H_7Li (3)	-201.48328 -201.47629	C2-Li=2.0649 C3-Li=2.0447	167.34 162.95	0.360135 0.313430
	B3LYP	C_5H_7Li (2) C_5H_7Li (3)	-202.22901 -202.21994	C2-Li= 2.0503 C3-Li= 2.0428	161.88 156.47	0.268910 0.221774
C_5H_7Na	MP2	C_5H_7Na (2) C_5H_7Na (3)	-355.86459 -355.86451	C2-Na=2.4349 C3-Na=2.4619	140.03 139.98	0.555994 0.520063
	B3LYP	C_5H_7Na (1) C_5H_7Na (3)	-356.98401 -356.98298	C1-Na=2.4122 C3-Na=2.4571	136.78 135.91	0.448987 0.362031
C_5H_7K	MP2	C_5H_7K (3)	-793.16404	C3-K=2.7625	122.41	0.698270
	B3LYP	C_5H_7K (3)	-794.59862	C3-K=2.7807	118.50	0.589575
C_7H_9Li	MP2	C_7H_9Li (2) C_7H_9Li (4)	-278.63486 -278.63238	C2-Li=2.0692 C4-Li=2.0636	155.55 153.99	0.373835 0.401254
	B3LYP	C_7H_9Li (2) C_7H_9Li (4)	-279.63708 -279.63333	C2-Li=2.0563 C4-Li=2.0512	149.83 147.73	0.286118 0.310325
C_7H_9Na	MP2	C_7H_9Na (2) C_7H_9Na (4)	-433.01766 -433.01669	C2-Na=2.4350 C4-Na=2.4264	129.17 128.56	0.573420 0.604455
	B3LYP	C_7H_9Na (2) C_7H_9Na (4)	-434.39363 -434.39119	C2-Na=2.4276 C4-Na=2.4017	125.68 124.60	0.471526 0.517614
C_7H_9K	MP2	C_7H_9K (3) C_7H_9K (4)	-870.31811 -870.31533	C3-K=2.7712 C4-K=2.7860	112.18 110.44	0.735153 0.797177
	B3LYP	C_7H_9K (3)	-872.00842	C3-K=2.7773	107.71	0.643907
$C_9H_{11}Li$	MP2	$C_9H_{11}Li$ (2) $C_9H_{11}Li$ (4)	-355.78630 -355.78411	C2-Li=2.0711 C4-Li=2.0672	147.36 145.99	0.379870 0.413597
	B3LYP	$C_9H_{11}Li$ (2) $C_9H_{11}Li$ (4)	-357.04515 -357.04137	C2-Li=2.0584 C4-Li=2.0558	141.41 139.29	0.294823 0.327068
$C_9H_{11}Na$	MP2	$C_9H_{11}Na$ (2) $C_9H_{11}Na$ (4)	-510.16988 -510.16983	C2-Na=2.4370 C4-Na=2.4291	121.47 121.44	0.582925 0.589690

	B3LYP	$C_9H_{11}Na$ (2)	-511.80260	C2-Na=2.4290	117.83	0.483759
		$C_9H_{11}Na$ (4)	-511.80076	C4-Na=2.4105	117.04	0.534838
		$C_9H_{11}Na$ (5)	-511.79955	C5-Na=2.4087	116.12	0.493544
$C_9H_{11}K$	MP2	$C_9H_{11}K$ (5)	-947.47212	C5-K=2.7702	105.61	0.766852
		$C_9H_{11}K$ (3)	-947.47152	C3-K=2.7751	105.23	0.746121
	B3LYP	$C_9H_{11}K$ (3)	-949.41836	C3-K=2.7826	100.47	0.659999
		$C_9H_{11}K$ (5)	-949.41799	C5-K=2.7755	100.44	0.695120
$C_{11}H_{13}Li$	MP2	$C_{11}H_{13}Li$ (2)	-432.93764	C2-Li=2.0716	141.30	0.383447
		$C_{11}H_{13}Li$ (6)	-432.93586	C6-Li=2.0692	140.19	0.424731
		$C_{11}H_{13}Li$ (4)	-432.93563	C4-Li=2.0685	140.05	0.418938
	B3LYP	$C_{11}H_{13}Li$ (2)	-434.45319	C2-Li=2.0603	135.12	0.300113
		$C_{11}H_{13}Li$ (4)	-434.44948	C4-Li=2.0578	133.05	0.334975
		$C_{11}H_{13}Li$ (6)	-434.44937	C6-Li=2.0586	132.99	0.341395
$C_{11}H_{13}Na$	MP2	$C_{11}H_{13}Na$ (6)	-587.32284	C6-Na=2.4291	116.43	0.629397
		$C_{11}H_{13}Na$ (4)	-587.32212	C4-Na=2.4306	115.98	0.625096
		$C_{11}H_{13}Na$ (2)	-587.32168	C2-Na=2.4371	115.70	0.588221
	B3LYP	$C_{11}H_{13}Na$ (2)	-589.21120	C2-Na=2.4302	111.92	0.491881
		$C_{11}H_{13}Na$ (6)	-589.21008	C6-Na=2.4152	111.48	0.548476
		$C_{11}H_{13}Na$ (4)	-589.20974	C4-Na=2.4150	111.29	0.543812
$C_{11}H_{13}K$	MP2	$C_{11}H_{13}K$ (5)	-1024.62543	C5-K=2.7783	100.79	0.773997
		$C_{11}H_{13}K$ (3)	-1024.62393	C3-K=2.7795	99.85	0.753244
	B3LYP	$C_{11}H_{13}K$ (5)	-1026.82776	C5-K=2.7830	95.24	0.706114
		$C_{11}H_{13}K$ (3)	-1026.82749	C3-K=2.7854	94.89	0.671424
$C_{13}H_{15}Li$	MP2	$C_{13}H_{15}Li$ (2)	-510.08892	C2-Li=2.0727	136.65	0.385466
		$C_{13}H_{15}Li$ (6)	-510.08740	C6-Li=2.0704	135.69	0.429343
		$C_{13}H_{15}Li$ (4)	-510.08702	C4-Li=2.0696	135.46	0.421843
	B3LYP	$C_{13}H_{15}Li$ (2)	-511.86118	C2-Li=2.0619	130.20	0.303510
		$C_{13}H_{15}Li$ (4)	-511.85754	C4-Li=2.0600	128.18	0.339446
		$C_{13}H_{15}Li$ (6)	-511.85744	C6-Li=2.0603	128.14	0.347855
$C_{13}H_{15}Na$	MP2	$C_{13}H_{15}Na$ (6)	-664.47506	C6-Na=2.4294	112.36	0.634970
		$C_{13}H_{15}Na$ (4)	-664.47396	C4-Na=2.4310	111.67	0.629002
		$C_{13}H_{15}Na$ (2)	-664.47324	C2-Na=2.4381	111.22	0.591863
	B3LYP	$C_{13}H_{15}Na$ (2)	-666.61960	C2-Na=2.4323	107.22	0.497573
		$C_{13}H_{15}Na$ (6)	-666.61887	C6-Na=2.4156	107.10	0.555448
		$C_{13}H_{15}Na$ (4)	-666.61834	C4-Na=2.4173	106.71	0.549120
$C_{13}H_{15}K$	MP2	$C_{13}H_{15}K$ (7)	-1101.77860	C7-K=2.7838	97.29	0.779432
		$C_{13}H_{15}K$ (5)	-1101.77777	C5-K=2.7836	96.80	0.778923
		$C_{13}H_{15}K$ (3)	-1101.77586	C3-K=2.7830	95.59	0.757878
	B3LYP	$C_{13}H_{15}K$ (7)	-1104.23727	C7-K=2.7895	91.29	0.714738
		$C_{13}H_{15}K$ (5)	-1104.23677	C5-K=2.7879	90.99	0.714258
		$C_{13}H_{15}K$ (3)	-1104.23621	C3-K=2.7880	90.46	0.679056

[a] The numeral in parentheses corresponds to the carbon above which the metal is stationed.

It is evident from Table 3.2 that the stable isomers have reasonably high E_{st}. The energy difference between the stable isomers of the same system

is very low. For example, $C_9H_{11}K$ (3) and $C_9H_{11}K$ (5) differ by an energy value of 0.233 kcal/mol. (B3LYP method). However, the isomers obtained via coplanar and non-coplanar substitutions differ considerably in their energies. For example, $C_9H_{11}K$ (1p) with an energy of –949.37826 Hartree differs from the stable isomer of the system, $C_9H_{11}K$ (3), (E = -949.47836 Hartree), by 25.16 kcal/mol. Similarly, the isomers $C_9H_{11}K$ (3) and $C_9H_{11}K$ (5p), E = -949.38870 Hartree, differ by 19.17 kcal/mol.

Generally speaking, the B3LYP and MP2 calculations give similar results. The position of the metals in different stable isomers is the same in both methods. However, there are certain discrepancies between the results of these two methods, when we discuss the order of stability of these isomers. For example, among the three isomers of $C_{13}H_{15}Na$, the order of stability is $C_{13}H_{15}Na$ (2) > $C_{13}H_{15}Na$ (6) > $C_{13}H_{15}Na$ (4), as per the B3LYP method. But in MP2 level, this order is changed as $C_{13}H_{15}Na$ (6) > $C_{13}H_{15}Na$ (4) > $C_{13}H_{15}Na$ (2). There are some more of such differences (see Table 3.2). Since we got the same set of stable isomers for these two methods, and since the energy difference between them in each method is almost insignificant, we just ignore these differences. Since the B3LYP and MP2 results are generally comparable, we have relied more on B3LYP for our further calculations because of its low computational cost.

The charges on the carbon atoms have great relevance when we discuss the position of the metal in the isomers. The stability of an isomer is related to the position of the metal. Hence, the Mulliken charges on the carbons of some sample polyenes, polyenic anions and the Li/Na/K polyenes, as recorded in the output file of the ab initio calculations (B3LYP) are presented in Tables 3.3 (a) to 3.3 (e). (Since our discussion is mainly based on B3LYP calculations, Mulliken values are taken from B3LYP results only)

Table 3.3(a): Mulliken charges (a.u) on the carbons in C_5H_8, $(C_5H_7)^-$ and C_5H_7M, where M= Li/Na/K.

System	C1	C2	C3	C4	C5
C_5H_8	-0.359	-0.059	-0.100	-0.105	-0.490
$(C_5H_7)^-$	-0.468	-0.039	-0.199	-0.039	-0.468
C_5H_7Li (2)	**-0.450**	**-0.078**	**-0.232**	-0.034	-0.389
C_5H_7Li (3)	-0.395	**-0.091**	**-0.238**	**-0.091**	-0.395
C_5H_7Na (1)	**-0.486**	**-0.108**	**-0.217**	-0.048	-0.404
C_5H_7Na (3)	**-0.431**	**-0.094**	**-0.226**	**-0.094**	**-0.431**
C_5H_7K (3)	**-0.466**	**-0.093**	**-0.253**	**-0.093**	**-0.466**

Table 3.3(b): Mulliken charges (a.u) on the carbons in C_7H_{10}, $(C_7H_9)^-$ and C_7H_9M, where M= Li/Na/K.

System	C1	C2	C3	C4	C5	C6	C7
C_7H_{10}	-0.490	-0.105	-0.100	-0.122	-0.126	-0.059	-0.358
$(C_7H_9)^-$	-0.444	-0.041	-0.187	-0.113	-0.187	-0.041	-0.444
C_7H_9Li (2)	**-0.447**	**-0.078**	**-0.237**	-0.096	-0.144	-0.055	-0.379
C_7H_9Li (4)	-0.388	-0.032	**-0.240**	**-0.116**	**-0.240**	-0.032	-0.388
C_7H_9Na (2)	**-0.479**	**-0.106**	**-0.224**	-0.112	-0.156	-0.055	-0.387
C_7H_9Na (4)	-0.404	-0.044	**-0.245**	**-0.146**	**-0.245**	-0.044	-0.404
C_7H_9K (3)	**-0.462**	**-0.098**	**-0.256**	**-0.155**	**-0.213**	-0.051	-0.400

Table 3.3(c): Mulliken charges (a.u) on the carbons in C_9H_{12}, $(C_9H_{11})^-$ and $C_9H_{11}M$, where M= Li/Na/K.

System	C1	C2	C3	C4	C5	C6	C7	C8	C9
C_9H_{12}	-0.491	-0.105	-0.100	-0.122	-0.126	-0.122	-0.125	-0.060	-0.358
$(C_9H_{11})^-$	-0.428	-0.045	-0.176	-0.113	-0.180	-0.113	-0.176	-0.045	-0.428
$C_9H_{11}Li$(2)	**-0.445**	**-0.079**	**-0.238**	-0.095	-0.144	-0.119	-0.139	-0.057	-0.372
$C_9H_{11}Li$(4)	-0386	-0.033	**-0.236**	**-0.120**	**-0.244**	-0.094	-0.143	-0.056	-0.378
$C_9H_{11}Na$(2)	**-0.475**	**-0.105**	**-0.226**	-0.111	-0.157	-0.119	-0.144	-0.056	-0.377
$C_9H_{11}Na$(4)	-0.400	-0.047	**-0.235**	**-0.150**	**-0.248**	-0.109	-0.155	-0.056	-0.387
$C_9H_{11}K$(3)	**-0.455**	**-0.098**	**-0.253**	**-0.157**	**-0.211**	-0.116	-0.153	-0.056	-0.385
$C_9H_{11}K$(5)	-0.398	-0.053	**-0.208**	**-0.162**	**-0.258**	**-0.162**	**0.208**	-0.053	-0.398

Table 3.3(d): Mulliken charges (a.u) on the carbons in $C_{11}H_{14}$, $(C_{11}H_{13})^-$ and $C_{11}H_{13}M$ where M= Li/Na/K

System	C1	C2	C3	C4	C5	C6	C7	C8	C9	C10	C11
$C_{11}H_{14}$	-0.358	-0.060	-0.124	-0.122	-0.125	-0.123	-0.126	-0.123	-0.010	-0.105	-0.491
$(C_{11}H_{13})^-$	-0.417	-0.047	-0.168	-0.115	-0.171	-0.114	-0.171	-0.115	-0.168	-0.047	-0.417
$C_{11}H_{13}Li$ (2)	**-0.444**	**-0.079**	**-0.238**	-0.094	-0.143	-0.119	-0.139	-0.120	-0.133	-0.057	-0.368
$C_{11}H_{13}Li$ (4)	-0.384	-0.034	**-0.233**	**-0.122**	**-0.244**	-0.093	-0.144	-0.120	-0.138	-0.057	-0.371
$C_{11}H_{13}Li$ (6)	-0.376	-0.057	-0.142	-0.096	**-0.239**	**-0.124**	**-0.239**	-0.096	-0.142	-0.057	-0.376
$C_{11}H_{13}Na$ (2)	**-0.472**	**-0.104**	**-0.227**	-0.111	-0.156	-0.119	-0.144	-0.120	-0.137	-0.057	-0.372
$C_{11}H_{13}Na$ (4)	-0.397	-0.048	**-0.230**	**-0.153**	**-0.247**	-0.109	-0.156	-0.120	-0.144	-0.056	-0.377
$C_{11}H_{13}Na$ (6)	-0.384	0.057	-0.153	-0.111	**-0.238**	**-0.154**	**-0.238**	-0.111	-0.153	-0.057	-0.387
$C_{11}H_{13}K$ (3)	**-0.451**	**-0.098**	**-0.252**	**-0.159**	**-0.207**	-0.117	-0.154	-0.121	-0.143	-0.056	-0.377
$C_{11}H_{13}K$ (5)	-0.394	-0.055	**-0.198**	**-0.162**	**-0.254**	**-0.165**	**-0.209**	-0.118	-0.152	-0.057	-0.383

Table 3.3(e): Mulliken charges (a.u) on the carbons in $C_{13}H_{16}$, $(C_{13}H_{15})^-$ and $C_{13}H_{15}M$ where M= Li/Na/K

System	C1	C2	C3	C4	C5	C6	C7	C8	C9	C10	C11	C12	C13
$C_{13}H_{16}$	-0.357	-0.060	-0.124	-0.122	-0.125	-0.123	-0.125	-0.123	-0.126	-0.123	-0.100	-0.105	-0.491
$(C_{13}H_{15})^-$	-0.409	-0.048	-0.162	-0.116	-0.166	-0.115	-0.165	-0.115	-0.166	-0.116	-0.162	-0.048	-0.409
$C_{13}H_{15}Li$(2)	**-0.443**	**-0.079**	**-0.238**	-0.095	-0.143	-0.120	-0.139	-0.120	-0.134	-0.121	-0.131	-0.058	-0.365
$C_{13}H_{15}Li$(4)	-0.383	-0.035	**-0.231**	**-0.123**	**-0.244**	-0.094	-0.143	-0.120	-0.139	-0.120	-0.133	-0.058	-0.367
$C_{13}H_{15}Li$(6)	-0.375	-0.057	-0.141	-0.096	**-0.237**	**-0.126**	**-0.239**	-0.095	-0.142	-0.121	-0.137	-0.058	-0.369
$C_{13}H_{15}Na$(2)	**-0.470**	**-0.103**	**-0.228**	-0.111	-0.156	-0.119	-0.144	-0.120	-0.138	-0.120	-0.134	-0.057	-0.369
$C_{13}H_{15}Na$(4)	-0.395	-0.049	**-0.226**	**-0.155**	**-0.247**	-0.109	-0.155	-0.120	-0.144	-0.120	-0.137	-0.057	-0.372
$C_{13}H_{15}Na$(6)	-0.381	-0.057	-0.151	-0.113	**-0.233**	**-0.158**	**-0.237**	-0.112	-0.153	-0.121	-0.142	-0.057	-0.375
$C_{13}H_{15}K$(3)	**-0.448**	**-0.099**	**-0.251**	**-0.160**	**-0.204**	-0.118	-0.153	-0.121	-0.143	-0.120	-0.137	-0.057	-0.372
$C_{13}H_{15}K$(5)	**-0.392**	**-0.056**	**-0.193**	**-0.163**	**-0.252**	**-0.168**	**-0.206**	**-0.119**	**-0.153**	-0.121	-0.142	-0.057	-0.378
$C_{13}H_{15}K$(7)	-0.380	-0.058	-0.149	-0.120	-0.199	-0.167	-0.250	-0.167	-0.199	-0.120	-0.149	-0.058	-0.380

The charge distribution highlights certain features in the polyenes. In all the systems, neutral, anionic and metal substituted polyenes, the terminal carbons possess the highest charges. In general, in all the neutral polyenes, the odd carbons have slightly higher charges than their neighbouring even carbons. This trend is retained in the polyenyl anions too. When the metals take position above different carbons, charges vary and the variation depends upon the nature of the segment pocketing the metal. For Li and Na, the carbon

on which the metal is stationed (even carbon) will have lesser charge and the two neighbouring atoms constituting an allylic segment will have higher charges. For K, the interaction involves a larger segment where the central carbon (odd carbon) will have higher charge that is repeated on alternate carbons of the interacting segment. The higher charges on different carbons of the polyenyl segment are highlighted in the Tables 3.3(a) to 3.3(e) by bold letters. The general trend, that the 'odd' having more and the 'even' having less, is more or less maintained.

When the charges on the hydrogens are summed on the heavier carbon atoms, the net charge on the carbons will be obtained. Table 3.4 gives the net charge on carbons of the different systems of the polyene C_9H_{12}.

Table 3.4: The net charge (a.u) on carbons (charges on hydrogens summed on carbons) in different systems (B3LYP/6-31G*).

System	C1	C2	C3	C4	C5	C6	C7	C8	C9
C_9H_{12}	-0.018	0.020	0.018	-0.001	-0.005	.00004	-0.003	0.065	-0.076
$(C_9H_{11})^-$	-0.283	0.019	-0.123	-0.050	-0.127	-0.050	-0.123	0.019	-0.283
$C_9H_{11}Li$ (2)	**-0.114**	**0.055**	**-0.033**	-0.012	-0.041	0.019	-0.097	0.068	-0.141
$C_9H_{11}Li$ (4)	-0.139	0.081	**-0.093**	**0.024**	**-0.101**	0.019	-0.042	0.052	-0.128
$C_9H_{11}Na$ (2)	**-0.200**	**0.030**	**-0.113**	-0.002	-0.060	-0.016	-0.044	0.051	-0.130
$C_9H_{11}Na$ (4)	-0.167	0.061	**-0.118**	**-0.017**	**-0.129**	-0.001	-0.061	0.046	-0.150
$C_9H_{11}K$ (3)	**-0.205**	**0.021**	**-0.156**	**-0.042**	**-0.108**	-0.013	-0.057	0.047	-0.146
$C_9H_{11}K$ (5)	-0.165	0.051	**-0.107**	**-0.047**	**-0.159**	**-0.047**	**-0.107**	0.051	-0.165

3.2.2.1 Position of the metal in the metal- polyenes

In all systems studied, the metal normally does not stay over the terminal carbon in the stable isomers. Usually, they stay above a carbon, odd or even, depending on the nature of the metal. Few metals stay exactly at 90^0 to the chain; very few of them maintain equal distance to the neighbouring carbons. For a comparison, some of these values are given in Table 3.5.

Table 3.5. Metal carbon distances and metal polyene bond angles in some selected systems (B3LYP/6-31G*).

System	C(i)- M (A^0)	C(i+1)-M (A^0)	C(i-1)-M (A^0)	MC(i)C(i+1) (deg.)	MC(i)H(i) (deg.)
$C_9H_{11}Li$ (2)	C2-Li=2.0584	C3-Li=2.1598	C1-Li=2.0968	74.42	118.60
$C_9H_{11}Li$ (4)	C4-Li=2.0558	C5-Li=2.1382	C3-Li=2.1420	73.56	118.32
$C_9H_{11}Na$ (2)	C2-Na=2.4290	C3-Na=2.6013	C1-Na=2.4547	80.68	112.65
$C_9H_{11}Na$ (4)	C4-Na=2.4105	C5-Na=2.5150	C3-Na=2.5432	77.49	112.40
$C_9H_{11}K$ (3)	C3-K=2.7826	C4-K=2.9550	C2-K=2.9382	82.78	89.35
$C_9H_{11}K$ (5)	C5-K=2.7755	C6-K=2.9464	C4-K=2.9464	82.57	91.10

Lithium is always positioned over an even carbon (e.g., 2, 4, 6, etc.), leading to several isomers that slightly differ in energy (even isomers). This even carbon is generally the 2nd (C2) in the most stable isomers, irrespective of the length of the carbon skeleton, which is in general agreement with the findings of Burke and Jesperson [2] (see Figure 3.3). The C (i)-M distance (Ri) is ca. 2.06 for Li. Except for the C_5 system, Na also gives even isomers, of which the most stable isomer has the metal over the C2 in most cases. The metal-carbon distance, Ri, is ca. 2.42 A^0 for Na-isomers.

(a) $C_9H_{11}^-$

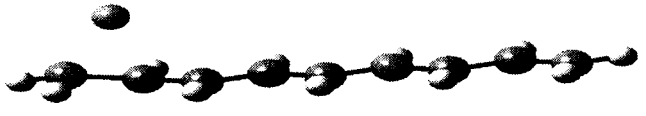

(b) $C_9H_{11}Li$ (2)

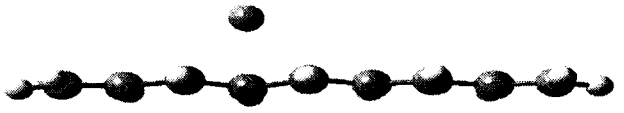

(c) $C_9H_{11}Li$ (4)

*rB

(d) $C_9H_{11}Na$ (2)

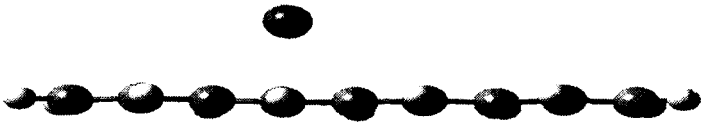

(e) $C_9H_{11}Na$ (4)

Figure 3.3: Optimized structures of the stable isomers of $C_9H_{11}Li$ & $C_9H_{11}Na$ (B3LYP/6-31G*)

Potassium, on the other hand, behaves in a totally different manner. Usually, it does not stay above an even carbon, but is stationed above an odd carbon. This odd carbon may be the centre of the polyene itself (e.g., at C3 in C_5H_7K and at C7 in $C_{13}H_{15}K$) or the centre of polyenic fragment containing odd number of carbons (e.g., at C3 in the fragment C_5H_7 of C_7H_9K and of $C_9H_{11}K$). K stays over an odd carbon, which causes a bend (warping) to the polyenic fragment. K usually forms only odd isomers. The C-M distance of K is ca. 2.78 A°, which is greater than that for Na and Li. It is curious to note that as the chain length increases, the most stable isomer of the polyenyl potassium tends to attain a symmetric shape (of a wide parabola) and it does so when the central carbon is odd as in $C_{13}H_{15}K$ (see Table 3.2). Figure 3.4 illuminates these features.

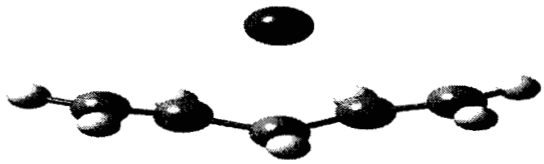

(a) C_5H_7K (3)

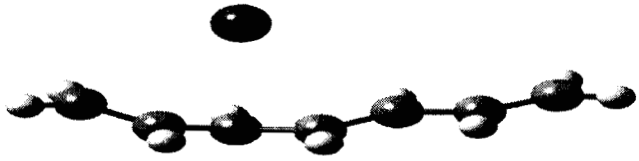

(b) C_7H_9K (3)

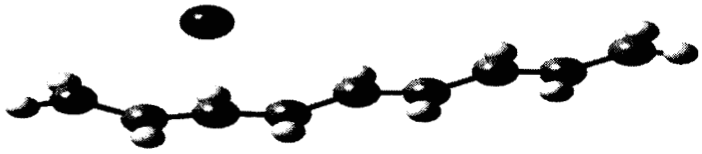

(c) $C_9H_{11}K$ (3)

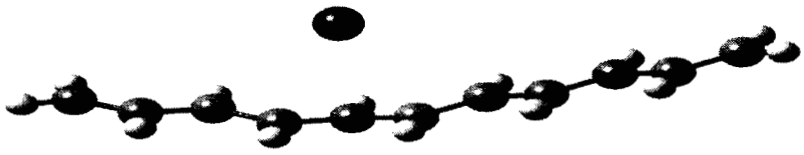

(d) $C_{11}H_{13}K$ (5)

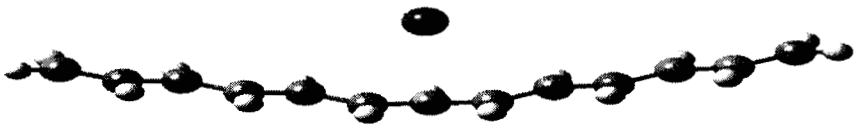

(e) $C_{13}H_{15}K$ (7)

Figure 3.4: The most stable isomers of different potassium- polyene systems (B3LYP/ 6-31G*)

As a sample study, we examined the effect of K-substitution on $C_{25}H_{28}$ at a low level Hartree-Fock method using 3-21G basis set. The results obtained are given in Table 3.6(a).

Table 3.6(a): The stable isomers of $C_{25}H_{27}K$ with their selected characteristics (HF/3-21G).

Stable isomer [a]	E (Hartree)	Ri (A^o)	Q_M (a.u)	$\Delta E=E_L-E_H$ (Hartree)
$C_{25}H_{27}K$ (3)	-1553.04253	2.7830	0.756617	0.16290
$C_{25}H_{27}K$ (5)	-1553.04429	2.7910	0.780508	0.16098
$C_{25}H_{27}K$ (7)	-1553.04543	2.7922	0.783187	0.16031
$C_{25}H_{27}K$ (9)	-1553.04595	2.7929	0.784499	0.15955
$C_{25}H_{27}K$ (11)	-1553.04617	2.7940	0.785037	0.15910
$C_{25}H_{27}K$ (13)	-1553.04623	2.7942	0.785190	0.15897

The different isomers obtained for $C_{25}H_{27}K$ confirm the tendency of K to move towards the centre, when it is substituted in a polyene. Of the six isomers obtained, $C_{25}H_{27}K$ (13) has got the lowest energy. The various isomers differ by small quantities of energy. The small energy difference between the isomers indicates the possibility for inter conversion between the isomers.

B3LYP calculations using 3-21G basis set for rubidium substituted $C_{13}H_{16}$ also showed the same trend as that of potassium. The results obtained for Rb substitution are presented in Table 3.6(b).

Table 3.6(b): Stable isomers of $C_{13}H_{15}Rb$ and their selected characteristics (B3LYP/3-21G)

Stable isomer [a]	E (Hartree)	Ri (A^o)	E_{st} (kcal/mol)	Q_M (a.u)	$\Delta E=E_L-E_H$ (Hartree)
$C_{13}H_{15}Rb$ (3)	-3428.10993	2.8917	94.35	0.671372	0.06067
$C_{13}H_{15}Rb$ (5)	-3428.11112	2.8952	95.10	0.698664	0.06157
$C_{13}H_{15}Rb$ (7)	-3428.11184	2.8990	95.55	0.699422	0.06275

The above results may be an indication to suggest that all large sized metals, when substituted in non-coplanar mode to the polyenes, always stick on to an odd carbon, which in turn will always be the centre of a polyenic fragment of odd carbons. The optimized structures of the stable isomers of $C_{13}H_{15}Rb$ are given below in Figure 3.5.

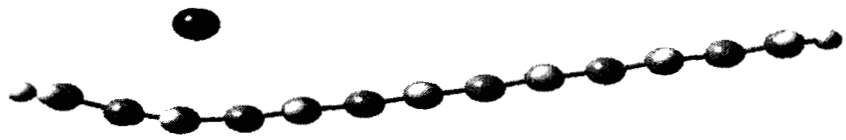

(a) $C_{13}H_{15}Rb$ (3)

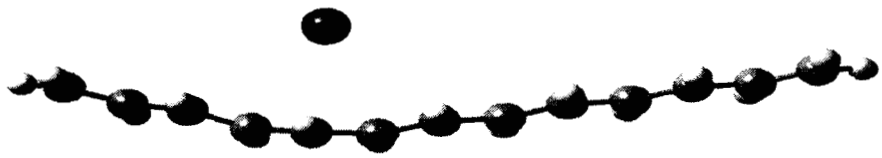

(b) $C_{13}H_{15}Rb$ (5)

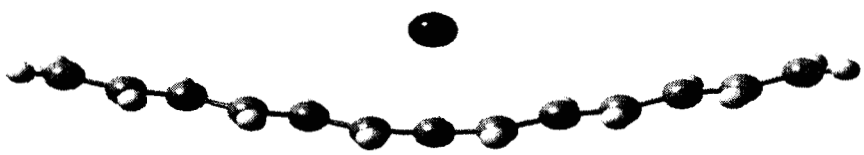

(c) $C_{13}H_{15}Rb$ (7)

Figure 3.5: Optimized structures of the stable isomers of $C_{13}H_{15}Rb$ (B3LYP/3-21G)

We have also examined the possibilities of locating odd isomers for Li and Na and even isomers for K and got some interesting results. Li gave an odd isomer only in the C_5 system, possessing a central odd carbon i.e., [C_5H_7Li (3)]. On the other hand, Na gave a high-energy odd isomer in all systems where an odd carbon is the centre of the polyene [e.g., are C_5H_7Na (3), $C_9H_{11}Na$ (5), $C_{13}H_{15}Na$ (7), etc.]. Similarly, with K, even isomers of high

energy are possible if the even carbon is the centre of a polyene. Examples for such isomers are C_7H_9K (4) and $C_{11}H_{13}K$ (6). In C_5 system, C_5H_7Li (3) has an optimized energy of –202.21994 Hartree, which is 4.39 kcal higher than that of the most stable isomer C_5H_7Li (2). Similarly, C_7H_9K (4) has an optimized energy of -870. 31533 Hartree, 1.74 kcal higher than that of the most stable isomer C_7H_9K (3) and $C_9H_{11}Na$ (5) has an optimized energy of -511.79955 Hartree, 1.95 kcal higher than that of the most stable isomer of the system $C_9H_{11}Na$ (2). Typical optimized structures of these three isomers are given in Figure 3.6.

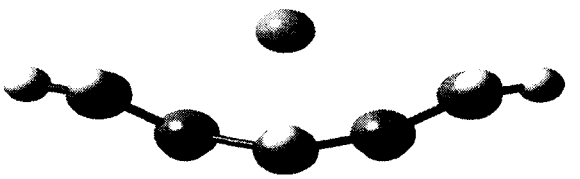

(a) C_5H_7Li (3)

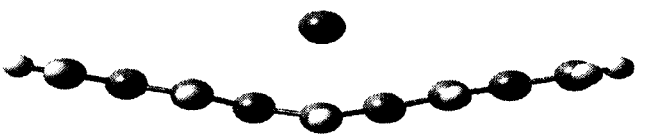

(b) $C_9H_{11}Na$ (5)

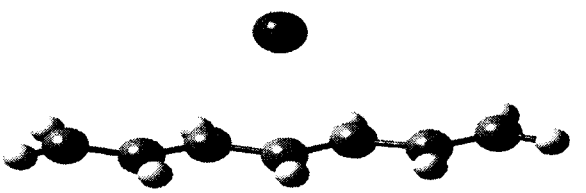

(c) C_7H_9K (4)

Figure 3.6: Optimized structures of the high-energy isomers (a) C_5H_7Li (3), (b) $C_9H_{11}Na$ (5) and (c) C_7H_9K (4) [B3LYP/6-31G*].

3.2.2.2 Effect of the position of metal on molecular parameters

The presence of the metal over a particular carbon causes a total rearrangement of the molecular parameters like bond length, bond angle and dihedral angle. Along with that, there is substantial change in the shape of the resultant species. All these may be indications to the interaction between the metal and the polyene.

(a) Localization of the delocalised π- cloud of the polyene

The B3LYP values of the C-C bond lengths in some of the systems are given in Table 3.7(a) and MP2 values in Table 3.7(b).

Table 3.7(a): Carbon- carbon bond lengths (A^0) in different polyenic systems (B3LYP/6-31G*)

System	C1-C2	C2-C3	C3-C4	C4-C5	C5-C6	C6-C7	C7-C8	C8-C9
C_9H_{12}	1.4983	1.3469	1.4461	1.3563	1.4406	1.3560	1.4476	1.3442
$(C_9H_{11})^-$	1.3613	1.4277	1.3864	***1.4047***	***1.4047***	1.3864	1.4277	1.3613
$C_9H_{11}Li$ (2)	***1.4008***	***1.4087***	1.4365	1.3644	1.4351	1.3597	1.4453	1.3461
$C_9H_{11}Li$ (4)	1.3473	1.4496	***1.4042***	***1.4090***	1.4397	1.3606	1.4451	1.3464
$C_9H_{11}Na$ (2)	***1.4036***	***1.4043***	1.4251	1.3718	1.4304	1.3628	1.4433	1.3475
$C_9H_{11}Na$ (4)	1.3515	1.4434	***1.4016***	***1.4096***	1.4315	1.3663	1.4421	1.3486
$C_9H_{11}K$ (5)	1.3515	1.4410	1.3863	***1.4121***	***1.4121***	1.3862	1.4410	1.3515
$C_9H_{11}K$ (3)	1.3752	1.42	***1.4041***	***1.3932***	1. 4281	1.3666	1. 4413	1. 3490

Table 3.7(b): Carbon- carbon bond lengths (A^0) in different polyenic systems (MP2/6-31G*)

System	C1-C2	C2-C3	C3-C4	C4-C5	C5-C6	C6-C7	C7-C8	C8-C9
C_9H_{12}	1.4947	1.3479	1.4453	1.3559	1.4408	1.3554	1.4475	1.3455
$(C_9H_{11})^-$	1.3597	1.4264	1.3833	**1.4017**	**1.4017**	1.3833	1.4264	1.3597
$C_9H_{11}Li$ (2)	**1.3994**	**1.4053**	1.4368	1.3618	1.4356	1.3579	1.4457	1.3465
$C_9H_{11}Na$ (2)	**1.3987**	**1.4042**	1.4265	1.3678	1.4311	1.3605	1.4439	1.3474
$C_9H_{11}K$ (3)	1.3730	**1.4182**	**1.4008**	1.3911	1.4277	1.3645	1.4413	1.3490
$C_9H_{11}K$ (5)	1.3514	1.4405	1.3841	**1.4088**	**1.4088**	1.3841	1.4405	1.3514

(From Tables 3.7(a) & 3.7(b), it is evident that both B3LYP and MP2 methods give almost identical values for the structural parameters. So, in the subsequent discussions, only B3LYP values are presented.)

The table shows that the C-C bond lengths in the free C_9H_{12} are not the typical single bond and double bond values (1.54 A^0 and 1.34 A^0 respectively). This change is due to the slight delocalisation of the electron cloud as a result of the extended conjugation. These bond lengths are substantially changed when the polyene is converted to its anion. There is intense delocalisation of the electron cloud and the central bonds attain identical bond lengths [see the C4-C5 and C5-C6 values of $(C_9H_{11})^-$ in Table 3.7] indicating total delocalisation at the centre. When a cation is doped to such an anion, i.e., when metal is substituted, the delocalised electron cloud on the polyene is dragged to the polyenic fragment on which the metal is stationed. This is evident from the bond length values inside the polyenic segment where these values are almost equal (showed in bold italics)-closer to the C-C bond length in the perfectly delocalised system benzene, i.e., 1.3966 A^0 (B3LYP/6-31G*). On the other hand, the bond length values outside the area of metal interaction are only slightly changed in comparison with the bond length values of the free polyene. These results strongly suggest that there exists an interaction between the cation and the highly delocalised π-electron cloud inside the polyenic segment.

(b) Distortion of the carbon skeleton of the polyene

Besides the change in the bond lengths, there is considerable change in the bond angles and dihedral angles, when a metal is substituted to the polyene in a non-coplanar fashion. This is an indication to the distortion of the carbon skeleton due to the metal substitution. The bond angles that we observe in the free polyene have been considerably altered in the polyenic portions where the metal resides. Also, the change in the dihedral angles

throws light into the influence that the substituted metal exerts on the carbon skeleton so as to distort its planarity. Selected bond angles and dihedral angles presented in Table 3.8(a) and Table 3.8(b) amply illustrate this fact.

Table 3.8(a): Selected bond angles in free C_9H_{12}, $(C_9H_{11})^-$ and the most stable metal- polyenes (B3LYP/6-31G*).

System	H1C1C2	C1C2C3	C2C3C4	C3C4C5	C4C5C6	C5C6C7	C6C7C8	C7C8C9	C8C9H9
C_9H_{12}	111.30	125.14	124.49	124.52	124.41	124.64	124.24	124.64	121.53
$(C_9H_{11})^-$	121.62	128.66	123.8	128.70	123.89	128.70	123.78	128.68	121.61
$C_9H_{11}Li$ (2)	119.50	126.37	124.08	126.99	123.92	125.83	124.03	125.49	121.57
$C_9H_{11}Na$ (2)	119.70	128.16	124.28	127.33	123.96	126.27	124.00	125.82	121.74
$C_9H_{11}K$ (3)	120.94	127.39	122.55	127.60	124.17	127.03	123.94	126.25	121.59

Table 3.8(b): Selected dihedral angles in free C_9H_{12}, $(C_9H_{11})^-$ and the most stable metal- polyenes (B3LYP/6-31G*)

System	H1C1C2C3	C1C2C3C4	C2C3C4C5	C3C4C5C6	C4C5C6C7	C5C6C7C8	C6C7C8C9	C7C8C9H9
C_9H_{12}	0.0	180.0	-180.0	-180.0	180.0	180.0	-180.0	0.0
$(C_9H_{11})^-$	0.0	180.0	-180.0	180.0	-180.0	180.0	-180.0	0.0
$C_9H_{11}Li$ (2)	**-26.20**	**-172.5**	**-172.89**	-179.09	-180.00	179.99	179.80	0.07
$C_9H_{11}Na$ (2)	**-21.65**	**-172.0**	**-179.26**	-178.82	179.55	-179.84	179.82	0.12
$C_9H_{11}K$ (3)	**-12.94**	**-150.58**	**-153.94**	**-175.26**	179.60	-178.77	179.29	0.24

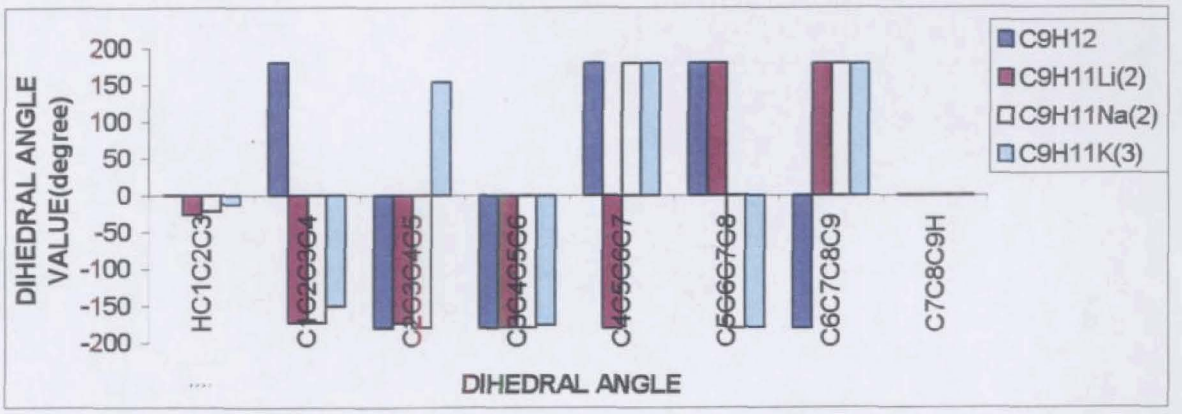

Figure 3.7: Graphical representation of the dihedral angles in C_9H_{12}, $C_9H_{11}Li$ (2), $C_9H_{11}Na$ (2) and $C_9H_{11}K$ (3).

The distortion in the planarity of the carbon skeleton on substitution is evident from Figures 3.3 to 3.6 and its intensity may be ascertained from the Tables 3.8(a) & 3.8(b). Figure 3.7 gives a comparison of the deviations in the carbon skeletons in terms of the changes in dihedral angles. Lithium and sodium, which form $C_nH_{n+2}M(i)$ type complexes where i = 2, 4, 6, etc., (even isomers), do not evoke considerable distortion on the carbon skeleton. But, potassium and higher members (e.g., rubidium), which form $C_nH_{n+2}M$ (i) type complexes, where i = 3, 5, 7, etc., (odd isomers), do cause a substantial distortion in the shape of the complex. In fact, the K-polyenes attain a warped shape, with the metal above the centre of a carbon pocket, always maintaining minimum most distance from the central carbon. The bent of the structure is towards the metal.

It may also be noted that the even isomers of potassium [e.g. C_7H_9K (4)] do not show warping, whereas, the odd isomers of Na [e.g., $C_9H_{11}Na$ (5)] do show warping (Figure 3.6). Thus, it appears that, the doped metal should stay over the odd carbon in order to effect a considerably warped carbon skeleton.

3.2.2.3 Enhancement of the conductance

The decreased gap between the HOMO and LUMO of the metal-polyenes suggests that as a result of metal substitution, there is a red shift in the optical properties of the metal-polyenes. This would also mean that the conductance of the system increases considerably on metal substitution. The HOMO energy (E_H) and LUMO energy (E_L) values of several systems are presented in Table 3.9.

Table 3.9: HOMO & LUMO energy values of different systems (B3LYP/6-31G*).

System	E_H (Hartree)	E_L (Hartree)	$\Delta E = E_L - E_H$ (kcal/mol)
C_9H_{12}	-0.19034	-0.05269	86.38
$(C_9H_{11})^-$	0.01951	0.12755	67.80
$C_9H_{11}Li$ (2)	-0.14841	-0.05333	59.66
$C_9H_{11}Na$ (2)	-0.13089	-0.07463	35.30
$C_9H_{11}K$ (3)	-0.12253	-0.06231	37.79
$C_{11}H_{14}$	-0.18318	-0.06239	75.80
$C_{11}H_{13}Li$ (2)	-0.14698	-0.05621	56.96
$C_{11}H_{13}Na$ (2)	-0.13120	-0.07767	33.59
$C_{11}H_{13}K$ (5)	-0.12304	-0.06542	36.16
$C_{13}H_{16}$	-0.17795	-0.06940	68.12
$C_{13}H_{15}Li$ (2)	-0.14602	-0.05874	54.77
$C_{13}H_{15}Na$ (2)	-0.13149	-0.08004	32.29
$C_{13}H_{15}K$ (7)	-0.12501	-0.06849	35.47
$C_{25}H_{27}K$ (13)	-0.13002	-0.07906	31.98
$C_{33}H_{35}K$ (17)	-0.13150	-0.08218	30.95

It can be seen from Table 3.9 that, as expected, the conductance increases as the length of the polyene increases. Maximum conductance is attained when Na is the substituent. It is curious to note that the effect of Na on conductance is not intermediate between that of Li and K, as one would expect from periodic behaviour.

3.2.2.4 Formation of different isomers

We have found that the doping of metal cation on to the polyenyl anion at different sites provided a number of stable isomers. As the length of the polyene increases, the number of isomers also increases (Table 3.2). We have identified that the C_3 system has only one isomer each for Li, Na and K,

namely C_3H_5M (2), where M= Li/Na/K. For C_5 system, K has only one isomer, i.e., C_5H_7K (3); but Na and Li have two isomers each, C_5H_7M (2) and C_5H_7M (3), where M= Li or Na. C_7 system forms two isomers each with Li, Na and K- C_7H_9Li (2) and C_7H_9Li (4) for Li, C_7H_9Na (2) and C_7H_9Na (4) for Na, but C_7H_9K (3) and C_7H_9K (4) for K, the K (4) isomer being revealed in the MP2 level calculation only. Table 3.2 shows the stable isomers of Li, Na and K for the C_3 to C_{13} systems. These isomers are very close in their energies. For example, the two isomers $C_9H_{11}K$ (3) and $C_9H_{11}K$ (5) differ by an energy value of mere 0.25 kcal/mol (B3LYP level). Of the three isomers of $C_{13}H_{15}K$, the most stable $C_{13}H_{15}K$ (7) differs from $C_{13}H_{15}K$ (3) by 0.67 kcal/mol (B3LYP level). Similarly, of the three isomers of $C_{13}H_{15}Rb$, the most stable $C_{13}H_{15}Rb$ (7) differs from the next isomer $C_{13}H_{15}Rb$ (5) by an energy of mere 0.45 kcal/mol and the total energy difference between the most stable one and the least stable $C_{13}H_{15}Rb$ (3) is just 1.2 kcal/mol [calculations at B3LYP/ 3-21G basis set, see Table 3.6(b)]. The small difference in the energies of the isomers implies the possibility of inter conversion between the isomers even at the availability of slight amount of energy. This scenario assumes more significance when we consider large systems, where there will be a number of isomers, each differing from the other by a small quantum of energy. This means, at a slight provocation, the metal cations will move throughout the chain, causing a migration of the delocalised π-cloud along with it.

3.3 Alkali metal substitution to substituted polyenes

When substituents are present on the polyene, they would exert some influence on the formation of metal polyenes. The influence will vary according to the nature of the substituents. If electron-withdrawing groups are present, they will adversely affect those reactions that are actually electrophilic. On the other hand, electron-donating groups will enhance the

rate of such reactions. Similarly, the interactions involving the π-cloud will be enhanced by electron donating groups and decreased by electron withdrawing groups. Unless other interactions are possible, the stabilization energy values will manifest the increase or decrease in the interaction.

We have already noted that the metal substitution is actually analogous to doping of metal ions to the polyenyl anion. In polyenyl anion, the extra electron present oscillates along the polyene exhibiting efficient pi-cloud delocalisation. In metal-polyenes this delocalised electron cloud is somewhat localized in a segment and it interacts strongly with the metal. When electron-donating groups are introduced in the polyene, there will be more cation-π interaction, provided the substituent sufficiently enriches the pi-cloud. On the other hand, when electron-withdrawing groups are the substituents in the polyene, the results will be just the opposite. When the pi- cloud is strongly withdrawn, cation-π interaction will diminish which will have a destabilizing effect on the metal polyenes. In order to verify these aspects, the metals were substituted on selected substituted polyenes and the subsequent changes were studied. For the sample study, C_9H_{12} system was selected along with an electron-donating group CH_3 and an electron-withdrawing group CN as the substituents.

3.3.1 Metal substitution to $C_9H_{11}CH_3$

At first, the methyl group was substituted on the carbon on which the metal stationed when it was substituted in the free polyene. This is C2 for Li and Na and C3 for K. The alkali metal was then substituted on the sp^3 carbon of $C_9H_{11}CH_3$ (j), where j =2 for Li and Na and j =3 for K. It was followed by substituting the metal on the sp^3 carbon of the polyene in which methyl group is substituted on its central carbon (C5). The most stable metal polyenes of C_9H_{12} and $C_9H_{11}CH_3$ systems with the alkali metals are presented in Table 3.10.

Table 3.10: The stable isomers of different metal-polyenes and methyl-substituted metal-polyenes and their selected characteristics (B3LYP/6-31G*).

Metal-polyene system	E (Hartree)	Ri (A°)	E_{st} (kcal/mol)	Q_M (a.u)	$\Delta E = E_L - E_H$ (Hartree)
$C_9H_{11}Li$ (2)	-357.04515	C2-Li=2.0584	141.41	0.294823	0.09508
$C_9H_{10}CH_3$ (2) Li (2)	-396.36049	C2-Li=2.0826	141.34	0.292159	0.09325
$C_9H_{10}CH_3$ (5) Li (2)	-396.36019	C2-Li=2.0590	141.29	0.295651	0.09450
$C_9H_{11}Na$ (2)	-511.80260	C2-Na=2.4290	117.83	0.483759	0.05626
$C_9H_{10}CH_3$ (2) Na (2)	-551.11731	C2-Na=2.4624	117.38	0.479902	0.05396
$C_9H_{10}CH_3$ (5) Na (2)	-551.11741	C2-Na=2.4251	117.62	0.490392	0.05580
C_9H_{11} K (3)	-949.41836	C3-K=2.7826	100.47	0.659999	0.06022
$C_9H_{10}CH_3$ (3) K (3)	-988.73781	C3-K=2.8088	102.25	0.598067	0.06784
$C_9H_{10}CH_3$ (5) K (5)	-988.73645	C5-K=2.7964	102.27	0.632005	0.06650
$C_9H_{10}CH_3$ (5) K (3)	-988.73186	C3-K=2.7932	99.56	0.685565	0.08260

It can be found from Table 3.10 that when metal was substituted on the sp^3 carbon of a methyl (CH_3) substituted polyene, the stabilisation energy is slightly decreased for Li and Na, but increased for K. In all the three cases metal-carbon distances (Ri) increase and charges on the metal decrease. Increase in the conductance is only for Li and Na complexes. In the case of K, the substitution of electron donating group decreases the conductance.

The measure of Mulliken charges present on the carbons on the polyene is another pointer to the interactive forces present in the system. For a comparison, the Mulliken charges on the carbons in different systems are presented in Table 3.11.

Table 3.11: Mulliken charges (a.u) on the carbons of Li/Na/K substituted C_9H_{12} & $C_9H_{11}CH_3$ (B3LYP/6-31G*).

System	C1	C2	C3	C4	C5	C6	C7	C8	C9
C_9H_{12}	-0.018	0.020	0.018	-0.001	-0.005	.00004	-0.003	0.065	-0.076
$C_9H_{11}Li$ (2)	**-0.445**	**-0.079**	**-0.238**	-0.095	-0.144	-0.119	-0.139	-0.057	-0.372
$C_9H_{10}CH_3$ (2) Li (2)	**-0.483**	**0.197**	**-0.297**	-0.093	-0.141	-0.121	-0.140	-0.057	-0.373
$C_9H_{10}CH_3$ (5) Li (2)	**-0.446**	**-0.071**	**-0.243**	-0.167	0.165	-0.172	-0.143	-0.050	-0.375
$C_9H_{11}Na$ (2)	**-0.475**	**-0.105**	**-0.226**	-0.111	-0.157	-0.119	-0.144	-0.056	-0.377
$C_9H_{10}CH_3$ (2) Na (2)	**-0.514**	**0.189**	**-0.293**	-0.106	-0.154	-0.121	-0.145	-0.056	-0.379
$C_9H_{10}CH_3$ (5) Na (2)	**-0.475**	**-0.098**	**-0.231**	-0.181	0.154	-0.173	-0.148	-0.049	-0.380
$C_9H_{11}K$ (3)	**-0.455**	**-0.098**	**-0.253**	**-0.157**	**-0.211**	-0.116	-0.153	-0.056	-0.385
$C_9H_{10}CH_3$ (3) K (3)	**-0.437**	**-0.148**	**0.060**	**-0.218**	**-0.200**	-0.114	-0.151	-0.057	-0.382
$C_9H_{10}CH_3$ (5) K (5)	-0.395	-0.049	**-0.199**	**-0.218**	**0.059**	**-0.217**	**-0.199**	-0.049	-0.395
$C_9H_{10}CH_3$ (5) K (3)	**-0.461**	**-0.103**	**-0.255**	**-0.227**	**0.109**	-0.173	-0.157	-0.050	-0.387

The enhanced negative charge on the carbons in the vicinity of the metal shows that the interaction between the metal and the cation is governed by electrostatics also. The positive charge on the carbon carrying the CH_3 is due to the replacement of hydrogen by carbon. The general trend that the even carbon carrying less negative charge and the odd carbon carrying more negative charge is true for substituted polyenes too.

The nature of the C-C bonds in the vicinity of the metal also gives a picture about the interaction in the system. C-C bond length values in concerned systems are presented in Table 3.12.

Table 3.12: Carbon-carbon bond lengths (A^0) in Li/Na/K substituted C_9H_{12} & $C_9H_{11}CH_3$ systems (B3LYP/6-31G*)

System	C1-C2	C2-C3	C3-C4	C4-C5	C5-C6	C6-C7	C7-C8	C8-C9
C_9H_{12}	1.4983	1.3469	1.4461	1.3563	1.4406	1.3560	1.4476	1.3442
$C_9H_{11}Li$ (2)	**1.4008**	**1.4087**	1.4365	1.3644	1.4351	1.3597	1.4453	1.3461
$C_9H_{10}CH_3$ (2) Li (2)	**1.4052**	**1.4185**	1.4354	1.3663	1.4341	1.3603	1.4449	1.3463
$C_9H_{10}CH_3$ (5) Li (2)	**1.4001**	**1.4104**	1.4375	1.3702	1.4457	1.3594	1.4472	1.3456
$C_9H_{11}Na$ (2)	**1.4036**	**1.4043**	1.4251	1.3718	1.4304	1.3628	1.4433	1.3475
$C_9H_{10}CH_3$ (2) Na (2)	**1.4069**	**1.4141**	1.4231	1.3746	1.4290	1.3637	1.4427	1.3478
$C_9H_{10}CH_3$ (5) Na (2)	**1.4020**	**1.4071**	1.4267	1.3773	1.4463	1.3626	1.4453	1.3469
$C_9H_{11}K$ (3)	**1.3752**	**1.4200**	**1.4041**	**1.3932**	1.4281	1.3666	1.4413	1.3490
$C_9H_{10}CH_3$ (3) K (3)	**1.3737**	**1.4276**	**1.4110**	**1.3926**	1.4318	1.3648	1.4421	1.3484
$C_9H_{10}CH_3$ (5) K (5)	1.3499	1.4446	**1.3859**	**1.4187**	**1.4187**	**1.3859**	1.4446	1.3499
$C_9H_{10}CH_3$ (5) K (3)	**1.3763**	**1.4211**	**1.4080**	**1.3966**	1.4349	1.3673	1.4431	1.3486

The bond length values show that the delocalisation of the pi electron cloud along the polyene is slightly modified in substituted metal-polyenes. The retention of delocalisation and the decrease in the charge on the metal imply slightly improved cation- π interaction, which is more effective in the case of K-substituted polyenes. However, when the methyl group is substituted on C5, there is decrease in the E_{st} and increase in the charge on the metal, which implies a less effective cation- π interaction. The structures of these species will explain more and they are given in Figure 3.8.

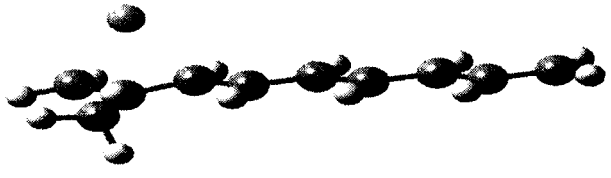

(a) $C_9H_{10}CH_3$ (2) Li (2)

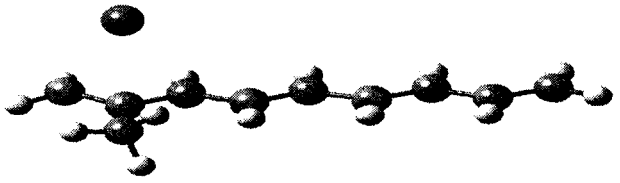

(b) $C_9H_{10}CH_3$ (2) Na (2)

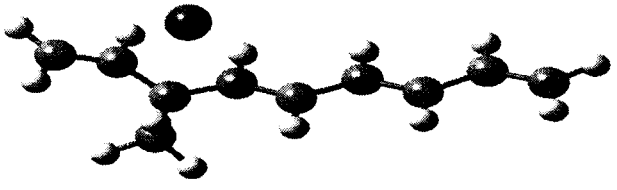

(c) $C_9H_{10}CH_3$ (3) K (3)

Figure 3.8: Optimized structures Li/Na/K substituted $C_9H_{11}CH_3$

(B3LYP/6-31G*)

3.3.2 Metal substitution to $C_9H_{11}CN$

The strong electron-withdrawing group, CN, was introduced into polyene C_9H_{12} and substitution of metals was done in the same fashion as in the previous section. When highly electronegative groups are present in the chain, there is a possibility of metal ion interacting with that group. Such an interaction will render extra stability to the system. This is more prominent in the case of larger ions like K^+, Rb^+ etc. If we could minimize the possibility for metal ion-CN interaction, the E_{st} values will be a good index to the nature of interaction in such polyenes. The results obtained when alkali metals were substituted to $C_9H_{11}CN$ are presented in Table 3.13.

Table 3.13: The most stable isomers of different metal-polyenes and CN substituted metal-polyenes and their selected characteristics (B3LYP/6-31G*).

Metal-polyene system	E (Hartree)	Ri (A°)	E_{st} (kcal/mol)	Q_M (a.u)	$\Delta E=E_L-E_H$ (Hartree)
$C_9H_{11}Li$ (2)	-357.04515	C2-Li=2.0584	141.41	0.294823	0.09508
$C_9H_{10}CN$ (2) Li (2)	-449.28648	C2-Li=2.0740	130.98	0.344380	0.09418
$C_9H_{10}CN$ (5) Li (2)	-449.29822	C2-Li=2.0920	130.37	0.337202	0.10443
$C_9H_{11}Na$ (2)	-511.80260	C2-Na=2.4290	117.83	0.483759	0.05626
$C_9H_{10}CN$ (2) Na (1)[a]	-604.05125	C1-Na=2.4308	111.72	0.447912	0.07608
$C_9H_{10}CN$ (5) Na (3)[b]	-604.07330	C3-Na=2.5413	117.57	0.505684	0.08718
$C_9H_{11}K$ (3)	-949.41836	C3-K=2.7826	100.47	0.659999	0.06022
$C_9H_{10}CN$ (3) K (1)[c]	-1041.6908	C1-K=3.0227	100.83	0.696237	0.08051

[a] Na, which was originally on C2 moves towards C1 and resides between C1 and CN to interact with CN, C1-Na=2.4308 and Na-CN=2.5998.

[b] Na moves towards C3 and interacts with the CN; note that Na-N=2.4183, but C3-Na=2.5413 and the complex has almost the same E_{st}.

[c] K, which was originally on C3 moves towards C1 and resides between C1 and CN to have strong interaction with CN.

From Table 3.13, it can be seen that E_{st} of $C_9H_{10}CN$ (2) Li (2) and $C_9H_{10}CN$ (2) Na (2) are less in comparison with their parent systems, namely, $C_9H_{11}Li$ (2) and $C_9H_{11}Na$ (2). In the former set of complexes, Li possesses a higher charge (due to less efficient cation - π interaction) and its distance from the carbon (C2) is larger than that in $C_9H_{11}Li$ (2). However, charge on Na in $C_9H_{10}CN$ (2) Na (1) is lesser than that on Na in $C_9H_{11}Na$ (2). Na moves away from C2 to a position from where it will have an effective interaction with the CN group. The C2-C-N bond angle that was 179.1^0 in $C_9H_{11}CN$ (2) distorts towards the metal and it becomes 167.02^0 in $C_9H_{10}CN$ (2) Na (1), which indicates a slight interaction between the metal and CN group.

There are systems in which the stabilization energy increases as the result of CN substitution. In such cases, the metals possess increased charges, which implies decreased cation-π interaction. These metals, though doped on different carbons, move to positions where they will have efficient interaction with the CN group. For example, in $C_9H_{10}CN$ (5) Na (3), Na, which was originally doped on C2, moves towards CN (substituted on C5) and rests at a position between C3 & C4. The distances of Na from different carbons are the following: C2-Na=3.4709 A^0, C3-Na=2.5413 A^0, C4-Na=2.8132 A^0, C^1-Na=2.5015 A^0 (C^1 is the carbon of CN group). Similar is the case with $C_9H_{10}CN$ (3) K (1). Here K, doped on C3, moves away from C3 and remains at a position closer to both C1 & C^1. The distances of K from different carbons are the following: C3-K=3.0527 A^0, C2-K=3.0734 A^0, C1-K=3.0227 A^0, C^1-K=2.7703 A^0. The bond angle C3-C^1-N that was originally 179.1^0, changes to 169.18^0. The increased value of E_{st} is due to the enhanced electrostatic interaction between the metal and the CN group, which renders extra stability to the system, compensating the loss of stability due to the diminished cation- π interaction in the system.

To get a clear picture on the electrostatic interactions present in the system, the Mulliken charges on the carbons may be helpful. In Table 3.14, the Mulliken charges on the carbons of Li/Na/K substituted C_9H_{12} & $C_9H_{11}CN$ are presented for the comparative study.

Table 3.14: Mulliken charges (a.u) on the carbons of Li/Na/K substituted C_9H_{12} & $C_9H_{11}CN$ (B3LYP/6-31G*)

System	C1	C2	C3	C4	C5	C6	C7	C8	C9
C_9H_{12}	-0.491	-0.105	-0.100	-0.122	-0.126	-0.122	-0.125	-0.060	-0.358
$C_9H_{11}CN$ (2)	-0.458	0.204	-0.221	-0.119	-0.169	-0.116	-0.169	-0.046	-0.417
$C_9H_{11}Li$ (2)	**-0.445**	**-0.079**	**-0.238**	-0.095	-0.144	-0.119	-0.139	-0.057	-0.372
$C_9H_{10}CN$ (2) Li (2)	**-0.476**	**0.100**	**-0.262**	-0.105	-0.135	-0.122	-0.133	-0.058	-0.365
$C_9H_{11}Na$ (2)	**-0.475**	**-0.105**	**-0.226**	-0.111	-0.157	-0.119	-0.144	-0.056	-0.377
$C_9H_{10}CN$ (2) Na (1)	**-0.536**	0.142	-0.184	-0.131	-0.130	-0.123	-0.132	-0.058	-0.366
$C_9H_{11}K$ (3)	**-0.455**	**-0.098**	**-0.253**	**-0.157**	**-0.211**	-0.116	-0.153	-0.056	-0.385
$C_9H_{11}CN$ (3)	-0.414	-0.073	0.067	-0.155	-0.170	-0.110	-0.166	-0.048	-0.410
$C_9H_{10}CN$ (3) K (1)	**-0.488**	-0.104	0.002	-0.155	-0.160	-0.115	-0.143	-0.057	-0.373

There is substantial increase in the negative charges on the carbons in the vicinity of substituted CN group, but the carbon to which CN is attached possess a positive charge. More charge on the carbons promotes strong electrostatic attraction with the metal. However, there is also a repulsive interaction between the metal and the nearest carbon as it carries a positive charge. Therefore, the net change in E_{st} due to the electrostatic interaction will be negligible. The second contribution comes from cation- π interaction. The C-C bond lengths may offer more explanation regarding the nature of cation- π interaction. C-C bond lengths of different metal polyenes are given in Table 3.15.

Table 3.15: C-C bond lengths (A^0) in Li/Na/K substituted C_9H_{12} & $C_9H_{11}CN$ systems (B3LYP/6-31G*).

System	C1-C2	C2-C3	C3-C4	C4-C5	C5-C6	C6-C7	C7-C8	C8-C9
C_9H_{12}	1.4983	1.3469	1.4461	1.3563	1.4406	1.3560	1.4476	1.3442
$C_9H_{11}Li(2)$	**1.4008**	**1.4087**	1.4365	1.3644	1.4351	1.3597	1.4453	1.3461
$C_9H_{10}CN(2)Li(2)$	**1.4175**	**1.4135**	1.4343	1.3647	1.4350	1.3592	1.4456	1.3455
$C_9H_{11}Na(2)$	**1.4036**	**1.4043**	1.4251	1.3718	1.4304	1.3628	1.4433	1.3475
$C_9H_{10}CN(2)Na(1)$	1.4455	1.3861	1.4218	1.3690	1.4313	1.3613	1.4442	1.3463
$C_9H_{11}K(3)$	1.3752	1.4200	**1.4041**	**1.3932**	1.4281	1.3666	1.4413	1.3490
$C_9H_{10}CN(3)K(1)$	1.3695	1.4381	1.4409	1.3652	1.4353	1.3599	1.4452	1.3463

It can be seen from the C-C bond length values that the delocalised pi cloud along C1, C2 & C3 is perfect in $C_9H_{11}Li$ (2) & $C_9H_{11}Na$ (2), somewhat depleted in $C_9H_{10}CN$ (2) Li (2) and totally disrupted in $C_9H_{10}CN$ (2) Na (1). Hence, the contribution from cation-π interaction towards the E_{st} will be less. So there will be a decrease in E_{st} for $C_9H_{10}CN$ (2) Li (2). However, in $C_9H_{10}CN$ (2) Na (1) there is extra electrostatic interaction between the Na and the CN, which explains why it is having almost the same E_{st}. Similarly, in $C_9H_{11}K$ (3), potassium interacts with the pentadienyl segment with a delocalised electron cloud. Such a pi cloud is almost nonexistent in $C_9H_{10}CN$ (3) K (1). But, since there exists a strong K-CN interaction, the complex has a slightly improved E_{st} value.

The optimized structures of these are more suggestive which are given in Figure 3.9 (B3LYP/6-31G*).

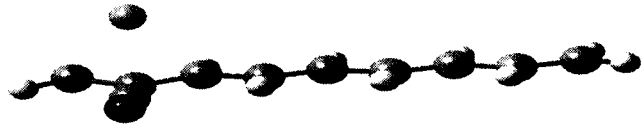

(a) $C_9H_{10}CN(2)Li(2)$

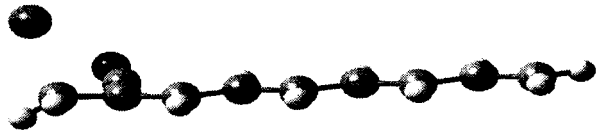

(b) $C_9H_{10}CN(2)Na(1)$

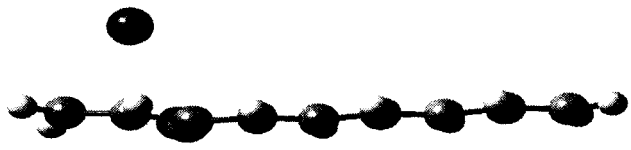

(c) $C_9H_{10}CN(3)K(1)$

Figure 3.9: Optimized structures of Li/Na/K substituted $C_9H_{11}CN$

3.4 Discussion

On metal substitution, the metal turns to a cation and takes a position above the carbon skeleton. Further, the sp^3 carbon (C1) undergoes a change of hybridization to sp^2. Thus, a metal-substituted polyene is essentially cation-polyenic anion system, or in other words, a cation-π system.

As the result of metal substitution, there occurs a rearrangement of C-C bond lengths along the carbon skeleton. The bond lengths inside the polyenic fragment with which the metal interacts attain almost identical values, suggesting a total delocalisation inside that fragment (see Tables 3.7(a) and 3.7(b). A comparison of bond lengths of free and metal substituted C_9 system is presented in Figure 3.10.

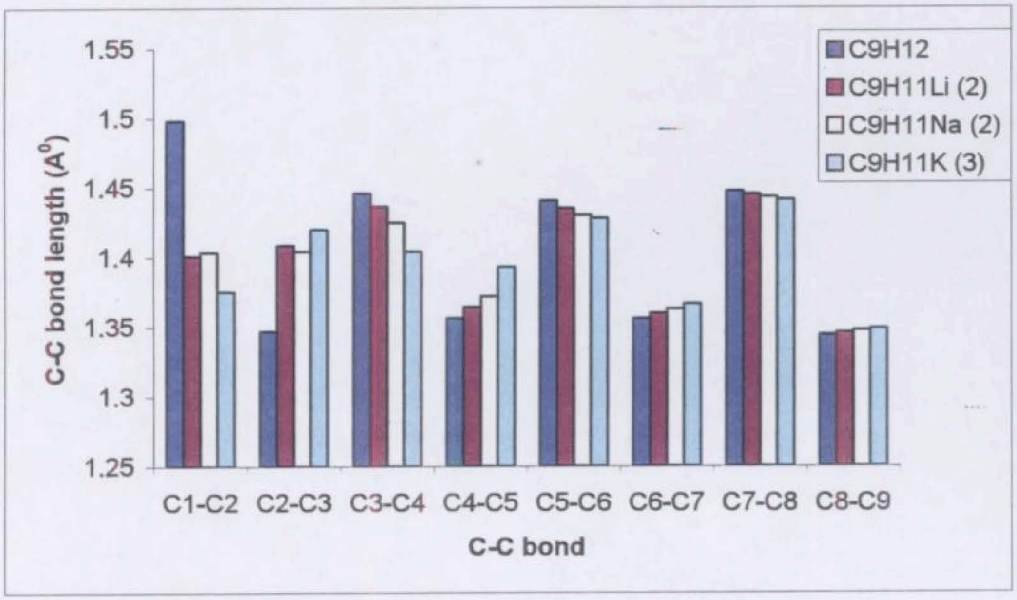

Figure 3.10: Comparison of C-C bond lengths in C_9H_{12} and its Li/Na/K substituted complexes

The metal-polyenes are characterized by high E_{st}. The E_{st} decreases as the length of the polyene increases (see Table 3.2). For example, the E_{st} of C_5H_7Li (2) is 161.88 kcal/mol. But for $C_9H_{11}Li$ (2), the value is 141.41 kcal/mol and for $C_{13}H_{15}Li$ (2), it is 130.20 kcal/mol. The high E_{st} of these

complexes is greater than the usual ionic bond strength. Such a high value indicates the stabilization achieved by the system due to some other interaction in addition to the strong Coulombic interaction between the cation and the polyenyl anion. The extra stability of the system is explained in terms of the intimate interaction between the cation and the pi cloud of the polyene. As the length of the polyene increases, the covalent character of the polyenyl anion increases and hence the strength of the ionic interaction decreases, which accounts for the decrease in E_{st}. A graph comparing the E_{st} of the different isomers of $C_9H_{11}K$ and $C_{13}H_{15}K$ is presented in Figure 3.11.

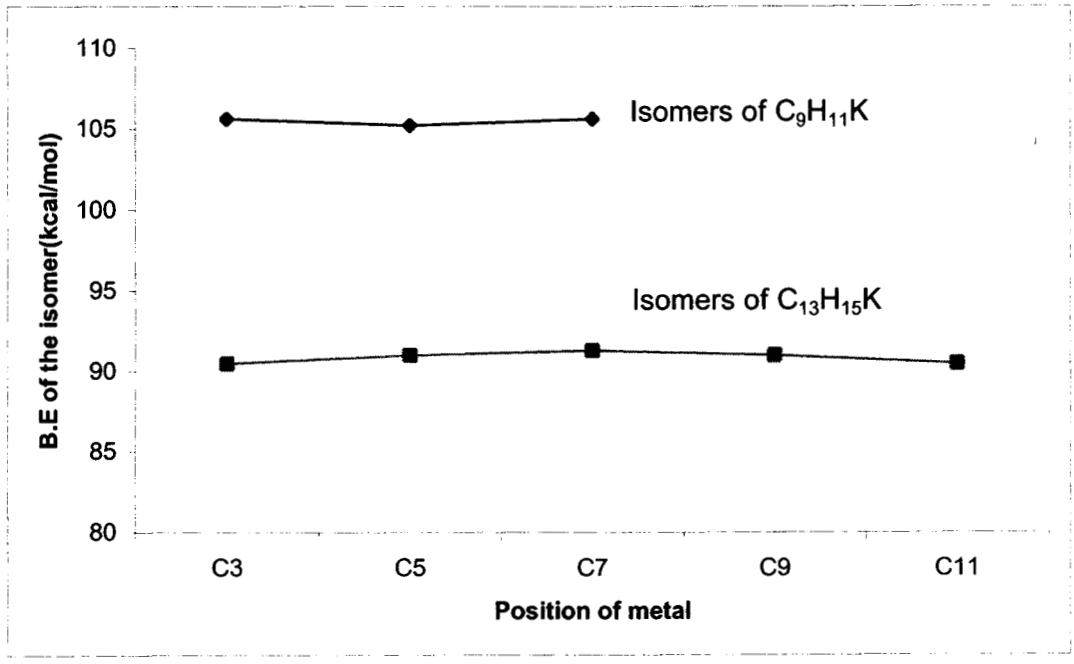

Figure 3.11: Comparison of the E_{st} of K-isomers of C_9 & C_{13} systems

The cation- pi cloud interaction involves two components- the interaction between the point charges on the metal and on the carbons of the interacting segment (type I interaction) and the interaction of the cation with the delocalised pi cloud, oscillating along this polyenyl fragment (type II interaction).

3.4.1 Stability of isomers in metal polyenes

The most stable metal-polyenes of lithium and sodium have the general formula $C_nH_{2n+2}M$ (2), where M = Li or Na. On the other hand, in potassium-polyenes, potassium is always stationed above an odd carbon, which is the centre of a polyenic fragment (see Figures 3.3 and 3.4). Potassium-polyene achieves more and more stability by assuming a higher symmetry (from C_1 to C_s point group) by moving to the top of the central odd carbon. The diverse behaviours of these alkali metals suggest that the stability of the metal-substituted complexes is not simply governed by the simple cation-anion interaction (ionic interaction) alone, but other factors characteristic of cation-π interactions (such as stability of the polyenic segment, size of the dopant, symmetry of the product, etc.) also appear to contribute to the stability of the system, which we shall consider below.

3.4.1.1 Coulombic interaction between cation and carbon skeleton (Type I interaction)

In the stable isomers of potassium–polyene systems, K carries higher positive charge than Li and Na. For instance, in the species $C_9H_{11}M$, Mulliken charges (B3LYP/6-31G*) of Li^+, Na^+ and K^+ are 0.295, 0.484 and 0.695 respectively (See Table 3.2). Further, the odd carbons of the chain possess considerably higher negative charge than the even carbons. The two terminal carbons carry maximum negative charge, which steadily decreases towards the centre of the carbon chain (Table 3.3). For instance, the Mulliken charges (B3LYP/6-31G*) on different carbons in $C_9H_{11}K$ (3) are C1 = -0.455, C2 =-0.098, C3 = -0.253, C4 = -0.157, C5 = -0.211, C6 = -0.116, C7 = -0.153, C8 = -0.056, C9 = -0.385. Thus, the preferential affinity of K towards odd carbons (see Figure 3.4) may be explained in terms of the attractive Coulombic interactions between them. The net charges on the carbons of different species given in Table 3.4 are shown graphically in Figure 3.12. From the Figure, it

can be seen that Li and Na, attached to the even carbons have two neighbouring carbons with higher negative charge. On the other hand, K interacts with a carbon of highest negative charge. On warping, it attains further interaction with two more neighbouring carbons of significant negative charges.

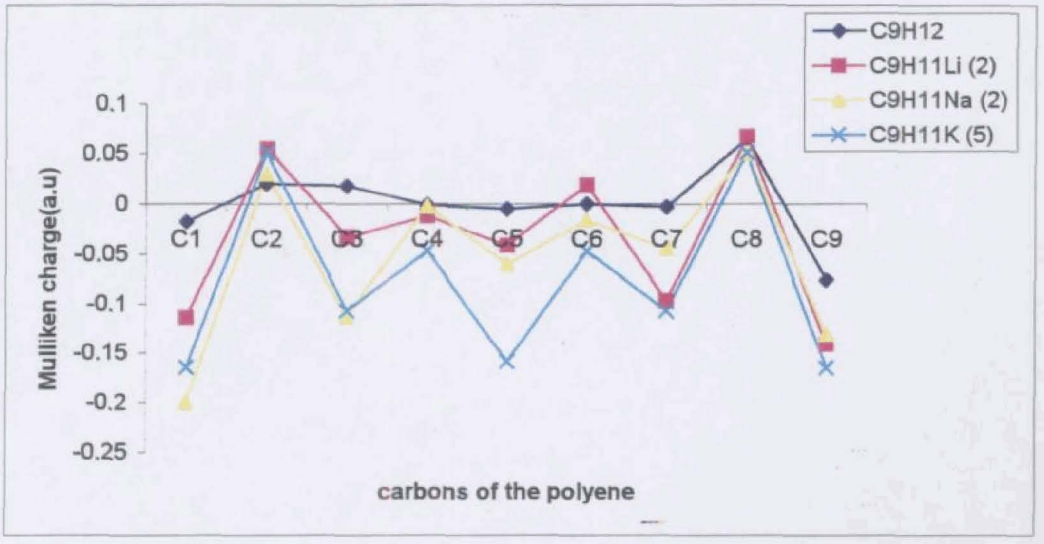

Figure 3.12: Comparison of Mulliken charges on carbons of C_9H_{12} and its Li/Na/K substituted complexes.

However, this simple model based on Coulombic interaction is insufficient, since the affinity of lithium and sodium in their stable isomers is towards even carbons carrying lower negative charge (Figure 3.3). Further, the cation doped at the terminal carbon carrying the maximum negative charge, usually does not stick on to it, but moves towards a carbon carrying lesser charge. The role of other factors contributing to stability is thus apparent.

3.4.1.2 Interaction between cation and π- electron cloud (Type II interaction)

The results show that Li^+ and Na^+ preferentially interact with a 3-carbon, 4 π electrons (allyl) fragment. However, K^+ interacts with a 5-carbon (6 π electrons), 9-carbon (10 π electrons) or 13- carbon (14 π electrons) fragment, producing stable isomers with the metal stationed over the middle carbons (i.e., the 3rd, 5th, 7th carbon) of these polyenic fragments (see Table 3.2 and Figure 3.4). We note that a 9-carbon fragment is obtained by the fusion of two pentadienyl groups. Similarly, a 13-carbon fragment is obtained by the fusion of three pentadienyl groups and so on. This means that in all its complexes, K^+ always interacts with a polyenic fragment carrying a cloud of (4n+2) π-electrons (n = number of pentadienyl groups fused together in the polyenic segment), in contrast with Li^+ and Na^+ which prefer to interact with a fragment of four-electron cloud. Hence, the proposal by Burke and Jesperson [3] that "the isomers containing 3-carbon 4 π-electron interaction sites appear favoured", is limited to the Li and Na polyenes only, but not true with K-polyene. Our results suggest that for potassium (and higher members of the group), the stability appears to be associated with an interaction between the cation and (4n+2) π electrons, rather than 4 π electrons. Therefore, in addition to the interaction of Type I, the number of interacting π electrons, in other words, the size of the π electron cloud also holds the key to the stability of the K-polyenes.

The reduction in the charge of the cation from +1 to a lower value in the complex is indicative of this cation – π cloud interaction (Type II). In the complex with the anion $(C_9H_{11})^-$, for instance, the Mulliken charges (B3LYP/6-31G*) of Li^+, Na^+ and K^+ reduced from 1 to 0.295, 0.484 and 0.695 respectively (Table 3.2). Thus, π electrons of the polyenic system 'flow' towards the cation resulting in an interaction between the cation and

the π cloud attributing stability to the complex. The flow of π electrons is maximum for lithium (lowest charge), signifying maximum stabilization of the Li-complex via this mechanism. The charge of the cation also indicates that the Type I interaction of electrostatic nature is maximum with K and least with Li.

The energies of reaction (E_R) of different metal-polyenes were determined as the difference between the total energy of the optimized metal-polyene and the sum of the energies of the corresponding metal cation and polyenic anion (The stabilisation energy, E_{st}, is then the negative of E_R). The lithium-polyene has got the highest E_{st} compared to its sodium and potassium counterparts (see Table 3.2). For example, the E_{st} in kcal/mol of $C_9H_{11}Li$ (2) is 141.41, that of $C_9H_{11}Na$ (2) is 117.83 and that of $C_9H_{11}K$ (5) is 100.47, indicating maximum stability for the Li-polyene, in agreement with the maximum π electron flow found for it. We have noted that the charge of Li^+ in the complex is low unlike in pure ionic compounds (e.g., LiCl) leading to relatively poor Coulombic interaction. Yet, the E_{st} is maximum for Li-polyene, which is evidently due a significant contribution towards stability by cation–π cloud interaction of type II. The situation is just the opposite in K-polyene, i.e., maximum Coulombic interaction (Type I) and minimum cation–π cloud interaction (though the pi cloud is large), because of the high point charge, the Na-polyene taking an intermediate position.

However, the question, why do Li and Na prefer to a smaller π-electron cloud for stability, remains to be answered. A plausible explanation may be found in terms of the size and charge of the dopant.

3.4.1.3 Size of the dopant

An examination of the stable isomers of different systems suggests that as the size of the cation increases, it tends to move towards the centre to attain maximum stability (Table 3.2). At larger size, the cations can effectively interact with more carbon atoms and presumably with a larger π-electron cloud. Hence K will have its stable isomers when it is stationed above the 3rd or 5th or 7th carbon of the chain, as observed. This is in agreement with the experimental observation made by Gokel [5] that the diacetylene is appropriate to bind Na^+, but too small to bind K^+. On the other hand, lower members Li and Na have their most stable isomers when they are stationed at the 2nd carbon of the terminal 3-carbon (allyl) pocket. They can also form less stable isomers by getting trapped at three carbon pockets with middle carbon at 4, 6, 8, etc., displaying their affinity towards even carbon. It is interesting to note that in any of the methods, HF / MP2 / B3LYP, on geometry optimization, we have not obtained an isomer with Li interacting with a 5-carbon or larger segment like potassium. Due to its smaller size, Li can be easily accommodated in a 3-carbon segment on an even carbon, inviting good Coulombic interactions with the neighbouring odd carbons even without warping. Also, Li^+ develops a strong interaction with the delocalised π cloud of the allyl system. This explains why we have the stable isomers $C_9H_{11}Li$ (2) and $C_9H_{11}Li$ (4), but never $C_9H_{11}Li$ (3) and $C_9H_{11}Li$ (5). The possibility for a 3-carbon 4-electron segment with an odd carbon at the centre interacting with Li is totally ruled out, since such a system will have a highly unstable polyenic arrangement as the extended conjugation of the chain will be disturbed which will destabilize the system. The same reasons can answer the formation of $C_9H_{11}Na$ (2) and $C_9H_{11}Na$ (4). However, the larger sized sodium forms a less stable isomer $C_9H_{11}Na$ (5) indicating the tendency to be contained in larger fragments, which is seen matured with K, and possibly

with higher members. Thus, as we move down the group, the dopants tend to attach to the odd carbon inviting an interaction with more carbons around it (and hence the bent structure).

The preferential binding of Li and Na to the 2nd carbon from the terminal may be explained in terms of the stabilization attained by the polyenic part via modified extended conjugation, which will be partially disturbed when the metal is attached to 4th or 6th etc. carbon [For instance, in $C_9H_{11}Li$, Li (2) isomer has 3 double bonds in conjugation, whereas Li (4) isomer has only 2 double bonds in conjugation and one in isolation (see Table 3.7(a)]. On the other hand, the Coulombic interactions between the higher members like K, Rb, etc., and the polyenic carbons are strong enough to exceed the destabilization energy resulting from the loss of conjugation and hence such complexes are fairly stable.

Table 3.2 shows a general decrease in the charge of the cation in the complex signifying a strong interaction between the cation and the π-electron cloud (Type II interaction). The gradation of the charge from K to Li clearly indicates the enhancement of cation–π cloud interaction with a decrease in the size of the cation. This is in agreement with the results (both experimental and computational) reported for cation-benzene complexes [6]. Further, this is an additional driving force for the confinement of the cation in an allylic pocket (e.g., Li & Na) or in a wider polyenic pocket (e.g., K).

3.4.1.4 Symmetry of the metal-polyene

It may be noted from Table 3.2 that in the most stable isomer of K-polyenes, K^+ is always positioned over the *central odd carbon*, except in C_9-system. Even in the C_9- system, the expected K (5) isomer is obtained when calculations were done with a higher basis set (6-311+G*). When the chain length increases, the most stable isomer is invariably the one with K^+ on the

central odd carbon followed by an enhancement in symmetry from C_1 to C_s, as seen in C_{13}-system. If the central carbon is even (as in C_{11}-system), in the most stable isomer, K^+ takes the position above the odd carbon next to the central carbon, exhibiting its preference to odd carbon over symmetry. The above behaviour of potassium prompts us to suggest that an increase in symmetry (from C_1 to C_s) of the metal-polyene also contributes to the stability of the isomer. This speculation derives weight from the fact that among the 6 stable isomers of $C_{25}H_7K$ (with K above C3, C5, C7, C9, C11 and C13), the isomer $C_{25}H_7K$ (13) is found to be the most stable on geometry optimization [Table 3.6(a)].

On the other hand, the symmetry factor plays a major role in Li and Na polyenes when the polyene has an even carbon at the centre. In such cases, Li and Na tend to move towards the centre to form symmetrical structures. Thus in C_{11} system, we have $C_{11}H_{13}Na$ (6) as the most stable isomer. This trend may be expected in higher polyenes also. Since the energy difference is very low, even the slight effects due to the basis sets may alter the order of stability. However, as a general rule, we can state that the metal polyenes tend to form symmetrical structures; and when other factors are favourable, symmetrical structures will have maximum stability.

3.4.2 Prominence of cation-π interaction

The results obtained for substituted polyenes support the prominence of cation-π interaction. When electron-donating groups like CH_3 are introduced into the polyene on the same carbon on which metal resides, there occurs an increase in the E_{st} of the K-polyenes. For Li and Na, the E_{st} decreases slightly (Table 3.10). The E_{st} difference between $C_9H_{11}Li$ (2) and $C_9H_{10}CH_3$ (2) Li (2) is 0.07 kcal/mol; between $C_9H_{11}Na$ (2) and $C_9H_{10}CH_3$ (2) Na (2) is 0.45 kcal/mol; but $C_9H_{10}CH_3$ (3) K (3) is higher in energy by 1.78 kcal/mol than $C_9H_{11}K$ (3). Since the M-C distances increase and charges on

the metals decrease, the Coulombic considerations should give a decreased E_{st} value. But instead, the energy remains almost the same (for Li & Na) or slightly increases (for K). This can be explained only in terms of enhanced cation-π interaction.

When electron-donating group is present in the polyene, there will be an enhanced pi electron cloud. The metal ion interacts more efficiently with this pi-cloud. The decrease in the charge on the metal may be due to this enhanced interaction. This stabilizes the metal-polyene too, as evident from the E_{st} values. The increased distance between the metal and the carbon may be due to the presence of CH_3 on the same carbon. It is evident from the B. E values that the substitution of methyl group on C5, the central carbon of the polyene, evokes no substantial change in the energy. The inability of CH_3 to effect considerable modification to the delocalised electron cloud over C1, C2 and C3 portion of the polyene supports the already reported property of cation-π interaction-that the substituent effects are inductive rather than mesomeric [7].

The results with polyenes having electron-withdrawing group also support this conclusion (Table 3.13). $C_9H_{10}CN$ (2) Li (2) has an E_{st} lesser by 10.43 kcal/mol than $C_9H_{11}Li$ (2). The efficient cation--π interaction decreases as the result of decrease in the π-electron density. The increased charge on Li, Na and K indicates the decreased cation-π interaction. The electron-withdrawing group in the polyene depletes or totally disrupts the delocalised electron cloud and hence chance for efficient cation-π interaction is minimized (See Table 3.15 for C-C bond lengths).

The data given in Table 3.2 is also supportive of this interaction. In most cases, the isomers of lower energy have the metals with higher Mulliken charges, but with reduced metal-carbon distances (For e.g., among the

isomers $C_9H_{11}Na$ (2) & (4), the former has higher E_{st}. The charges on Na in two species are 0.483759 and 0.534838 and Na-C (i) distances are 2.4290 and 2.4105 respectively). Naturally, if Coulombic interactions were the deciding factor in metal polyenes, it should ensure higher stabilization energy for species with higher charge on metal and lower M-C (i) distance. Since the stabilization energy is in the reverse order, a still more prominent interaction should be present in these systems. The nature of the delocalised electron cloud along the polyenyl fragment with which the metal interacts suggests that cation--π interaction could be that force of stabilization.

3.5 Conclusion

The studies on metal substituted polyenes suggest that cation-π interaction is an important binding force to be reckoned with in metal polyenes. The larger sized metals have a tendency to go for type I interaction for stability, which brings in peculiar structural changes in the complex. These structural changes (especially the warping in K-polyenes) are significant phenomena for the future. Addressing this property may lead us to new compounds, whose structures are being modified by metal substitution. Also, the metal binding ability of conjugated polyenes arising out of their delocalised pi cloud may be employed to convert them as potential metal carriers in appropriate fields.

3.6 References:

1. A. J. Heeger, Synthetic Metals, 125 (2002) 23-42.
2. X. Lin, J. Li, S. Yip, Physical Review Letters, 95, 198303 (2005) 1-4.
3. L. A. Burke & K. K. Jesperson, Journal of Molecular Modeling, 6, 2 (2000) 248- 256.

4. X. Lin, J. Li, E. Smela, S. Yip, International Journal of Quantum Chemistry, 102 (2005) 980-985.

5. "Dekker Encyclopedia of Nanoscience and Nanotechnology", J. A. Schwarz, C. I. Contescu, K. Putyera, ed., Amazon. Com., 213.

6. J. C. Ma & D. A. Dougherty, Chem. Rev., 97 (1997) 1303-1324.

7. S. Mecozzi, A. P. West Jr., D. A. Dougherty, J. Am. Chem. Soc., 118 (1996) 2307-2308.

A THEORETICAL STUDY OF THE CATION – π INTERACTION IN ALKALI METAL POLYENES AND POLYENE COMPLEXES

THESIS

Submitted to the
University of Calicut
in partial fulfillment of the requirements
for the award of the degree of
Doctor of Philosophy
in Chemistry,
under the Faculty of Science

By

FR. JOSE T. M.

Forwarded

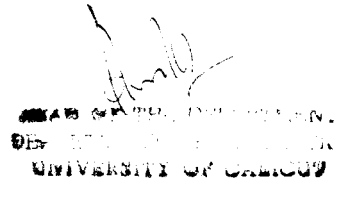

Department of Chemistry,
University of Calicut,
Calicut University P.O.,
673 635

April 2007

CHAPTER 4

ALKALI METAL DOPED CONJUGATED POLYENES

4.1 Introduction

In the previous chapter, we were discussing the effect of metal substitution to conjugated polyenes. Since we wanted to mimic a metal doping like situation, exactly the same that exists in conducting polymers [1], doping of alkali metals to conjugated polymers, starting from C_5 system, was studied. The odd and even systems are separately studied in order to assess the effect of terminal methyl group in the substrate polyene during doping. The studies gave certain interesting results, which would help us to peep into the possible mechanism playing in conducting polymers. Also, it could give us a good opening in our studies involving biomolecules having polyenic chain with extended conjugation.

4.2 Doping of alkali metals to odd numbered all-trans conjugated polyenes

On doping the alkali metals into odd numbered, all-trans polyenes and subsequent optimization, we get certain complexes, characterized by very low binding energies (E_{st}). When compared with the products of metal substitution, Li doped complexes are somewhat similar. The complexes formed by doping Na are totally different, especially those obtained for lower polyenes. For K, such complexes are different when the polyenes are small; but they slowly attain the characteristics of metal-substituted polyenes as the length of the polyene increases. The different isomers obtained, when Li, Na and K were doped into C_5H_8, C_7H_{10}, C_9H_{12} and $C_{11}H_{14}$ are given in Table 4.1 along with their total energy (E), stabilisation energy (E_{st}), shortest metal-

carbon distance (Ri), charge on the metal (Q_M) and HOMO-LUMO energy gap (ΔE).

Table 4.1: Stable isomers of Li, Na and K complexes of C_5, C_7, C_9 and C_{11} systems with their important characteristics (B3LYP/6-31G*).

Metal-doped polyene	Stable isomers [a]	E (Hartree)	E_{st} (kcal/mol)	Ri (A°)	Q_M (a.u)	$\Delta E=E_L-E_H$ (Hartree)
C_5H_8Li	C_5H_8Li (4)	-202.81878	10.01	C4-Li=2.0982	0.064539	0.06736
C_5H_8Na	C_5H_8Na (5)	-357.59556	02.01	C5-Na=2.9592	***-0.076969*** [b]	0.06840
C_5H_8K	C_5H_8K (5)	-795.20549	01.65	C5-K=3.5267	***-0.066163***	0.05557
$C_7H_{10}Li$	$C_7H_{10}Li$ (6)	-280.23245	15.11	C6-Li=2.0608	0.244287	0.06190
	$C_7H_{10}Li$ (3)	-280.22758	11.91	C3-Li=2.0693	0.202398	0.05715
$C_7H_{10}Na$	$C_7H_{10}Na$ (7)	-435.00278	02.65	C7-Na=2.8172	***-0.03712***	0.05148
	$C_7H_{10}Na$ (4)	-435.00076	01.21	C4-Na=3.3739	***-0.09910***	0.05534
$C_7H_{10}K$	$C_7H_{10}K$ (7)	-872.61249	02.09	C7-K = 3.3660	***-0.01862***	0.03840
	$C_7H_{10}K$ (6)	-872.61239	02.02	C6-K= 3.2039	0.049492	0.03317
	$C_7H_{10}K$ (4)	-872.61116	01.55	C4-K=3.7458	***-0.085664***	0.03840
$C_9H_{12}Li$	$C_9H_{12}Li$ (8)	-357.64512	18.61	C8-Li=2.0605	0.277739	0.06524
	$C_9H_{12}Li$ (6)	-357.63836	14.59	C6-Li= 2.0538	0.280595	0.05447
	$C_9H_{12}Li$ (3)	-357.63961	15.13	C3-Li=2.0577	0.276513	0.06018
$C_9H_{12}Na$	$C_9H_{12}Na$ (9)	-512.41082	03.41	C9-Na=2.7096	0.018860	0.04309
	$C_9H_{12}Na$ (6)	-512.40643	00.97	C6-Na=2.7083	0.052152	0.03223
	$C_9H_{12}Na$ (4)	-512.40786	01.21	C4-Na=3.3418	***-0.099071***	0.04287
$C_9H_{12}K$	$C_9H_{12}K$ (8)	-950.02215	04.61	C8-K= 2.9960	0.289659	0.03086
	$C_9H_{12}K$ (6)	-950.01991	03.30	C6-K= 3.0130	0.287108	0.02770
	$C_9H_{12}K$ (4)	-950.01930	02.71	C4-K=3.0204	0.219703	0.02815
$C_{11}H_{14}Li$	$C_{11}H_{14}Li$ (10)	-435.05622	20.97	C10-Li=2.0612	0.290707	0.06683
	$C_{11}H_{14}Li$ (8)	-435.05045	17.62	C8-Li= 2.0530	0.328364	0.05983
	$C_{11}H_{14}Li$ (5)	-435.04956	17.06	C5-Li=2.0540	0.326850	0.05879
	$C_{11}H_{14}Li$ (3)	-435.05052	17.41	C3-Li=2.0579	0.294349	0.06181
$C_{11}H_{14}Na$	$C_{11}H_{14}Na$ (11)	-589.81914	04.20	C11-Na=2.6357	0.075670	0.03856
	$C_{11}H_{14}Na$ (7)	-589.81584	02.15	C7-Na=2.7963	0.052930	0.02939
	$C_{11}H_{14}Na$ (6)	-589.81570	02.04	C6-Na=2.8174	0.032573	0.02936
	$C_{11}H_{14}Na$ (4)	-589.81536	01.35	C4-Na=3.2533	***-0.09689***	0.03347
$C_{11}H_{14}K$	$C_{11}H_{14}K$ (9)	-1027.43218	06.73	C9-K=2.9193	0.434572	0.03050
	$C_{11}H_{14}K$ (7)	-1027.43081	06.09	C7-K=2.8994	0.486464	0.02763
	$C_{11}H_{14}K$ (6)	-1027.43061	05.89	C6-K=2.9003	0.462644	0.02766
	$C_{11}H_{14}K$ (4)	-1027.42904	04.68	C4-K=2.9163	0.382695	0.02721

[a] The numeral in parentheses corresponds to the carbon above which the metal is stationed.
[b] The values in bold italics are the negative charges on the alkali metals.

The large distance between the metal and polyenic carbon implies decreased interaction between the metal and the polyene. There is significant change in the carbon- carbon bond length values, but the intense warping, as in the case of potassium-substituted polyenes, is missing, especially in the lower polyenes. The Mulliken charges on the doped atoms show that in some isomers, especially in lower polyenes, Na and K exist as their negative ions [e.g., C_5H_8K (1), $C_7H_{10}Na$ (1), $C_9H_{12}Na$ (4), etc.].

The charges on the carbons of the free and metal-doped systems are presented in Tables 4.2(a) to (d) (B3LYP/6-31G*).

Table 4.2(a): Mulliken charges (a.u) on the carbons of C_5H_8 and its metal-doped complexes

System	C1	C2	C3	C4	C5
C_5H_8	-0.490	-0.105	-0.100	-0.059	-0.359
C_5H_8Li (4)	-0.478	-0.112	**-0.174**	**-0.143**	**-0.379**
C_5H_8Na (5)	-0.492	-0.098	-0.101	-0.057	**-0.405**
C_5H_8K (5)	-0.495	-0.100	-0.105	-0.069	**-0.387**

Table 4.2(b): Mulliken charges (a.u) on the carbons of C_7H_{10} and its metal-doped complexes

System	C1	C2	C3	C4	C5	C6	C7
C_7H_{10}	-0.490	-0.105	-0.100	-0.122	-0.126	-0.059	-0.358
$C_7H_{10}Li$ (6)	-0.485	-0.121	-0.104	-0.117	**-0.209**	**-0.116**	**-0.431**
$C_7H_{10}Li$ (3)	-0.468	**-0.172**	**-0.135**	**-0.228**	-0.117	-0.063	-0.376
$C_7H_{10}Na$ (7)	-0.492	-0.103	-0.102	-0.118	-0.128	-0.058	**-0.424**
$C_7H_{10}Na$ (4)	-0.497	-0.098	**-0.117**	**-0.143**	**-0.122**	-0.058	-0.351
$C_7H_{10}K$ (7)	-0.492	-0.103	-0.102	-0.120	**-0.133**	**-0.070**	**-0.406**
$C_7H_{10}K$ (6)	-0.492	-0.106	-.103	-0.130	**-0.161**	**-0.101**	**-0.400**

Table 4.2(c): Mulliken charges (a.u) on the carbons of C_9H_{12} and its metal-doped complexes.

System	C1	C2	C3	C4	C5	C6	C7	C8	C9
C_9H_{12}	-0.491	-0.105	-0.100	-0.122	-0.126	-0.122	-0.125	-0.060	-0.358
$C_9H_{12}Li$ (8)	-0.486	-0.117	-0.102	-0.134	-0.132	-0.111	**-0.218**	**-0.101**	**-0.438**
$C_9H_{12}Li$ (6)	-0.486	-0.121	-0.100	-0.121	**-0.217**	**-0.165**	**-0.206**	-0.038	-0.381
$C_9H_{12}Na$(9)	-0.491	-0.106	-0.101	-0.123	-0.129	-0.120	-0.130	-0.060	**-0.443**
$C_9H_{12}Na$(6)	-0.491	-0.106	-0.096	-0.139	**-0.179**	**-0.175**	**-0.143**	-0.056	-0.360
$C_9H_{12}K$(8)	-0.487	-0.115	-0.101	-0.132	-0.135	-0.153	**-0.199**	**-0.112**	**-0.425**
$C_9H_{12}K$(6)	-0.489	-0.116	-0.099	-0.170	**-0.186**	**-0.183**	**-0.175**	-0.060	-0.374

Table 4.2(d): Mulliken charges (a.u) on the carbons of $C_{11}H_{14}$ and its metal-doped complexes.

System	C1	C2	C3	C4	C5	C6	C7	C8	C9	C10	C11
$C_{11}H_{14}$	-0.491	-0.105	-0.010	-0.123	-0.126	-0.123	-0.125	-0.122	-0.124	-0.060	-0.358
$C_{11}H_{14}Li$(10)	-0.487	-0.114	-0.100	-0.132	-0.129	-0.132	-0.134	-0.106	**-0.225**	**-0.094**	**-0.440**
$C_{11}H_{14}Li$(8)	-0.486	-0.117	-0.102	-0.136	-0.131	-0.112	**-0.223**	**-.146**	**-0.225**	-0.035	-0.383
$C_{11}H_{14}Na$(11)	-0.490	-0.107	-0.100	-0.125	-0.127	-0.124	-0.130	-0.120	-0.133	-0.162	**-0.458**
$C_{11}H_{14}Na$(7)	-0.490	-0.107	-0.101	-0.125	-0.126	**-0.114**	**-0.191**	**-0.173**	-0.121	-0.060	-0.361
$C_{11}H_{14}K$(9)	-0.487	-0.116	-0.099	-0.135	-0.130	-0.134	**-0.143**	**-0.161**	**-0.218**	**-0.111**	**-0.438**
$C_{11}H_{14}K$(7)	-0.486	-0.121	-0.101	-0.139	**-0.133**	**-0.185**	**-0.206**	**-0.186**	**-0.191**	-0.059	-0.384

From the Mulliken charges given above, it can be found that the trend followed in metal doping is the same as that of substitution. The metals generally show a tendency to spare a portion of their valence electrons to the pi-system and develop partial positive charge (Table 4.1) so that they can bind with the pi-system by cation-π interaction. Li and K as cations (though with lesser charge on them) move over the π-cloud and interact with the carbons of higher charges on either side of their nearest carbon. The net charge on the carbons (obtained by summing up the charges on the hydrogens) will give more clarity to this idea. For scrutiny, the net charges on the carbons of a few metal-doped and undoped C_9 systems are given in Table 4.3.

Table 4.3: Net Mulliken charges (a.u) on the carbons of free and Li/Na/K doped C_9H_{12}.

System	C1	C2	C3	C4	C5	C6	C7	C8	C9
C_9H_{12}	-0.018	0.020	0.018	-0.001	-0.005	.00004	-0.003	0.065	-0.076
$C_9H_{12}Li$ (8)	-0.042	-0.005	0.0005	-0.030	-0.029	0.003	**-0.079**	**0.042**	**-0.138**
$C_9H_{12}Li$ (6)	-0.043	-0.011	0.005	-0.002	**-0.075**	**-0.027**	**-0.069**	0.074	-0.135
$C_9H_{12}Na$(9)	-0.019	0.018	0.016	-0.003	-0.008	0.003	-0.003	0.079	**-0.105**
$C_9H_{12}Na$(6)	-0.019	0.020	0.027	0.0001	**-0.037**	**-0.033**	**-0.004**	0.073	-0.078
$C_9H_{12}K$(8)	-0.034	0.0003	0.008	-0.020	-0.020	-0.030	**-0.079**	**0.018**	**-0.133**
$C_9H_{12}K$(6)	-0.033	0.001	0.015	-0.046	**-0.062**	**-0.060**	**-0.051**	0.059	-0.109

The net charges on carbons suggest why the metals prefer to some positions when they are doped to the system. The carbons in the interacting segment are having slightly larger negative charge. Thus, in the doped systems too, there exists a feeble electrostatic interaction between the carbons and the cation, which may be the stabilizing factor for such complexes. As per the observations, the doping brings in more influence on Li and K. They lose some of their electrons to the polyene to make them partially positive and the polyene, partially negative. On the other hand, Na is almost unaffected and it remains almost in its free state keeping a large distance from the terminal carbon of the polyene. This may account for the peculiar behaviour of Na-doped polyene.

4.2.1 Position of the metal on the polyene

The doping of metals to odd numbered polyenes gave different types of isomers for different metals. Here, the metals are found not exactly above a single carbon, but above a carbon-carbon bond, often at the middle of it. Though they are above the carbon skeleton, they are not perpendicular to the carbon chain. They prefer to lie as far from the sp^3 end as possible to achieve better stability. The selected metal-carbon distances and bond angles for a few systems to highlight the above statements are given in Table 4.4.

Table 4.4: Metal-carbon distances and metal polyene bond angles in some selected systems.

System	C(i+1)-M (A^0)	C(i)-M (A^0)	C (i-1)-M (A^0)	MC(i)C(i+1) (deg.)	MC(i)H(i) (deg.)
$C_9H_{12}Li$ (8)	C9-Li=2.0955	C8-Li=2.0605	C7-K=2.1841	71.53	116.52
$C_9H_{12}Li$ (6)	C7-Li=3.2197	C6-Li= 2.0538	C5-Li=3.1485	77.17	110.78
$C_9H_{12}Na$ (9)	---	C9-Na= 2.7096	C2-Na=3.2421	---	91.73
$C_9H_{12}Na$ (6)	C7-Na=3.0534	C6-Na=2.7083	C5-Na=2.7175	90.72	98.92
$C_9H_{12}K$ (8)	C9-K=3.2057	C8-K= 2.9960	C7-K=3.0236	85.96	102.23
$C_9H_{12}K$ (6)	C7-K=3.3370	C6-K= 3.0130	C5-K=3.0249	91.01	97.64

On doping to polyenes, Li always gave the most stable isomer with the general formula, C_nH_{n+3} Li (n-1). Thus we have C_5H_8Li (4), $C_7H_{10}Li$ (6), $C_9H_{12}Li$ (8), etc., as the most stable isomers in their respective systems. In other isomers too, the metal is near to an even carbon, a trend that it exhibited in substitution to polyenes. When coming closer to the sp^3 carbon, it stays over the third carbon- still, the 2nd sp^2 carbon from that end [The exception is C_5H_8Li (2)- see Figure 4.1 (b)]. Examples for the less stable isomers are $C_7H_{10}Li$ (3), $C_9H_{12}Li$ (3), $C_{11}H_{14}Li$ (3), etc. The optimized structures of a few stable isomers given below in Figure 4.1 will explain more.

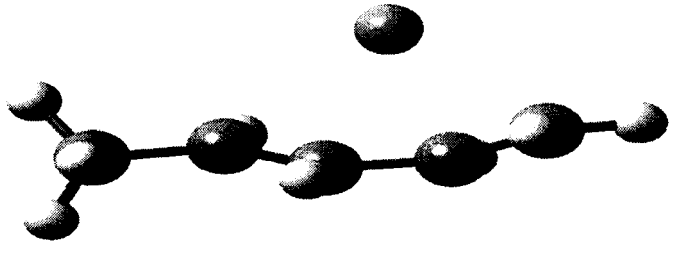

(a) C_5H_8Li (4)

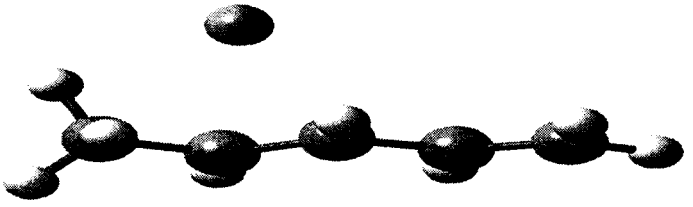

(b) C_5H_8Li (2)

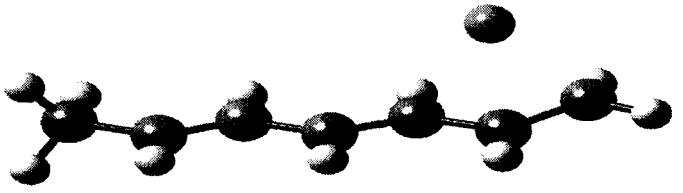

(c) C_7H_{10} Li (6)

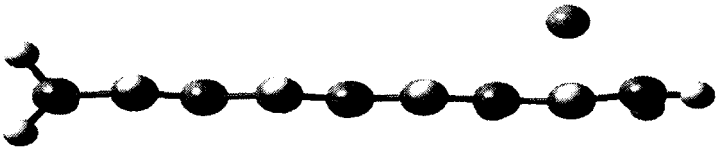

(d) $C_9H_{12}Li$ (8)

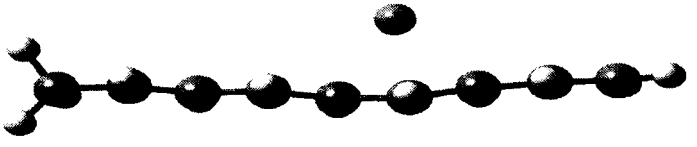

(e) $C_9H_{12}Li$ (6)

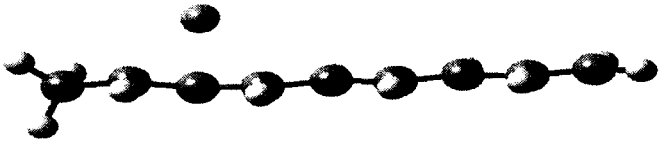

(f) $C_9H_{12}Li$ (3)

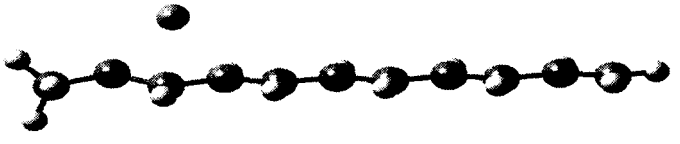

(g) $C_{11}H_{14}Li$ (3)

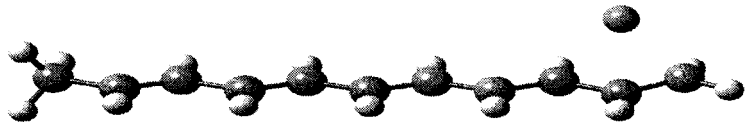

(h) $C_{11}H_{14}Li$ (10)

Figure 4.1: Optimized structures of stable isomers of Li-doped polyenes (B3LYP/6-31G*)

On the other hand, Na-doped polyenes showed some peculiar behaviour. The most stable isomers in all the cases were those in which the metal stays above the terminal sp^2 carbon, the general formula being C_nH_{n+3} Na (n). Thus we have $C_7H_{10}Na$ (7), $C_9H_{12}Na$ (9) and $C_{11}H_{14}Na$ (11) as the most stable isomers of Na for C_7, C_9 and C_{11} systems. Other stable isomers of higher energy have the metal closer to an even carbon in almost all the cases- a trend similar to that seen in metal polyenes. For a detailed analysis, the structures of some of the Na-isomers are given in Figure 4.2.

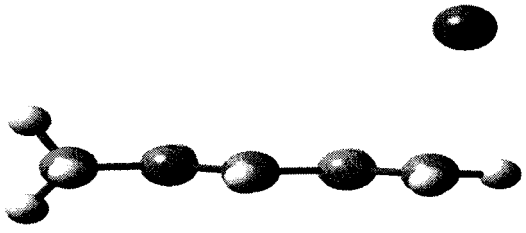

(a) C_5H_8Na (5)

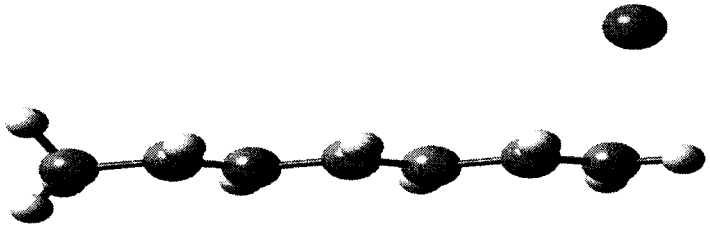

(b) $C_7H_{10}Na$ (7)

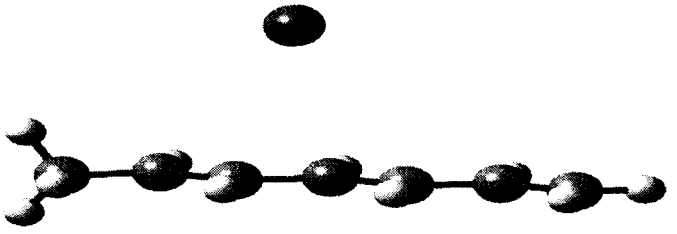

(c) $C_7H_{10}Na$ (4)

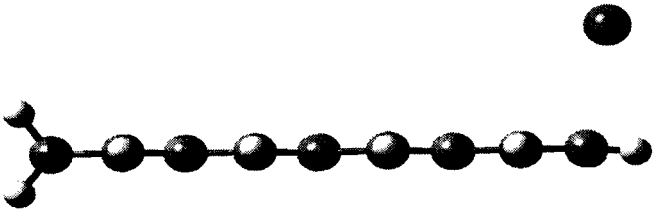

(d) $C_9H_{12}Na$ (9)

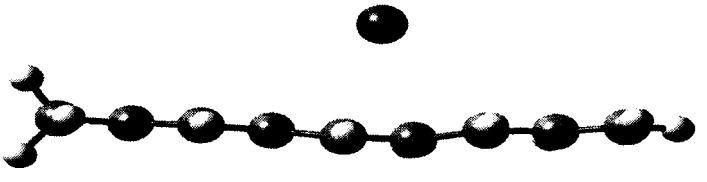

(e) $C_9H_{12}Na$ (6)

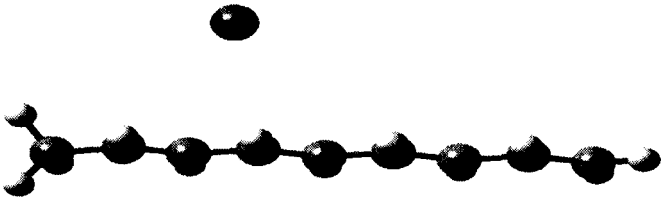

(f) $C_9H_{12}Na$ (4)

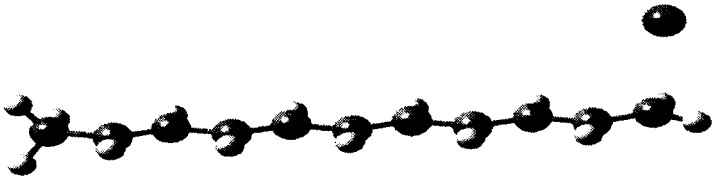

(g) $C_{11}H_{14}Na$ (11)

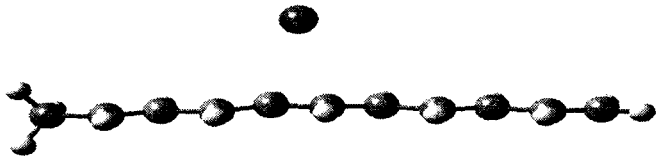

(h) $C_{11}H_{14}Na$ (6)

Figure 4.2: Optimized structures of stable isomers of Na-doped polyenes (B3LYP/6-31G*)

When K was doped to the polyenes, except for lower ones (C_5H_8 and C_7H_{10}), the trend is almost the same as that of Li doping. The most stable isomer has the metal over the terminal allyl fragment. The general formula of the isomer is C_nH_{n+3} K (n-1). To be precise, K resides over the bond between Cn-1 & Cn-2. Examples are $C_9H_{12}K$ (8), $C_{11}H_{14}K$ (9). In lower systems like C_5 and C_7, K is negatively charged and form isomers, which show a resemblance to the trend of Na. Figure 4.3 reveals some of the features of these complexes.

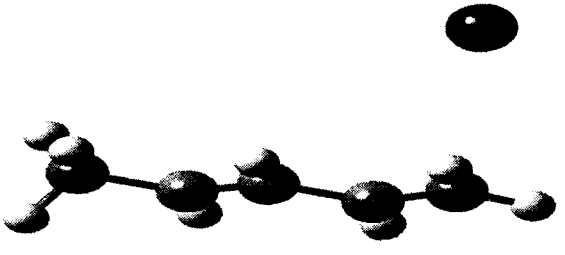

(a) C_5H_8K (5)

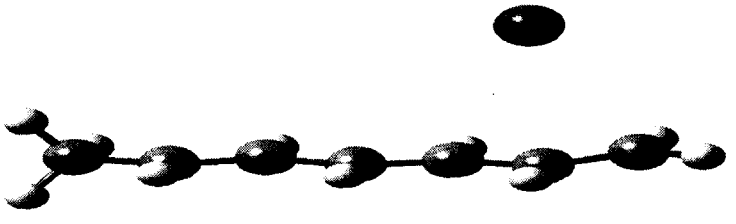

(b) $C_7H_{10}K$ (6)

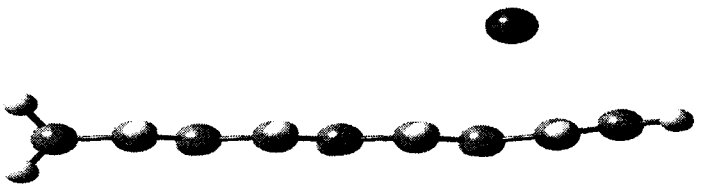

(c) $C_9H_{12}K$ (8)

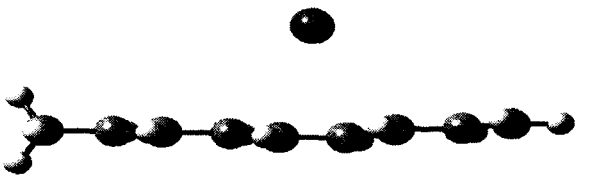

(d) $C_9H_{12}K$ (6)

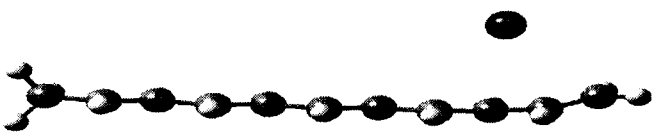

(e) $C_{11}H_{14}K$ (9)

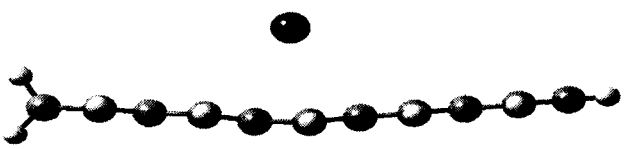

(f) $C_{11}H_{14}K$ (6)

Figure 4.3: Optimized structures of the stable isomers of potassium doped polyenes (B3LYP/6-31G*)

4.2.2 Doping- induced changes in the molecular parameters

As a result of metal doping, there occur substantial changes in the values of carbon- carbon bond lengths, bond angles and dihedral angles. The changes are, however, not so intense as in the case of metal substitution. It may be a pointer to the feeble interaction in these complexes resulting in very low stabilisation energy.

4.2.2.1 Enhanced delocalisation of the electrons

The bond length values in metal free polyenic system C_9H_{12}, polyenic anion $(C_9H_{11})^-$ and metal-doped polyenes are given in Table 4.5 for a comparison.

Table 4.5: C-C bond lengths (A^0) in C_9H_{12}, $(C_9H_{11})^-$ and the stable Li/Na/K doped C_9H_{12} (B3LYP/6-31G*)

System	C1-C2	C2-C3	C3-C4	C4-C5	C5-C6	C6-C7	C7-C8	C8-C9
C_9H_{12}	1.4983	1.3469	1.4461	1.3563	1.4406	1.3560	1.4476	1.3442
$(C_9H_{11})^-$	1.3613	1.4277	1.3864	**1.4047**	**1.4047**	1.3864	1.4277	1.3613
$C_9H_{12}Li(8)$	1.4986	1.3603	**1.4259**	**1.3906**	**1.3973**	**1.4204**	**1.4103**	**1.4086**
$C_9H_{12}Li(6)$	1.4985	1.3618	**1.4263**	**1.4034**	**1.4153**	**1.4135**	1.4419	1.3532
$C_9H_{12}Li(3)$	1.5097	**1.4044**	**1.4151**	**1.4180**	**1.3996**	**1.3891**	**1.4271**	1.3580
$C_9H_{12}Na(9)$	1.4978	1.3492	1.4421	1.3621	1.4319	1.3671	1.4307	1.3664
$C_9H_{12}Na(6)$	1.4976	1.3507	1.4435	**1.3765**	**1.4265**	**1.3764**	1.4453	1.3482
$C_9H_{12}K(8)$	1.4985	1.3534	1.4362	**1.3714**	**1.4262**	**1.3844**	**1.4248**	**1.3710**
$C_9H_{12}K(6)$	1.4982	1.3540	1.4404	**1.3823**	**1.4205**	**1.3824**	1.4412	1.3523

It is evident from the bond length values that there is extensive delocalisation in the doped polyenes in the portion excluding the sp^3 carbon, which is somewhat different from the pattern in polyenyl anion. The terminal single bond involving the sp^3 carbon is almost unchanged. There is total delocalisation in the fragment interacting with Li (the bond length values are very close); partial delocalisation in the fragment interacting with K; but the fragment interacting with Na has poorly delocalised pi electron cloud (See values in bold letters in Table 4.5). The efficiency of delocalisation is in the order Li-doped complex > K-doped complex > Na-doped complex. It may be noted that the charge density of the dopant varies in the same order (see Table 4.1).

4.2.2.2 Distortion to the carbon skeleton of the polyene

With regard to the distortion due to doping, which is indicated by the deviation in the bond angles and dihedral angles, it is observed that the K-doped complexes are more distorted than their Na and Li counterparts. In fact, in Na-complexes, the carbon skeleton remains almost unchanged. The Li-complexes exhibit almost similar traits as the Li substituted polyenes. The bond angles and dihedral angles of the metal–polyene complexes, given in Tables 4.6 & 4.7, highlight the effect of metal doping on the carbon skeleton.

Table 4.6: Selected bond angles in free C_9H_{12} and the most stable Li/Na/K-C_9H_{12} complexes (B3LYP/6-31G*).

System	HC1C2	C1C2C3	C2C3C4	C3C4C5	C4C5C6	C5C6C7	C6C7C8	C7C8C9	C8C9H
C_9H_{12}	111.30	125.14	124.49	124.52	124.41	124.64	124.24	124.64	121.53
$C_9H_{12}Li(8)$	111.42	125.37	125.81	124.87	125.17	126.27	123.25	125.51	120.71
$C_9H_{12}Na(9)$	111.34	125.13	124.56	124.56	124.43	124.89	124.01	125.75	121.22
$C_9H_{12}K(8)$	111.59	125.03	125.22	124.61	125.16	125.55	124.63	126.08	121.42

Table 4.7: Selected dihedral angles in free C_9H_{12} and the most stable Li/Na/K-C_9H_{12} complexes (B3LYP/6-31G*).

System	HC1C2C3	C1C2C3C4	C2C3C4C5	C3C4C5C6	C4C5C6C7	C5C6C7C8	C6C7C8C9	C7C8C9H
C_9H_{12}	0.0	180.0	-180.0	-180.0	180.0	180.0	-180.0	0.0
$C_9H_{12}Li(8)$	-0.11	179.97	-179.95	179.95	-179.25	**176.89**	**-168.27**	-27.58
$C_9H_{12}Na(9)$	0.35	180.0	-179.83	179.91	-179.81	179.89	-177.96	**-6.31**
$C_9H_{12}K(8)$	-0.46	-179.83	179.50	-179.68	178.10	**-175.19**	**162.22**	-10.65

As the result of alkali metal doping, slight distortion in the planarity of the carbon skeleton takes place; but the distortion does not turn out as a visible bent as that we found in K substituted polyenes (see Figure 4.4).

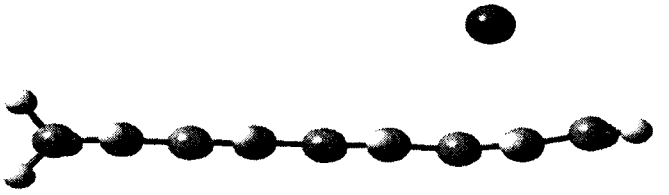

(a) $C_9H_{12}K$ (8)

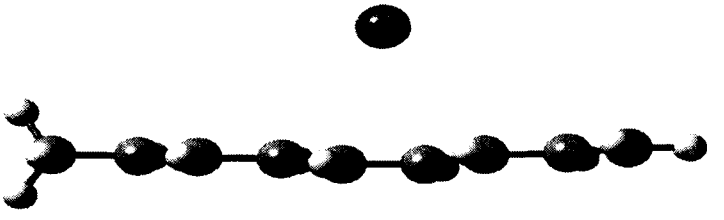

(b) $C_9H_{12}K$ (6)

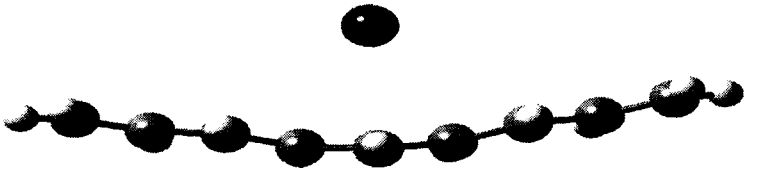

(c) $C_9H_{11}K$ (5)

Figure 4.4: Potassium doped and substituted C_9 systems (B3LYP/6-31G*)

4.2.3 Enhancement of the conductance

The values of HOMO-LUMO gap of all the isomers of metal-doped systems are presented in Table 4.1. The HOMO and LUMO energy (E_H & E_L) values indicate that the metal-doped species are having more conductance than the metal substituted polyenes. The values of a few systems are compared with the corresponding metal-free systems in Table 4.8.

Table 4.8: Values of HOMO-LUMO energy gap of some metal-free and metal-doped polyenic systems (B3LYP/6-31G*).

System	E_H (Hartree)	E_L (Hartree)	$\Delta E = E_L - E_H$ (kcal/mol)
C_7H_{10}	-0.20081	-0.03841	101.91
$C_7H_{10}Li$ (6)	-0.11214	-0.05024	38.84
$C_7H_{10}Na$ (7)	-0.10867	-0.05719	32.30
$C_7H_{10}K$ (7)	-0.09366	-0.05526	24.10
C_9H_{12}	-0.19034	-0.05269	86.38
$C_9H_{12}Li$ (8)	-0.11733	-0.05209	40.94
$C_9H_{12}Na$ (9)	-0.10985	-0.06676	27.04
$C_9H_{12}K$ (8)	-0.09530	-0.06444	19.36
$C_{11}H_{14}$	-0.18318	-0.06239	75.80
$C_{11}H_{14}Li$ (10)	-0.12104	-0.05421	41.94
$C_{11}H_{14}Na$ (11)	-0.11159	-0.07303	24.20
$C_{11}H_{14}K$ (9)	-0.09911	-0.06961	19.14

The conductance has increased considerably by the metal doping as is evident from the HOMO-LUMO gap. The values show that potassium doping gave the maximum conductance whereas the lithium doping effected a minimum only. Also, it can be noticed that the conductance was almost doubled when metals were doped instead of being substituted (Compare Tables 3.9 and 4.8). As the chain length increases, the conductance also increases, which points to the possible effect of metal doping in long polyenes. It should be recalled that the PA chain, an enlarged form of conjugated polyenes, attains electrical conductance when doped with alkali metals [2].

4.2.4 Formation of different isomers

We have found that the segment interacting with the doped metal is the part excluding the sp^3 carbon and hence the odd-even numbering is less significant here. Table 4.1 provides the list of stable isomers obtained when Li, Na and K were doped to the polyenes ranging from C_5 to C_{11}. These isomers bring out the general features of alkali metal-doped polyenes. Only Li shows a uniform character- its most stable isomer in all the metal-doped systems is $C_nH_{n+3}Li(n-1)$. Thus we have C_5H_8Li (4), $C_7H_{10}Li$ (6), $C_9H_{12}Li$ (8), etc., as the stable isomers of different systems. Isomers of higher energy are also possible for these systems. In all of them, Li tends to attach on to an even carbon. The C-C bond lengths in different isomers show that Li always interact with an allyl fragment with delocalised electron cloud (Table 4.5).

As for Na, apart from the most stable isomer with the general formula $C_nH_{n+3}Na$ (n), there are other isomers; but they are of very low E_{st}. All of them tend to attach to an even carbon, which is the part of an allyl fragment. Examples for Na isomers with higher energy or lower E_{st} are $C_7H_{10}Na$ (4), $C_9H_{12}Na$ (6), $C_9H_{12}Na$ (4), $C_{11}H_{14}$ Na (7), etc.

K-doped polyenes do not follow a general pattern. In C_5 and C_7 systems, most stable isomers are C_5H_8K (5) and $C_7H_{10}K$ (7). But when we reach C_9H_{12}, the most stable isomer becomes $C_9H_{12}K$ (8), others isomers being $C_9H_{12}K$ (6) and $C_9H_{12}K$ (4). In $C_{11}H_{14}$, the stable isomers are $C_{11}H_{14}K$ (9), $C_{11}H_{14}K$ (7), $C_{11}H_{14}K$ (6) and $C_{11}H_{14}K$ (4). However, it should be remembered that the metal is very often above a C-C bond rather than being above a carbon. Also, since the interacting part is the fragment with conjugated double bond, the odd even distinction becomes less relevant in odd polyenes.

The number of isomers possible in each system can be predicted easily. Since all the metals interact possibly with an allyl fragment, each allyl fragment can contribute one stable isomer. Thus, C_5 system can have one, C_7 can have two, C_9 can have three and so on, the number increasing with increase in the length of the polyene.

It is remarkable that the different isomers of the same system differ by small amounts of energy. For example, in C_{11} system, the most stable $C_{11}H_{14}K$ (9) differs from the nearest isomer $C_{11}H_{14}K$ (7) by mere 0.64 kcal/mol. Energy difference between $C_{11}H_{14}K$ (7) and $C_{11}H_{14}K$ (6) is just 0.20 kcal/mol. On the other hand, the most stable Li isomer differs in energy by appreciable amounts from its counterparts of lesser E_{st}. In C_9 system, $C_9H_{12}Li$ (6) is higher than $C_9H_{12}Li$ (8) in energy by 4.02 kcal/mol. However, the lower Li-isomers are mutually very close in their energies. The same is the case with Na-isomers of different systems.

In order to get a better understanding of metal doping to polyenes, doping to even polyenes, where the sp^3 carbon is absent, is also necessary. Hence some samples of even polyenes are also doped with alkali metals and the results are presented in the next section.

4.3 Doping of alkali metals to even numbered all-trans conjugated polyenes

Since substitution of metals in an even numbered conjugated polyene is a planar substitution delivering no significant result (See discussion in 3.2.1) we considered the even polyenes for doping reactions only. Even numbered all trans polyenes are almost similar to the odd polyenes with regard to doping, as they differ only by a non-interacting CH_3 group. Hence, the doping of alkali metal atom into conjugated even polyenes should give identical products as those obtained for odd polyenes. In order to verify this

assumption, we studied the doping of alkali metals to three polyenes, namely C_6H_8, C_8H_{10} and $C_{10}H_{12}$, the first one closer to C_7H_{10}, second closer to C_9H_{12} and the last closer to $C_{11}H_{14}$. True to our expectations, the doping to C_6H_8, C_8H_{10} and $C_{10}H_{12}$ gave almost identical products, with comparable binding energies. This suggests that as in odd polyenes, doping in even polyenes also results in weak interactive forces between the metal and the polyene. Mulliken charges on the doped metals were also in the same range as in the metal-odd polyene complexes. A difference was that the number of isomers was less, as the even polyene is symmetric with respect to the two terminals. The stable isomers obtained on alkali metal doping with some of their characteristics are presented in Table 4.9.

Table 4.9: The stable isomers of Li/Na/K doped C_6, C_8 and C_{10} systems with their important characteristics (B3LYP/6-31G*).

Metal-polyene complex	Stable isomers [a]	E (Hartree)	E_{st} (kcal/mol)	Ri (A°)	Q_M (a.u)	$\Delta E=E_L-E_H$ (Hartree)
C_6H_8Li	C_6H_8Li (2)	-240.91360	15.10	C2-Li=2.0615	0.261470	0.06556
C_6H_8Na	C_6H_8Na (1)	-395.68241	02.50	C1-Na=2.7913	*-0.012103*	0.04992
C_6H_8K	C_6H_8K (2)	-833.29241	02.16	C2-K=3.0572	0.183787	0.03316
$C_8H_{10}Li$	$C_8H_{10}Li$ (2)	-318.32596	19.25	C2-Li=2.0617	0.285942	0.06776
	$C_8H_{10}Li$ (4)	-318.31948	15.47	C4-Li=2.0526	0.308065	0.05818
$C_8H_{10}Na$	$C_8H_{10}Na$ (1)	-473.09065	03.51	C1-Na=2.6814	0.048531	0.04225
	C_8H_{10} Na (4)	-473.08654	01.42	C4-Na=2.6268	0.151541	0.03363
$C_8H_{10}K$	$C_8H_{10}K$ (2)	-910.70279	05.31	C2-K=2.9679	0.357919	0.03167
	$C_8H_{10}K$ (5)	-910.70066	04.17	C5-K=2.9623	0.389450	0.02821
$C_{10}H_{12}Li$	$C_{10}H_{12}Li$ (2)	-395.73684	21.43	C2-Li=2.0622	0.296187	0.06876
	$C_{10}H_{12}Li$ (4)	-395.73126	18.21	C4-Li=2.0552	0.335609	0.06223
$C_{10}H_{12}Na$	$C_{10}H_{12}Na$(2)	-550.49839	04.45	C2-Na=2.5661	0.229626	0.03356
	$C_{10}H_{12}Na$(5)	-550.49620	03.09	C5-Na=2.5628	0.250329	0.03235
$C_{10}H_{12}K$	$C_{10}H_{12}K$(3)	-988.11293	07.43	C3-K=2.8872	0.491595	0.03175
	$C_{10}H_{12}K$(5)	-988.11185	07.06	C5-K=2.8605	0.566187	0.02912

[a] The numeral in parentheses corresponds to the carbon to which the metal is having smallest distance.

The charges on the metals and the carbons of the polyenyl chain play a significant role in the formation of different isomers. The Mulliken charges on each carbon of the polyene and of the complexes obtained via metal doping are presented in Table 4.10(a), 4.10(b) & 4.10(c) (B3LYP/6-31G*).

Table 4.10(a): Mulliken charges (a.u) on the carbons in C_6H_8 and its stable Li/Na/K-doped complexes

System	C1	C2	C3	C4	C5	C6
C_6H_8	-0.355	-0.060	-0.122	-0.122	-0. 060	-0.355
C_6H_8Li (2)	-0.432	-0.113	-0.209	-0.115	-0.168	-0.376
C_6H_8Na (2)	-0.427	-0.059	-0.124	-0.119	-0.162	-0.355
C_6H_8K (2)	-0.410	-0.112	-0.178	-0.148	-0.064	-0.366

Table 4.10(b): Mulliken charges (a.u) on the carbons in C_8H_{10} and its stable Li/Na/K-doped complexes

System	C1	C2	C3	C4	C5	C6	C7	C8
C_8H_{10}		-0.060	-0.122	-0.123	-0.122	-0.122	-0.060	-0.356
$C_8H_{10}Li$ (2)	**-0.438**	**-0.100**	**-0.219**	-0.110	-0.131	-0.132	-0.065	-0.370
$C_8H_{10}Li$ (4)	-0.381	-0.038	**-0.212**	**-0.161**	**-0.216**	**-0.119**	-0.065	-0.377
$C_8H_{10}Na$ (1)	**-0.448**	-0.061	-0.129	-0.121	-0.126	-0.123	-0.061	-0.358
$C_8H_{10}Na$ (4)	-0.364	-0.057	**-0.151**	**-0.182**	**-0.182**	-0.151	-0.057	-0.365
$C_8H_{10}K$ (2)	**-0.430**	**-0.113**	**-0.204**	-0.160	-0.134	-0.133	-0.063	-0.372
$C_8H_{10}K$ (5)	-0.378	-0.061	-0.182	**-0.189**	**-0.189**	**-0.182**	-0.061	-0.378

Table 4.10(c): Mulliken charges (a.u) on the carbons in $C_{10}H_{12}$ and its stable Li/Na/K-doped complexes

System	C1	C2	C3	C4	C5	C6	C7	C8	C9	C10
$C_{10}H_{12}$	-0.356	-0.060	-0.123	-0.122	-0.123	-0.123	-0.122	-0.123	-0.060	-0.356
$C_{10}H_{12}Li(2)$	**-0.440**	**-0.093**	**-0.226**	-0.105	-0.134	-0.131	-0.127	-0.131	-0.062	-0.367
$C_{10}H_{12}Li(4)$	-0.383	-0.036	**-0.225**	**-0.146**	**-0.223**	-0.111	-0.130	-0.134	-0.064	-0.371
$C_{10}H_{12}Na(2)$	**-0.427**	**-0.116**	**-0.182**	-0.128	-0.133	-0.128	-0.125	-0.129	-0.061	-0.364
$C_{10}H_{12}Na(5)$	-0.370	-0.056	-0.161	**-0.181**	**-0.194**	**-0.155**	-0.123	-0.129	-0.061	-0.368
$C_{10}H_{12}K(3)$	**-0.441**	**-0.112**	**-0.222**	**-0.166**	**-0.146**	-0.136	-0.128	-0.136	-0.060	-0.372
$C_{10}H_{12}K(5)$	-0.387	-0.060	**-0.194**	**-0.188**	**-0.211**	**-0.194**	**-0.134**	-0.142	-0.062	-0.379

The distribution of charges indicates that there is an enhanced charge concentration in the region where the metal resides in the metal polyenyl complex. The charge distribution extends over a pentadienyl segment in cases where the metal is closer to an odd carbon. Examples are $C_{10}H_{12}K$ (3) and $C_{10}H_{12}K$ (5). A clear picture emerges when the net Mulliken charges on the carbons in different systems are examined. They are presented in Table 4.11.

Table 4.11: The net charges (a.u) on the carbons of $C_{10}H_{12}$ and its Li/Na/K doped complexes.

System	C1	C2	C3	C4	C5	C6	C7	C8	C9	C10
$C_{10}H_{12}$	-0.070	0.066	0.001	0.002	0.001	0.001	0.002	0.001	0.066	-0.070
$C_{10}H_{12}Li(2)$	**-0.134**	**0.054**	**-0.084**	0.012	-0.028	-0.023	-0.019	-0.021	0.051	-0.105
$C_{10}H_{12}Li(4)$	-0.134	0.079	**-0.084**	**-0.004**	**-0.080**	-0.006	0.024	-0.027	0.045	-0.114
$C_{10}H_{12}Na(2)$	**-0.110**	**0.027**	**-0.054**	-0.002	-0.015	-0.013	-0.011	-0.014	0.058	-0.094
$C_{10}H_{12}Na(5)$	-0.101	0.066	-0.028	**-0.043**	**-0.058**	**-0.022**	-.003	-0.015	0.054	-0.101
$C_{10}H_{12}K(3)$	**-0.165**	**0.014**	**-0.110**	**-0.047**	**-0.036**	-0.029	-0.021	-0.030	0.050	-0.117
$C_{10}H_{12}K(5)$	-0.139	0.051	**-0.081**	**-0.071**	**-0.097**	**-0.078**	**-0.025**	-0.039	0.045	-0.132

4.3.1 Position of the metal

In C_6H_8, C_8H_{10} and $C_{10}H_{12}$, Li behaved in the same pattern as in the odd polyenes- that the metal stationed above even carbons in its stable isomers and the most stable isomer has it over the 2nd carbon. Na behaved differently in the three systems; in C_6H_8 complex, it has only one isomer i.e., C_6H_8Na (1), in C_8H_{10} complex, its two isomers are $C_8H_{10}Na$ (1) and $C_8H_{10}Na$ (4) whereas in $C_{10}H_{12}$ complex, the two isomers are $C_{10}H_{12}Na$ (2) and $C_{10}H_{12}Na$ (5). For K, the trend is different in these systems, the different sets of isomers being C_6H_8K (2) for C_6H_8, $C_8H_{10}K$ (2) and $C_8H_{10}K$ (5) for C_8H_{10} and $C_{10}H_{12}K$ (3) and $C_{10}H_{12}K$ (5) for $C_{10}H_{12}$. There are two factors to be noted here before terming the above phenomena as irregular. As the metal moves towards the centre of the polyene, the odd-even difference assumes less

significance in even numbered conjugated polyenes. Secondly, in most of the isomers, the metals are actually residing almost at the centre of the C(i)-C(i±1) bond [C(i) is the carbon to which the metal has the shortest distance]. The different isomers of C_{10} system and their metal-carbon distances and relevant bond angles are presented in Table 4.12.

Table 4.12. Metal carbon distances and metal polyene bond angles in some selected systems (B3LYP/6-31G*).

System	C(i-1)-M (A^0)	C(i)- M (A^0)	C(i+1)-M (A^0)	MC(i)C(i+1) (deg.)	MC(i)H(i) (deg.)
$C_{10}H_{12}Li$ (2) [a]	2.0997	2.0622	2.1790	75.12	117.30
$C_{10}H_{12}Li$ (4)	2.1647	2.0552	2.1605	74.52	115.16
$C_{10}H_{12}Na$ (2)	2.6060	2.5661	2.7759	82.97	106.05
$C_{10}H_{12}Na$ (5)	2.5673	2.5628	2.9354	90.87	98.17
$C_{10}H_{12}K$ (3)	2.9277	2.8872	3.2420	91.61	92.73
$C_{10}H_{12}K$ (5)	2.9127	2.8605	3.1566	88.72	96.54

[a] The numeral in parentheses corresponds to the carbon to which the metal is having smallest distance.

It can be found from Table 4.12 that Li in $C_{10}H_{12}Li$ (2) is between carbons C1 & C2. Similarly, Na in $C_{10}H_{12}Na$ (5) is between C4 & C5. The same trend is retained in other systems also. In $C_8H_{10}Li$ (2), lithium is over C1-C2 bond (C1-Li = 2.097; C2-Li = 2.062) and in $C_8H_{10}Li$ (4), the metal is over C4-C5 bond (C4-Li = 2.05; C5-Li = 2.15). Similarly, in $C_8H_{10}K$ (2), C2-K = 2.968 and C3-K = 2.978 and in $C_{10}H_{12}K$ (5), C4-K = 2.9127 and C5-K = 2.8605. All these indicate that the doped metals are situated above the C-C bond. The bond angles (Table 4.12) suggest that the metals reside approximately vertically above the carbon atoms. The structures of the different free polyenes and the stable isomers of their metal-doped complexes are given in Figure 4.5.

(a) C_6H_8

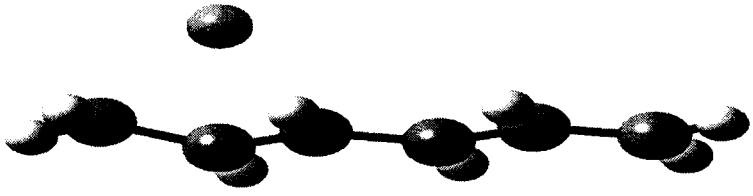

(b) C_6H_8Li (2)

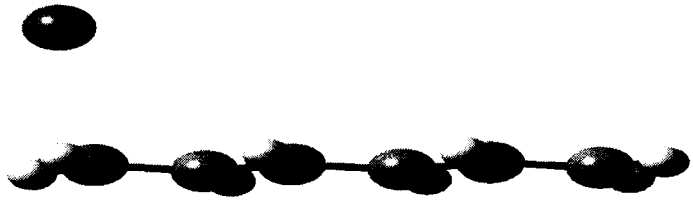

(c) C_6H_8Na (1)

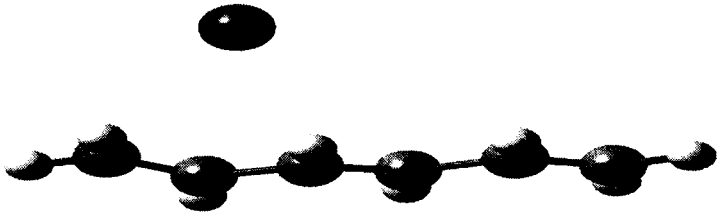

(d) C_6H_8K (2)

(e) C_8H_{10}

(f) $C_8H_{10}Li$ (2)

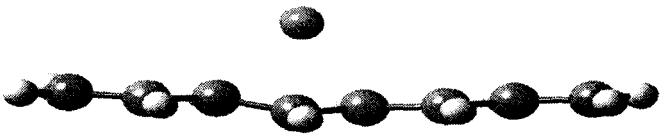

(g) $C_8H_{10}Li$ (4)

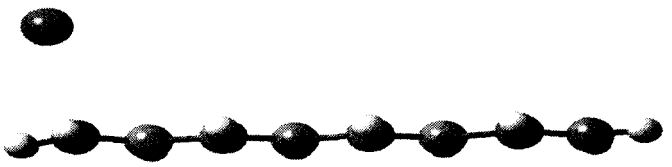

(h) $C_8H_{10}Na$ (1)

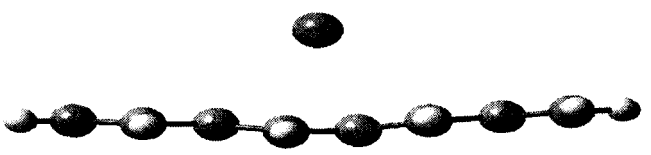

(i) $C_8H_{10}Na$ (4)

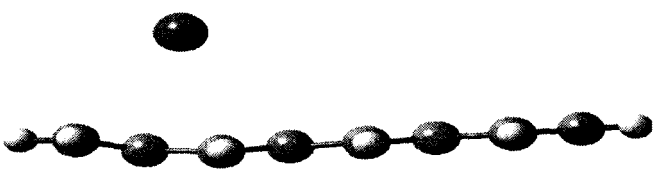

(j) $C_8H_{10}K$ (2)

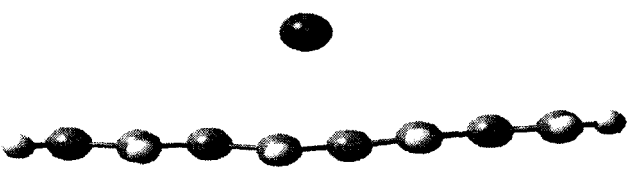

(k) $C_8H_{10}K$ (5)

(l) $C_{10}H_{12}$

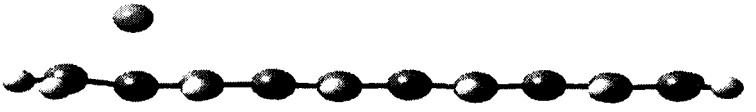

(m) $C_{10}H_{12}Li$ (2)

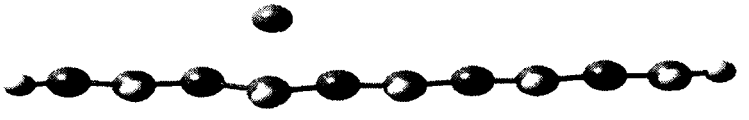

(n) $C_{10}H_{12}Li$ (4)

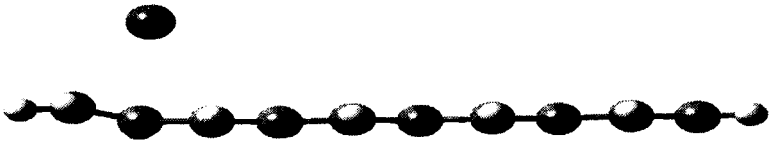

(o) $C_{10}H_{12}Na$ (2)

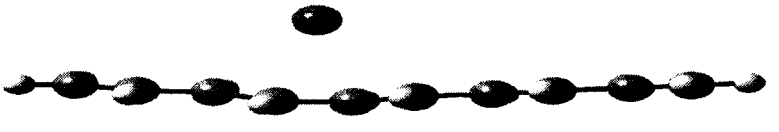

(p) $C_{10}H_{12}Na$ (5)

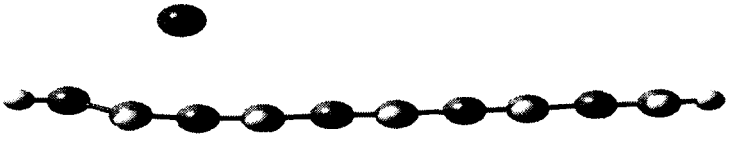

(q) $C_{10}H_{12}K$ (3)

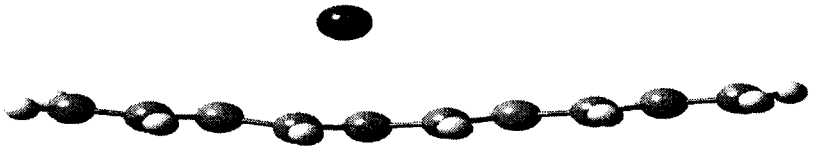

(r) $C_{10}H_{12}K$ (5)

Figure 4.5: Free C_6H_8, C_8H_{10} and $C_{10}H_{12}$ and the stable isomers of their Li/Na/K doped complexes (B3LYP/6-31G*)

4.3.2 Doping induced changes in the molecular parameters

The doping of the metal in a conjugated polyene of even number causes significant changes to the molecular parameters such as bond lengths, bond angles and dihedral angles. The structural deviation is very much evident from the figure itself (Figure 4.5). As the polyenic chain length increases, these changes become more and more pronounced.

4.3.2.1 Change in carbon- carbon bond lengths

For a comparison of the changes in the C-C bond lengths, the optimized bond length values of the free $C_{10}H_{12}$ and its stable isomers of Li/Na/K doped complexes are given in Table 4.13.

Table 4.13: Optimized C-C bond lengths (A^0) in free $C_{10}H_{12}$ and its Li/Na/K doped complexes (B3LYP/6-31G*)

System	C1-C2	C2-C3	C3-C4	C4-C5	C5-C6	C6-C7	C7-C8	C8-C9	C9-C10
$C_{10}H_{12}$	1.3446	1.4468	1.3573	1.438	1.3598	1.438	1.3573	1.4468	1.3446
$C_{10}H_{12}Li$ (2)	**1.4042**	**1.4106**	**1.4243**	**1.3874**	**1.4025**	**1.4057**	**1.3819**	1.4315	1.3546
$C_{10}H_{12}Li$ (4)	1.3511	1.4446	**1.4110**	**1.4122**	**1.4166**	**1.4007**	**1.3875**	**1.4282**	1.3570
$C_{10}H_{12}Na$(2)	**1.3827**	**1.4187**	**1.3894**	**1.4158**	**1.3791**	**1.4220**	**1.3686**	1.4393	1.3493
$C_{10}H_{12}Na$(4)	1.3510	1.4418	**1.3818**	**1.4170**	**1.3930**	**1.4265**	**1.3700**	1.4379	1.3502
$C_{10}H_{12}K$ (3)	**1.3765**	**1.4194**	**1.3956**	**1.4136**	**1.3876**	**1.4156**	**1.3744**	1.4358	1.3521
$C_{10}H_{12}K$ (5)	1.3556	1.4367	**1.3926**	**1.4101**	**1.4004**	**1.4189**	**1.3791**	1.4326	1.3545

As the result of extended conjugation, there is considerable delocalisation of the electron cloud in the $C_{10}H_{12}$ system, which is clear from the C-C bond lengths. This delocalisation is further enhanced as the result of metal doping. For Li-doped complexes, the delocalisation is more efficient, especially inside the polyenic fragment above which the metal is residing (the bond length values are close to one another). This may be taken as an evidence for the interaction between the Li^+ and the pi-electron cloud. In Na and K-doped complexes, there is enhanced oscillation of the pi-electrons, but to a lesser extent in comparison with Li complexes. In all these complexes, the doped neutral metal atom loses some of its electron (for e.g., in $C_{10}H_{12}Li$ (2), the charge of the metal increased from zero to ca. 0.296), which may be the contributing factor to the stabilization of such complexes.

4.3.2.2 Distortion of the carbon skeleton of the polyene

The distortion in the carbon skeleton can be determined by comparing the bond angles and dihedral angles of the free polyene and that of the metal-doped polyenes. Selected bond angles and dihedral angles in free $C_{10}H_{12}$ and Li/Na/K doped $C_{10}H_{12}$ are given in Tables 4.14(a) & 4.14(b).

Table 4.14(a): Selected bond angles in free $C_{10}H_{12}$ and the most stable Li/Na/K- $C_{10}H_{12}$ complexes (B3LYP/6-31G*).

System	H1C1C2	C1C2C3	C2C3C4	C3C4C5	C4C5C6	C5C6C7	C6C7C8	C7C8C9
$C_{10}H_{12}$	121.54	124.56	124.26	124.55	124.43	124.43	124.55	124.26
$C_{10}H_{12}Li(2)$	119.46	125.91	125.15	125.99	124.96	124.70	125.38	124.19
$C_{10}H_{12}Na(2)$	120.87	126.06	124.63	125.56	124.75	124.67	125.05	124.22
$C_{10}H_{12}K(3)$	121.07	126.56	124.47	126.11	125.37	124.85	125.56	124.24

Table 4.14(b): Selected dihedral angles in free $C_{10}H_{12}$ and the most stable Li/Na/K- $C_{10}H_{12}$ complexes (B3LYP/6-31G*).

System	H1C1C2C3	C1C2C3C4	C2C3C4C5	C3C4C5C6	C4C5C6C7	C5C6C7C8	C6C7C8C9	C7C8C9C10
$C_{10}H_{12}$	0.0	180.0	-180.0	180.0	-180.0	180.0	-180.0	180.0
$C_{10}H_{12}Li(2)$	**-26.42**	**169.79**	**-175.68**	179.16	-179.83	179.96	-179.99	179.95
$C_{10}H_{12}Na(2)$	**-14.55**	**163.29**	**-176.11**	179.23	-179.81	179.87	-179.96	179.94
$C_{10}H_{12}K(3)$	**12.49**	**158.23**	**-169.93**	179.29	-179.66	179.07	-179.88	179.94

The bond angle and the dihedral angle values show that there is considerable distortion taking place as the result of metal doping to even numbered conjugated polyenes. However, the parabola type warping that we found with K substitution in odd numbered polyene has not been achieved. Also it should be noted that the distortion increases as the length of the polyene increases. As the length of the polyene increases, the positive charge on the doped metal also increases.

4.3.3 Increase in the conductance

The HOMO and the LUMO energies (E_H & E_L) and their differences in the free polyenes and their Li/Na/K- doped complexes are given in Table 4.15.

Table 4.15: HOMO-LUMO difference in free C_6H_8, C_8H_{10}, $C_{10}H_{12}$ and their Li/Na/K- doped complexes (B3LYP/6-31G*).

System	E_H (Hartree)	E_L (Hartree)	$\Delta E = E_L - E_H$ (kacl/mol)
C_6H_8	-0.20923	-0.04436	103.46
C_6H_8Li (2)	-0.11694	-0.05138	41.14
C_6H_8Na (1)	-0.11169	-0.06177	31.33
C_6H_8K (2)	-0.09423	-0.06107	20.81
C_8H_{10}	-0.19700	-0.05771	87.41
$C_8H_{10}Li$ (2)	-0.12155	-0.05379	45.52
$C_8H_{10}Na$ (1)	-0.11274	-0.07049	26.51
$C_8H_{10}K$ (2)	-0.09818	-0.06651	19.87
$C_{10}H_{12}$	-0.18870	-0.06672	76.54
$C_{10}H_{12}Li$ (2)	-0.12473	-0.05597	43.15
$C_{10}H_{12}Na$ (2)	-0.11204	-0.07848	21.06
$C_{10}H_{12}K$ (3)	-0.10181	-0.07006	19.92

Due to the metal doping in conjugated polyenes, the conductance has a substantial increase as indicated by the decreased HOMO- LUMO gap. The alkali metals, being good reducing agents, provide their electrons to the already delocalised electron system which enhances charge carrier ability and thereby the conductance.

4.3.4 Formation of different isomers

Doping of alkali metals to even polyenes gave different isomers. As in the case of odd polyenes, here too only Li shows a uniform character- the most stable isomer in the three systems has the general formula $C_nH_{n+2}Li$ (2) and the second isomer has the general formula $C_nH_{n+2}Li$ (4). In general, the isomers of Li show an affinity towards the even carbons.

In the case of Na, its most stable isomer in C_6 and C_8 systems has the general formula $C_nH_{n+2}Na$ (n), whereas in C_{10} system it becomes $C_{10}H_{12}Na$ (2). In the C_{10} system, Na loses some of its electrons to attain a charge of 0.2296 and moves to the second carbon to have effective interaction with the allylic fragment. The second isomer for Na-doped C_8 system is $C_8H_{10}Na$ (4) whereas that of C_{10} system is $C_{10}H_{12}Na$ (5).

K too gives different isomers for different systems. The most stable isomer in C_6 and C_8 systems are C_6H_8K (2) and $C_8H_{10}K$ (2) respectively. On the other hand, the most stable isomer in C_{10} system is $C_{10}H_{12}K$ (3). The second isomer in all the systems studied, which is of slightly higher energy, has the metal over the C5, with the general formula $C_nH_{n+2}K$ (5).

The energy difference between the different isomers of the same system is very low for K/Na-complexes, but considerably high for Li-complexes. For example, $C_{10}H_{12}K$ (3) and $C_{10}H_{12}K$ (5) differ by 0.37 kcal/mol only and the Na- isomers of the same system differ by 1.36 kcal/mol. However, for Li isomers, the energy difference is higher. From Table 4.9, it

can be noted that $C_{10}H_{12}Li$ (2) is lower in energy by 3.22 kcal/mol than the second stable isomer of the system, $C_{10}H_{12}Li$ (4). It may be assumed that the interactive forces rendering stability to the K and Na isomers are almost the same irrespective of their position on the polyene. On the other hand, for Li-complexes, such forces get minimized as the metal moves towards the center of the polyene.

4.4 Alkali metal doping to substituted polyenes

When metals are doped to the polyenes, the interaction arises due to the flow of electron from the metal to the polyene. When electron-donating groups are present in the polyene, they will enhance the electron cloud in the polyene and hence electron flow from the metal to the polyene will be retarded. This implies that there will be less intense interaction between the polyene and the metal. i.e., lesser stability to the product. On the other hand, when electron-withdrawing groups are present, there will be relative decrease of pi cloud in the polyene. Then, the electron flow from the metal to the polyene will be more. i.e., more stability to the metal-doped substituted polyene. Thus the trend will be exactly the opposite of what we found in metal substitution to substituted polyenes.

4.4.1 Metal doping to $C_9H_{11}CH_3$

Alkali metals were doped to $C_9H_{11}CH_3$ and the E_{st} and other parameters of the complexes thus obtained were determined. They were compared with those of the metal-doped complexes to find out the effect of substitution on E_{st} and other parameters. In Table 4.16 the different characteristics of Li/Na/K doped C_9H_{12} and $C_9H_{11}CH_3$ (8) are presented (B3LYP/6-31G*).

Table 4.16: The most stable Li/Na/K doped complexes of C_9H_{12} and $C_9H_{11}CH_3$ (8)

Metal-polyene system	E (Hartree)	E_{st} (kcal/mol)	Ri (A^o)	Q_M (a.u)	$\Delta E = E_L - E_H$ (Hartree)
$C_9H_{12}Li$ (8)	-357.64512	18.61	C8-Li=2.0605	0.277739	0.06524
$C_9H_{11}CH_3$(8)Li (8)	-396.96091	17.56	C8-Li=2.0820	0.267949	0.06283
$C_9H_{12}Na$(9)	-512.41082	03.41	C9-Na= 2.7096	0.018860	0.04309
$C_9H_{11}CH_3$(8)Na(9)	-551.72875	03.68	C9-Na=2.7326	-0.007821	0.04637
$C_9H_{12}K$(8)	-950.02215	04.61	C8-K= 2.9960	0.289659	0.03086
$C_9H_{11}CH_3$(8)K (8)	-989.33979	04.52	C8-K=3.0221	0.232285	0.03413

From the E_{st} values we can infer that Li-doped and K-doped polyenes are having more stability than their substituted polyene counter parts [i.e., $C_9H_{12}Li$ (8) is more stable than $C_9H_{11}CH_3$ (8)Li (8)]. In such systems, metals have lower charges on them, but the metal- carbon distance exhibits an increase of ca. 0.03 A^0. There is modification in the conductance of the system too - Na and K complexes show lower values, whereas Li complexes show higher values. In Na-doped substituted polyenes, Na possesses a small negative charge (-0.0078). This shows that the electron flow is from the polyene to the metal. Hence introduction of electron donating group slightly increases the energy of stabilization of that complex. However, for Li and K doped substituted polyenes, the E_{st} is actually decreasing- a direct effect of electron donating group.

In Table 4.17, the Mulliken charges on different carbons of different systems are presented.

Table 4.17: Mulliken charges (a.u) on the carbons of Li/Na/K doped $C_9H_{11}CH_3$ and free $C_9H_{11}CH_3$ (B3LYP/6-31G*).

System	C1	C2	C3	C4	C5	C6	C7	C8	C9
C_9H_{12}	-0.491	-0.105	-0.100	-0.122	-0.126	-0.122	-0.125	-0.060	-0.358
$C_9H_{11}CH_3$ (8)	-0 .491	-0.106	-0.100	-0.126	-0.119	-0.122	-0.177	0.237	-0.413
$C_9H_{12}Li$ (8)	-0.486	-0.117	-0.102	-0.134	-0.132	-0.111	**-0.218**	**-0.101**	**-0.438**
$C_9H_{11}CH_3$(8)Li (8)	-0.486	-0.117	-0.102	-0.137	-0.127	-0.110	**-0.276**	**0.173**	**-0.472**
$C_9H_{12}Na$(9)	-0.491	-0.106	-0.101	-0.123	-0.129	-0.120	-0.130	-0.060	**-0.443**
$C_9H_{11}CH_3$(8)Na(9)	-0.491	-0.106	-0.100	-0.126	-0.121	-0.117	-0.181	0.235	**-0.489**
$C_9H_{12}K$(8)	-0.487	-0.115	-0.101	-0.132	-0.135	-0.153	**-0.199**	**-0.112**	**-0.425**
$C_9H_{11}CH_3$(8)K (8)	-0.488	-0.113	-0.101	-0.133	-0.126	-0.147	**-0.242**	**0.181**	**-0.467**

The charges on the carbons show that the introduction of methyl group brings in a positive charge on C8. However, the charges on other carbons show an increase as the result of methyl substitution. The charge accumulation is on those carbons in the polyenyl fragment, which interact with the metal.

How are the bonds affected by the introduction of methyl group in to the polyene? It will be partially revealed by the C-C bond lengths in the system. The C-C bond lengths in different systems are given in Table 4.18.

Table 4.18: C-C bond lengths (A^0) in Li/Na/K doped C_9H_{12} & $C_9H_{11}CH_3$ systems (B3LYP/6-31G*).

System	C1-C2	C2-C3	C3-C4	C4-C5	C5-C6	C6-C7	C7-C8	C8-C9
C_9H_{12}	1.4983	1.3469	1.4461	1.3563	1.4406	1.3560	1.4476	1.3442
$C_9H_{12}Li$ (8)	1.4986	1.3603	**1.4259**	**1.3906**	**1.3973**	**1.4204**	**1.4103**	**1.4086**
$C_9H_{11}CH_3$ (8)Li(8)	1.4987	1.3595	**1.4272**	**1.3885**	**1.4008**	**1.4186**	**1.4187**	**1.4119**
$C_9H_{12}Na$ (9)	1.4978	1.3492	1.4421	1.3621	1.4319	1.3671	1.4307	1.3664
$C_9H_{11}CH_3$(8)Na(9)	1.4980	1.3483	1.4436	1.3599	1.4362	1.3634	1.4449	1.3676
$C_9H_{12}K$ (8)	1.4985	1.3534	1.4362	1.3714	**1.4262**	**1.3844**	**1.4248**	**1.3710**
$C_9H_{11}CH_3$ (8)K (8)	1.4984	1.3515	1.4390	1.3667	**1.4324**	**1.3787**	**1.4373**	**1.3720**

The bond length values show that there is slight modification in the delocalised electron cloud of the polyene, as the result of methyl substitution. This change is more prominent in the portion that interacts with the metal. It may be assumed that the electron donating nature of methyl group stalls the electron flow from the metal to the polyene. A decrease in the delocalisation of the pi cloud along the polyene is the result, which is manifested by the bond length values.

The structures of the new complexes are given below in Figure 4.6.

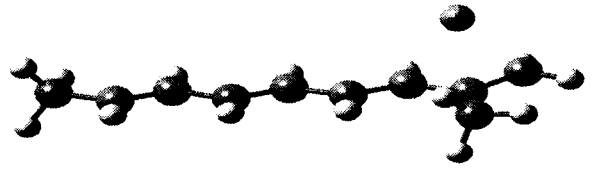

(a) $C_9H_{11}CH_3$ (8)Li (8)

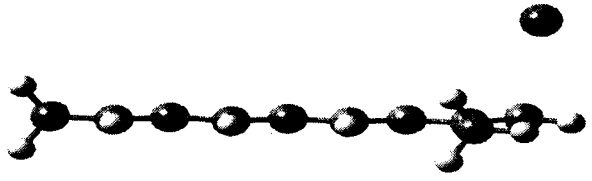

(b) $C_9H_{11}CH_3$ (8)Na (9)

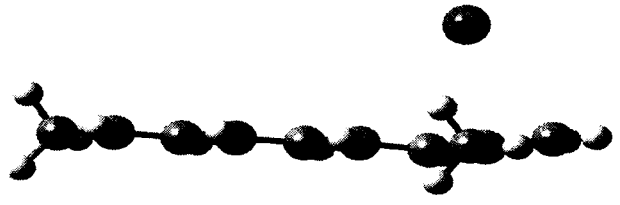

(c) $C_9H_{11}CH_3$ (8)K (8)

Figure 4.6: Optimized structures of Li/Na/K doped $C_9H_{11}CH_3$ (8) (B3LYP/6-31G*)

4.4.2 *Metal doping to $C_9H_{11}CN$*

When an electron-withdrawing group is used as the substituent in the polyene, the result of metal doping should be different altogether. In presence of such groups, the delocalised pi cloud of the chain will be depleted and the flow of electron from the doped metal to the polyene will be enhanced. As a result, metals will possess increased charge, and will interact with the polyene with more intensity. Accordingly, the E_{st} values will be higher than that of metal-doped polyenes. Such changes are observed when CN group is a substituent in the polyene. The different characteristics of metal-doped $C_9H_{11}CN$ and metal-doped C_9H_{12} are presented in Table 4.19 for further study.

Table 4.19: The most stable Li/Na/K doped complexes of C_9H_{12} and $C_9H_{11}CN$ (B3LYP/6-31G*)

Metal-polyene system	E (Hartree)	E_{st} (kcal/mol)	Ri (A^o)	Q_M (a.u)	$\Delta E = E_L - E_H$ (Hartree)
$C_9H_{12}Li$ (8)	-357.64512	18.61	C8-Li=2.0605	0.277739	0.06524
$C_9H_{11}CN(8)Li(8)$	-449.89169	21.65	C8-Li=2.0738	0.330579	0.07656
$C_9H_{12}Na$ (9)	-512.41082	03.41	C9-Na= 2.7096	0.018860	0.04309
$C_9H_{11}CN(8)Na(9)$	-604.66116	09.95	C9-Na=2.5385	0.373629	0.05886
$C_9H_{12}K(8)$	-950.02215	04.61	C8-K= 2.9960	0.289659	0.03086
$C_9H_{11}CN(8)K(8)$[a]	-1042.27633	11.50	C8-K=2.8408	0.597047	0.05056

[a] K moves towards the CN to have strong interaction with it. Hence it is away from carbons C7, C8 & C9, but is closer to CN. Note that K-CN = 2.8326 A^0

The energy values suggest that the electron-withdrawing group in the polyene is actually stabilizing the system by promoting the flow of electrons from the metal to the polyene. As a result, the metals possess enhanced charges in the complex. The metal-carbon distances have decreased in Na and K doped complexes, but increased in Li doped complex. Another notable

change is in the value of HOMO-LUMO energy difference. Substitution of an electron-withdrawing group adversely affects the conductance of the system.

The Mulliken charges on the carbons of $C_9H_{11}CN$, metal-doped C_9H_{12} and metal-doped $C_9H_{11}CN$ are given in Table 4.20.

Table 4.20: Mulliken charges (a.u) on the carbons of $C_9H_{11}CN$, Li/Na/K doped $C_9H_{11}CN$ and Li/Na/K doped C_9H_{12} (B3LYP/6-31G*).

System	C1	C2	C3	C4	C5	C6	C7	C8	C9
C_9H_{12}	-0.491	-0.105	-0.100	-0.122	-0.126	-0.122	-0.125	-0.060	-0.358
$C_9H_{11}CN$ (8)	-0.493	-0.100	-0.102	-0.119	-0.124	-0.121	-0.160	0.204	-0.379
$C_9H_{12}Li$ (8)	-0.486	-0.117	-0.102	-0.134	-0.132	-0.111	**-0.218**	**-0.101**	**-0.438**
$C_9H_{11}CN(8)Li(8)$	-0.490	-0.108	-0.102	-0.130	-0.125	-0.115	**-0.221**	**0.035**	**-0.454**
$C_9H_{12}Na(9)$	-0.491	-0.106	-0.101	-0.123	-0.129	-0.120	-0.130	-0.060	**-0.443**
$C_9H_{11}CN(8)Na(9)$	-0.489	-0.111	-0.100	-0.133	-0.121	-0.140	-0.159	0.106	**-0.495**
$C_9H_{12}K(8)$	-0.487	-0.115	-0.101	-0.132	-0.135	-0.153	**-0.199**	**-0.112**	**-0.425**
$C_9H_{11}CN(8)K(8)$	-0.487	-0.117	-0.100	-0.143	-0.123	-0.188	-0.201	0.057	-0.469

The Mulliken charges on the carbons of Li/Na/K doped $C_9H_{11}CN$ show that the doping of alkali metals results in an increase of the negative charge (in comparison with the $C_9H_{11}CN$), especially in the fragment of interaction. The carbon carrying the CN group possesses a positive charge.

The C-C bond lengths given in Table 4.21 will give an idea about the distribution of electrons along the polyene.

Table 4.21: C-C bond lengths (A^0) in Li/Na/K doped C_9H_{12} & $C_9H_{11}CN$ systems (B3LYP/6-31G*).

System	C1-C2	C2-C3	C3-C4	C4-C5	C5-C6	C6-C7	C7-C8	C8-C9
C_9H_{12}	1.4983	1.3469	1.4461	1.3563	1.4406	1.3560	1.4476	1.3442
$C_9H_{11}CN$ (8)	1.4973	1.3471	1.4454	1.3565	1.4401	1.3544	1.4590	1.3519
$C_9H_{12}Li$ (8)	1.4986	1.3603	**1.4259**	**1.3906**	**1.3973**	**1.4204**	**1.4103**	**1.4086**
$C_9H_{11}CN(8)Li(8)$	1.4980	1.3538	1.4348	**1.3751**	**1.4150**	**1.3960**	**1.4309**	**1.4306**
$C_9H_{12}Na$ (9)	1.4978	1.3492	1.4421	1.3621	1.4319	1.3671	1.4307	1.3664
$C_9H_{11}CN(8)Na(9)$	1.4986	1.3507	1.4401	1.3665	**1.4261**	**1.3748**	**1.4287**	**1.4257**
$C_9H_{12}K$ (8)	1.4985	1.3534	1.4362	**1.3714**	**1.4262**	**1.3844**	**1.4248**	**1.3710**
$C_9H_{11}CN(8)K(8)$	1.4991	1.3512	1.4399	1.3674	1.4299	**1.3832**	**1.4336**	**1.4123**

The C-C bond lengths show that $C_9H_{11}CN$ (8) Li (8) and $C_9H_{11}CN$ (8) Na (9) are characterized by a modified delocalised pi cloud along the polyenic fragment where the metal is stationed. The bond lengths suggest that the density of the pi cloud is slightly depleted, still the efficiency of the interaction is retained/ magnified as the result of electron flow to the system. $C_9H_{11}CN$ (8)K (8) also has a partially delocalised electron cloud with which the metal is interacting.

The structures of different metal-doped substituted polyenes are presented in Figure 4.7.

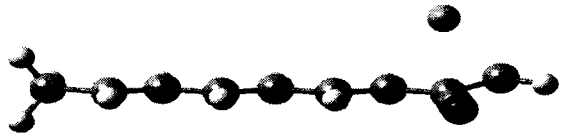

(a) $C_9H_{11}CN$ (8) Li (8)

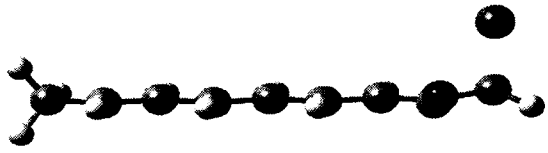

(b) $C_9H_{11}CN$ (8) Na (9)

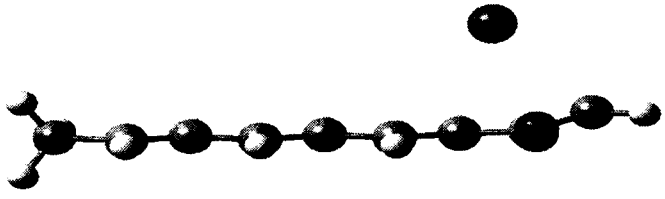

(c) $C_9H_{11}CN$ (8) K (8)

Figure 4.7: Optimized structures of Li/Na/K doped $C_9H_{11}CN$ (8) (B3LYP/6-31G*)

4.5 Discussion

The metal-doped polyenes, whether odd or even, are characterized by low stabilisation energy, low charge on the metal, high conductance, extensively delocalised C-C bonds in the polyene and a less distorted carbon skeleton. The E_{st} value increases as the length of the carbon skeleton increases. A uniform pattern for these complexes with regard to the position of the metal is attained only after they reach a particular length. For Li, from C_7 system onwards, a regular pattern is observed. For K, it is from C_9 system onwards. In the case of Na, still larger polyenes are needed so that it follows the pattern of Li and K doped polyenes. The variation of E_{st} with respect to the length of the polyene is presented in Figure 4.8.

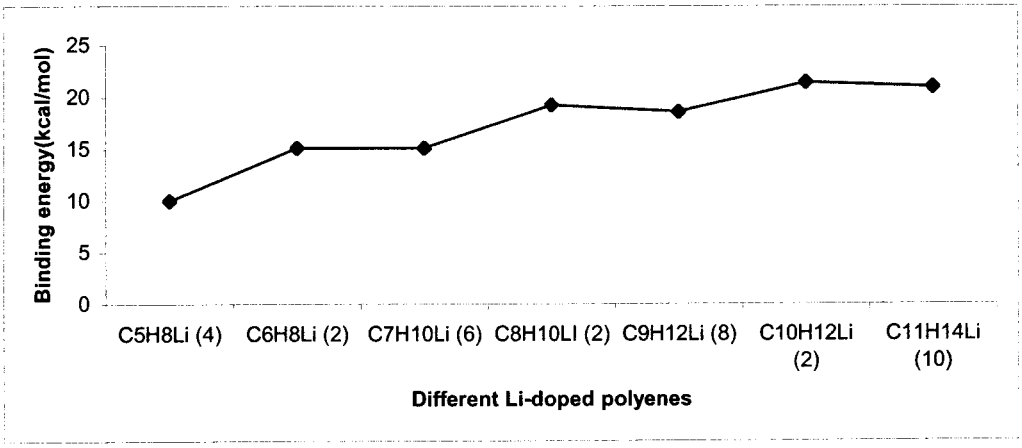

Figure 4.8: E_{st} values of the most stable isomers of Li-doped polyenes

The underlying mechanism, which controls the properties of metal-doped polyenes, could be the same as that in conducting polymers. In conducting polymers, the doped metal loses its outermost electron to the polymer part. This causes an electron delocalisation along the backbone of the polymer chain [1]. The cation then interacts with the polymer, possessing an anionic character. Hence, the metal-doped polymers are termed as salts [1].

Our observations have revealed that in metal-doped polyenes, the same type of mechanism is taking place. The doped metal loses some of its electron while the polyene acquires a partial negative charge and a delocalised electron cloud. The subsequent interaction between the two species stabilizes the system. The increasing E_{st} in proportion to the length of the polyene and charge on the metal may be solid evidences for this mechanism.

4.5.1 Stability of the isomers of metal-doped polyenes

In general, the most stable metal-doped polyene complex has the metal stationed over the 2nd carbon from the terminal, or rather over the allyl fragment (see Tables 4.1 & 4.9). The doped metal possesses a charge of 0.20 a.u and above. The exception for Li is its complex with C_5 system [charge on Li in C_5H_8 Li (4) is 0.065 a.u] and for Na & K are their complexes with C_9H_{12} and lower polyenes. Such complexes are characterized by very low E_{st}. In some of these complexes, Na and K carry even negative charges. For example, in $C_7H_{10}K$ (7), K carries –0.019 a.u. Similarly in $C_7H_{10}Na$ (7), Na carries –0.037 a.u.

Comparatively high E_{st}, the smallest being 10.01 kcal/mol for C5 system, characterizes almost all the Li-doped polyenes. As the length of the polyene increases, the E_{st} energy also increases. Except for C_5H_8Li (4), in all the Li-polyene complexes, Li has somewhat high charge that is almost equal to the charge on it in the Li-polyenes like C_7H_9Li (2), $C_9H_{11}Li$ (2) etc. For example, in C_9 system, Li has a charge of 0.295 when it was substituted and 0.278 when it was doped. Similarly, in C_{11} system, Li has a charge of 0.300 in substitution and 0.291 in doping. The most stable Li-isomer has the metal over the terminal allyl fragment, very often near to C2, at a distance between 2.05 and 2.1 A^0.

On the other hand, Na-doped polyenes are characterized by small E_{st}. This varies from 2.01(in C_5 system) to 4.5 kcal/mol (in C_{10} & C_{11} systems). Usually, these values are smaller than its K- counterparts. For small polyenes, the metal is almost in its free state, very often having a charge, positive or negative, lesser than 0.1 a.u. Its stable isomer has the metal over the terminal sp^2 carbon at a large distance, between 2.55 and 3.5 A^0. In complexes, where the metal possesses the negative charge, the Na-C distance will be very large. As the length of the polyene increases, Na tends to attain higher charge and moves to the second carbon in its most stable isomer of that system (e.g., $C_{10}H_{12}Na$ (2)- Table 4.9).

The low E_{st} of Na-doped complexes may be explained in terms of the explanation given by Zhu and Lu [3] for the low energy of adsorption for Na in graphite. According to them, the SOMO (singly occupied molecular orbital) of Na atom, being at the middle point between the HOMO and LUMO of graphite layer, cannot form a stable interaction with either the HOMO or LUMO. Exactly the same situation takes place when Na is doped in conjugated polyenes. For example, when Na is doped in C_6H_8, the SOMO-HOMO difference is 0.08026 Hartree and SOMO-LUMO difference is 0.08461 Hartree. This means Na will have no efficient interaction with the polyene. As a result, the E_{st} values of Na-doped polyenes will be comparatively lower than that of Li and K doped polyenes. Note that the SOMO-HOMO and SOMO-LUMO differences for Li and C_6H_8 are 0.07586 and 0.08901 Hartree respectively and that for K and C_6H_8 are 0.10265 and 0.06222 Hartree respectively.

K-doped polyenes are also characterized by low E_{st}. But in higher polyenes, it attains a significant value (1.65 kcal/mol in C_5 system and ca. 7.5 kcal/mol in C_{10} system). In small polyenes, the charge on the metal will be very small, but it increases as the length of the polyene increases (-0.07 a.u. in

C_5 system and ca. 0.50 a.u. in C_{10} system). The K-carbon distance also varies considerably- from $3.5A^0$ to 2.9 A^0. The most stable isomer has the metal over the terminal allyl unit, over the C8-C7 bond in C_9 system and over C2-C3 bond in C_{10} system (see Tables 4.4 & 4.12).

Which are the interactions playing vital roles to stabilize these systems? What are the factors guiding the formation of different isomers? Low E_{st} values of these complexes imply that strong electrostatic interactions are absent. However, since the E_{st} increases with the increase in the charge on the metal, discarding them totally from the discussion may not be appropriate. Apart from Coulombic interaction, the possibilities for other types of interactions such as cation-π interaction, ion-dipole interaction, van der Waals' interaction etc., are also explored.

4.5.1.1 Coulombic interaction

In lower polyenes, when metals are doped, a complex with a low E_{st} is formed. For the first instance we may think of a Coulombic interaction. However, the charge on the metal is so small that a Coulombic interaction between the metal and the polyene culminating in an ionic bond cannot be reasonably conceived. It is true; the metals do attain some positive charge in larger polyenes, while the polyenes attain some amount of negative charge. Still, it is not appropriate to call it purely as a Coulombic interaction. The E_{st} energy range existing in these complexes [10 to 20 kcal/mol for Li complexes, 2 to 5 kcal/mol for Na complexes and 1.5 to 7.5 kcal/mol for K complexes] also supports this hypothesis.

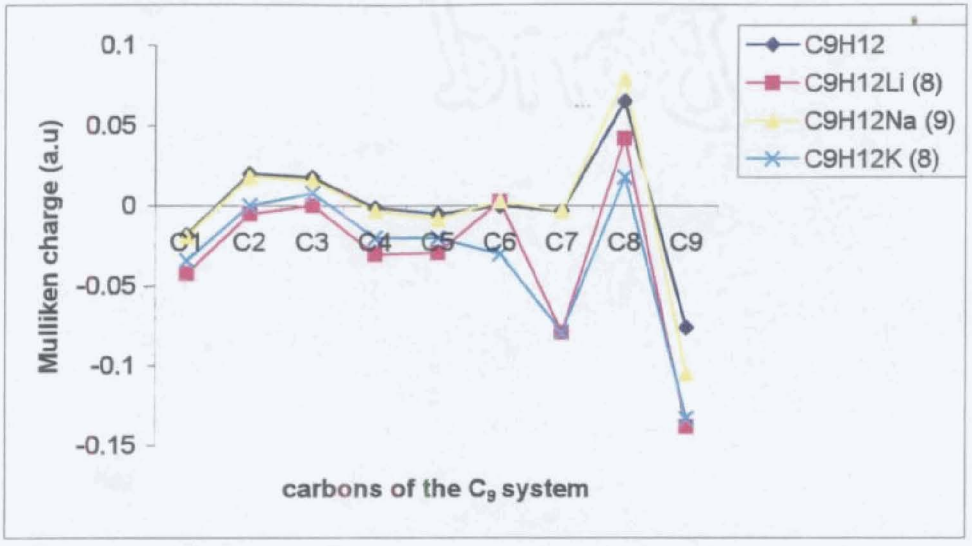

Figure 4.9: Mulliken charges on the carbons of C_9H_{12} and its Li/Na/K doped complexes

There are some more facts to be mentioned here. The first one is the large metal- carbon (polyene) distances (ca. 2.06 A^0 for Li, 2.7A^0 for Na and 2.91 A^0 for K) existing in these complexes, which do not favor an efficient Coulombic interaction. Secondly, the variation in E_{st} of different complexes of the same metal is not justifiable in terms of pure Coulombic interaction alone. For example, E_{st} of $C_9H_{12}K$ (8) is 4.61 kcal/mol and that of $C_{11}H_{14}K$ (9) is 6.73 kcal/mol. The charges on K in these two complexes are 0.289659 and 0.434573 respectively and the K-C distances are 2.9960 A^0 and 2.9193 A^0. On the other hand, the E_{st} of $C_9H_{12}Li$ (8) and $C_{11}H_{14}Li$ (10) are 18.61 and 20.97 respectively, while the charges of Li in these two complexes are 0.277739 and 0.290707 and Li-C distances are 2.0605 and 2.0612 respectively.

However, the electrostatic nature of this interaction cannot be ruled out. It can be observed that when the charge on the metal decreases, accordingly the E_{st} also decreases and vice versa. There must be an electrostatic interaction between the metal and the negatively charged carbons of the polyene. In all the isomers formed, the carbons in the polyene closer to the metals are found to have higher charges, which will result in Coulombic

interaction to some extent. Also, in all the systems, the most stable isomer has the metal associated with the terminal allyl segment [e.g. $C_9H_{12}Li$ (8)] or pentadienyl segment [$C_{11}H_{14}K$ (9)]. The metal prefers to these terminal segments due to the higher charge on the terminal carbon, which facilitates stronger Coulombic interaction. Hence, we have to search for some other interaction, which is feeble in nature, but involves some amount of electrostatics in its functioning. Ion-dipole interaction and cation-π interaction are two such interactions, which are feeble in strength but involving electrostatics.

4.5.1.2 Cation-π interaction

In alkali metal-doped polyenes, the dopant donates its outer electron to the polyene. As the metal loses electron to the polyene, there occurs two changes to the system simultaneously- formation of a cationic system above the polyene and a slightly improved pi- electron cloud perpendicular to the plane of the carbon skeleton of the polyene (See Tables 4.5 & 4.13). The delocalisation is extensive in Li-doped polyenes, less intense in K-doped polyenes and nominal in Na-doped polyenes. The partially ionized metal stations above a polyenic fragment inviting interaction from it. The carbon-carbon bond lengths along this fragment show that they are totally or partially delocalised. This entails in reasonably strong cation-π interaction that contributes to the stability of the system. The range of E_{st} in these complexes also supports this proposal of cation- π interaction.

For example, in $C_9H_{12}Li$ (8), Li interacts with the fragment with C-C bond lengths of 1.4103 and 1.4086. Similarly, in $C_9H_{12}K$ (8), K is pocketed by a fragment with C-C bond lengths of 1.3844, 1.4248 and 1.3710. However, for Na, such a fragment with delocalised electron cloud is not identified in C_9 system, as the metal exists almost in its unionized state. In cases where the metal is partially ionized during doping, the system is fairly stabilized. For

example, in $C_{10}H_{12}Na$ (2), Na has a higher charge (0.230) and hence it stations over C2 inviting interaction from the allylic unit with a partially delocalised electron cloud (C-C bond lengths are 1.3827 & 1.4187). This accounts for the comparatively high E_{st} (4.45 kcal/mol) of $C_{10}H_{12}Na$ (2). [For more details see Tables 4.1, 4.5, 4.9 & 4.13]. Figure 4.10 gives a comparison of the bond lengths in different metal-doped C_9H_{12} system. Consecutive bond lengths closer to 1.4 A^0 indicate the presence of a delocalised electron cloud and such a delocalisation is found in Li-isomer and to a certain extent in K-isomer.

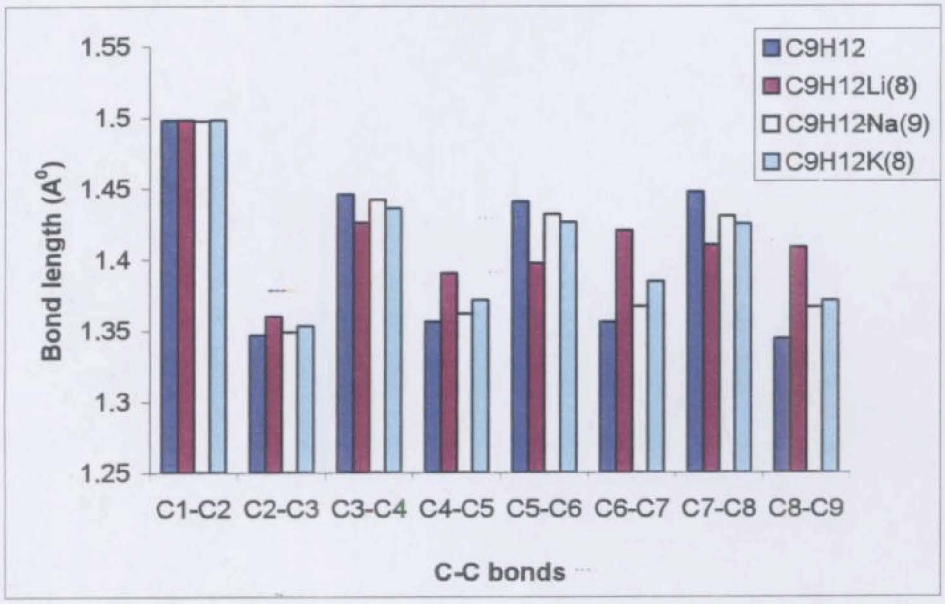

Figure 4.10: Comparison of C-C bond lengths in C_9H_{12} and its Li/Na/K doped complexes

Hence, as per the above discussion, there occurs an efficient metal-π cloud interaction in Li-doped polyene, less efficient one in K-doped polyene and least efficient one in Na-doped polyene. This explains why Li-doped polyenes have fairly high E_{st}, K-complexes have lesser and the Na-complexes have the least E_{st}.

Full-fledged formation of metal ions does not take place in metal-doped lower polyenes. Hence, the possibility for an ion-dipole interaction does not arise. Similar is the case with other non-covalent interactions.

These explanations go well with the stability of higher polyene complexes; but in lower polyenes, such interactions are almost non-existent. Their stability may be due to some other interactions of very feeble strength and the best-suited one to explain these aspects is van der Waals' interaction.

4.5.1.3 van der Waals' interaction

Metal-doped lower polyene complexes (especially Na-doped complexes) are characterized by very low E_{st}. For example, C_5H_8Li (4) has a E_{st} of 10.01 kcal/mol, C_5H_8Na (5) has 2.01 kcal/mol, C_5H_8K (5) has 1.65 kcal/mol, $C_9H_{12}Na$ (4) has 1.21 kcal/mol. etc. In all such complexes, the metal is almost in neutral state. In C_5 complex, charge on Li is +0.064539, charge on Na is –0.076969 and that on K is –0.066163. (In all the low energy Na-doped complexes, Na has charges varying from –0.099 to +0.052). Hence, in such complexes, an interaction involving electrostatics is not possible (see Table 4.1: The M-C distances in them are also very high). The C-C bond lengths in C_5 complexes of Na and K (1.3508, 1.4509 & 1.3472, 1.4540 respectively) also rule out the possibility of such interactions. Hence, the only interaction possible in such complexes is weak van der Waals' interactions. The small E_{st} values confirm this conclusion.

The C-C bond lengths (1.3912, 1.4306) in C_5 complex of Li explain why it has a high E_{st}. Li, with a charge of +0.064539, interacts with the partially delocalised pi cloud in C_5 system and renders it some stability.

All these explanations relate the stability to the charge on the metal and the delocalisation of the pi electrons. But they cannot explain why the metals

prefer to certain positions in the polyene. This is guided by some other factors.

4.5.1.4 Extended conjugation

A conjugate polyene is stabilized by extended conjugation. Even in metal-doped polyenes, the tendency is to retain this conjugation. When the doped metal is over the terminal allyl fragment, the system attains stability via cation- pi interaction . In addition to that, further stabilization is also gained by the retention of the conjugation in the polyene. Hence, the most stable isomers in metal-doped polyenes have the metal over the terminal (allyl or pentadienyl) fragment. Examples are $C_9H_{12}Li$ (8), $C_{10}H_{12}Li$ (2). As the metal moves towards the center, the stabilization via extended conjugation will be disturbed and hence such isomers are less favored. In all the metal-doped complexes in our study, we have found them possessing higher energy than those where the metal stays above the terminal segment (for details, Tables 4.1 & 4.9).

4.5.1.5 Affinity towards odd/even carbons

As in metal polyenes, in metal-doped polyenyl complexes too, Li retains its affinity towards the even carbon. Binding on to the middle carbon of an allylic portion, Li efficiently interacts with it, stabilizing the system considerably. Since the interaction of the metal is exclusively with the polyenic part with conjugate double bonds, its isomers will have the metal over the even carbon from either end of the polyene, the numbering starting from the sp^2 carbon. Thus, Li has its complex isomers with C_9 system in which the metal stays on C8, C6 and C3 (2^{nd} sp^2 carbon from the sp^3 carbon terminal). In C_{10} system, the isomers will have the metal over C2 & C4. As the length of the chain increases, the affinity towards even carbon increases and a slightly distorted carbon skeleton is formed.

Na, when doped in lower polyenes, remains as such and stays away from the polyene. It is having only a van der Waals' interaction with the terminal carbon. However, as the length of the polyene increases, Na slowly attains positive charge, interacts with the even carbons and form complexes, almost in the same fashion of Li. An improvement from the nave character in lower polyenes to the refined and ordered character in higher polyenes is visible in the case of Na. In longer systems, Na primarily prefers to even carbons in stable isomers.

In lower polyenes, K behaves exactly like Na. It withholds its electrons (hence low charge) and prefers to even carbons, which means an allyl-K interaction. In such complexes, the metal possesses only a fraction of charge and interacts from a larger distance (see Table 4.1& 4.9) and hence the size factor does not play a significant role. However, as the length of the polyene increases, K loses more of its valence electron, comes closer to the polyene, attaches to odd carbons and interacts with a pentadienyl fragment evoking slight warping to the carbon skeleton. Thus K forms $C_9H_{12}K$ (8), $C_9H_{12}K$ (6) and $C_9H_{12}K$ (4) with C_9 system, whereas it forms $C_{11}H_{14}K$ (9), $C_{11}H_{14}K$ (7), $C_{11}H_{14}K$ (6) and $C_{11}H_{14}K$ (4) with C_{11} system and $C_{10}H_{12}K$ (3) & (5) with C_{10} system.

On the basis of the above observations, we can predict that when alkali metals are doped to long polyenes, the complexes obtained will exhibit more or less the same characteristics of metal substituted polyenes, including the warping of carbon skeleton. This implies that the distinction between doping and substituting becomes irrelevant in the case of long conjugated polyenes.

4.5.2 Prominence of cation-π interaction

The analysis of the results obtained for the doping of alkali metals in substituted polyenes gives some important insights. When an electron-

donating group, CH3, was present in the C_9 system, the Li & K complexes were destabilized whereas the Na complex was stabilized (Table 4.16). In the stabilized Na-complex, Na is carrying a negative charge. This means, the presence of a group in the polyene, which enhances the electron cloud, will promote the flow of electrons to Na and hence will render stability to the system. On the other hand, when an electron-withdrawing group CN was present, all the three systems were stabilized (Table 4.19). The influence of these groups on the E_{st} gives an idea about the interactions present in metal-doped polyenes.

We have found that the stability of the metal-doped polyene is dependent on the interaction between the metal and the delocalised electron cloud of the polyene. For a doped metal, to have high charge, it should lose its electron to the polyene. Usually, the metal ionizes to a certain extent only. The electron lost by it, is gained by the polyene and its pi cloud gets modified. The interaction between the polyene and the metal is the result of these two steps. Any substituent, which retards either the loss of electrons from the metal or the modification of the pi cloud, will destabilize the system. In substituted polyenes, CH_3 group retards the flow of electrons from the metal to the polyene as it itself enriches the pi cloud of the polyene. Hence, the E_{st} is low for methyl substituted metal-doped polyenes.

On the other hand, electron-withdrawing groups act in the reverse direction. They abstract electron cloud from the polyene and facilitate the electron flow from the metal to the polyene. This results in enhanced charge on the metal and improved electron cloud in the polyene. As a result, type II & I interactions in the system are considerably increased. Interaction between the metal ion and the carbons of the polyene is the type I and the interaction between the metal ion and the pi cloud is the type II. Therefore, the

complexes with polyene, substituted by an electron-withdrawing group will have high E_{st}.

Both these observations highlight the presence of cation- π interaction in metal-doped polyenes. Perhaps, the only significant interaction in such complexes is cation- π interaction.

In $C_9H_{11}CN$ (8)Na (8) and $C_9H_{11}CN$ (8)K (8), there is another stabilizing factor- the Na^+ and K^+, possessing higher charges interact with the CN group. Apart from the enhanced cation- pi interaction, this electrostatic interaction also accounts for the steep increase in the E_{st}.

4.6 Conclusion

As the result of alkali metal doping in conjugated polyenes, there occurs slight distortion to the carbon skeleton. The intensity of distortion increases as the size of the polyene and that of the dopant increases. The principal binding force in such complexes is found to be the cation-π interaction. Since the effect of doping of alkali metals becomes significant only when the polyene has a substantial size, we may suggest that this trend will be matured in long polyenes like PA. As the size of the polyene increases, the difference between substitution and doping may narrow down and the complexes obtained in both type will exhibit almost identical characteristics. As an example, we made a study on $C_{32}H_{34}$ and $C_{33}H_{36}$. The former was doped with K and the latter was substituted and doped with K. The optimization results support our conclusion. HOMO-LUMO gap [26.17 kcal/mol for $C_{32}H_{34}K$ (16), 25.87 kcal/mol for $C_{33}H_{36}K$ (16) & 30.95 kcal/mol for $C_{33}H_{35}K$ (17)] suggests that they have almost equal conductance. The charges on potassium in these species [0.751029 a.u for $C_{32}H_{34}K$ (16), 0.750359 a.u for $C_{33}H_{36}K$ (16) & 0.742741 a.u for $C_{33}H_{35}K$ (17)] are very close, suggesting almost identical interactions stabilizing them. Their

structures (Figure 4.11) are also very similar. All these may be taken as indications to suggest that the complexes obtained by doping and substituting alkali metals to large polyenes exhibit almost identical chemical and electrical properties.

(a) $C_{33}H_{35}K$ (17)

(b) $C_{33}H_{36}K$ (16)

(c) $C_{32}H_{34}K$ (16)

Figure 4.11: Optimized structures of $C_{33}H_{35}K$ (17), $C_{33}H_{36}K$ (16) and $C_{32}H_{34}$ K(16) [B3LYP/6-31G*)

4.7 References:

1. A. J. Heeger, Synthetic Metals, 125 (2002) 23-42.
2. A.G. MacDiarmid, Synthetic Metals, 125 (2002) 11-22.
3. Z. H. Zhu & G. Q. Lu, Langmuir, 20 (2004) 10751-10755

A THEORETICAL STUDY OF THE CATION – π INTERACTION IN ALKALI METAL POLYENES AND POLYENE COMPLEXES

THESIS

Submitted to the
University of Calicut
in partial fulfillment of the requirements
for the award of the degree of
Doctor of Philosophy
in Chemistry,
under the Faculty of Science

By

FR. JOSE T. M.

Forwarded

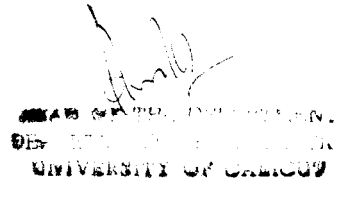

Department of Chemistry,
University of Calicut,
Calicut University P.O.,
673 635

April 2007

CHAPTER 5

ALKALI METAL ION DOPED CONJUGATED POLYENES

5.1 Introduction

We have found that the metal doping in conjugated polyenes renders a partial anionic character to the polyene and the resulting cation-pi cloud interaction is the stabilizing factor of metal-doped polyenes. This means, the characteristics of such complexes are determined, at least partially, by the odd electron oscillating along the carbons of the polyene. If cation-π interaction plays a significant role in metal-doped polyenes, a still more pronounced interaction would be there, if the metal is doped in the form of a cation to such a conjugated polyene. There are reports about the high stabilisation energy (E_{st}) of alkaline earth metal dication/benzene complexes [1]. In the early studies of cation-π interaction, cations were introduced into the pi system and their stabilisation energies were determined [2-6]. It has been shown that the interaction between cation and graphite is important for the development of battery materials [7]. Since conjugated polyenes possess a delocalised electron cloud, the introduction of a cation must evoke strong cation-π interaction. Therefore, a study of the effects of cation doping in conjugated polyenes is significant not only from the academic point of view, but such results may find application in the field of material manufacture. With these targets fixed at, computational studies were performed on polyenic systems, doped with alkali metal cations.

5.2 Doping of alkali metal cations in odd numbered all-trans conjugated polyenes

Cation doping to the odd numbered conjugated polyenes is characterized by the formation of isomers of almost identical structures with relatively high E_{st}. The carbon- metal distance (Ri) is increased in the case of Li, decreased for Na and almost unchanged for K, in comparison with the metal-doped systems. The delocalisation of the electron cloud (in the cation-doped complexes) is enhanced with respect to the free polyene, but diminished with respect to the metal-doped complexes. Selected properties such as total energy (E), stabilisation energy (E_{st}), carbon- metal distance (Ri), charge on the metal (Q_M), HOMO-LUMO gap (ΔE) etc., of the stable isomers of different cation-doped polyenic systems are given below in Table 5.1.

Table 5.1: The stable isomers of Li^+, Na^+ and K^+ doped complexes of different polyenes and their important characteristics (B3LYP/6-31G*).

Cation-polyene complex	Stable isomers [a]	E (Hartree)	E_{st} (kcal/mol)	Ri (A^o)	Q_M (a.u)	$\Delta E = E_L - E_H$ (Hartree)
$C_5H_8Li^+$	$C_5H_8Li^+$ (4)	-202.65462	35.15	2.2010	0.550549	0.19851
$C_5H_8Na^+$	$C_5H_8Na^+$ (4)	-357.47377	24.60	2.5669	0.695011	0.18476
$C_5H_8K^+$	$C_5H_8K^+$ (4)	-795.06280	15.53	3.0410	0.843074	0.18350
$C_7H_{10}Li^+$	$C_7H_{10}Li^+$ 6)	-280.06720	38.92	2.1807	0.527501	0.15182
	$C_7H_{10}Li^+$(4)	-280.06485	37.52	2.1961	0.539862	0.16007
$C_7H_{10}Na^+$	$C_7H_{10}Na^+$(6)	-434.84447	27.30	2.5526	0.683105	0.14993
	$C_7H_{10}Na^+$ (4)	-434.84256	26.13	2.5585	0.684038	0.15297
$C_7H_{10}K^+$	$C_7H_{10}K^+$ (6)	-872.47242	17.54	3.0231	0.835848	0.15201
	$C_7H_{10}K^+$ (4)	-872.47077	16.57	2.9997	0.836555	0.15611

$C_9H_{12}Li^+$	$C_9H_{12}Li^+$ (8)	-357.47918	41.89	2.1654	0.506712	0.12237
	$C_9H_{12}Li^+$ (6)	-357.47622	40.20	2.1798	0.532630	0.13469
	$C_9H_{12}Li^+$ (3)	-357.47629	40.24	2.1735	0.521020	0.13000
$C_9H_{12}Na^+$	$C_9H_{12}Na^+$(8)	-512.25488	29.34	2.5373	0.672217	0.12874
	$C_9H_{12}Na^+$(6)	-512.25307	28.28	2.5549	0.677762	0.13433
	$C_9H_{12}Na^+$(3)	-512.25255	27.90	2.5666	0.674527	0.12855
$C_9H_{12}K^+$	$C_9H_{12}K^+$(8)	-949.88194	19.00	3.0148	0.829745	0.12756
	$C_9H_{12}K^+$(6)	-949.88061	18.27	2.9995	0.830787	0.13499
	$C_9H_{12}K^+$(4)	-949.87985	17.75	2.9836	0.829925	0.13287
$C_{11}H_{14}Li^+$	$C_{11}H_{14}Li^+$(10)	-434.89058	44.37	2.1536	0.489496	0.10282
	$C_{11}H_{14}Li^+$(8)	-434.88725	42.49	2.1611	0.518737	0.11348
	$C_{11}H_{14}Li^+$(5)	-434.88694	42.26	2.1725	0.523874	011642
	$C_{11}H_{14}Li^+$(3)	-434.88745	42.62	2.1600	0.504341	0.10922
$C_{11}H_{14}Na^+$	$C_{11}H_{14}Na^+$(10)	-589.66505	31.03	2.5265	0.662813	0.10568
	$C_{11}H_{14}Na^+$(8)	-589.66311	29.98	2.5401	0.671003	0.11493
	$C_{11}H_{14}Na^+$(6)	-589.66285	29.78	2.5480	0.671166	0.11742
	$C_{11}H_{14}Na^+$(4)	-589.66256	29.58	2.5348	0.666328	0.11066
$C_{11}H_{14}K^+$	$C_{11}H_{14}K^+$(10)	-1027.29136	20.27	3.0021	0.825350	0.10881
	$C_{11}H_{14}K^+$(8)	-1027.29006	19.58	2.9886	0.826622	0.11556
	$C_{11}H_{14}K^+$(6)	-1027.28967	19.33	2.9831	0.825073	0.11790
	$C_{11}H_{14}K^+$(4)	-1027.28914	18.94	2.9663	0.825510	0.11430

[a] The numeral in parentheses corresponds to the carbon to which the metal is having smallest distance.

Comparatively high stabilisation energy values for the cation-doped polyene complexes point towards strong interactive forces existing in them (between the cation and polyene). The charges on the metals in different complexes have decreased from +1 to different values between 0.5 and 0.85. This indicates the electron flow from the polyene to the metal.

The Mulliken charges often explain why certain isomers are formed and some are not formed. Also,they give a clue about the nature of interaction existing in these complexes. The Mulliken charges on the carbons of free polyenes and their cation doped complexes are given in Tables 5.2 (a), (b), (c) and (d) (B3LYP/6-31G*).

Table 5.2(a): Mulliken charges (a.u) on the carbons of free C_5H_8 and its Li^+/ Na^+/ K^+doped complexes.

System	C1	C2	C3	C4	C5
C_5H_8	-0.490	-0.105	-0.100	-0.059	-0.359
$C_5H_8Li^+$ (4)	-0.511	-0.044	**-0.204**	**-0.130**	**-0.323**
$C_5H_8Na^+$ (4)	-0.510	-0.081	**-0.179**	**-0.128**	**-0.359**
$C_5H_8 K^+$ (4)	-0.508	-0.097	**-0.179**	**-0.124**	**-0.392**

Table 5.2(b): Mulliken charges (a.u) on the carbons of free C_7H_{10} and its Li^+/Na^+/ K^+doped complexes.

System	C1	C2	C3	C4	C5	C6	C7
C_7H_{10}	-0.490	-0.105	-0.100	-0.122	-0.126	-0.059	-0.358
$C_7H_{10}Li^+$(6)	-0.509	-0.069	-0.112	-0.061	**-0.240**	**-0.112**	**-0.347**
$C_7H_{10}Li^+$(4)	-0.506	-0.069	**-0.184**	**-0.229**	**-0.076**	-0.073	-0.317
$C_7H_{10}Na^+$(6)	-0.506	-0.078	-0.115	-0.095	**-0.215**	**-0.119**	**-0.373**
$C_7H_{10}Na^+$(4)	-0.508	–0.097	**-0.172**	**-0.212**	**-0.113**	-0.077	-0.327
$C_7H_{10}K^+$(6)	-0.504	-0.085	-0.117	-0.112	**-0.217**	**-0.119**	**-0.401**
$C_7H_{10}K^+$(4)	-0.506	-0.106	**-0.169**	**-0.200**	**-0.162**	-0.080	-0.340

Table 5.2(c): Mulliken charges (a.u) on the carbons of free C_9H_{12} and its Li^+/ Na^+/ K^+doped complexes.

System	C1	C2	C3	C4	C5	C6	C7	C8	C9
C_9H_{12}	-0.491	-0.105	-0.100	-0.122	-0.126	-0.122	-0.125	-0.060	-0.358
$C_9H_{12}Li^+$ (8)	-0.506	-0.072	-0.109	-0.092	-0.137	-0.064	**-0.243**	**-0.104**	**-0.361**
$C_9H_{12}Li^+$ (6)	-0.506	-0.077	-0.109	-0.076	**-0.232**	**-0.209**	**-0.095**	-0.070	-0.324
$C_9H_{12}Na^+$(8)	-0.504	-0.079	-0.108	-0.099	-0.141	-0.095	**-0.219**	**-0.115**	**-0.382**
$C_9H_{12}Na^+$(6)	-0.504	-0.084	-0.114	-0.110	**-0.213**	**-0.201**	**-0.123**	-0.075	-0.331
$C_9H_{12}K^+$(8)	-0.502	-0.085	-0.109	-0.105	**-0.145**	**-0.117**	**-0.225**	**-0.118**	**-0.400**
$C_9H_{12}K^+$(6)	-0.503	-0.089	-0.115	**-0.125**	**-0.210**	**-0.195**	**-0.159**	**-0.183**	-0.341

Table 5.2(d): Mulliken charges (a.u) on the carbons of free $C_{11}H_{14}$ and its Li^+/ Na^+/ K^+doped complexes.

System	C1	C2	C3	C4	C5	C6	C7	C8	C9	C10	C11
$C_{11}H_{14}$	-0.491	-0.105	-0.010	-0.123	-0.126	-0.123	-0.125	-0.122	-0.124	-0.060	-0.358
$C_{11}H_{14}Li^+$(10)	-0.505	-0.076	-0.106	-0.095	-0.133	-0.096	-0.138	-0.066	**-0.245**	**-0.098**	**-0.371**
$C_{11}H_{14}Li^+$(8)	-0.505	-0.077	-0.108	-0.097	-0.136	-0.073	**-0.240**	**-0.194**	**-0.114**	-.066	-0.329
$C_{11}H_{14}Na^+$(10)	-0.502	-0.082	-0.106	-0.100	-0.134	-0.101	-0.142	-0.095	**-0.223**	**-0.112**	**-0.389**
$C_{11}H_{14}Na^+$(8)	-0.503	-0.082	-0.108	-0.103	-0.140	-0.107	**-0.219**	**-0.196**	**-0.131**	-0.074	-0.335
$C_{11}H_{14}K^+$(10)	-0.500	-0.086	-0.106	-0.104	-0.135	-0.106	**-0.146**	**-0.117**	**-0.230**	**-0.116**	**-0.406**
$C_{11}H_{14}K^+$(8)	-0.503	-0.127	-0.166	-0.223	**-0.143**	**-0.144**	**-0.111**	**-0.131**	**-0.107**	-0.068	-0.333

As in the previous systems studied, there is an enhanced charge concentration in the region where the metal ion resides in the metal polyenyl complex. In cases where the K^+ is the dopant, the carbons of the pentadienyl segment with which the cation interacts, possess higher charges. e.g., are $C_{11}H_{14}K^+$ (10) and $C_{11}H_{14}K^+$ (8). A clear picture emerges when the net Mulliken charges on the carbons in different isomers are examined. For a scrutiny, the net charges on the carbons of C_9H_{12} and its different cation doped species are presented in Table 5.3.

Table 5.3: The net charges (a.u) on the carbons of C_9H_{12} and its $Li^+/Na^+/K^+$ doped complexes (B3LYP/6-31G*).

System	C1	C2	C3	C4	C5	C6	C7	C8	C9
C_9H_{12}	-0.018	0.020	0.018	-0.001	-0.005	.00004	-0.003	0.065	-0.076
$C_9H_{12}Li^+$ (8)	0.062	0.091	0.045	0.068	0.020	0.108	**-0.053**	0.096	0.055
$C_9H_{12}Li^+$ (6)	0.065	0.087	0.048	0.098	**-0.041**	**-0.017**	0.082	0.097	0.048
$C_9H_{12}Na^+$(8)	0.049	0.077	0.038	0.054	0.010	0.068	**-0.048**	0.072	0.007
$C_9H_{12}Na^+$(6)	0.053	0.074	0.038	0.055	**-0.036**	**-0.022**	0.044	0.085	0.030
$C_9H_{12}K^+$(8)	0.040	0.067	0.034	0.043	0.001	0.038	**-0.066**	0.052	**-0.037**
$C_9H_{12}K^+$(6)	0.043	0.064	0.030	0.029	**-0.050**	**-0.032**	**-0.003**	0.079	0.009

5.2.1 Position of the metal on the polyene

The different stable isomers obtained for Li^+/ Na^+/ K^+doped C_9H_{12} systems as listed in Table 5.1 may suggest that all the cations have an affinity towards the even carbon, i.e., 8, 6, 4 etc. It is true; the cations keep minimum distance from the even carbons (Ci), but their actual position is almost at the middle of the C(i)-C(i+1) bond. For e.g., in $C_9H_{12}K^+$ (8), K is between C8 and C7 (C8-K= 3.01, C7-K= 3.04 and C9-K= 3.28). The same is the case with $C_9H_{12}Li^+$ (8) and $C_9H_{12}Na^+$ (8). The large distance between the cation and polyene decreases the Coulombic interaction, but the interaction of the cation with the delocalised pi- cloud stabilizes the system.

For a detailed analysis, the different distances of the cation from different carbons of the interacting segment and the relevant bond angles are given in Table 5.4.

Table 5.4: Cation- carbon distances (A^0) and cation polyene bond angles (degree) in some selected systems (B3LYP/6-31G*).

System	C(i+1)-M (A^0)	C(i)-M (A^0)	C(i-1)-M (A^0)	MC(i)C(i+1) (deg.)	MC(i)H(i) (deg.)
$C_9H_{12}Li^+$ (8)	2.3550	2.1654	2.2452	80.29	114.46
$C_9H_{12}Li^+$ (6)	2.6527	2.1798	2.1939	93.97	105.43
$C_9H_{12}Na^+$(8)	2.7575	2.5373	2.6396	84.36	108.65
$C_9H_{12}Na^+$ (6)	2.9977	2.5549	2.5717	94.88	102.49
$C_9H_{12}K^+$ (8)	3.2824	3.0148	3.0431	88.99	104.53
$C_9H_{12}K^+$ (6)	3.3099	2.9995	3.0700	90.72	101.51

The optimized structures of a few stable isomers of Li^+ doped polyenes are given below in Figure 5.1 from which the effect of Li^+ doping can be ascertained.

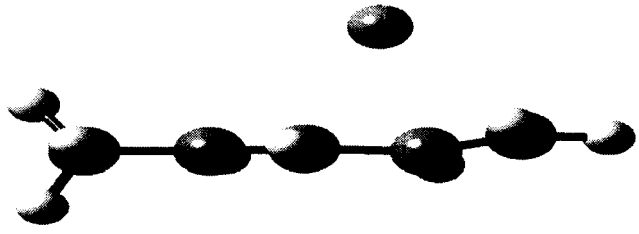

(a) $C_5H_{10}Li^+$ (4)

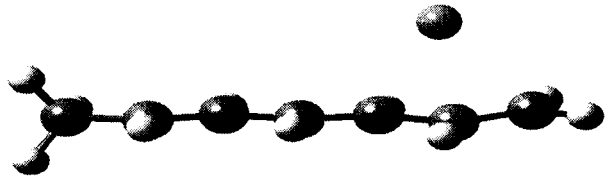

(b) $C_7H_{10}Li^+$ (6)

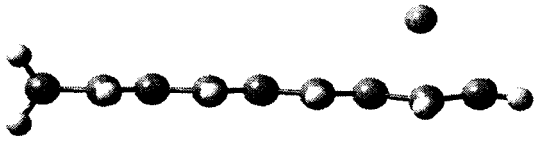

(c) $C_9H_{12}Li^+$ (8)

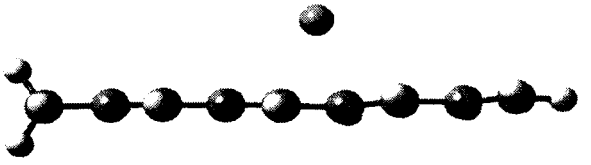

(d) $C_9H_{12}Li^+$ (6)

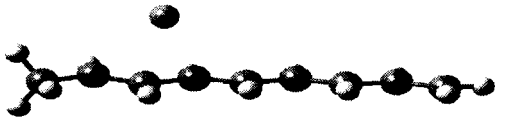

(e) $C_9H_{12}Li^+$ (3)

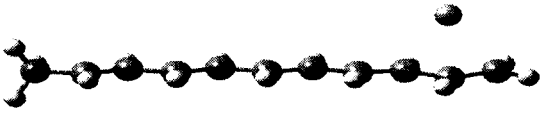

(f) $C_{11}H_{14}Li^+$ (10)

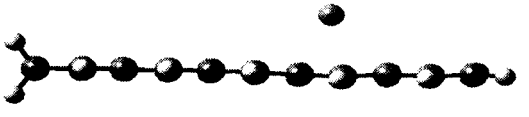

(g) $C_{11}H_{14}Li^+$ (8)

(h) $C_{11}H_{14}Li^+$ (3)

Figure 5.1: Optimized structures of a few stable isomers of Li^+ doped polyenes (B3LYP/6-31G*)

From the figure, it can be seen that Li^+ prefers to station above some even sp^2 carbon from the terminal. However, if the ion is closer to the sp^3 carbon of the chain, it moves to the third carbon, again an sp^2 carbon, which comes second from that side, if only the sp^2 carbons are considered. As the ion moves towards the center, the correct position of the metal is between adjacent carbons- an indication to the irrelevance in differentiating carbons into odd and even.

The optimized structures of a few isomers of Na^+ doped polyenes are presented in Figure 5.2.

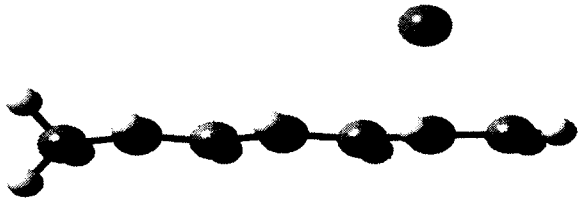

(a) $C_7H_{10}Na^+$ (6)

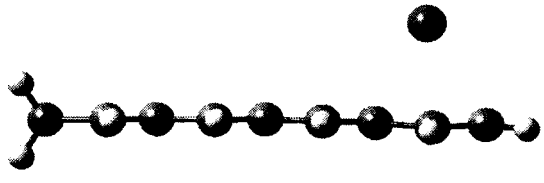

(c) $C_9H_{12}Na^+$(8)

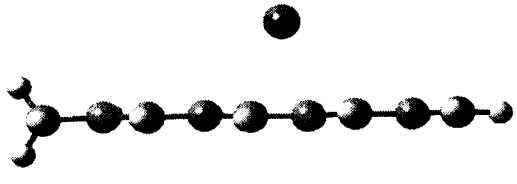

(d) $C_9H_{12}Na^+$(6)

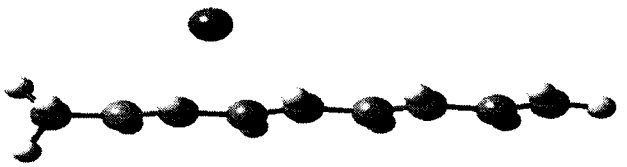

(e) $C_9H_{12}Na^+(3)$

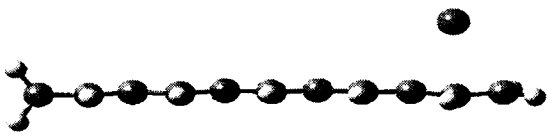

(f) $C_{11}H_{14}Na^+$ (10)

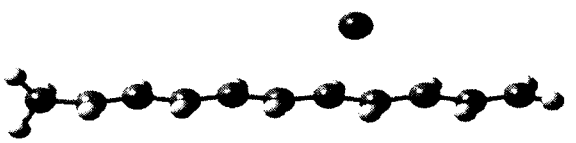

(f) $C_{11}H_{14}Na^+$ (8)

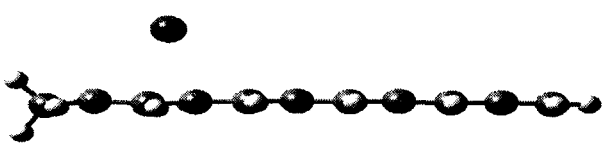

(g) $C_{11}H_{14}Na^+$ (4)

Figure 5.2: Optimized structures of a few stable isomers of Na^+ doped polyenes (B3LYP/6-31G*)

Except for the isomer in which the metal is at the terminal allylic segment, all others are having the metal almost at the middle of the carbon-carbon bond. In general, in all the isomers, the closest carbon of the polyene to the metal is an even carbon.

In Figure 5.3 optimized structures of a few stable isomers of K^+ doped polyenes are given.

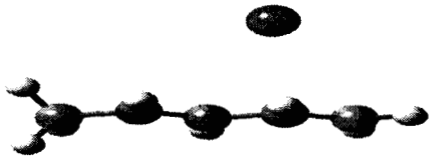

(a) $C_5H_8K^+$ (4)

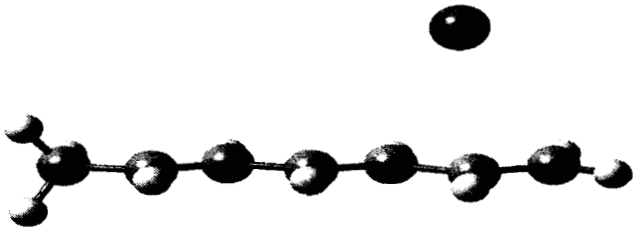

(b) $C_7H_{10}K^+$ (6)

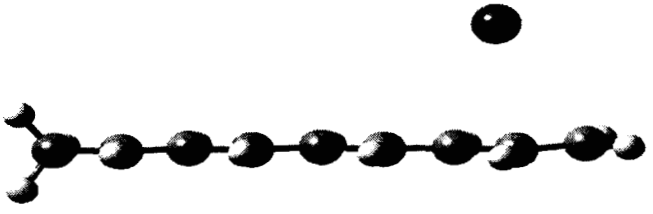

(c) $C_9H_{12}K^+$(8)

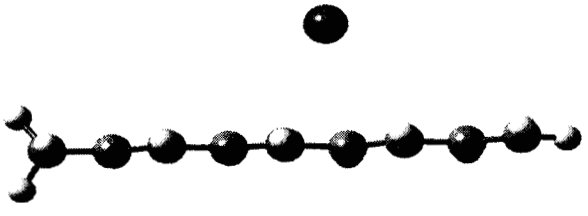

(d) $C_9H_{12}K^+$(6)

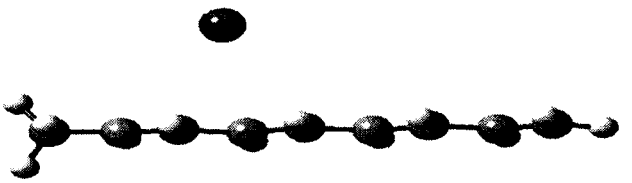

(e) $C_9H_{12}K^+(4)$

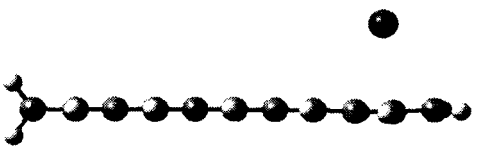

(e) $C_{11}H_{14}K^+$ (10)

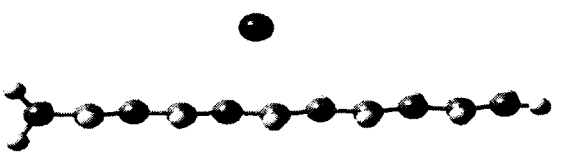

(f) $C_{11}H_{14}K^+$ (6)

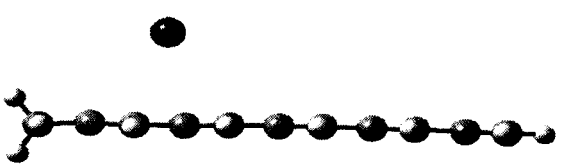

(g) $C_{11}H_{14}K^+$ (4)

Figure 5.3: Optimized structures of a few stable isomers of K^+ doped polyenes (B3LYP/6-31G*)

The structures show that the cation-doped systems are less distorted when compared with the metal-doped systems (see Figures 4.1-4.3). As the size of the dopant increases, the tendency to form stable isomers with the metal in the vicinity of sp^3 carbon decreases. Thus, when Li^+ forms $C_nH_{n+3}Li^+$

(3) type complexes in C_9 and higher systems, K^+ never forms such complexes. Na^+ rarely forms such complexes- true to its intermediate character trait.

5.2.2 Doping induced changes in the molecular parameters

In comparison with the metal doping, the cation doping evokes lesser changes in the molecular parameters. The planarity of the carbon chain is almost retained and the warping that we observed in the case of metal substitution is totally missing. The stabilisation energy values suggest a strong interaction; however, it evokes less distortion or induces no warping at all.

5.2.2.1 Change in the carbon- carbon bond lengths

The C-C bond length values partially explain the nature of the interaction in cation-doped polyenes. The interaction is strong enough to induce significant changes in carbon- carbon bond lengths. The interaction of the cation seems to be limited to the polyenic part where the π-cloud is oscillating. The carbon-carbon bond length values of free C_9H_{12}, $(C_9H_{11})^-$ and cation doped systems are presented in Table 5.4.

Table 5.4: C-C bond lengths (A^0) in C_9H_{12}, $(C_9H_{11})^-$ and the most stable isomers of $Li^+/Na^+/K^+$ doped C_9H_{12} (B3LYP/6-31G*).

System	C1-C2	C2-C3	C3-C4	C4-C5	C5-C6	C6-C7	C7-C8	C8-C9
C_9H_{12}	1.4983	1.3469	1.4461	1.3563	1.4406	1.3560	1.4476	1.3442
$(C_9H_{11})^-$	1.3613	1.4277	1.3864	1.4047	1.4047	1.3864	1.4277	1.3613
$C_9H_{12}Li^+(8)$	1.4902	1.3541	1.4331	1.3686	1.4222	1.3782	1.4516	1.3606
$C_9H_{12}Na^+(8)$	1.4920	1.3519	1.4369	1.3646	1.4292	1.3711	1.4529	1.3574
$C_9H_{12}K^+(8)$	1.4933	1.3504	1.4397	1.3619	1.4348	1.3661	1.4519	1.3526

It is evident from Table 5.4 that the delocalisation of the π-cloud is not as pronounced as in the case of metal doping. Further, we can say that there is no localization of the delocalised electron cloud that we observed in metal substituted polyenes. The terminal carbon-carbon bond is only marginally

affected which suggests the limited interaction of the cation with the sp^3 carbon.

5.2.2.2 Structural distortion of the polyene

For evaluating the cation-induced structural change of the polyene, the bond angles and the dihedral angles were studied. The comparatively insignificant deviations in them suggest the retention of the original structure to a certain extent even after the cation doping. For a closer study, the bond angles and dihedral angles of the Li^+/ Na^+/ K^+doped C_9H_{12} and the free C_9H_{12} are presented in Tables 5.5(a) & (b)

Table 5.5(a): Selected bond angles (degree) in free C_9H_{12} and the most stable $Li^+/Na^+/K^+$- C_9H_{12} complexes (B3LYP/6-31G*).

System	H1C1C2	C1C2C3	C2C3C4	C3C4C5	C4C5C6	C5C6C7	C6C7C8	C7C8C9	C8C9H9
C_9H_{12}	111.30	125.14	124.49	124.52	124.41	124.64	124.24	124.64	121.53
$C_9H_{12}Li^+(8)$	110.42	125.38	122.55	124.95	122.29	125.80	123.41	124.85	121.50
$C_9H_{12}Na^+(8)$	110.55	125.36	122.85	124.98	122.72	125.71	123.57	125.49	121.45
$C_9H_{12}K^+(8)$	110.65	125.34	123.15	124.96	123.17	125.60	123.87	125.39	121.52

Table 5.5(b): Selected dihedral angles (degree) in free C_9H_{12} and the most stable $Li^+/Na^+/K^+$ - C_9H_{12} complexes (B3LYP/6-31G*).

System	H1C1C2C3	C1C2C3C4	C2C3C4C5	C3C4C5C6	C4C5C6C7	C5C6C7C8	C6C7C8C9	C7C8C9H9
C_9H_{12}	0.0	180.0	-180.0	-180.0	180.0	180.0	-180.0	0.0
$C_9H_{12}Li^+(8)$	-0.23	-179.69	179.31	-178.52	178.76	**-176.56**	**171.33**	**-178.83**
$C_9H_{12}Na^+(8)$	-0.29	-179.54	179.09	-178.52	178.15	**-177.09**	**175.14**	**-178.59**
$C_9H_{12}K^+(8)$	-0.45	-179.59	179.57	-179.09	179.51	**-179.13**	**174.60**	**-178.37**

Among the three cation-doped complexes of C_9H_{12}, Li^+-C_9H_{12} complex shows maximum distortion, which, in comparison with the Li substituted C_9H_{12} and Li doped C_9H_{12}, is the poorest. The minimal distortion for the carbon backbone in K^+- C_9H_{12} complex is not even comparable with the distortion in $C_9H_{11}K$ (3), though it is somewhat closer to K-doped C_9H_{12}. But

it should be borne in mind that the intensity of distortion may not be a pointer to the intensity of interaction. Of the two species, K^+- C_9H_{12} and K- C_9H_{12}, the former is more stable though it has a less distorted structure.

5.2.3 Increase in the conductance

The HOMO and the LUMO energies and their differences in free polyenes and their $Li^+/Na^+/K^+$- doped complexes are given in Table 5.6.

Table 5.6: HOMO-LUMO difference in free C_9H_{12} and $Li^+/Na^+/K^+$- C_9H_{12} complexes

System	E_H (Hartree)	E_L (Hartree)	$\Delta E = E_L - E_H$ (kcal/mol)
C_5H_8	-0.21767	-0.01519	127.06
$C_5H_8Li^+$ (4)	-0.41569	-0.21718	124.57
$C_5H_8Na^+$ (4)	-0.39337	-0.20861	115.94
$C_5H_8K^+$ (4)	-0.37259	-0.18909	115.15
C_7H_{10}	-0.20081	-0.03841	101.91
$C_7H_{10}Li^+$ (6)	-0.36931	-0.21749	95.27
$C_7H_{10}Na^+$ (6)	-0.35201	-0.20208	94.08
$C_7H_{10}K^+$ (6)	-0.33699	-0.18498	95.39
C_9H_{12}	-0.19034	-0.05269	86.38
$C_9H_{12}Li^+$(8)	-0.33659	-0.21422	76.79
$C_9H_{12}Na^+$(8)	-0.32200	-0.19756	80.79
$C_9H_{12}K^+$(8)	-0.31126	-0.18370	80.05
$C_{11}H_{14}$	-0.18318	-0.06239	75.80
$C_{11}H_{14}Li^+$ (10)	-0.31286	-0.21004	64.52
$C_{11}H_{14}Na^+$ (10)	-0.29999	-0.19431	66.32
$C_{11}H_{14}K^+$ (10)	-0.29094	-0.18213	68.28

The HOMO-LUMO energy difference for different systems shows that there is only a slight increase in the conductance of the polyene as the result of cation doping. However, it is significantly lesser than the conductance attained/effected by the metal doping or metal substitution. The low

conductance may be due to the lesser extent of delocalisation of pi electron cloud along the polyene (see Table 5.4). Here too, it is noteworthy that as the length of the polyene increases, there is increase in the conductance of the species. However, it seems that there is no any specific order of ascendance or increase in the case of different cations.

5.2.4 Formation of different isomers

Table 5.1 provides the complete list of stable isomers obtained when Li^+, Na^+ and K^+ were doped to the polyenes ranging from C_5 to C_{11}. These isomers bring out the general features of alkali cation-doped polyenes. It can be seen that the different isomers of the same system differ by a small quantity of energy. For example, Li (6) & Li (4) isomers of C_7H_{10} are separated by 1.4 kcal/mol. Similarly, the K (10) & K (8) isomers of $C_{11}H_{14}$ differ by 0.69 kcal/mol only. Li (10) & Li (8) isomers of the same system differ by 1.88 kcal/ mol. The small energy difference between the isomers may be an indication to the possibility of cation jump from one position to another at the availability of slight energy to the system.

The number of isomers possible for each system depends on the number of allyl fragments possible in the given system (The nature of isomers shows that there exists a cation- allyl interaction in cation-doped polyenes). Since the fragment of the polyene that interacts with the cation excludes the sp^3 carbon, the counting should be done excluding terminal sp^3 carbon. Thus C_5 system can have only one stable isomer, C_7 can have two, C_9 can have three and so on. Since the energy difference between the isomers is very small, especially for longer polyenes, the hopping of metal ion throughout the chain will be easier, which signifies the possibility of drastic changes in the electric properties of the material.

5.3 Doping of alkali metal cations in even numbered all-trans conjugated polyenes

Even polyenes are similar to odd polyenes; they differ only by a non-interacting methyl group. Hence the odd and even systems will have almost the same characteristics. Only two even systems (i.e., C_8H_{10} & $C_{10}H_{12}$) were analyzed with cation doping and they agreed with the predictions made above. The E_{st} of the cation-polyene complexes was of the same order as in odd polyene complexes. The stable isomers of $Li^+/Na^+/K^+$ doped C_8H_{10} & $C_{10}H_{12}$ with their important characteristics are given in Table 5.7.

Table 5.7: The stable isomers of $Li^+/Na^+/K^+$ doped C_8H_{10} and $C_{10}H_{12}$ systems with their important characteristics (B3LYP/6-31G*)

System	Stable isomers [a]	E (Hartree)	E_{st} (kcal/mol)	Ri (A^o)	Q_M (a.u)
$C_8H_{10}Li^+$	$C_8H_{10}Li^+(2)$	-318.15430	38.92	2.1738	0.519264
	$C_8H_{10}Li^+(4)$[b]	-318.15160	37.37	2.1977[c]	0.543167
$C_8H_{10}Na^+$	$C_8H_{10}Na^+(2)$	-472.93099	26.98	2.5466	0.680043
	$C_8H_{10}Na^+(5)$	-472.92936	26.03	2.5753	0.685368
$C_8H_{10}K^+$	$C_8H_{10}K^+(2)$	-910.55871	17.09	3.0269	0.834315
	$C_8H_{10}K^+(5)$	-910.55755	16.43	3.0390	0.835748
$C_{10}H_{12}Li^+$	$C_{10}H_{12}Li^+(2)$	-395.56638	41.79	2.1608	0.499876
	$C_{10}H_{12}Li^+(4)$	-395.56303	39.87	2.1719	0.529096
$C_{10}H_{12}Na^+$	$C_{10}H_{12}Na^+(2)$	-550.34164	28.97	2.5341	0.669012
	$C_{10}H_{12}Na^+(4)$	-550.33963	27.81	2.5496	0.677123
$C_{10}H_{12}K^+$	$C_{10}H_{12}K^+(2)$	-987.96849	18.54	3.0102	0.828669
	$C_{10}H_{12}K^+(4)$	-987.96711	17.77	3.0000	0.830407

[a] The numeral in parentheses corresponds to the carbon to which the metal is having the smallest distance.
[b] The metal is exactly at the middle of C4-C5 bond.
[c] C4-Li= C5- Li = 2.1977

Similar to the cation doping in odd polyenes, here too, high stabilisation energy is obtained for the Li-isomers, the order being the same,

i.e., Li> Na > K. In all the isomers, the metal ions are stationed almost above the C-C bond. Also, towards the center, the odd- even distinction becomes irrelevant in a conjugated polyene of even carbons.

The formation of different isomers for different polyenes may be explained in terms of the Mulliken charges. The values are presented in Tables 5.8(a) & (b).

Table 5.8(a): Mulliken charges (a.u) on the carbons in C_8H_{10} and its stable $Li^+/Na^+/K^+$-doped complexes (B3LYP/6-31G*).

System	C1	C2	C3	C4	C5	C6	C7	C8
C_8H_{10}		-0.060	-0.122	-0.123	-0.122	-0.122	-0.060	-0.356
$C_8H_{10}Li^+(2)$	**-0.354**	**-0.108**	**-0.240**	-0.064	-0.133	-0.092	-0.073	-0.314
$C_8H_{10}Li^+(4)$	-0.319	-0.072	-0.084	**-0.219**	**-0.219**	-0.084	-0.072	-0.319
$C_8H_{10}Na^+(2)$	**-0.377**	**-0.118**	**-0.215**	-0.096	-0.137	-0.098	-0.072	-0.322
$C_8H_{10}Na^+(5)$	-0.365	-0.057	0.151	**-0.182**	**-0.182**	-0.151	-0.057	-0.365
$C_8H_{10}K^+$ (2)	**-0.397**	**-0.119**	**-0.219**	-0.117	-0.140	-0.105	-0.071	-0.329
$C_8H_{10}K^+$ (5)	-0.378	-0.061	-0.182	**-0.189**	**-0.189**	-0.182	-0.061	-0.378

Table 5.8(b): Mulliken charges (a.u) on the carbons in $C_{10}H_{12}$ and its stable $Li^+/Na^+/K^+$-doped complexes (B3LYP/6-31G*).

System	C1	C2	C3	C4	C5	C6	C7	C8	C9	C10
$C_{10}H_{12}$	-0.356	-0.060	-0.123	-0.122	-0.123	-0.123	-0.122	-0.123	-0.060	-0.356
$C_{10}H_{12}Li^+(2)$	**-0.366**	**-0.101**	**-0.243**	-0.066	-0.136	-0.095	-0.129	-0.095	-070	-0.319
$C_{10}H_{12}Li^+(4)$	-0.326	-0.068	-0.104	**-0.203**	**-0.234**	-0.076	-0.131	-0.097	-0.072	-0.320
$C_{10}H_{12}Na^+(2)$	**-0.386**	**-0.114**	**-0.220**	-0.096	-0.140	-0.101	-0.129	-0.100	-0.069	-0.326
$C_{10}H_{12}Na^+(4)$	-0.332	-0.075	-0.126	**-0.200**	**-0.214**	-0.110	-0.136	-0.103	-0.071	-0.326
$C_{10}H_{12}K^+$ (2)	**-0.403**	**-0.117**	**-0.226**	-0.117	-0.144	-0.107	-0.130	-0.104	-0.068	-0.331
$C_{10}H_{12}K^+$ (4)	-0.342	-0.077	-0.159	**-0.195**	**-0.210**	-0.127	-0.137	-0.108	-0.071	-0.331

It may be concluded that the doped metal ions prefer to a carbon where maximum charge-charge interaction is possible. In other words, wherever the cation resides, there the net charge is negative. In order to illumine this fact,

the net charge on the carbons of different cation-doped isomers of $C_{10}H_{12}$ system is presented in Table 5.9.

Table 5.9: The net charges (a.u) on the carbons of $C_{10}H_{12}$ and its $Li^+/Na^+/K^+$ doped complexes (B3LYP/6-31G*).

System	C1	C2	C3	C4	C5	C6	C7	C8	C9	C10
$C_{10}H_{12}$	-0.070	0.066	0.001	0.002	0.001	0.001	0.002	0.001	0.066	-0.070
$C_{10}H_{12}Li^+(2)$	0.048	**0.097**	**-0.055**	0.104	0.020	0.063	0.026	0.063	0.090	0.043
$C_{10}H_{12}Li^+(4)$	0.043	0.097	0.073	**-0.012**	**-0.045**	0.096	0.027	0.061	0.087	0.045
$C_{10}H_{12}Na^+(2)$	0.001	**0.073**	**-0.050**	0.066	0.010	0.051	0.019	0.052	0.085	0.025
$C_{10}H_{12}Na^+(4)$	0.027	0.085	0.040	**-0.022**	**-0.038**	0.053	0.018	0.049	0.083	0.028
$C_{10}H_{12}K^+(2)$	**-0.041**	**0.052**	**-0.068**	0.037	0.002	0.041	0.015	0.043	0.081	0.011
$C_{10}H_{12}K^+(4)$	0.008	0.078	**-0.032**	**0.041**	**-0.051**	0.027	0.010	-0.004	0.080	0.014

5.3.1 Position of the metal

The most stable isomer for all the systems with any of the metal ion doped has the same formula, $C_nH_{n+2}M^+(2)$. When other isomers of higher energy are considered, $C_{10}H_{12}$ has all of them with the metal over C4. In C_8H_{10}, all of them are near to C5. However, the position is in between C4 and C5 in either system, which shows a preference to the C4-C5 bond. Another feature to be noted is that the doped cation is not exactly at a vertical position, but resides in a slightly slanted position. A close examination of the relevant values, taken from the optimized data file of some of the isomers is given in Table 5.10, will pronounce the above features more clearly.

Table 5.10: M^+-carbon distances and metal polyene bond angles in some selected isomers of $Li^+/Na^+/K^+$ doped $C_{10}H_{12}$ (B3LYP/6-31G*)

System	C(i-1)-M (A^0)	C(i)- M (A^0)	C(i+1)-M (A^0)	MC(i)C(i+1) (deg.)	MC(i)H(i) (deg.)
$C_{10}H_{12}Li^+(2)$	2.3374	**2.1608**	**2.2437**	73.91	114.94
$C_{10}H_{12}Li^+(4)$	2.6038	**2.1719**	**2.1993**	71.62	106.75
$C_{10}H_{12}Na^+(2)$	2.7399	**2.5341**	**2.6406**	77.79	109.23
$C_{10}H_{12}Na^+(4)$	2.9829	**2.5496**	**2.5750**	74.52	102.59
$C_{10}H_{12}K^+$ (2)	3.2710	**3.0102**	**3.0403**	77.28	104.83
$C_{10}H_{12}K^+$ (4)	3.3157	**3.0000**	**3.0638**	78.69	101.48

Figure 5.4 gives more details on the isomers and the positions of the metals. In comparison with the metal-doped systems, cation-doped systems are less distorted and the chain almost retains its planarity. No bent is visible even in large systems-a noted deviation from metal-doped polyenes.

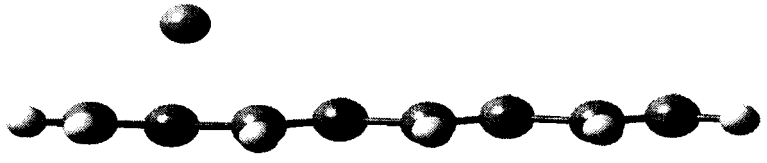

(a) $C_8H_{10}Li^+$ (2)

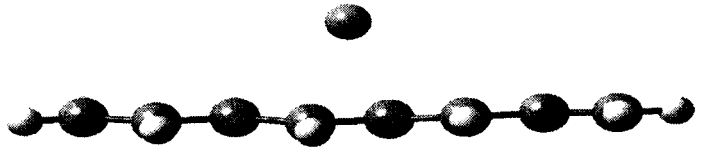

(b) $C_8H_{10}Li^+$ (4)

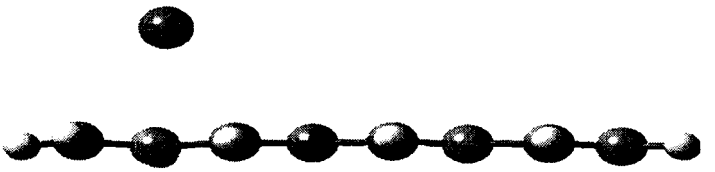

(c) $C_8H_{10}Na^+$ (2)

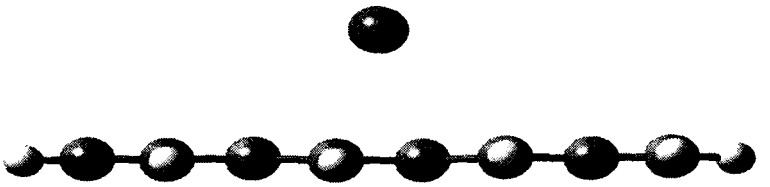

(d) $C_8H_{10}Na^+$ (5)

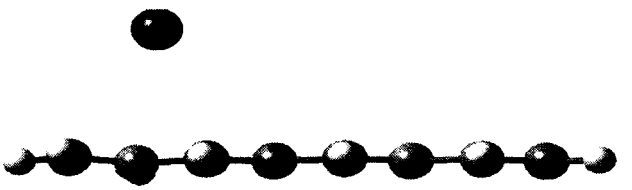

(e) $C_8H_{10}K^+$ (2)

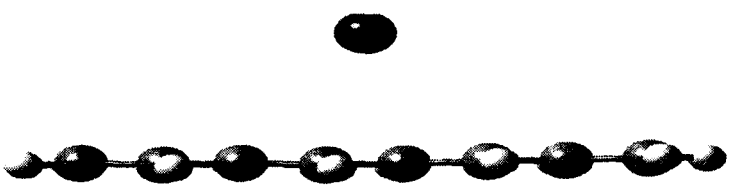

(f) $C_8H_{10}K^+$ (4)

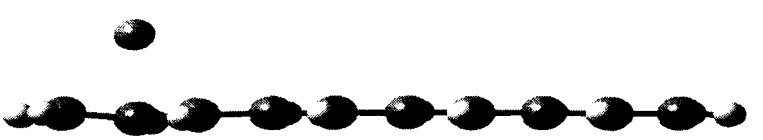

(g) $C_{10}H_{12}Li^+$ (2)

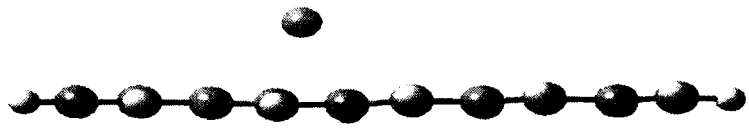

(h) $C_{10}H_{12}Li^+$ (4)

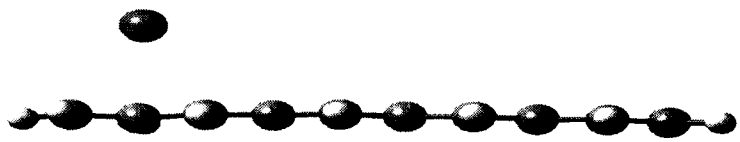

(i) $C_{10}H_{12}Na^+$ (2)

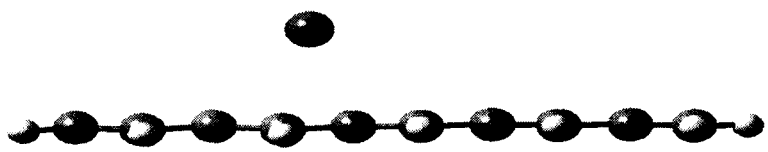

(j) $C_{10}H_{12}Na^+$ (4)

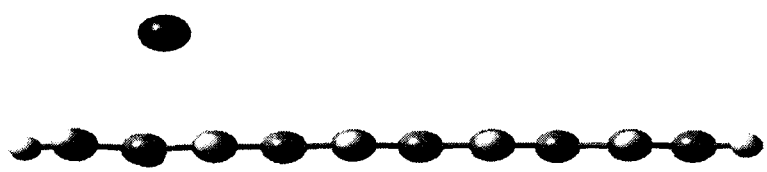

(k) $C_{10}H_{12}K^+$ (2)

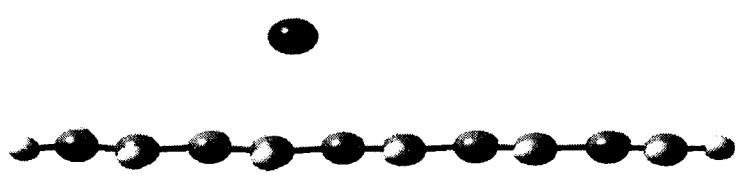

(l) $C_{10}H_{12}K^+$ (4)

Figure 5.4: The optimized structures of a few stable isomers of $Li^+/Na^+/K^+$ doped complexes of C_8H_{10} and $C_{10}H_{12}$ (B3LYP/6-31G*)

5.3.2 Doping induced changes in the molecular parameters

Compared to the metal doping, the cation doping brings in only minute changes to the structural parameters. The less intensity may not be due to the absence of strong interaction, because the stabilisation energy values of these complexes are very high. The flow of electron towards the cation may be reducing the pi-electron cloud that may have a dampening effect on the distortion of the carbon skeleton.

5.3.2.1 Change in the C-C bond lengths

Since the carbon- carbon bond lengths will suggest whether a bond is localised or delocalised, the optimized C-C bond lengths of free polyene and its cation-complexes are given in Table 5.11 for a closer examination. The positioning of such a delocalised electron cloud is also significant in judging the nature of interaction existing in cation doped polyenyl complexes.

Table 5.11: Optimized C-C bond lengths (A^0) in free $C_{10}H_{12}$ and its most stable $Li^+/Na^+/K^+$ doped complexes (B3LYP/6-31G*).

System	C1-C2	C2-C3	C3-C4	C4-C5	C5-C6	C6-C7	C7-C8	C8-C9	C9-C10
$C_{10}H_{12}$	1.3446	1.4468	1.3573	1.438	1.3598	1.438	1.3573	1.4468	1.3446
$C_{10}H_{12}Li^+(2)$	**1.3619**	**1.4495**	**1.3809**	**1.4183**	1.3732	1.4242	1.3653	1.4399	1.3471
$C_{10}H_{12}Li^+(4)$	1.3450	1.4482	**1.3701**	**1.4521**	**1.3754**	1.4303	1.3632	1.4417	1.3463
$C_{10}H_{12}Na^+(2)$	**1.3585**	**1.4513**	**1.3732**	1.4528	1.3686	1.4286	1.3626	1.4422	1.3461
$C_{10}H_{12}Na^+(4)$	1.3450	1.4484	**1.3672**	**1.4502**	**1.3712**	1.4343	1.3612	1.4434	1.3455
$C_{10}H_{12}K^+(2)$	1.3533	**1.4506**	**1.3678**	1.4319	1.3656	1.4317	1.3608	1.4436	1.3454
$C_{10}H_{12}K^+(4)$	1.3451	1.4494	**1.3639**	**1.4449**	1.3673	1.4361	1.3600	1.4445	1.3451

The values show that the delocalisation of the electron cloud is less intense in the segment above which the metal is stationed. At the same time, there is enhanced delocalisation, (though not so intense as in metal-doped polyenes), along the carbon skeleton than the parent polyene, as indicated by the values.

5.3.2.2 Distortion to the carbon skeleton

Intensity of distortion to the carbon skeleton may be found out from the bond angles and the dihedral angles. Apparently, as the Figure 5.4 suggests, the distortion is very minimum. However, an interaction that amounts to a stabilisation energy of about 42 kcal/mol cannot leave the system totally undisturbed. For a close examination, the bond angles and dihedral angles of free $C_{10}H_{12}$ and its most stable $Li^+/Na^+/K^+$ doped complexes are given in Tables 5.12(a) & (b).

Table 5.12(a): Selected bond angles (degree) in free $C_{10}H_{12}$ and the most stable $Li^+/Na^+/K^+$- $C_{10}H_{12}$ complexes (B3LYP/6-31G*).

System	H1C1C2	C1C2C3	C2C3C4	C3C4C5	C4C5C6	C5C6C7	C6C7C8	C7C8C9
$C_{10}H_{12}$	121.54	124.56	124.26	124.55	124.43	124.43	124.55	124.26
$C_{10}H_{12}Li^+(2)$	121.47	124.91	123.44	125.84	122.37	124.94	122.68	124.54
$C_{10}H_{12}Na^+((2)$	121.49	125.58	123.55	125.77	122.75	124.97	122.96	124.53
$C_{10}H_{12}K^+(2)$	121.60	125.44	123.88	125.63	123.2	124.94	123.24	124.52

Table 5.12(b): Selected dihedral angles (degree) in free $C_{10}H_{12}$ and the most stable $Li^+/Na^+/K^+$ - $C_{10}H_{12}$ complexes (B3LYP/6-31G*).

System	H1C1C2C3	C1C2C3C4	C2C3C4C5	C3C4C5C6	C4C5C6C7	C5C6C7C8	C6C7C8C9	C7C8C9C10
$C_{10}H_{12}$	00.00	-180.0	-180.0	-180.0	180.0	180.0	180.0	180.0
$C_{10}H_{12}Li^+(2)$	**-10.07**	**-171.81**	**-176.34**	178.65	-178.55	179.24	-179.73	179.85
$C_{10}H_{12}Na^+((2)$	**-06.44**	**-175.65**	**-176.87**	178.01	-178.54	179.13	-179.65	179.80
$C_{10}H_{12}K^+(2)$	**-04.76**	**-174.66**	**-179.09**	179.55	-179.14	179.71	-179.77	179.94

As the bond angles and dihedral angles suggest, there is only minor distortion to the carbon skeleton, in comparison with the metal polyenes. However, there is a significant deviation from the dihedral values of free polyene when cations are doped. This suggests that there exist some strong interactive forces between the cation and the polyene. They account for the high stabilisation energy of these systems.

5.3.3 *Increase of conductance*

A minor increase in conductance may be observed in the cation-doped polyenes. The HOMO and LUMO energies of the free polyenes and their cation-doped complexes are given in Table 5.13.

Table 5.13: HOMO-LUMO difference in free C_8H_{10}, $C_{10}H_{12}$ and their $Li^+/Na^+/K^+$ - doped complexes.

System	E_H (Hartree)	E_L (Hartree)	$\Delta E = E_L - E_H$ (kcal/mol)
C_8H_{10}	-0.19700	-0.05771	87.41
$C_8H_{10}Li^+$ (2)	-0.34860	-0.22142	79.81
$C_8H_{10}Na^+$ (2)	-0.33343	-0.20370	81.41
$C_8H_{10}K^+$ (2)	-0.32167	-0.18939	83.01
$C_{10}H_{12}$	-0.18870	-0.06672	76.54
$C_{10}H_{12}Li^+$ (2)	-0.32251	-0.21601	66.83
$C_{10}H_{12}Na^+$ (2)	-0.30925	-0.19968	68.76
$C_{10}H_{12}K^+$ (2)	-0.29986	-0.18723	70.68

The increase in conductance for the cation-doped polyenes is very negligible in comparison with the high conductance exhibited by metal-doped polyenes. Since the cation does not donate an electron to the pi-cloud of the polyene, but abstracts some of the electron cloud, there is no chance for a vastly improved conductance. That explains why cation-doped polyenes have lesser conductance in comparison with the metal-doped polyenes.

5.3.4 *Formation of different isomers*

As in the case of odd polyenes, here too, different isomers of cation-doped polyenes are formed. All of them retain a general characteristic that the metal ions in them prefer to settle above a C-C bond. The different isomers are close in energies. For example, $C_{10}H_{12}Li$ (2) & (4) differ by 1.92 kcal/mol; $C_{10}H_{12}K$ (2) & (4) differ by 0.77 kcal/mol. The different isomers are possible

because of the possible cation-allyl interaction. Therefore, the number of possible isomers is equal to the number of allyl fragments present in the polyene.

5.4 Alkali metal ion doping to substituted polyenes

We have already presented the results of alkali metal cation doping to conjugated polyenes. In order to evaluate the effects of substituents in the polyene on the characteristics of cation-doped polyenes, cation doping was done on substituted C_9 system. The groups substituted on the polyene were CH_3 and CN, representatives from electron-donating and electron-withdrawing groups.

5.4.1 Metal ion doping to $C_9H_{11}CH_3$

When electron-donating groups are present in a system, it would enhance the electron cloud of the system. Accordingly, electrophilic reactions or interactions will be favoured. Hence, from the reaction results, we can conclude whether the interaction is electrophilic or not. The characteristics of the $Li^+/Na^+/K^+$ doped complexes of C_9H_{12} and $C_9H_{11}CH_3$ (8) are presented in Table 5.14.

Table 5.14: The most stable $Li^+/Na^+/K^+$ doped complexes of C_9H_{12} and $C_9H_{11}CH_3$ (8) [B3LYP/6-31G*]

Metal-polyene system	E (Hartree)	E_{st} (kcal/mol)	Ri (A^o)	Q_M (a.u)	$\Delta E=E_L-E_H$ (Hartree)
$C_9H_{12}Li^+$ (8)	-357.47918	41.89	2.1654	0.506712	0.12237
$C_9H_{11}CH_3(8)Li^+(8)$	-396.79826	42.93	2.1928	0.496498	0.12355
$C_9H_{12}Na^+(8)$	-512.25488	29.34	2.5373	0.672217	0.12874
$C_9H_{11}CH_3(8)Na^+(8)$	-551.57321	29.88	2.5762	0.663888	0.12357
$C_9H_{12}K^+$ (8)	-949.88194	19.00	3.0148	0.829745	0.12756
$C_9H_{11}CH_3(8)K^+(8)$	-989.19970	19.23	3.0380	0.831213	0.12685

From Table 5.14, it is clear that the presence of electron donating group, CH_3, is actually stabilizing the system by increasing its E_{st}. The metal-carbon distance is larger for $Li^+/Na^+/K^+$ doped substituted polyenes, in comparison with free polyene counterparts. But the charge on the metal is less in Li^+ and Na^+ doped complexes; but K has more charge on it in $C_9H_{11}CH_3$ $(8)K^+(8)$ than that in $C_9H_{12}K^+$ (8).

The Mulliken charges on different carbons in different systems are presented in Table 5.15 for comparing the interactions in them.

Table 5.15: Mulliken charges (a.u) on the carbons in $Li^+/Na^+/K^+$ doped $C_9H_{11}CH_3$ (8) & C_9H_{12} (B3LYP/6-31G*)

System	C1	C2	C3	C4	C5	C6	C7	C8	C9
$C_9H_{11}CH_3$ (8)	-0 .491	-0.106	-0.100	-0.126	-0.119	-0.122	-0.177	0.237	-0.413
$C_9H_{12}Li^+$ (8)	-0.506	-0.072	-0.109	-0.092	-0.137	-0.064	-0.243	-0.104	-0.361
$C_9H_{11}CH_3(8)Li^+(8)$	-0.506	-0.074	-0.109	-0.096	-0.132	-0.061	-0.293	0.180	-0.413
$C_9H_{12}Na^+(8)$	-0.504	-0.079	-0.108	-0.099	-0.141	-0.095	-0.219	-0.115	-0.382
$C_9H_{11}CH_3(8)Na^+(8)$	-0.503	-0.081	-0.108	-0.102	-0.136	-0.090	-0.274	0.183	-0.436
$C_9H_{12}K^+$ (8)	-0.502	-0.085	-0.109	-0.105	-0.145	-0.117	-0.225	-0.118	-0.400
$C_9H_{11}CH_3(8)K^+(8)$	-0.501	-0.086	-0.109	-0.108	-0.140	-0.112	-0.280	0.180	-0.462

There is an increase in the charges on the carbons of the polyenic segments interacting with the metals, but the same on other carbons are slightly less. The carbon carrying the substituent carries positive charge.

A close analysis of the C-C bond lengths in different cation-doped systems will give certain indications, regarding the nature of electronic distributions in those complexes. Hence, the C-C bond length values in such systems are presented in Table 5.16.

Table 5.16: C-C bond lengths (A^0) in $Li^+/Na^+/K^+$ doped $C_9H_{11}CH_3$ (8) & C_9H_{12} (B3LYP/6-31G*)

System	C1-C2	C2-C3	C3-C4	C4-C5	C5-C6	C6-C7	C7-C8	C8-C9
$C_9H_{12}Li^+$ (8)	1.4902	1.3541	1.4331	1.3686	1.4222	1.3782	1.4516	1.3606
$C_9H_{11}CH_3(8)Li^+(8)$	1.4907	1.3534	1.4343	1.3673	1.4250	1.3761	1.4650	1.3651
$C_9H_{12}Na^+(8)$	1.4920	1.3519	1.4369	1.3646	1.4292	1.3711	1.4529	1.3574
$C_9H_{11}CH_3(8)Na^+(8)$	1.4924	1.3513	1.4380	1.3634	1.4320	1.3691	1.4664	1.3614
$C_9H_{12}K^+$ (8)	1.4933	1.3504	1.4397	1.3619	1.4348	1.3661	1.4519	1.3526
$C_9H_{11}CH_3(8)K^+(8)$	1.4936	1.3500	1.4405	1.3610	1.4372	1.3646	1.4639	1.3563

In comparison with $Li^+/Na^+/K^+$ doped C_9H_{12}, the C-C bond lengths in $Li^+/Na^+/K^+$ doped $C_9H_{11}CH_3$ (8) are slightly modified, the modification extending throughout the chain. In either case, a perfectly delocalised electron cloud spread over a particular segment, as in the case previous systems, is not observed here.

The structures of above complexes of substituted polyenes are given in Figure 5.5.

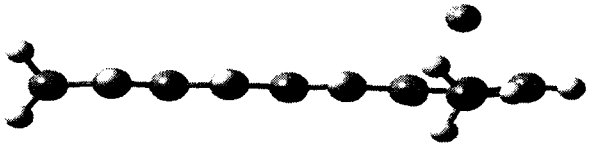

(a) $C_9H_{11}CH_3$ (8)Li^+(8)

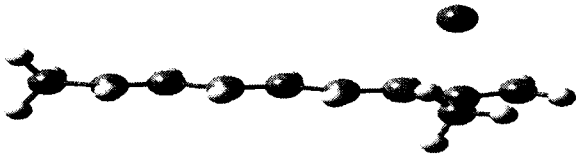

(b) $C_9H_{11}CH_3(8)Na^+(8)$

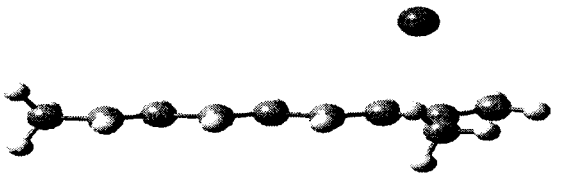

(c) $C_9H_{11}CH_3$ (8)K^+(8)

Figure 5.5: Optimized structures of $Li^+/Na^+/K^+$ doped complexes of C_9H_{12} and $C_9H_{11}CH_3$ (8) [B3LYP/6-31G*]

5.4.2 Metal ion doping to $C_9H_{11}CN$

Introduction of an electron-withdrawing group to a conjugated polyene will decrease the available electron cloud. Hence, any interaction favoured by enhanced pi electron cloud will be retarded by such substitution. In cation-doped systems, the cation interacts with the polyene to give a stable complex and hence the introduction of electron withdrawing groups in the polyene will destabilize the system. However, if the new entrant can have direct interaction with the cation, the system will be strongly stabilized. If highly polarized systems are present, such interactions will take place, rendering extra stability to the system. The products obtained when cations are doped on $C_9H_{11}CN$ (8) and C_9H_{12}, along with their characteristics are classified in Table 5.17.

Table 5.17: The most stable $Li^+/Na^+/K^+$ doped complexes of C_9H_{12} and $C_9H_{11}CN$ (8)-(B3LYP/6-31G*)

Metal-polyene system	E (Hartree)	E_{st} (kcal/mol)	Ri (A^o)	Q_M (a.u)	$\Delta E=E_L-E_H$ (Hartree)
$C_9H_{12}Li^+$ (8)	-357.47918	41.89	2.1654	0.506712	0.12237
$C_9H_{11}CN(8)Li^+(6)$[a]	-449.71921	40.23	2.3833	0.518909	0.12053
$C_9H_{12}Na^+(8)$	-512.25488	29.34	2.5373	0.672217	0.12874
$C_9H_{11}CN(8)Na^+(6)$[b]	-604.49861	30.82	2.8101	0.674467	0.12247
$C_9H_{12}K^+$ (8)	-949.88194	19.00	3.0148	0.829745	0.12756
$C_9H_{11}CN(8)K^+(8)$[c]	-1042.13737	27.80	5.2451	0.901772	0.11546

[a] Li^+ doped on C8 moves on to C6 to have effective interaction with the CN group.
[b] Na^+ doped on C8 moves on to C6 to have effective interaction with the CN group.
[c] K^+, doped on C8, moves away from the polyene and sticks on the nitrogen of CN group. K-N=2.6438

From Table 5.17, the result of cation doping to substituted polyene can be analyzed. In comparison with the cation-doped free polyenes, substituted polyene-cation complexes of Li are less stable. For Na^+ and K^+, such complexes are highly stabilized via the electrostatic interaction between the metal and the CN group. All the metals move away from the interacting polyenic segment and establish a partial bonding with the nitrogen of CN. The charge on the metal increases slightly for Li^+ and Na^+, but makes a jump in the case of K^+. The conductance of the system also increases as the result of substitution.

The Mulliken charges on the carbons in cation-doped free polyenes and cation –doped substituted polyenes are presented in Table 5.18.

Table 5.18: Mulliken charges (a.u) on the carbons in $Li^+/Na^+/K^+$ doped $C_9H_{11}CN$ (8) & C_9H_{12} (B3LYP/6-31G*)

System	C1	C2	C3	C4	C5	C6	C7	C8	C9
$C_9H_{11}CN(8)$	-0.493	-0.100	-0.102	-0.119	-0.124	-0.121	-0.160	0.204	-0.379
$C_9H_{12}Li^+$ (8)	-0.506	-0.072	-0.109	-0.092	-0.137	-0.064	**-0.243**	**-0.104**	**-0.361**
$C_9H_{11}CN(8)Li^+(6)$	-0.505	-0.079	-0.106	-0.117	**-0.125**	**-0.227**	**-0.167**	0.167	-0.345
$C_9H_{12}Na^+(8)$	-0.504	-0.079	-0.108	-0.099	-0.141	-0.095	**-0.219**	**-0.115**	**-0.382**
$C_9H_{11}CN(8)Na^+(6)$	-0.503	-0.085	-0.106	-0.128	**-0.133**	**-0.192**	**-0.174**	0.171	-0.350
$C_9H_{12}K^+$ (8)	-0.502	-0.085	-0.109	-0.105	-0.145	-0.117	**-0.225**	**-0.118**	**-0.400**
$C_9H_{11}CN(8)K^+(8)$	-0.498	-0.091	-0.103	-0.113	-0.122	-0.118	-0.154	0.196	-0.367

The polyenic carbons that are closer to the metals have comparatively higher Mulliken charges. However, in the case of $C_9H_{11}CN$ (8)K^+(8), such a phenomenon is not visible. It may be due to the migration of metal from the polyenic carbons to the exclusive interaction with the nitrogen of CN group.

The carbon- carbon bond lengths in different cation-doped complexes, which give a measure of the extent of delocalisation, are given in Table 5.19.

Table 5.19: C-C bond lengths (A^0) in $Li^+/Na^+/K^+$ doped $C_9H_{11}CN$ (8) & C_9H_{12} (B3LYP/6-31G*)

System	C1-C2	C2-C3	C3-C4	C4-C5	C5-C6	C6-C7	C7-C8	C8-C9
$C_9H_{12}Li^+$ (8)	1.4902	1.3541	**1.4331**	**1.3686**	**1.4222**	**1.3782**	1.4516	1.3606
$C_9H_{11}CN(8)Li^+(6)$	1.4912	1.3525	**1.4373**	**1.3662**	**1.4396**	**1.3655**	1.4784	1.3473
$C_9H_{12}Na^+(8)$	1.4920	1.3519	**1.4369**	**1.3646**	**1.4292**	**1.3711**	1.4529	1.3574
$C_9H_{11}CN(8)Na^+(6)$	1.4925	1.3511	**1.4398**	**1.3639**	**1.4403**	**1.3617**	1.4723	1.3491
$C_9H_{12}K^+$ (8)	1.4933	1.3504	**1.4397**	**1.3619**	**1.4348**	**1.3661**	1.4519	1.3526
$C_9H_{11}CN(8)K^+(8)$	1.4950	1.3488	1.4422	1.3589	1.4369	1.3568	1.4560	1.3557

The C-C bond lengths show that neither in the cation-doped free polyenes nor in the cation-doped substituted polyenes, the metal interacts with a highly delocalised electron cloud. Instead, as the result of cation doping, there develops a more separation between the C-C double bond and single bond (less delocalisation) in the substituted polyenes in comparison with the same in cation-doped free polyenes.

The optimized structures of the cation-doped substituted polyenes are given in Figure 5.6. The position of the metal gives a clue about the nature of interaction existing in them.

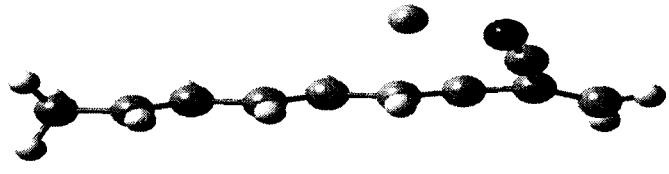

(a) $C_9H_{11}CN$ (8) Li^+ (6)

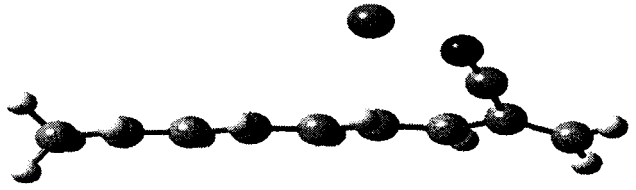

(b) $C_9H_{11}CN$ (8) Na^+ (6)

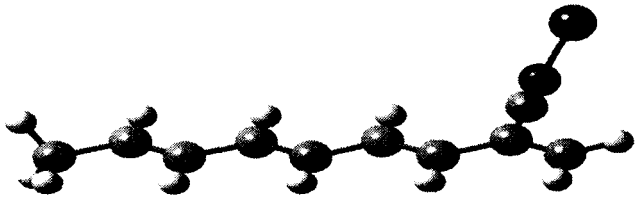

(c) $C_9H_{11}CN$ (8) K^+ (N)*

* K^+, doped on C8, moves away from the polyene and is bonded to the nitrogen of CN

Figure 5.6: Optimized structures of $Li^+/Na^+/K^+$ doped $C_9H_{11}CN$ (8) (B3LYP/6-31G*)

From the structures, it can be seen that interaction of the metals are primarily with the nitrogen of the CN group. This is maximum for K^+ and minimum for Li^+. Hence, the stabilization of these complexes is primarily via the coulombic interaction between the cation and the CN.

5.5 Discussion

Alkali metal ion-doped odd and even polyenes possess considerably high E_{st}, which increases as the length of the polyene increases (For Li-complexes, 35.15 kcal/mol in C_5 system, 38.92 kcal/mol in C_7 system and 41.89 kcal/mol in C_9 system). The carbons of the polyene have slightly diminished Mulliken charges (see Figure 5.7), but the metal has a charge that is much higher than its charge in the corresponding metal polyene. The charge on the metal decreases as the length of the polyene increases (0.551 a.u in C_5

system, 0.528 a.u in C_7 system and 0.489 a.u in C_{11} system- all for Li). The conductance increases slightly as the result of cation doping, but the increase is far below than their metal-doped counter parts. Also, these complexes are characterized by a larger metal- polyene distance (2.201 A^0 in C_5 system, 2.181 A^0 in C_7 system and 2.165 A^0 in C_9 system), which also decreases as the length of the polyene increases. Details can be had from Tables 5.1 & 5.7. The distortion to the carbon skeleton as the result of cation doping is very negligible [see Tables 5.5(a) & (b), 5.12(a) & (b) and Figures 5.1- 5.4].

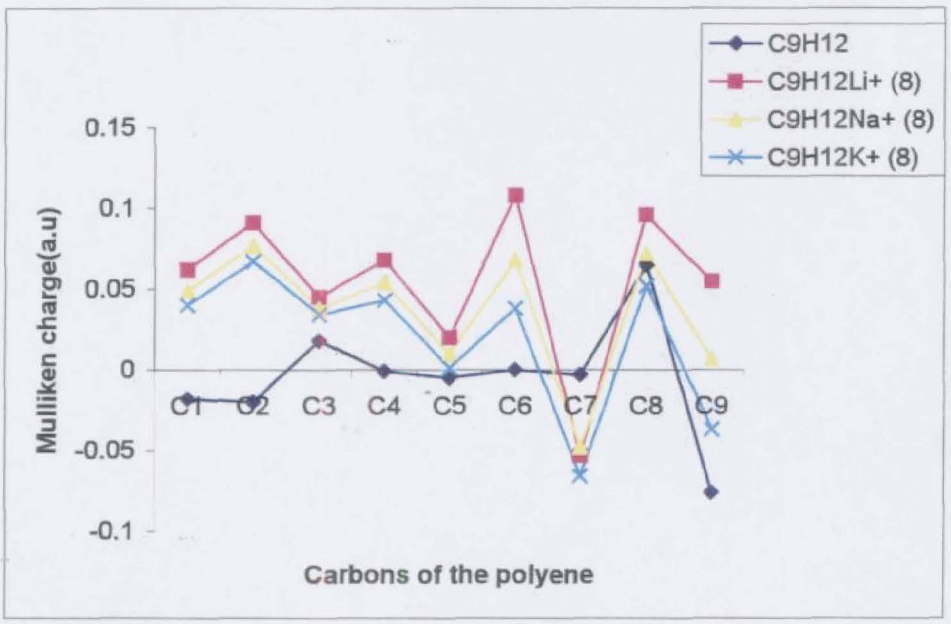

Figure 5.7: Mulliken charges on different carbons of C_9H_{12} and its $Li^+/Na^+/K^+$ doped complexes.

5.5.1 Stability of the isomers of Alkali metal ion doped polyenes

The relatively high E_{st} is a strong evidence to infer that powerful interactions are present in cation-doped polyenes. However, this interaction cannot be any of the conventional binding forces. Since the interacting species of the system are a cation and a polyene, ion- ion interaction, mutual sharing of electrons or extension of lone pair of electron for bonding are not possible

in this system. Strictly speaking, the stability of the complex can be explained only in terms of the non-covalent interaction, cation-π cloud interaction. There are reports that the major attractive contributions to this high stabilisation energy emerge from electrostatic and induction energies [8]. The electrostatic energy arises due to the charge-charge interaction and the induction energy arises due to the interaction between the HOMO of the π-system and the LUMO of the cation. We have already classified them as the Type I and Type II interactions, which collectively contribute to the total cation-π interaction.

Unlike the metal substituted and metal-doped systems, the cation-doped polyenes do not have extensively delocalised C-C bonds and localized pi cloud above the allylic unit interacting with the metal (Table 5.4 & 5.11). In general, the most stable metal ion -doped polyene complex has the metal stationed over the 2nd carbon from the terminal, or rather over the terminal allyl fragment. In other isomers too, the metal ions are closer to the even carbons. However, it should be noted that when the metal moves towards the center, it resides over a bond and not on a particular carbon (Table 5.4 & 5.11). Though there is a flow of electron from polyene to the metal as evidenced by the decreased charge on the cation, there is improved delocalisation of the electron cloud in the carbon chain (see Tables 5.4 & 5.11).

5.5.1.1 Cation-π interaction- type I or type II?

The polyene possesses a pi electron cloud, which is partially delocalised along the carbon skeleton. When the cation is placed at a site perpendicular to the carbon skeleton, there takes place a flow of the pi cloud from the polyene to the degenerate p-orbitals of the cation- a partial p-p overlapping. Thus, the stabilizing interaction in cation-doped complex is efficient cation- π interaction. This interaction is made possible by the small

energy gap between these two levels. For example, the energy difference between the HOMO of C_9H_{12} (-0.19034 Hartree) and the closest UMO of Li^+ (-0.16801 Hartree) is 0.0223 Hartree (Actually, the LUMO of the metal ion is s-orbital with an energy value much lower than the HOMO of the polyene and hence the probable interaction will be with the p-level, having an energy closer to that of HOMO and having the same symmetry). Similarly, with Na^+, the energy gap is 0.03991 Hartree and with K^+, it is 0.07673 Hartree. The interaction between the polyenic pi cloud and the cation stabilizes the system and this accounts for the high E_{st} of the system. The cation- pi cloud interaction is manifested by the decreased charge on the doped cation.

The efficiency of the interaction, as manifested by high E_{st}, suggests that the cation-π interaction in cation-doped polyenes is predominantly Coulombic in nature (type I interaction). The highly charged metal ion is involved in strong charge- charge interaction with the negatively charged carbons of the polyene. Since, no polyenic segment with highly delocalised electron cloud is there to pocket the cation, intense cation- allyl/polyenyl interaction (type II interaction) must be negligible. (Figure 5.8 given below) The small energy difference between the different isomers of the same system (see Figure 5.9) indicates that the position of the metal has only slight influence on the energy of the system. However, a mild interaction of the cation with the whole π-cloud oscillating along the carbon skeleton is possible, which is almost the same in all the isomers.

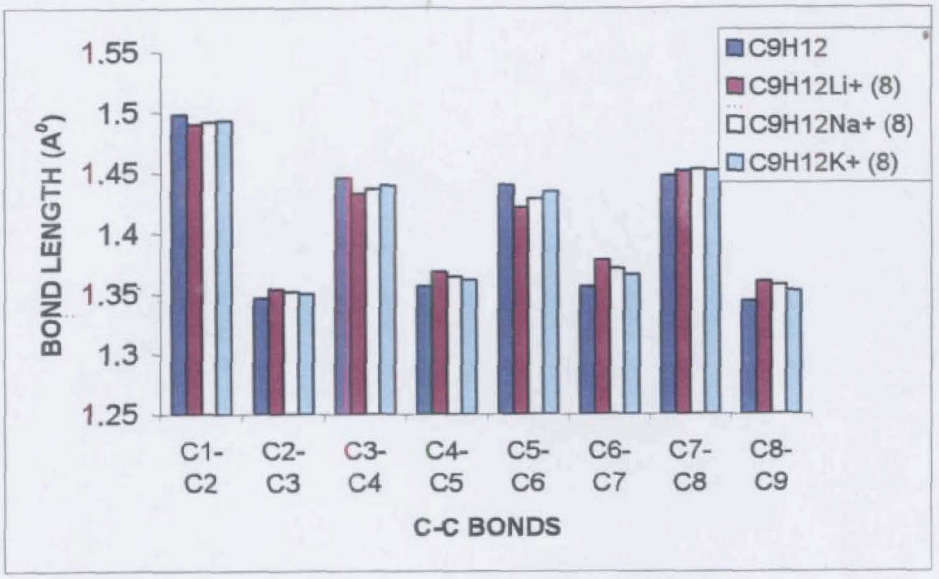

Figure 5.8: C-C bond lengths in C_9H_{12} and its $Li^+/Na^+/K^+$ doped complexes

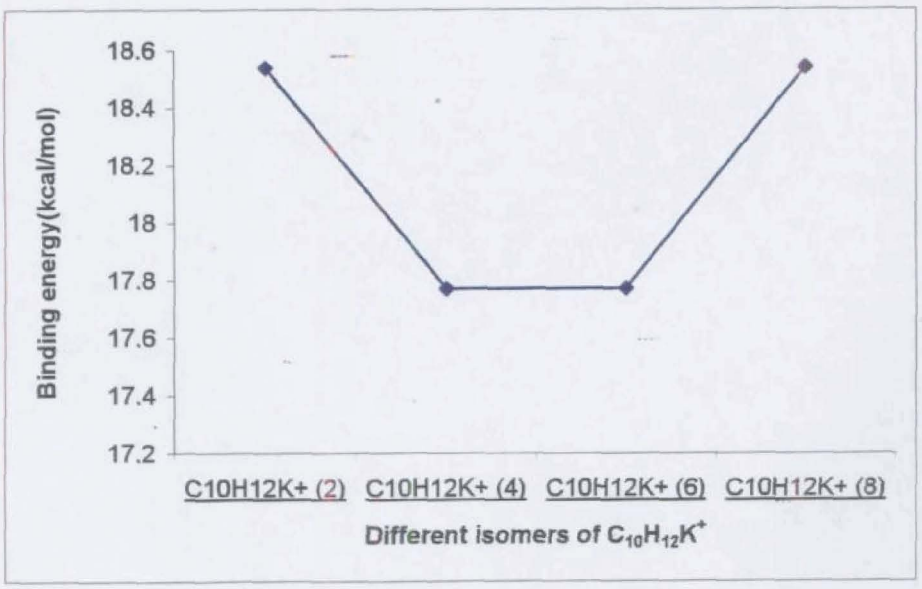

Figure 5.9: E_{st} of the different isomers of $C_{10}H_{12}K^+$

In fact, the same type of pπ-p interaction is found in metal substituted polyenes. It is due to this extra interaction in those systems that they have been stabilized by an energy value, much higher than the usual ion- ion

interaction energy. On the other hand, the stabilisation in metal-doped polyenes is due to a less efficient s-π^* interaction, which contributes only slightly to the E_{st}. (In metals, the HOMO is s-orbital from which the electron flows to the polyene during the complex formation. The LUMO of the conjugated polyene is a π^*orbital and hence the interaction is weak s-π^* overlapping). Thus, the E_{st} in metal-doped polyenes is comparatively low.

5.5.1.2 Affinity for even carbons

The important and most stable isomer has the general formula, $C_nH_{n+3}M$ (2) for all odd polyenes and $C_nH_{n+2}M$ (2), for all even polyenes, where $M=Li^+/Na^+/K^+$. In most other isomers, the metals tend to attach to the even carbons of the chain. Thus we have C_9H_{12} M (8), $C_{10}H_{12}$ M (4), $C_8H_{10}M$ (4) etc., where $M=Li^+/Na^+/K^+$. It is interesting to note that in $C_8H_{10}Li$ (4), Li is exactly at the middle of the C4-C5 bond with equal distance to C5 too. We have to note that in C_8H_{10}, C4 & C5 are identical. The affinity for even carbons may be explained in terms of the higher charges carried by the carbons of the interacting segment. Also, when the metal is closer to even carbons, the extended conjugation is less disturbed which also contributes to the stability of the system.

5.5.1.3 Insignificance of the size of the metal

In cation-doped polyenes, the metals are at larger distances from the polyene (in C_9 system Li^+ is at a distance of 2.165 A^0, Na^+ at 2.537 A^0 and K^+ at 3.015 A^0 –for details see Tables 5.1 & 5.7). Therefore, the size of the cation is less significant in deciding the position of the metal in the complex. Hence, the interactions of cations like K^+ with larger polyenic segments and the consequent warping in the region in order to increase the charge-charge interaction between the metal ion and the carbons of higher charge are absent from the complex. As a result, warped cation-doped polyenyl complexes are

not obtained. The symmetry factor, which had some role in the stabilization of metal polyenes, is also insignificant; in even polyenes due to the absence of a central carbon and in odd polyenes, due to the restriction of cation-polyene interaction into the segment of sp^2 carbons. However, in isomers in which the metals are almost in the middle, the metals tend to stay over the central bond to attain a better symmetry. Examples for such isomers are $C_8H_{10}Li^+$ (4), $C_8H_{10}Na^+$ (5), $C_8H_{10}K^+$ (4), etc.

5.5.2 Prominence of Cation-Pi interaction

The detailed analysis of the cation doped systems shows that cation-π interaction is the major binding factor in cation-doped polyenes. Geometry optimizations with substituted polyenes also support our conclusion. When cations were doped to polyenes with electron donating group (CH_3), the E_{st} was found to be increasing (Table 5.14). The electron-donating group enhances the pi cloud; the pi cloud then strongly interacts with the cation to yield a more stable product. On the other hand, the electron-withdrawing groups will destabilize the system, as it will decrease the electron cloud of the polyene. Hence the E_{st} of the system will be less. However, when we performed the calculation with CN, there occurred an increase in the E_{st} of the system due to the direct interaction between the metal and the CN group. Still, the Li-complex shows a decrease in the total E_{st} as the result of substituting CN group in the polyene (see Table 5.17).

5.6 Conclusion

The cation-doped conjugated polyenes are stabilized by high amount of energy. There are no significant structural changes for the complexes. The principal binding force existing in them is found to be cation-π interaction in which the type I interaction is more prominent. Calculations show that the E_{st} in $C_7H_{10}Li^+$ (6) is almost equal to the E_{st} in Li-C_6H_6 complex (the former has a

E_{st} of 38.92 kcal/mol whereas the E_{st} of the latter is 38.3 kcal/mol) [9]. Since the E_{st} is large enough to make them potential metal ion carriers, the application of these complexes in biological world may be explored further.

5.7 References:

1. S. Tsuzuki, T. Uchimaru, M. Mikami, J. Phys. Chem. A., 107 (2003) 10414- 10418.

2. R. A. Kumpf & D. A. Dougherty, Science, 261 (1993) 1708-1710.

3. S. Mecozzi, A. P. West Jr., D. A. Dougherty, J. Am. Chem. Soc., 118 (1996) 2307 -2308.

4. S. Mecozzi, A. P. West Jr., D. A. Dougherty, Proc. Natl. Acad. Sci. USA, 93 (1996) 10566-10571.

5. J. W. Caldwell & P. A. Kollman, J. Am. Chem. Soc., 117 (1995) 4177-4178.

6. R. C. Dunbar, S. J. Klippenstein, J. Hrusak, D. Stockigt, H. Schwarz, J. Am. Chem. Soc., 118 (1996) 5277-5283.

7. "Handbook of battery materials"; J. O. Besenhard, ed., Wiley VCH: Weinheim, Germany, 1999.

8. D. Kim, S. Hu, P. Tharakeswar, K. S Kim, J. M. Lisy, J. Phys. Chem. A, 107 (2003) 1228-1238.

9. J. C. Ma & D. A. Dougherty, Chem. Rev., 97 (1997) 1303-1324.

A THEORETICAL STUDY OF THE CATION – π INTERACTION IN ALKALI METAL POLYENES AND POLYENE COMPLEXES

THESIS

Submitted to the
University of Calicut
in partial fulfillment of the requirements
for the award of the degree of
Doctor of Philosophy
in Chemistry,
under the Faculty of Science

By

FR. JOSE T. M.

Forwarded

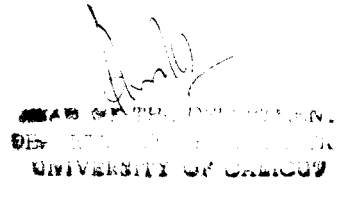

Department of Chemistry,
University of Calicut,
Calicut University P.O.,
673 635

April 2007

CHAPTER 6

SUMMARY AND CONCLUSION

6.1 Introduction

The computational studies on the addition of alkali metals or alkali metal ions to conjugated polyenes reveal certain important and peculiar features. These important features, which were presented and discussed in the previous chapters, are summarized and their possible applications and extensions are highlighted in this chapter.

6.2 Summary

6.2.1 Alkali metal substitution to conjugated polyenes

The substitution of alkali metals on the sp^3 carbon (C1) of conjugated all-trans odd polyenes (C_nH_{n+3}) causes the following changes in the polyene:

(i) C1 undergoes a change of hybridisation from sp^3 to sp^2 resulting in a polyenic anion $(C_nH_{n+2})^{-1}$ and the metal (M) moves in the form of a cation on to the i^{th} carbon, producing isomers of the general formula $C_nH_{n+2}M$ (i), where i= 2,4,6...for Li and Na and i= 3,5,7...for K.

(ii) The most stable isomer of Li and Na polyenes is the one in which the metal resides above the even carbon C2. This structure preserves maximum extended conjugation.

(iii) The most stable isomer of K-polyenes is the one in which the metal resides above the central odd carbon or above the odd carbon closer to the centre- i.e., the most stable isomer will possess a higher symmetry.

(iv) The interaction of Li and Na is with an allyl fragment in which there is a delocalised electron cloud and that of K is with a pentadienyl fragment or with fused multiples of pentadienyl fragments, having delocalised electron cloud.

(v) There occurs a rearrangement of C-C bond lengths along the carbon skeleton and a distortion to the carbon skeleton with considerable deviations in the bond angles and dihedral angles.

(vi) For K-substitution, the distortion of the carbon skeleton turns out into a dramatic warping.

(vii) The conductance increases substantially as indicated by a huge decrease in the HOMO-LUMO gap (e.g., in C_9 system, about 30 to 60 % increase).

(viii) The metal polyenes derive stability through (i) ionic interaction between the metal cation and polyenic anion (ii) cation-carbon skeleton interaction (Type I interaction) and (iii) cation-π cloud interaction (Type II interaction). Type II and Type I interactions are together termed as cation-π interaction.

(ix) The interaction of the metal with the polyene enhances the delocalisation of the π-electrons, which can lead to an enhancement in the conductance of the metal-polyene.

(x) The stabilization energies (E_{st}) of the metal-polyenes are relatively high since the binding involves ionic interaction, in addition to the cation-π interaction.

(xi) The small differences in the E_{st} of the isomers, especially with K-polyenes, suggest the possibility of the movement of the metal ion along the carbon chain.

(xii) For a given metal, the E_{st} decreases as the chain length of the polyene increases and for a given polyene, E_{st} is maximum for Li and minimum for K.

6.2.2 Alkali metal doping to conjugated polyenes

Though alkali metal doping to conjugated polyenes does not evoke dramatic changes to the carbon skeleton, the following features characterize such complexes:

(i) The most stable isomer of Li-doped odd polyene has the general formula $C_nH_{n+3}Li$ (n-1) and that of Li-doped even polyene has the general formula $C_nH_{n+2}Li$ (2). Thus, in the most stable isomer, Li lies above the 2^{nd} sp^2 carbon from the sp^2-terminal.

(ii) The most stable isomer of Na-doped polyenes has different structures: in lower polyenes, Na is above the terminal sp^2 carbon and in higher polyenes, it is above the 2^{nd} sp^2 carbon from the terminal.

(iii) The most stable isomer of K-doped polyenes has the metal above the 3^{rd} sp^2 carbon from the terminal. Lower polyenes show exceptions by assuming positions at 1 and 2.

(iv) The positions of the metal in other isomers are similar to that in substituted polyenes. This is especially so as chain length increases

(v) The bond lengths are rearranged and the carbon skeleton is distorted as in substituted polyenes. Extensive delocalisation of electron cloud along the carbon skeleton is also observed.

(vi) The conductance of the doped polyenes increases to a large extent as indicated by the huge reduction in the HOMO-LUMO gap (e.g., in C_9 system, about 50 to 65 % increase).

(vii) The metal-doped polyenes achieve stability by developing into a system involving cation-π interaction via. the partial flow of electron from the metal to the polyene. The ionic interaction, found in the substituted polyenes, is absent.

(viii) The interaction of the metal with the polyene is cation-π interaction (mainly Type II). However, as the length of the polyene increases, charge on the metal also increases and hence Type I interaction becomes significant.

(ix) The E_{st} of the doped polyene is low due to the absence of ionic interactions. However, the E_{st} increases as the chain length increases.

(x) When the chain length increases, the characteristics of the substituted and doped polyene tend to merge in terms of position of the metal, charge on the metal, metal-carbon distance, number of isomers, HOMO-LUMO gap etc. (e.g., K-doped $C_{32}H_{34}$ and K-substituted $C_{33}H_{36}$ –see 4.6).

6.2.3 Alkali metal cation doping to conjugated polyenes

The doping of alkali metal ions to the conjugated polyenes evokes no considerable changes on the structural parameters of the polyene. The following features characterize the alkali metal ion-doped conjugated polyenes:

(i) The stable isomers have the metal over an even carbon, the most stable isomer being the one in which the metal is above the 2nd sp^2 carbon from the terminal, irrespective of the nature of the metal.

(ii) The general formula of the most stable isomer of any odd system is $C_nH_{n+3}M^+$ (n-1) and any even system is $C_nH_{n+2}M^+$ (2).

(iii) Metal ion doping slightly modifies the delocalised electron cloud along the carbon skeleton, but evokes negligible distortion to the planarity of the polyene, the distorting effect being in the order $Li^+ > Na^+ > K^+$.

(iv) The increase in the conductance of the complex is also negligible (e.g., about 10% increase in C_9 system).

(v) The system achieves stability via. cation-π interaction (mainly Type I)

(vi) The interaction of the cation with the polyene causes a partial flow of electron from the π cloud to the cation. The delocalisation of the electron cloud along the carbon skeleton is also very poor. This results in a very little change in the conductance of the cation-doped system.

(vii) These complexes are having higher E_{st} than that of the metal-doped polyenes.

6.2.4 General features of metal addition to conjugated polyenes

The detailed analysis and discussions of alkali metal-substituted polyenes (chapter 3), alkali metal-doped polyenes (chapter 4) and alkali metal ion-doped polyenes (chapter 5) show that cation- π interaction is a significant binding force existing among them. The former two systems, which are

enriched by an electron given by the alkali metals, behave almost identically as the polyenes attain a critical length. For instance consider the results obtained for potassium doping in $C_{32}H_{34}$ and potassium substitution in $C_{33}H_{36}$ (see 4.6). The cation-doped polyenes differ from the other two in their electronic and structural parameters. Since the first and second systems differ from the third essentially by the presence of an extra electron in the π^*-level of the polyene, we may conclude that the electronic and structural differences exhibited by them are due to this extra pi-electron in the polyene.

Comparison of the net Mulliken charges on the different carbons of various polyenic systems will explain more about the electron flow and the subsequent changes in the electrostatics along the polyene. The net Mulliken charges on the carbons of C_9 system in its various forms (free, anionic, Li-substituted, Li-doped and Li^+-doped) are given in Table 6.1

Table 6.1: The net Mulliken charges (a.u) on different carbons of C_9H_{12}, $(C_9H_{11})^-$, $C_9H_{11}Li$ (8), $C_9H_{12}Li$ (8) and $C_9H_{12}Li^+$ (8) (B3LYP/6-31G*).

System	C1	C2	C3	C4	C5	C6	C7	C8	C9	Q_M [a]
C_9H_{12}	-0.018	0.020	0.018	-0.001	-0.005	0.00004	-0.003	0.065	-0.076	--
$(C_9H_{11})^-$	-0.283	0.019	-0.123	-0.050	-0.127	-0.050	-0.123	0.019	-0.283	--
$C_9H_{11}Li$ (8)	-0.141	0.068	-0.097	0.019	-0.041	-0.012	-0.033	0.055	-0.114	0.2948
$C_9H_{12}Li$ (8)	-0.042	-0.005	0.0005	-0.030	-0.029	0.003	-0.079	0.042	-0.138	0.2777
$C_9H_{12}Li^+$(8)	0.062	0.091	0.045	0.068	0.020	0.108	-0.053	0.096	0.055	0.5067

[a] Charge on Li

A comparison of the net charges on the carbons of different systems is given in Figure 6.1.

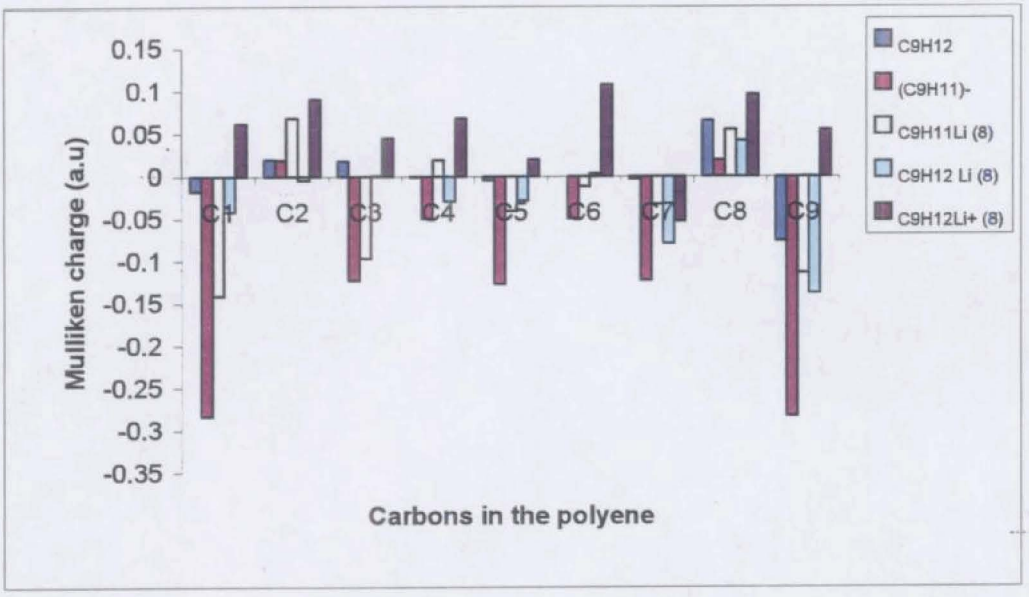

Figure 6.1: Comparison of the net charges on different carbons of the C_9H_{12}, $(C_9H_{11})^-$, $C_9H_{11}Li$ (8), $C_9H_{12}Li$ (8) and $C_9H_{12}Li^+$ (8).

The net charges on the different carbons of the free C_9H_{12}, $(C_9H_{11})^-$, $C_9H_{11}Li$ (8), $C_9H_{12}Li$ (8) and $C_9H_{12}Li^+$ (8) are given in a graphical form. From the graph, it can be seen that when metal is substituted on the polyene [e.g., $C_9H_{11}Li$ (2)], except the 2nd and 4th carbons, all others carry more negative charge. In metal-doped system [e.g., $C_9H_{12}Li$ (8)], only C6 has lesser negative charge than the carbons of free polyene whereas in cation-doped system [e.g., $C_9H_{12}Li^+$ (8)], only one carbon (C7) has more negative charge. This gives an idea on the nature of the electron flow during the metal substitution, metal doping and metal ion doping in free polyenes.

The important characteristics of the free, anionic, metal-substituted, metal-doped and metal ion doped polyenes and the observed parameters that explain them are given in Table 6.2.

Table 6.2: Important characteristics of C_9H_{12} and its alkali metal substituted/doped, metal ion doped complexes (B3LYP/6-31G*).

System	C_9H_{12}	$C_9H_{11}^-$	C_9H_{11} Li (8)	C_9H_{12} Li (8)	C_9H_{12} Li^+ (8)	C_9H_{11} Na (2)	C_9H_{12} Na (9)	C_9H_{12} Na^+ (8)	C_9H_{11} K (7)	C_9H_{12} K (8)	C_9H_{12} K^+ (8)
E_{st}	---	---	141.41	18.61	41.89	117.83	03.41	29.34	100.47	04.61	19.00
ΔE	86.38	67.80	59.66	40.94	76.79	35.30	27.04	80.79	37.79	19.36	80.05
Ri	---	---	2.0584	2.0605	2.1654	2.4290	2.7096	2.5373	2.7826	2.9960	3.0148
C9-C8	1.3442	1.3613	1.4008	1.4086	1.3606	1.4036	1.3664	1.3574	1.3752	1.3710	1.3526
C8-C7	1.4476	1.4277	1.4087	1.4103	1.4516	1.4043	1.4307	1.4529	1.4200	1.4248	1.4519
C7-C6	1.3560	1.3864	1.4365	1.4204	1.3782	1.4251	1.3671	1.3711	1.4041	1.3844	1.3661
C6-C5	1.4406	1.4047	1.3644	1.3973	1.4222	1.1.3718	1.4319	1.4292	1.3932	1.4262	1.4348
C9C8C7C6	-180.0	-180.0	-172.5	-168.27	171.33	-172.0	-177.96	175.14	-150.6	162.22	174.6
Structural features	Planar	Planar	Distorted	Slightly distorted	Slightly distorted	Distorted	Planar	Slightly distorted	Warped	Distorted	Slightly distorted
Q_M	---	---	0.2948	0.2777	0.5067	0.4838	0.0189	0.6722	0.6600	0.2897	0.8297
Q_{C9}	-0.358	-0.428	-0.445	-0.438	-0.361	-0.475	-0.443	-0.382	-0.455	-0.425	-0.400
Q_{C8}	-0.060	-0.045	-0.079	-0.101	-0.104	-0.105	-.0.060	-0.115	-0.098	-0.112	-0.118
Q_{C7}	-0.125	-0.176	-0.238	-0.218	-0.243	-0.226	-0.130	-0.219	-0.253	-0.199	-0.225
Q_{C6}	-0.122	-0.113	-0.095	-0.111	-0.064	-0.111	-0.120	-0.095	-0.157	-0.153	-0.117

E_{st}= Stabilisation energy of the system in kcal/mol; ΔE= LUMO-HOMO gap in kcal/mol; Ri= shortest metal-carbon distance (A^0); C9-C8, C8-C7, C7-C6 & C6-C5=C-C bond lengths (A^0); C9C8C7C6 = dihedral angle (deg.); Q_M = Mulliken charge on the metal (a.u); Q_{C9}, Q_{C8}, Q_{C7} and Q_{C6}= Mulliken charges on carbons (a.u).

Table 6.2 gives the relevant data with respect to C_9H_{12} as the substrate, featuring the important characteristics of the three systems we have studied. It is evident from the table that the presence of a metal above the polyene having a delocalised electron cloud is directly related to the conductance of the system. Also, it gives a clue about the relation of charge on the metal and stability of the complex formed. The importance of an extra electron in metal-polyene system for invoking structural deviations is also well exemplified. Based on the evaluation of metal-substituted, metal-doped and metal ion doped systems and the data presented in Table 6.2, an attempt is made to

converge the important characteristics of metal/cation added conjugated polyenes as follows:

(i) Cation-doped polyene constitutes a natural cation-π system and is stabilized by cation-π interaction involving cation-carbon skeleton interaction (electrostatic, Type I) and cation-π cloud interaction (non electrostatic, Type II). On the other hand, metal-substituted and metal-doped polyenes develop into cation-π systems by the partial flow of electron from the metal to the polyene and thereby get stabilized by cation-π interaction.

(ii) In metal added (substituted/doped) systems as well as the cation added systems, smaller atoms (Li & Na) prefer to interact with an allyl fragment of the polyene, whereas larger atoms (K & Rb) generally prefer to a pentadienyl fragment or its multiples.

(iii) Generally, interaction of the metal enhances the charges in the carbons of the allyl/pentadienyl fragment and also enhances the delocalisation of the π-electrons in the fragment (as seen from the C-C bond lengths- Table 6.2).

(iv) Enhancement of the charges on the carbon atoms leads to stronger Type I interaction, whereas enhanced delocalisation implies a stronger Type II interaction.

(v) In all the three systems, several isomers differing in stabilisation energies are possible for a given metal and polyene, depending on the positions of the metal above the carbon skeleton.

(vi) The metal takes position above the carbon skeleton so as to derive maximum stability via. (1) enhancing delocalisation of π-electrons and (2) imparting maximum charges to the carbons.

(vii) In the most stable isomers of both metal substituted and metal-doped systems, Li and Na generally prefer to stay above the terminal fragment, whereas K prefers to the central fragment. However, in cation-doped systems, all the three metals prefer to the terminal fragment.

(viii) The stability of the metal-substituted complexes decreased with increase in the length of the polyenes; but for metal-doped or metal ion-doped complexes, stability increased with increase in the length of the polyene.

(ix) The structures of the metal added (substituted/doped) complexes show that the carbon skeletons get distorted as a result of metal addition. The distortion is minimum with cation-doped complexes (Table 6.2).

(x) In the metal-added systems, the cation-π interaction is predominantly non-electrostatic, whereas in cation-doped system it is predominantly electrostatic (Table 6.2).

(xi) The reduction in the HOMO-LUMO energy gap leading to enhanced conductance appears to be a direct consequence of the enhanced delocalisation of the π-electrons along the polyene (Table 6.2).

(xii) Substitution and doping of alkali metals considerably increase the conductance of the system, whereas cation doping causes only a very slight increase in the conductance (Table 6.2).

(xiii) The small difference in the stabilisation energies of the isomers suggests the possibility of the movement of the metal species along the carbon chain, under suitable conditions.

Our studies of alkali metal doping/substitution and cation doping to conjugated polyenes reveal that only metal doping or substitution causes significant electronic and structural changes to the polyenes. Since we have found out cation-π interaction as the major force existing in alkali metal doped polyenes, we may further pursue our study to develop a satisfactory model to explain the mechanism in conducting polymers. The formation of different isomers and the role of the doped metal in stabilizing them may have something to offer in explaining this phenomenon.

6.3 Conclusion

The computational studies on metal polyenes and metal-doped polyene complexes show that cation- π interaction is an important interaction, controlling the energetics of such systems. Extending the above conclusion to conducting polymers, we can expect the same types of interactions governing the characteristics of the conducting polymers. The mechanism of transition from non metal to metal, which we observe in 'synthetic metals' [1], a topic still being debated in the field of conjugated polymers, may be explained in a new dimension, basing on the observations we have gathered in our work.

Today, the research on conductive polymers is wide open. An era has dawned on us where we are more concerned with the super conducting materials, obtained by the doping of alkali metals in fullerenes [2]. With the observation [3] and synthesis [4] of fullerenes, a field of 3-D molecules has been developed. They possess high electron affinity [5] and have pi- orbitals radiating in all directions [2] and interstitial sites large enough to accommodate the alkali metal cations [6]. Further, their potassium doped sample, K_3C_{60} [6], and rubidium-doped sample, Rb_3C_{60} [7], are found to be possessing super conductivity, an important milestone in the research of conducting polymers. Thus, in fullerenes too, the key to conductivity is the dopant atom, namely the alkali metal. Hence, the understanding about the

interactive forces in alkali metal doped polyenes may find its relevance in this new field of enormous application.

The ab initio calculations have shown that when alkali metals are substituted or doped in conjugated polyenes, various isomers are possible. These isomers differ each other by small quantities of energy. The small difference in energies among the isomers (See Table 3.2 for C_{13} system) implies a far-reaching consequence, viz., the possibility of transformation of one isomer to another by tunneling from one potential well to another leading to the oscillation of M^+ from one end of the chain to the other. This novel phenomenon may find application in the preparation of new materials with interesting electronic, electrical, magnetic and optical properties. The substantial decrease in the HOMO-LUMO gap of the K-complexes (see Tables 3.8, 3.14 & 3.20) is a pointer to the above speculation.

The curious structural changes that occur in the conjugated polyenes, as the result of metal substitution and doping, may endear them in the field of catalysis. The structural changes, particularly the phenomenon of warping, can evoke substantial deviations in the physico-chemical behaviour of the polyenic ligand. It can also affect the properties of the complex in which it acts as ligand. Thus, these results may be of use in the field of catalysis involving organo metallics in modifying or tuning or activating them.

Our studies have proved the metal binding ability of conjugated polyenes. We propose the extension of this property to the pharmaceutical field too. There is a group of polyene antibiotics [8] that are used as fungicides. They contain a hydrophobic conjugated double bond system in one portion of the molecule and a markedly hydrophilic polyhydroxyl system in another portion. Two fungicides used for treating fungal diseases are nystatin and amphotericin B (Figure 6.2). Amphotericin B, though efficient in curing fungal infections, is very toxic to humans. The toxicity is due to

membrane damage, an action due to pore formation and leakage of K^+ and Mg^{2+} ions. Its toxicity can be controlled if we could rectify the loss of K^+ ions on using this medicine. As amphotericin B contains a conjugated polyene part, it can act as a good cation binder, just like $C_{10}H_{12}$ binds a cation. Hence, K^+ ions can be introduced into the cell membrane along with the medicine. Thus the toxicity of the medicine can be minimized. Since the binding force is weak, the cleavage of K^+ from the medicine may be attained easily.

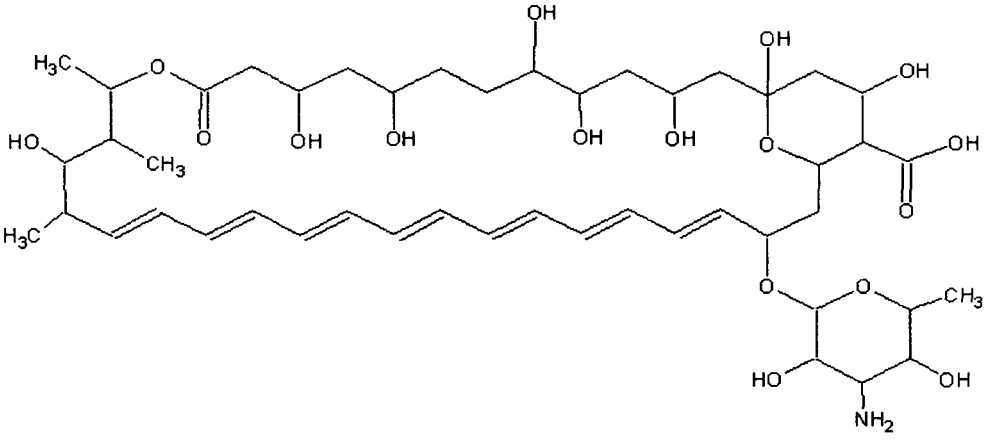

Figure 6.2: Amphotericin B

In similar fashion, β-carotenoids (Figure 1.2) and its derivatives can act as good metal carriers, as they contain polyenic part with extended conjugation. Our calculations have proved that K^+ binds to molecules with extended conjugation with appreciable strength, the binding being the result of cation-π interaction. For example, K^+ binds with the hypothetical molecule given in Figure 6.3, which resembles β-carotene to a certain extent, with a stabilisation energy of 20.88 kcal/mol. On the basis of above calculation, we suggest that the carotenoids, which are having medicinal value even otherwise, may be utilized as potential metal carriers.

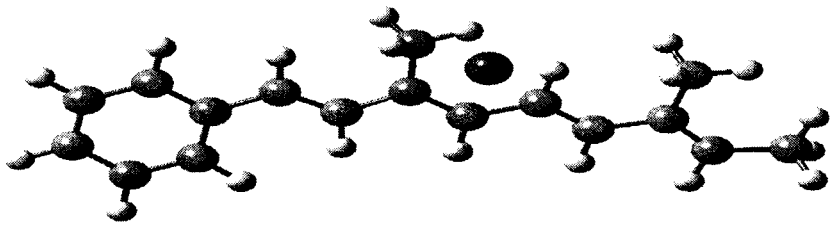

Figure 6.3: Optimized structure of $C_{17}H_{20}K$

We have found the structural changes that the metal doping or substitution evoked in conjugated polyenes. As the structure gets modified, accordingly the properties of the system will also change. This phenomenon may be applied in the field of biomass-gasification. The introduction of alkali metal atoms to the graphitic systems of the bio mass will cause the surface modification, which will eventually promote the rate of biomass gasification process.

The above-mentioned cases are a few of the many applications of metal-doped polyenes in the modern world. Many more additions to this study are yet to come. Further explorations in this field may help us make substantial manipulations of these features to the welfare of the humanity. Also, the stabilizing interaction of these complexes, namely cation-π interaction, can be tuned well to have a glimpse to the wonderful world of protein chemistry.

6.4 References:

1. A.G. MacDiarmid, Synthetic Metals, 125 (2002) 11-22.

2. R. C. Haddon, Pure & Appl. Chem., 65 (1993) 11-15.

3. H. W. Kroto, J. R. Heath, S. C. O'Brien, R. F. Curl, R. E. Smalley, Nature, 318 (1985) 162-164.

4. W. Kratschmer, L. D. Lamb, K. Fostiropoulos, D. R. Huffman, Nature, 347 (1990) 354-358.

5. R. C. Haddon, L. E. Brus, K. Raghavachari, Chem. Phys. Lett., 125 (1986) 459-464.

6. R. C. Haddon, A. F. Hebard, M. J. Rosseinsky, D. W. Murphy, S. J. Duclos, K. B. Lyons, B. Miller, J. M. Rosamilia, R. M. Fleming, A. R. Kortan, S. H. Glarum, A. V. Makhija, A. J. Muller, R. H. Eick, S. M. Zahurak, R. Tycko, G. Dabbagh, F. A. Thiel, (1991) 321-322.

7. S. H. Glarum, S. J. Duclos, R. C. Haddon, J. Am. Chem. Soc., 114 (1992) 1996-2001.

8. A. Z. Mahmoudabadi, D. B. Drucker, Indian Journal of Pharmacology, 38 (2006) 423-426.